

**TWO SETS OF INTESTINAL PACEMAKERS:
NEUROMODULATION, Ca²⁺-DEPENDENCE,
AND ELECTRICAL COUPLING**

**INTERACTION OF TWO SETS OF PACEMAKERS IN
CANINE ILEUM: NEUROMODULATION, Ca^{2+} -
DEPENDENCE, AND ELECTRICAL COUPLING**

by

FRANCISCO SANDOVAL CAYABYAB, B.Eng. (McMaster University)

A Thesis

Submitted to the School of Graduate Studies

in Partial Fulfilment of the Requirements

for the Degree

M. Eng. in Electrical and Computer Engineering

McMaster University

© Copyright by Francisco S. Cayabyab, September 1995

MASTER OF ENGINEERING (1995)
(Electrical and Computer Engineering)

McMASTER UNIVERSITY
Hamilton, Ontario

TITLE: Interaction of Two Sets of Pacemakers in Canine Ileum:
 Neuromodulation, Ca²⁺-Dependence, and Electrical Coupling

AUTHOR: Francisco Sandoval Cayabyab, B.Eng. (McMaster University)

SUPERVISORS: Dr. Hubert DeBruin and Dr. Edwin E. Daniel

NUMBER OF PAGES: xxi, 223

ABSTRACT

We investigated the origins, neural modulation, ionic mechanisms, and electrical coupling properties of the pacemaker systems in the canine ileum by simultaneously recording the intracellular electrical activity and accompanying mechanical activity in cross-sectioned slabs of the muscularis externa or in the isolated circular muscle. In the whole thickness preparation, intracellular recordings were taken from the circular muscle near the myenteric plexus (MyP), deep muscular plexus (DMP), and intermediate areas between the MyP and DMP and in the isolated circular muscle preparation from similar areas except near the myenteric plexus.

One type of slow wave, sigmoidal or triangular in shape, was recorded from impalements near the DMP region in the whole-thickness preparation. Another type observed from the MyP region oscillated at nearly the same frequency (9-10 cycles/min) and was characterized by a fast upstroke and a square shape. A mixture of these two patterns was recorded in intermediate areas (the outer circular muscle or OCM) while triangular slow waves were present near the submucosal plexus (SMP) inner circular muscle.

Neither type of slow waves was affected by atropine, guanethidine, propranolol, and phentolamine (all 1 μ M). Under these conditions of inhibition of NANC (non-adrenergic, non-cholinergic) nerves, electrical field stimulation (EFS) produced a fast, monophasic inhibitory junction potential (IJP) followed by a triggered slow wave (TSW)

which could be premature or delayed and whose amplitude was maximum near the MyP region and decayed progressively in the other areas (minimum in SMP region). The K⁺ channel blocker, apamin at 10⁻⁶ M, did not affect resting membrane potentials or spontaneous slow waves but inhibited the amplitude of the IJP up to 70% and slightly but significantly enhanced (30%) the amplitude of the TSW. Long duration, single pulses (50-100 msec square waves, 10-20 V) elicited TSWs without IJPs. Both the slow waves and TSWs were associated with contractions of circular muscle which were significantly enhanced by apamin but not by blockers of adrenergic and cholinergic nerves.

When the IJPs recorded near the MyP or DMP were abolished by tetrodotoxin (TTX, 1 μM) or by the NO synthase (NOS) inhibitor, N^ω nitro L-arginine (L-NNA, 50 μM), the occurrence of the TSW in response to EFS was advanced in time and increased in amplitude. The effects of L-NNA were reversed by L- but not D-arginine (both 1 mM). L-arginine significantly prolonged the durations of IJPs from the MyP and DMP regions. In contrast, the N-type Ca²⁺ channel blocker ω-conotoxin GVIA (ω-CTX, 1-3 x10⁻⁷M) abolished the IJP but delayed the induction of the TSW. Subsequent addition of either TTX or L-NNA advanced the onset of the TSW. The TSWs elicited by 50-100 msec single pulses were resistant to TTX, ω-CTX, or L-NNA. All treatments which abolished the IJP significantly increased contractions of circular muscle associated with spontaneous slow waves and TSWs.

In the isolated circular muscle preparation (with the DMP intact) triangular slow waves were recorded near the DMP or close to the MyP border. The frequency and

amplitude of the slow waves recorded near the DMP were significantly smaller than those recorded in similar areas in the full thickness preparation. EFS of this preparation evoked IJPs of 18 - 20 mV in amplitude. The IJPs were biphasic, lasted 5s and showed a fast and a slow component. No TSW occurred after the fast component of the IJPs; slow repolarization was observed instead. Long duration single pulses did not induce TSWs. In this preparation, the NOS inhibitor, N^ω nitro L-arginine methyl ester (L-NAME, 3x10⁻⁴M), abolished the IJPs and regularized the slow waves, but TSWs could not be evoked.

Superfusion of inhibitory neuromediators had different effects on pacemaking activity. SIN-1, a donor of NO, hyperpolarized the membrane, significantly increased slow wave frequency but reduced its amplitude, and abolished contractions. VIP (less effective) and PACAP (more effective) reduced slow wave frequency and amplitude without changing resting membrane potentials. PACAP, but not VIP, increased circular muscle tone at 10⁻⁶ M.

Nifedipine (10⁻⁷ and 3 x 10⁻⁷ M), an L-type calcium channel blocker, did not modify the shape of slow waves in any area of the full thickness preparation. It also did not reduce the amplitude of the IJP or TSW. Ni²⁺ at 200 μM, a Ca²⁺ channel blocker, inhibited slow wave frequency and amplitude and contractions. In Ca²⁺-free Krebs (0.1 mM EGTA) for 10-15 min, the amplitude and frequency of the slow waves were gradually reduced. The TSW in response to 100 msec single pulses was still recorded near the MyP but never near the DMP region. The inhibitory effect of Ca²⁺-free solution

on slow wave amplitude was more rapid in onset near the DMP region. The intracellular Ca^{2+} store pump inhibitor, cyclopiazonic acid (10-30 μM), enhanced slow wave frequency and contractions. This differential sensitivity to removal of Ca^{2+} may be related to the morphological and functional observations which suggested that different electrical coupling properties between the pacemaker networks existed. The MyP pacemakers were less electrically well-coupled by visible gap junctions (low resistive cell-to-cell contacts) to outer circular muscle and hence showed greater susceptibility to 1 mM octanol (a gap junction blocker). The DMP pacemakers made numerous gap junction contacts to circular muscle, and slow waves paced from this region were less susceptible to 1 mM octanol.

We conclude that 1) the pacemaker system of the canine ileum consists of two types of pacemakers that correspond to the presence of two networks of pacemaker cells found in the MyP and the DMP. The MyP network appeared to dominate pacemaking activity. 2) The slow waves and the TSW originated independently of neural activity but were delayed by IJPs. The MyP and the DMP provide two independent inhibitory neural inputs, where NO is released to mediate IJPs and relaxation and influence the delay in the occurrence of the TSW. 3) The TSW originates exclusively from the MyP region from which it spreads passively to other areas. It can reset the timing of slow waves in both pacemaker networks. 4) Ca^{2+} entry through non L- or N-type Ca^{2+} channels initiates slow waves. Intracellular Ca^{2+} stores modulate slow waves. 5) Different nature of electrical coupling of the MyP and DMP pacemakers to circular muscle may explain the differential sensitivity of slow waves to Ca^{2+} removal and gap junction blockade.

ACKNOWLEDGEMENTS

I would like to thank my supervisors, Drs. Hubert deBruin and Edwin E. Daniel, for their strong support, encouragement, and counsel throughout the many stages of this research project. I thank Dr. deBruin for his instrumental role as my advisor during a probationary period in Electrical Engineering, and for his willingness and enthusiasm to be my co-supervisor for my M. Eng. thesis. At various stages of my career at McMaster, I was privileged to have the opportunity to be inspired and trained as a biomedical scientist by Dr. Daniel despite my training as an engineer.

This research was supported financially by the N.S.E.R.C. and M.R.C. of Canada.

I would also like to thank the many colleagues who have come and left the Lab 4N75, for sharing their expertise with me and for their friendship and camaraderie. Thanks to Drs. Patri Vergara (Spain), Marcelo Jimenez (Spain), Masato Inazu (Japan), Hiroyoki Shimamoto (Japan), Louis Montano (Mexico), and John Zhang (China).

I also extend my gratitude to the past and present residents of Lab 4N75 for making the whole experience at McMaster an enriching one. Thank you Dr. Andrew Abela ("Trigger"), Jennifer Jury, Dr. Amy Low, Ita McGrogan, Sylva Cipris, Frank Christinck, Peter Darby, Ted Watson, Anne Marie Salapatek, Zofia Woskowska, Dr. Y.K. Mao, and Dr. Y.F. Wang.

Deeply felt love and appreciation go to my best friend, Sheila Savedia, and her family for their love, support and encouragement, especially during the last stages of

writing this thesis. I wish to acknowledge Sheila for her help in histological and light microscopic studies in this thesis, and for the countless hours she spent helping to organize this thesis.

Finally, I wish to express thanks to my loving parents (Francisco and Gregoria Cayabyab) and my brothers and sisters, for their constant support and encouragement throughout my university career.

I would like to close with the following quotation which impacted me personally while living and studying as a graduate student. "It must always be remembered that scientific research is a very difficult art, in which ninety-nine per cent of frustration and perspiration is not always balanced by one per cent of inspiration and elation. It requires peculiar self-confidence and will-power not to follow a line that promises relatively easy returns." (Excerpt from PUBLIC KNOWLEDGE, The Social Dimension of Science by Jonh Ziman [Cambridge University Press])

To my parents

TABLE OF CONTENTS

	PAGE
Title page	i
Descriptive note	ii
Abstract	iii
Acknowledgements	vii
Dedication	ix
Table of contents	x
List of tables	xiv
List of figures	xvi
List of abbreviations	xx

CHAPTER 1: INTRODUCTION

1.1	Function and regulation of the small intestine	2
1.2	Morphology of the canine small intestine	3
1.3	The interstitial cells of Cajal as putative pacemakers	16
1.4	The role of interstitial cells of Cajal in NANC neurotransmission	17
1.5	Possible role of NO and NANC neuromediators in pacemaking	18
1.6	Tissue preparation and electrophysiological studies	18

1.7	Rationale for using the dog model	20
1.8	Statement of the problem	21

CHAPTER 2: OBJECTIVES AND HYPOTHESIS

2.1	To obtain evidence for a dual pacemaking mechanism for slow wave in the canine intestine	24
2.2	To determine the roles of nitric oxide (NO) release from nerves and from non-neural sources in the regulation of slow wave activity and response to electrical field stimulation (EFS) in canine ileum	25
2.3	To investigate the roles of Ca ²⁺ in slow wave generation, nerve activation and contraction in canine ileum	26
2.4	To study the contribution of gap junctions in slow wave generation and excitation-contraction coupling	27

CHAPTER 3: METHODS AND RESULTS

3.1	Paper #1	28
	"Heterogeneity in electrical activity of the canine ileal circular muscle: interaction of two pacemakers"	
3.2	Paper #2	66
	"Influence of nitric oxide on the spontaneous and triggered electrical and mechanical activities of the canine ileum"	

3.3	Paper #3	113
	"Ca²⁺ influx modulation of the spontaneous and triggered electrical and mechanical activities of the canine ileum"	
3.4	Paper #4	162
	"Canine ileum myenteric and deep muscular plexus slow waves: electrical coupling of interstitial cells of Cajal to myocytes"	

CHAPTER 4: DISCUSSION

4.1	Dual Pacemaking Mechanism in Canine Ileum: Role of Interstitial Cells of Cajal	187
4.1.1	Electrical Coupling Mechanisms in Gastrointestinal Musculature ..	187
4.1.2	Electrical Coupling of ICC as Pacemakers in Canine Ileum	188
4.2	Role of NO and Other Neuromediators in Pacemaking Activity	191
4.2.1	NO as NANC Mediator	191
4.2.2	Possible Non-Neural Source of NO	192
4.2.3	NO, VIP and PACAP and Their Modulation of Pacemaking Activity	193
4.2.4	Future Studies to Understand Functions of and Interplay Among NO, VIP and PACAP	197
4.3	Role of Gap Junctions and Other Cell Contacts in Electrical and Mechanical Coupling of Pacemaking Activity	199

4.4	White Noise Current Input to Obtain Junctional Resistance and Capacitance	201
4.5	Biological Oscillators and Modelling	203
4.6	Conclusion	205
<u>BIBLIOGRAPHY</u>		208
<u>LIST OF PUBLICATIONS</u>		220

LIST OF TABLES

Chapter 3

3.1

- 3.1.1 Electrophysiological effects of NANC blockers (all at 10^{-6} M) on cells near the regions of the myenteric plexus (MyP) (A) and deep muscular plexus (DMP) (B) 64
- 3.1.2 Characteristics of the resting membrane potentials, slow waves and responses to electrical field stimulations in the different regions of the circular muscle layer of the canine ileum 65

3.2

- 3.2.1 Electrophysiological effects of tetrodotoxin (10^{-7} M) on cells near the regions of the myenteric plexus (MyP) (A) and the deep muscular plexus (DMP) (B) 110
- 3.2.2 A. Electrophysiological effects of L-NNA (50 μ M), D- and L-ARG (both 1 mM) on cells near the region of the myenteric plexus (MyP) 111
- B. Electrophysiological effects of L-NNA (50 μ M), D- and L-ARG (both at 1 mM) on cells near the deep muscular plexus (DMP) 112

3.3

- 3.3.1 Electrophysiological effects of the N-type Ca^{2+} channel blocker, ω -conotoxin GVIA (ω -CTX) at 10^{-7} - 3×10^{-7} M, and the L-type Ca^{2+} channel antagonists, nifedipine at 10^{-7} - 3×10^{-7} M, on cells near the myenteric plexus (MyP) (A) and the deep muscular plexus (DMP) (B) in the full-thickness preparations 158
- 3.3.2 Electrophysiological effects of 200 μM Ni^{2+} on cells near the myenteric plexus (MyP) (A) and the deep muscular plexus (DMP) (B) in the full-thickness preparations 159
- 3.3.3 Electrophysiological effects of 0 Ca^{2+} (100 μM EGTA) on cells near the regions of the myenteric plexus (MyP) (A) and the deep muscular plexus (DMP) (B) of the full-thickness preparations and near the DMP region of isolated circular muscle (ICM) (C) 160

3.4

- 3.4.1 Effects of octanol (1 mM) in the myenteric plexus (MyP, A) and deep muscular plexus (DMP, B) regions of the canine ileum 185

Chapter 4

- 4.1 Effects of vasoactive intestinal polypeptide (VIP) and pituitary adenylate cyclase activating peptide (PACAP) on pacemaking

activity in the canine ileum 194

LIST OF FIGURES

Chapter 1

Fig. 1. The smooth muscle layers and enteric nerve plexuses of the small intestine 5

Fig. 2. The muscularis externa, submucosa, and mucosa of canine ileum7

Fig. 3. The muscle layers bordered by the myenteric plexus in canine ileum 9

Fig. 4. The muscle layers bordered by the deep muscular plexus in canine ileum 11

Fig. 5. Transmission electron micrograph of the canine ileum circular muscle 13

Chapter 3.1

Fig. 1. Heterogeneity in electrical slow waves in canine ileum circular muscle 58

Fig. 2.	Gradient in IJPs and resting potentials in canine ileum circular muscle	59
Fig. 3.	Spontaneous slow waves and triggered activity near the pacemaking regions	60
Fig. 4.	Origin of triggered slow waves in canine ileum circular muscle	61
Fig. 5.	Slow waves and IJPs in isolated circular muscle preparations	62
Fig. 6.	Lack of triggered activity in isolated circular muscle preparation	63

Chapter 3.2

Fig. 1.	Spontaneous slow waves and IJPs near pacemaking regions	100
Fig. 2.	Blockade of nerve function with tetrodotoxin and its effects on spontaneous and triggered slow waves	101
Fig. 3.	Effects of nitric oxide synthesis blockers on slow waves and IJPs in different regions of circular muscle	102
Fig. 4.	Effect of nitric oxide synthesis blockers on time delays of triggered slow waves	103
Fig. 5.	Effects of nitric oxide synthesis blockers on slow waves and IJPs in isolated circular muscle	104
Fig. 6.	Nitric oxide synthesis blockers enhance slow waves and contractions	105

Fig. 7.	Blockade of nerve function with ω -conotoxin GVIA and its effects on triggered slow wave delays	106
Fig. 8.	Effects of K^+ channel blocker, apamin, on slow waves and contractions	107
Fig. 9.	Effects of nerve and muscle antagonists on motility index .	108
Fig. 10.	Effects of nitric oxide donors on slow waves and contractions	109

Chapter 3.3

Fig. 1.	Slow waves and IJPs in whole thickness and isolated circular muscle preparations	149
Fig. 2.	Effects of ω -conotoxin GVIA on IJPs and triggered slow waves	150
Fig. 3.	Effects of L-type Ca^{2+} channel blocker, nifedipine, on slow waves and contractions	151
Fig. 4.	Effects of Ca^{2+} influx blocker, Ni^{2+} , on slow waves and contractions	152
Fig. 5.	Inhibitory effects of Ni^{2+} , nifedipine, and Ca^{2+} removal on contractions	153
Fig. 6.	Differential effects of Ca^{2+} removal on slow waves and triggered activity	154
Fig. 7.	Summary of inhibitory effects of Ca^{2+} removal on slow waves and	

	membrane potentials	155
Fig. 8.	Electromechanical effects of cyclopiazonic acid near the deep muscular plexus	156
Fig. 9.	Electromechanical effects of cyclopiazonic acid near the myenteric plexus	157
 Chapter 3.4		
Fig. 1.	Octanol inhibition of slow waves and contractions	180
Fig. 2.	Octanol effects on IJPs near two pacemaking regions	181
Fig. 3.	Electron micrograph of the deep muscular plexus	182
Fig. 4.	Electron micrograph of the myenteric plexus: gap junctions	183
Fig. 5.	Electron micrograph of the myenteric plexus: close appositions	184
 Chapter 4		
Fig. 1.	Effects of PACAP on slow waves, IJPs and contractions in canine ileum	196

LIST OF ABBREVIATIONS

BK - large conductance Ca^{2+} -activated K^+ channels

Ca^{2+} -ATPase - Ca^{2+} adenosinetriphosphatase

Ca_i^{2+} - intracellular Ca^{2+}

Ca_o^{2+} - extracellular Ca^{2+}

CICR - Ca^{2+} -induced Ca^{2+} -release

CM - circular muscle

CPA - cyclopiazonic acid

D-ARG - D-arginine

DMP - deep muscular plexus

E-C - excitation-contraction

EFS - electrical field stimulation

EGTA - ethyleneglycol-bis(betaaminoethylether)-N,N,N,N-tetraacetic acid

EJP - excitatory junction potential

ICC - interstitial cells of Cajal

IJPs - inhibitory junction potentials

L-ARG - L-arginine

L-NAME - N^ω nitro L-arginine methyl ester

L-NNA - N^ω nitro L-arginine

MyP - myenteric plexus

NANC - nonadrenergic noncholinergic

NO - nitric oxide

NOS - nitric oxide synthase

OCM - outer circular muscle

ω -CTX - ω -conotoxin GVIA

SIN-1 - 3-morpholino-sydnonimine-hydrochloride

SMP - submucosal plexus

SR - sarcoplasmic reticulum

TSWs - triggered slow waves

TTX - tetrodotoxin

VIP - vasoactive intestinal polypeptide

CHAPTER 1

INTRODUCTION

1.1 Function and Regulation of the Small Intestine.

The small intestine, comprising the duodenum, jejunum and ileum, is the major site for absorption of nutrients and digestion products from the gastrointestinal tract. This absorptive function is facilitated by the peristaltic contractions (mixing or segmental contractions) that propagate from proximal to distal regions of the gut only for a short distance. This pattern of propulsive motility is known to be regulated by neurons of the myenteric plexus involving non-adrenergic, non-cholinergic (NANC) nerves [46]. Neural inputs to the effector musculature are responsible for the coordinated propulsive and receiving components of propulsive motility of the gut [69,75]. It is of interest that in the gut, there may be interplay among various neuromediators (*e.g.*, adenosine triphosphate or ATP, nitric oxide or NO, vasoactive intestinal polypeptide or VIP) with the regulation of the descending relaxation of intestinal peristalsis. Such relaxation is preceded by transient membrane hyperpolarization known as inhibitory junction potential (IJP), which may be mediated by NO, VIP or ATP released from inhibitory NANC nerves as has been described in several intestinal musculature of various species [50,69,107].

Normal patterns of motor activity of the small intestine depend on the interactions between smooth muscle cells and between smooth muscle cells and interstitial cells of Cajal or ICC (putative pacemakers of the gut). These motor patterns are influenced by the regulatory controls of both inhibitory and excitatory nerves and endocrine cells. Intestinal motility depends on the coordinated contractile activity of the musculature, which manifests electrophysiologically as the rhythmic electrical oscillations known

variously as slow waves, pace-setter potentials, or spike-like action potentials. These slow waves are temporally associated with phasic contractions of the smooth muscle. For my thesis research the segment of the small intestine being investigated is the ileum.

1.2 Morphology of the Canine Small Intestine

A schematic diagram of the entire cross section of the small intestine is depicted in Figure 1 and a representative light microscopic cross-section of a segment of canine ileum used in the present studies is shown in Figure 2A. Extrinsic innervation and vascularization of the small intestine enters at the mesenteric border. Just below the loose connective tissue serosa is the longitudinal muscle layer. It represents roughly one-third of the entire muscularis externa (Figure 2A). It has been widely accepted that visible gap junctions are absent in the longitudinal muscle layer [54], and alternative means of electrical coupling between longitudinal smooth muscle cells have been proposed such as electrical field coupling introduced by close appositional cell contacts [59].

The myenteric plexus separates the longitudinal and circular muscle layer (Figures 1 and 2). This plexus houses nerve ganglia interconnected with nerve fibers (Figures 1 and 3) and it also contains other cell populations (for example, interstitial cells of Cajal, macrophage-like cells, endothelial cells, etc.) that are not readily apparent under light microscopy but are identifiable when viewed with electron microscopy. There are regions in the myenteric plexus border where these ganglia do not appear (Figure 3A) and it is believed that interstitial cells of Cajal or ICC (the putative pacemaking cells) are the only cell type connecting the longitudinal and outer circular muscle cells.

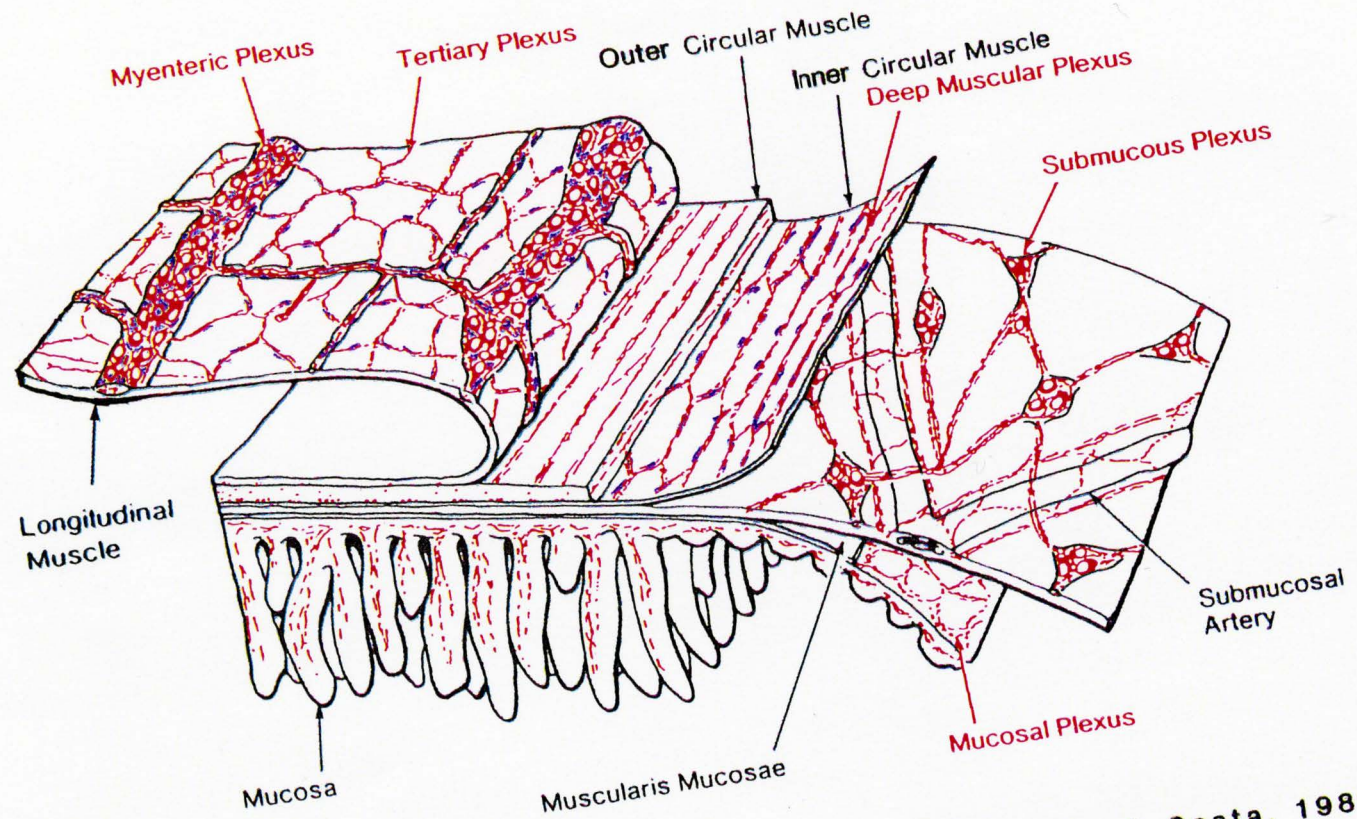
The circular muscle layer is subdivided into the outer circular muscle (OCM) and inner circular muscle (ICM). These two circular muscle layers, with the inner circular muscle also known as the dense layer, are bordered by the deep muscular plexus (see Figures 1 and 4). This plexus represents the narrow region where (continued to page 15)

Legend to Figure 1

The smooth muscle layers and enteric nerve plexuses of the canine ileum.

For our electrophysiological studies, note that the mucosa and submucosa were removed, and only the muscularis externa and the nerve plexuses (shaded red) and their respective pacemaking cells (labelled in blue) were used. Note also the locations of the inner circular muscle (ICM), the deep muscular plexus (DMP), the outer circular muscle (OCM), the myenteric plexus (MyP), and the longitudinal muscle. Adapted from Furness and Costa, 1980 [45].

The Canine Small Intestine



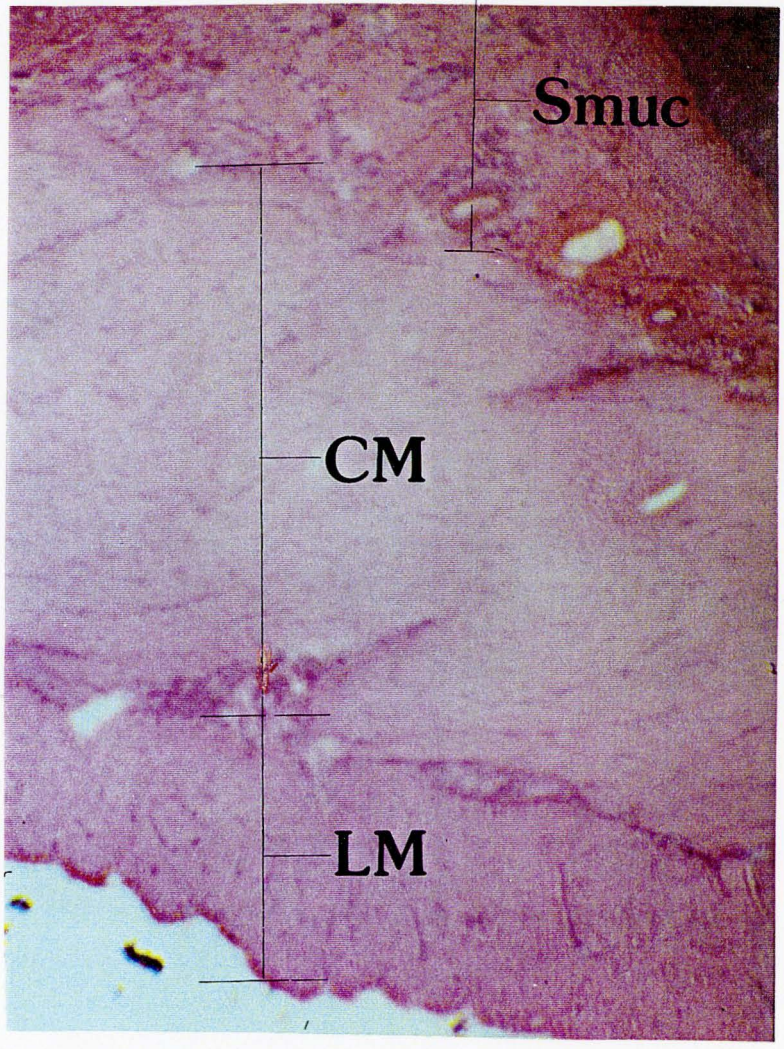
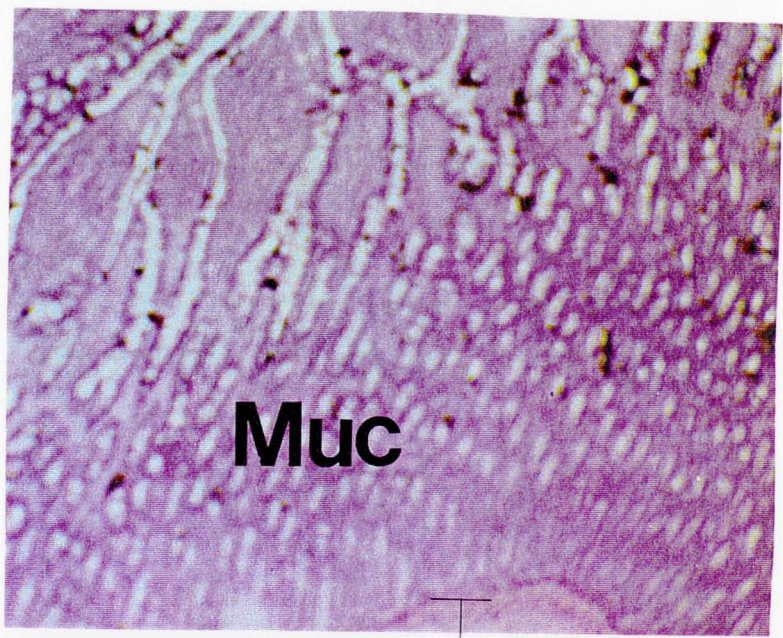
Furness & Costa, 1980

ICC

Legend to Figure 2

The muscularis externa, submucosa, and mucosa of canine ileum.

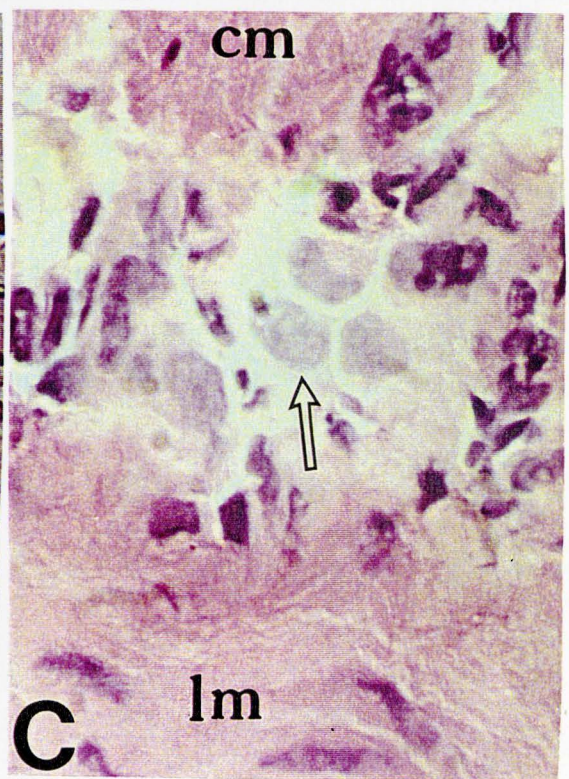
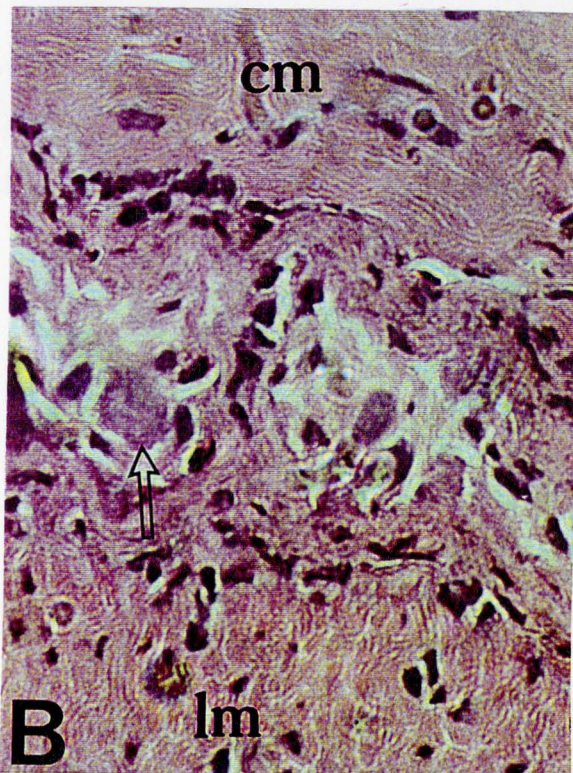
A 5 μm cryostat section through the canine ileum which is stained with hematoxylin and eosin (H&E), shows the mucosa (Muc), the submucosa (Smuc), the circular muscle (CM), and the longitudinal muscle (LM). Magnification X4.



Legend to Figure 3

The muscle layers bordered by the myenteric plexus in canine ileum.

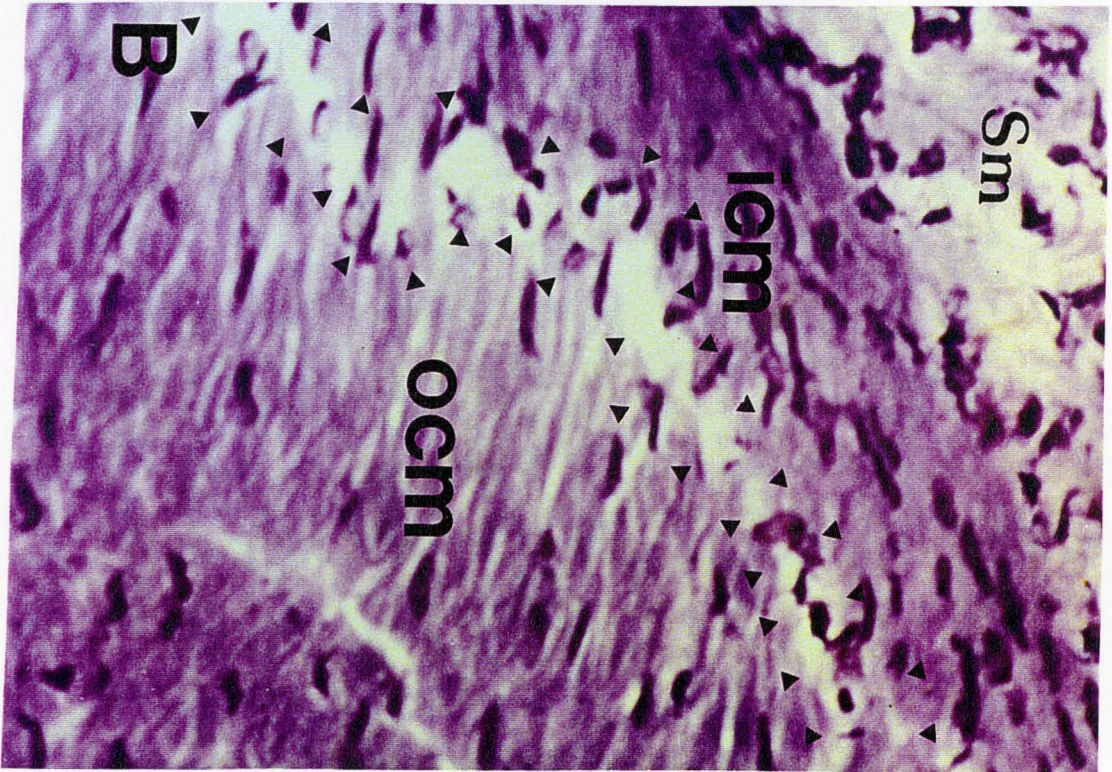
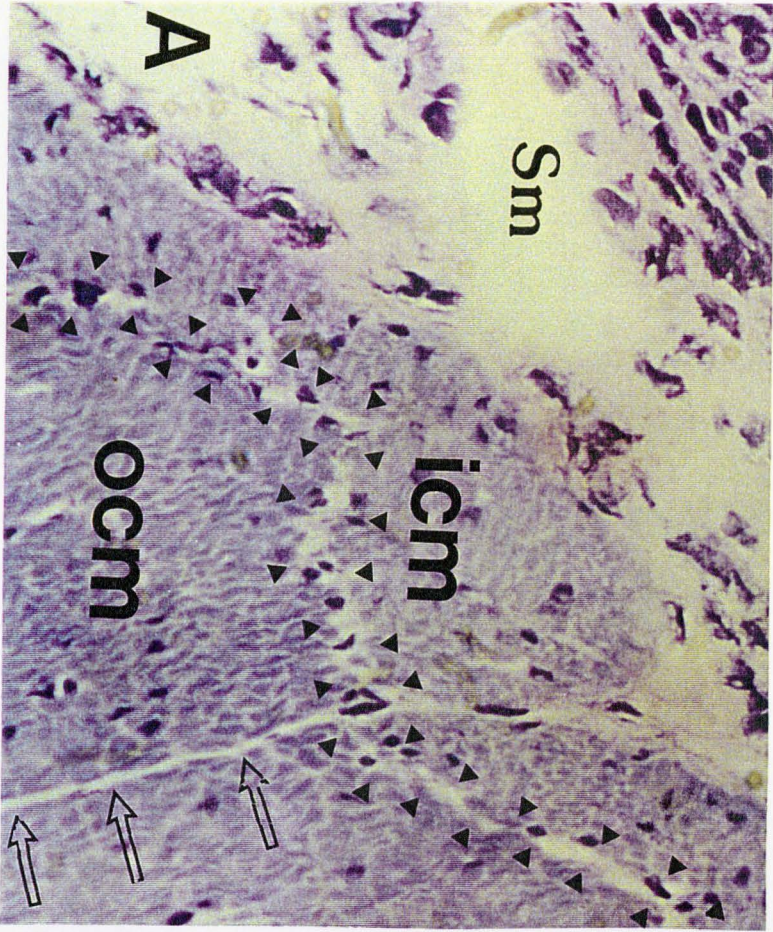
All sections are 5 μm thick and stained with H&E. **A.** Magnification X25. A section cut parallel to circular muscle (CM) cells and perpendicular to longitudinal muscle (LM). **B.** Magnification X63. A section cut parallel to circular muscle (CM). **C.** A section cut parallel to longitudinal muscle (LM). Hollow arrows in **A-C** indicate nerve ganglia. Solid arrows in **A** indicate regions of no visible ganglia present.



Legend to Figure 4

The muscle layers bordered by the deep muscular plexus in canine ileum.

A toluidine blue (A) and a combination of toluidine blue and eosin (B) stained sections showing the submucosa connective tissue (Sm), the inner circular muscle (icm), the outer circular muscle (ocm) and the deep muscular plexus region (bordered by small arrowheads). A was cut perpendicular to circular muscle cells (see cross-sections of cell nuclei) while B was cut parallel to the circular muscle (see outline of cell cytoplasm). Note connective tissue septa in A (hollow arrows). Magnification 63X.



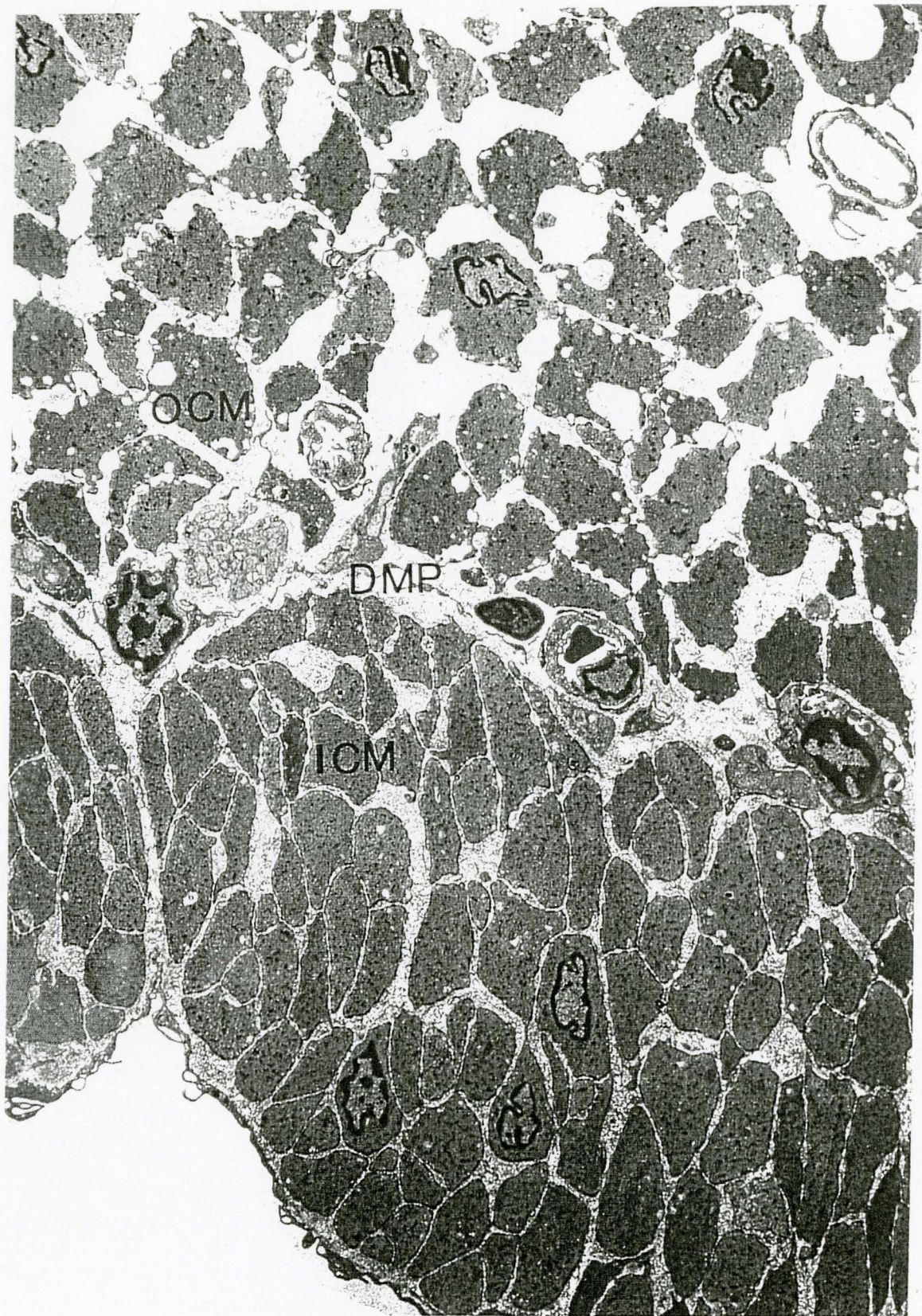
Legend to Figure 5

Transmission electron micrograph of the canine ileum circular muscle.

This micrograph shows that the dissection procedures to remove the mucosa and submucosa connective tissue do not damage the deep muscular plexus (DMP). That is, nerve endings and interstitial cells of Cajal are intact (not shown at this magnification).

ICM: inner (dense) circular muscle layer; OCM: outer circular muscle layer.

Magnification 4,500X. From Christinck, 1990 [23].



nerve varicosities were found to be closely associated with the ICC representing the other set of pacemaker cells in this region [9,10,12,13,14,57,115]. Bundles of circular muscle are often separated by connective tissue septae which may function to provide electrical isolation of individual circular muscle bundles or lamellae (Figure 4A). These connective tissue septae often appear to run continuously along the circular muscle bundle and to connect the deep muscular plexus and the myenteric plexus, but arrays of connected ICC were not found to provide coupling of the two sets of pacemakers [Daniel, E.E., personal communication; 91,92,95]. Cells in the inner (submucosal) circular muscle layer appear smaller and more densely packed than cells in the outer circular muscle layer [36; see also Figure 5]. Gap junctions are rare in the inner layer but are abundant in the outer circular muscle layer. The deep muscular plexus houses nerve varicosities but few or no ganglion cells [54], and nerves and the ICC network have been suggested to act as mechanoreceptors [36].

Above the inner circular muscle and lying within the connective tissue of the submucosa lies the submucous plexus, consisting of ganglia and nerve fibers (Figure 1). The muscularis mucosae, a thin layer of smooth muscle, lies between the submucosa connective tissue and the villi (extremely numerous finger-like projections). The mucosal side of the muscularis mucosae contain plexus of axons and small nerve bundles, known as the mucosal plexus, which forms connection with the submucous plexus.

1.3 The Interstitial Cells of Cajal as Putative Pacemakers.

Slow waves have been known to regulate gastrointestinal smooth muscle cell excitability and contractility. In several intestinal muscles, slow waves *in vitro* can exert control by directly initiating contractions with or without accompanying action potentials [51,96,97,111]. Recent evidence suggests that the slow waves of the small intestine might not be myogenic in origin per se, but might be derived from a network of interstitial cells of Cajal (ICCs) [51,113], located in the myenteric plexus (MyP) and in the deep muscular plexus (DMP) in several species including mouse [94,113], dog [36] and human [92,95]. Thuneberg (1982) [113] first marshalled the hypothesis that both networks of ICC can function as a network of pacemakers in mouse small intestine. Subsequent electrophysiological studies in various regions of the canine gut, including gastric antrum [7], proximal duodenum [8], jejunum [51], and colon [101], reported that the presence of ICCs at each of the plexuses can determine the homogeneity or heterogeneity in slow wave configurations. The shape of the slow waves was reported to be homogeneous when recorded at the myenteric and submucosal sides of the proximal duodenum [8] while differences in slow wave configurations between the two regions was described in gastric antrum [7]. Hara *et al.* (1986) [51] observed that in the canine jejunum slow potentials with superimposed spike bursts were the predominant pattern of electrical activity recorded in the inner circular muscle while square slow waves were recorded near the MyP. These workers evaluated slow wave production from various regions and dissected parts of the muscularis externa and concluded that the main pacemaker network was

located in or near the MyP while the DMP had a limited or subsidiary role in pacemaking. However, in the present study using canine ileum in the whole-thickness and isolated circular muscle preparations, we have established that each pacemaking network was capable of having an independent role in pacemaking activity.

1.4 The Role of Interstitial Cells of Cajal in NANC Neurotransmission.

ICCs have also been postulated to play a crucial role in the neurotransmission of non-adrenergic, non-cholinergic (NANC) inhibitory activity [28]. The ICCs from the MyP are usually near nerve profiles and make close contact with one another and with longitudinal and circular smooth muscle [91,93,113], while the ICCs from the DMP make gap junction contact with one another and with circular muscle cells [32,36,91,92,115] and are in close (<100 nm) contact with nerve axons and varicosities. Thus if ICC networks provide for pacemaking activity, the slow waves they generate are likely to be modulated by neural inputs. In fact, ICCs observed in the circular muscle of oesophagus, small intestine and colon have been found close to nerve endings often containing large granular vesicles [9,12,13,14]. The neuropeptide in these nerves has often been identified as vasoactive intestinal polypeptide (VIP). However, VIP had no discernible effect on electrical and mechanical activities of canine intestinal circular muscle [22] and no VIP receptors could be found on circular muscle membranes [77].

1.5 Possible Role of NO and NANC Neuromediators in Pacemaking.

Nitric oxide (NO), another putative NANC mediator, has been shown to be present in nerves with NO synthase (NOS) in the MyP of the guinea pig intestine and canine colon [15,47,82,118] and in the synaptosomes of the DMP of the canine ileum [70]. Recently, NOS and VIP have been shown to be found in the same nerve varicosities from both plexuses in the canine ileum and colon [14]. Moreover, inhibitory responses mediated by NO have been reported in several areas of the gastrointestinal tract such as the opossum lower oesophageal sphincter and body circular muscle [22,61,116], the canine pylorus [3], proximal duodenum, jejunum and ileum [8,22,105,106] and colon [26,67,117]. Controversy exists regarding the origin of NO in the gastrointestinal tract. The fact that inhibitory junction potentials (IJPs) were abolished by tetrodotoxin [105] suggested that NO was released from nerves to the smooth muscle either directly or by an intermediate cell. However the mechanism of storage and release of NO is not yet well understood [14,28,107] and how NO-mediated effects might influence spontaneous slow waves or triggered slow waves (TSWs) remains to be elucidated. Indeed, IJPs were shown to be able to drive slow waves in rabbit intestine [12,20]

1.6 Tissue Preparation and Electrophysiological Studies.

We aimed to develop two isolated canine ileum muscle slab preparations for study with intracellular microelectrodes of the functions and nature of electrical coupling of the two sets of pacemakers and the nerves that modulate their pacemaking function. Tissue

strips, which were used for studies which focussed only on the deep muscular plexus pacemaking activity, comprised of the outer and inner circular muscle layer. Both preparations are 1-2 mm thick and cut in the long axis of the circular muscle which preserves the circumferential nerve circuitry; one is the whole muscularis externa or full-thickness preparation, the other is the isolated circular muscle with the longitudinal muscle and myenteric plexus removed. Both preparations produce slow waves and inhibitory junction potentials (IJPs). The isolated circular muscle is devoid of myenteric plexus (MyP) and contains only the deep muscular plexus (DMP) which has only nerve endings and one set of putative pacemakers of slow waves (interstitial cells of Cajal or ICC). The other set of pacemakers is found in the MyP. Transmission electron microscopy of the ileal circular muscle preparations used in this thesis confirmed that the outer circular muscle layer, deep muscular plexus, and inner circular muscle layer, as well as the myenteric plexus and longitudinal muscle, were all preserved by the methods of fine dissection (see Figure 5, and also reference [23]).

Tissue strips (1 mm x 10 mm) were cut parallel with the circular muscle fibres and placed in a 5 ml organ chamber for electrophysiological recordings. The strips were pinned to the floor of the chamber in regions selected to record the intracellular electrical activity. About 1 cm of unpinned region was connected to a force transducer for recording of mechanical activity. This unpinned region was stretched by 2 g once, and the whole preparation was allowed to equilibrate for two to three hours before impalements were attempted. The tissue was superfused constantly by Krebs solution at

a rate of 3 ml/min (37°C). Glass electrodes filled with 3 M KCl with resistances ranging from 30 to 80 M Ω were used to impale the cells. Membrane potential changes were measured using a standard electrometer (World Precision Instruments KS-700). The signal was monitored on a dual beam oscilloscope (Tektronix D13; 5A22N differential amplifier; 5B12N dual time base) and recorded on 1/4 inch magnetic tape with a Hewlett-Packard instrumentation recorder and on chart paper (Gould 2200). A microscope (M3C, Wild Leitz) with calibrated eyepiece graticule was used to select accurately the position of the recording electrode. The electrical activity was studied in the following areas of the circular muscle: 1) near the MyP (0-10% of the total width close to the longitudinal muscle, 2) outer circular muscle (OCM) (10-40% from the MyP-longitudinal muscle border, 3) near the DMP (60-90% from the MyP, and 4) close to the submucosal plexus border (SMP) (90-100% from the MyP). The isolated circular muscle was studied near the DMP and in the OCM.

1.7 Rationale for Using the Dog Model

The canine ileum has already been studied in our laboratory using techniques of biochemistry [77], immunocytochemistry [74], electron microscopy [9,10,11,12,13,14,15], and electrophysiology [22,23,24], so that the wealth of knowledge that has already been gained would facilitate the investigation of neuromodulation, ionic mechanisms, and intercellular communication of pacemaking origins. Some features of this study could only be executed in an animal of sufficient size. We need to be able to separate the

various intestinal layers and their plexuses and study them separately. The morphology of the canine ileum is similar to that of the human.

1.8 Statement of the Problem

As the structural or cellular organization in the circular muscle of the canine ileum has been well established, the main objective of the present study was to investigate the hypothesis that the pattern of electrical activity (slow waves and IJPs) was heterogeneous throughout the circular muscle layer and related to two independent sets of pacemakers. To test this hypothesis, recordings from a cross-sectioned preparation of the entire muscularis externa were compared to those from an isolated circular muscle preparation devoid of longitudinal muscle and MyP. Microelectrodes were used to obtain intracellular recordings at precise distances from the MyP. Once the heterogeneity in slow wave activity and the distribution of IJPs within the circular muscle bundle was established, we next investigated the origin of TSW activity (triggered by the ending of an IJP, or by various stimulation parameters that did not induce an IJP) by using pharmacological neural toxins and by changing the availability of endogenous NO using NOS inhibitors to block the NANC IJP. We also extended the study to provide preliminary information on the ionic mechanisms underlying the different configurations of slow waves recorded near the MyP and the DMP. We then attempted to elucidate the electrical coupling mechanisms of the two types of slow waves by correlating morphological evidence to functional studies of gap junctions (major intercellular low resistive pathways).

Earlier the canine ileum circular muscle was studied electrophysiologically using extracellular recording techniques (single and double sucrose gap apparatus), but in this study electrical slow waves were not recorded [23]. A new tissue preparation, suitable for intracellular microelectrode studies, was developed to facilitate studies of pacemaking activity and neural modulation of pacemaking activity in canine ileum.

The following specific questions were asked:

1. What are the nature and origin of pacemaking activity in canine ileum;
2. What are the roles of enteric innervation on pacemaking function of interstitial cells of Cajal;
3. What are the electrophysiological characteristics of circular muscle cells across the circular muscle layer, including the response to electrical field stimulation;
4. What are the ionic mechanisms of ileum slow waves;
5. How are the two sets of pacemakers electrically coupled; and finally
6. Could nitric oxide, vasoactive intestinal polypeptide, and pituitary adenylate cyclase activating peptide beco-transmitters of intestinal inhibition.

CHAPTER 2

OBJECTIVES AND HYPOTHESIS

1. *Objective:* To obtain evidence for a dual pacemaking mechanism for the generation of distinct slow waves in the canine ileum.

Hypothesis: The interstitial cells of Cajal (ICC), putative pacemaking cells of the gut musculature, are concentrated and form networks in the myenteric plexus and deep muscular plexus. In canine ileum, each network of ICC may independently pace slow waves recorded from muscle cells near each pacemaking region.

Results: Recordings of intracellular electrical activity allowed the detailed study of the origins and characteristics of pacemaker system in the circular muscle of the canine ileum. Differences in resting membrane potentials, inhibitory junction potentials, and properties of the slow waves in the various levels of the circular muscle layer were shown. We propose that the first, and more dominant, source of pacemaking is situated in the region of the myenteric plexus and generates slow waves which are characterized by a rapid upstroke and plateau; the second, which can be entrained by the first, is located in the region of the deep muscular plexus and generates slow waves which are more triangular in shape.

2. *Objective:* To determine the roles of nitric oxide (NO) release from nerves and from non-neural sources in the regulation of slow wave activity and response to electrical field stimulation (EFS) in canine ileum.

Hypothesis: The interstitial cells of Cajal (ICC), pacemaker cells, located in the regions of the myenteric plexus (MyP) and deep muscular plexus (DMP) are closely innervated and may facilitate communication between the enteric nerves and smooth muscle cells to which they are electrically coupled. Inhibitory NO-releasing neural inputs mediate the EFS-induced inhibitory junction potentials (IJPs) and modulate pacemaking function of ICC of the MyP and DMP.

Results: Using a variety of neural blockers and NO synthase inhibitors, we examined the spontaneous and triggered slow wave (TSW) activity, IJPs, and mechanical activity. We suggest that slow waves originated independently of neural activity but that NO released from nerves can cause IJPs and affect pacemaker activity originating at the MyP region and that NO from non-neural sources can enhance neural NO effects at the DMP region.

3. *Objective:* To investigate the roles of Ca^{2+} in slow wave generation, nerve activation, and contraction in canine ileum.

Hypothesis: Neurotransmitter release and the generation of electrical slow waves and their coupling to contractions require different voltage-operated Ca^{2+} channel conductances. The intracellular Ca^{2+} stores modulate pacemaking function of ICC.

Results: Ca^{2+} influx through neither L- nor N- Ca^{2+} channels are involved in slow wave generation; L- Ca^{2+} channels are involved in coupling excitations by slow waves to contractions. Nerve-mediated inhibitory junction potentials require Ca^{2+} influx into nerves through N- Ca^{2+} channels. Intracellular Ca^{2+} stores modulate pacemaking activity, which is dominated by the myenteric plexus pacemakers under normal and reduced extracellular Ca^{2+} levels.

4. *Objective:* To study the contribution of gap junctions in slow wave generation and excitation-contraction coupling.

Hypothesis: Marked differences in gap junction density across the circular muscle of the canine ileum provide a physiological basis for the observed heterogeneity in electrical activity. Numerous visible gap junctions near the deep muscular plexus (DMP) and the paucity of gap junctions near the myenteric plexus (MyP) give rise to different sensitivity of slow waves to blockade of gap junction function.

Results: Slow waves generated from the DMP were less effectively blocked by octanol, a gap junction blocker. In contrast, the greater susceptibility of MyP slow waves to octanol provides a physiological evidence consistent with the paucity of gap junctions found in this region. The inhibitory effects of octanol on inhibitory junction potentials and the disappearance of phasic contractions associated with slow waves may reflect blockade of Ca^{2+} influx into nerves and muscle by octanol.

CHAPTER 3

CHAPTER 3.1

PAPER No. 1

HETEROGENEITY IN ELECTRICAL ACTIVITY OF THE CANINE ILEAL CIRCULAR MUSCLE: INTERACTION OF TWO PACEMAKERS

Submitted March, 1995 to the *American Journal of Physiology (Gastrointestinal and Liver Physiology)* in revision

Francisco Cayabyab's contribution:

- (i) performance of 75% of all electrophysiological experiments
- (ii) data presentation and statistical analysis
- (iii) writing, revising, and preparing manuscript for submission to American Journal of Physiology

HETEROGENEITY IN ELECTRICAL ACTIVITY OF THE CANINE ILEAL CIRCULAR MUSCLE: INTERACTION OF TWO PACEMAKERS

Marcel Jiménez³, Francisco S. Cayabyab^{1,2}, Patri Vergara³, and Edwin E. Daniel¹.

Departments of Biomedical Sciences¹ and Electrical & Computer Engineering²,

McMaster University, 1200 Main Street West, Hamilton, Ontario L8N 3Z5; and

Department of Cell Biology and Physiology³. Universitat Autònoma de Barcelona,

Bellaterra 08193 Barcelona, Spain.

Running title: Origins of slow waves and IJPs in the canine ileum

Address for correspondence: E.E. Daniel, PhD

Division of Physiology and Pharmacology

Department of Biomedical Sciences

Faculty of Health Sciences

McMaster University

1200 Main Street West

Hamilton, Ontario, Canada L8N 3Z5

Telephone no: 1-905-525-9140ext. 22130. Fax no. 1-905-524-3795

ABBREVIATIONS

DMP - deep muscular plexus

EFS - electrical field stimulation

ICC - interstitial cells of Cajal

IJs - inhibitory junction potentials

MyP - myenteric plexus

OCM - outer circular muscle

SMP - submucosal plexus

TSWs - triggered slow waves

ABSTRACT

The origins of the pacemaker system in the canine ileum were studied by simultaneously recording the intracellular electrical and mechanical activity in cross-sectioned slabs of the muscularis externa or in the isolated circular muscle devoid of longitudinal muscle and myenteric plexus (MyP). Intracellular recordings were obtained from the circular muscle near the MyP, the deep muscular plexus (DMP, inner circular muscle), an intermediate area between the MyP and DMP (OCM, outer circular muscle), or near the submucosal plexus (SMP) in both preparations. One type of slow wave, sigmoidal or triangular in shape, was recorded from impalements near the DMP region in the whole-thickness preparation. Another type observed from the MyP region oscillated at nearly the same frequency (9-10 cycles/min) and was characterized by a fast upstroke and a square shape. A mixture of these two patterns was recorded in the OCM while triangular slow waves were present near the SMP. The amplitudes (15-25 mV) and frequencies of slow waves recorded from the MyP and DMP were slightly but significantly higher than those recorded from either the OCM or the SMP. Occasional slow waves of large amplitudes (30-40 mV) were recorded in the MyP and DMP regions but never in the OCM and SMP regions. A 10-15 mV gradient in resting membrane potential (more hyperpolarized near MyP) existed across the circular muscle layer. In the full-thickness preparation, neither type of slow waves was affected by atropine, guanethidine, propranolol, and phentolamine (all at 10^{-6} M). Under these conditions high frequency (25-30 pps) electrical field stimulation (EFS) produced a fast, monophasic inhibitory junction potential (IJP) followed by a triggered slow wave (TSW) which could be premature or delayed and whose

amplitude was maximum near the MyP region and decayed progressively in the other areas. The TSWs could be evoked by a long duration (50-100 msec), single pulse which did not induce an IJP. Both the slow waves and TSWs were associated with contractions of circular muscle. In the isolated circular muscle preparation (with the DMP intact) triangular slow waves were recorded everywhere. The frequency and amplitude of the slow waves recorded near the DMP were significantly less than those recorded in similar areas in the full thickness preparation. EFS (25-30 pps) evoked IJPs of 18 - 20 mV in amplitude. The IJPs were biphasic, showing a fast and a slow component and were not followed by TSWs. Long duration, single pulses also did not induce TSWs. We conclude that the MyP pacemaker network generated a plateau-type slow wave while the DMP one induced a triangular slow wave. Although each source was capable independently of pacemaking activity, the MyP network may dominate pacemaking activity by keeping the DMP slow waves entrained and phase-locked. Separate neural inputs near each pacemaking regions produced IJPs. TSWs originated from the MyP region and spread to the other areas of the circular muscle. They reset the timing of slow waves in both pacemaker networks.

Key words: spontaneous and triggered slow waves, interstitial cells of Cajal, inhibitory junction potentials, myenteric plexus, deep muscular plexus, ileum motility

INTRODUCTION

Slow waves are known to regulate gastrointestinal smooth muscle cell excitability and contractility. In several intestinal muscles, slow waves *in vitro* can exert control by directly initiating contractions with or without accompanying action potentials (8, 15, 16, 19). Recent evidence suggests that the slow waves of the small intestine might not be myogenic in origin *per se*, but might be derived from or paced by a network of interstitial cells of Cajal (ICC) (8, 21), located in the myenteric plexus (MyP) and in the deep muscular plexus (DMP) in several species including mouse (14, 21), dog (7), and human (12, 13). Thuneberg (21) first proposed the hypothesis that both networks of ICC can function as a network of pacemakers in mouse small intestine. Subsequent electrophysiological studies in various regions of the canine gut, including proximal duodenum (1), jejunum (8), and colon (17) which has an ICC network at the inner border of circular muscle (2), reported that the presence or absence of similar ICC plexuses can affect the homogeneity or heterogeneity in slow wave configurations. The shape of the slow waves was reported to be homogeneous when recorded at the myenteric and submucosal sides of the proximal duodenum (1). Hara *et al.* (8) observed that in the canine jejunum slow potentials with superimposed spike bursts were the predominant pattern of electrical activity recorded in the innermost circular muscle while square slow waves were recorded near the MyP. These workers evaluated slow wave production from various regions accessible by wedge-shaped dissections and from dissected parts of the muscularis externa and concluded that the main pacemaker network was located in or near the MyP while the DMP had a limited or subsidiary role in pacemaking. However, the

present study using canine ileum in the whole-thickness and isolated circular muscle preparations suggests that each pacemaking network is capable of pacemaking activity independent of the other.

An intestinal muscle slice, obtained from two parallel cuts through the whole thickness of the intestinal wall, was used for intracellular electrical recordings at precise distances from the MyP. This is similar to the preparation pioneered by Smith *et al.* (17) in the colon. Thus our aim was to investigate the hypothesis that the pattern of electrical activity was heterogeneous throughout the circular muscle layer and related to two pacemakers capable of independent function. To test this hypothesis, recordings from a cross-sectioned preparation of the entire muscularis externa were compared to those from an isolated circular muscle preparation devoid of longitudinal muscle and MyP. We also examined the production of inhibitory junction potentials (IJPs) in both these preparations as well as the triggering of slow waves in them. We also investigated the origin of triggered slow waves (TSWs), triggered by the ending of an IJP or by various stimulation parameters that did not induce an IJP. We observed a gradient in membrane potentials across the circular muscle bundle, as well as gradients in the amplitudes of IJPs and TSWs. Preliminary accounts of some of this work have been published (4, 10).

MATERIALS AND METHODS

Preparation of ileal circular muscle

Healthy adult mongrel dogs of either sex, ranging from 10 to 25 Kg, were euthanized using intravenous sodium pentobarbitone (65 mg/kg). This procedure was approved by the McMaster University Animal Care Committee. The abdomen was immediately opened along the midline and a segment of ileum (10 cm) was removed from a position about 10 cm oral to the ileocaecal junction. The dissection was made at room temperature in normal oxygenated Krebs solution. The segment of ileum was cleaned of external fat and connective tissue and opened along the mesenteric border. The mucosa and submucosa were removed taking care not to damage the circular muscle. The longitudinal muscle was also removed in the isolated circular strips using the same technique already described (5). Electron micrographs of this preparation confirmed that the longitudinal muscle and the MyP were completely removed and the DMP undamaged.

Tissue strips (1 x 10 mm) were cut parallel with the circular muscle fibres and placed in a 5 ml organ chamber for electrophysiological recordings. The strips were pinned to the floor of the chamber to immobilize regions to be used for recording of intracellular electrical activity. About 1 cm of unpinned region was connected to a force transducer for recording of mechanical activity. This unpinned region was stretched by 2 g once, and the whole preparation was allowed to equilibrate for two to three hours before impalements were attempted. The strips were superfused with normal Krebs at a rate of 3 ml/minute (37 °C). The Krebs solution (in mM: NaCl, 115.5; NaH₂PO₄, 1.6; NaHCO₃, 21.9; KCl, 4.2; CaCl₂, 2.5; MgSO₄, 1.2 and glucose, 11.1) was continuously

aerated with 95% O₂ - 5% CO₂ to maintain pH of approximately 7.4. Atropine, guanethidine, propranolol, phentolamine (all 10⁻⁶ M, all from Sigma, CA, U.S.A.) were introduced to the Krebs reservoir and superfused for at least 25-30 minutes. Glass electrodes filled with 3 M KCl with resistances ranging from 30 to 80 MΩ were used to impale the cells. Membrane potential changes were measured using a standard electrometer (World Precision Instruments KS-700). The signal was monitored on a dual beam oscilloscope (Tektronix D13; 5A22N differential amplifier; 5B12N dual time base) and recorded on 1/4 inch magnetic tape with a Hewlett-Packard instrumentation recorder and on chart paper (Gould 2200). A microscope (M3C, Wild Leitz) with calibrated eyepiece graticule was used to select accurately the position of the recording electrode. The electrical activity was studied in the following areas of the circular muscle (see Figure 1A): 1) near the MyP (0-10% of the total width close to the longitudinal muscle, n = 50), 2) outer circular muscle (OCM) (10-40% from the MyP-longitudinal muscle border, n = 18), 3) near the DMP (60-90% from the MyP, n = 38), and 4) close to the submucosal plexus border (SMP) (90-100% from the MyP, n = 10). The isolated circular muscle was studied near the DMP (n = 20) and in the (OCM) (n = 6). The number of strips from at least three different animals used from each type of experiment is indicated by n, and a total of 64 animals were used in this study.

Electrical field stimulation

Electrical field stimulation was achieved using a pore-type silver electrode in contact with the tissue on one side of the strip, and a silver ground electrode on the other side. Stimuli were provided by a Grass S88 stimulator through a stimulus isolation unit

(Grass SIU5). A range of parameters was used to obtain the supramaximal IJPs in each strip. The pulse rate was 25-30 pps, the train duration 300 msec, supramaximal voltage 120 - 150 V, 0.3-0.4 msec pulses. Single pulse stimulation was achieved by using 50-100 msec square wave (10-20 V).

Recordings and statistical analysis.

The resting membrane potential, frequency, duration and amplitude of slow waves, and the durations and amplitudes of IJPs and TSWs were analysed for each record. TSWs were differentiated from spontaneous slow waves by their occurrence, advanced occasionally or delayed in time relative to the expected occurrence of the next spontaneous slow wave. These parameters were analysed during the control period (20 minutes) and every 5 minutes following the drug infusion (30 minutes). Frequencies of slow waves were determined by averaging the number of slow waves occurring over a period of 3 minutes. Data are presented as mean \pm S.E.M. Ordinary ANOVA (analysis of variance, with Bonferroni correction) or Student *t*-tests, as appropriate, were performed to check for statistical significance. Mean values were considered significantly different when $P < 0.05$. Significances are denoted as follows: * = $P < 0.05$, ** = $P < 0.01$, *** = $P < 0.001$, **** = $P < 0.0001$.

RESULTS

Resting membrane potentials and spontaneous and triggered slow waves in the full-thickness preparation

Figure 1A (left) shows a schematic of the full-thickness preparation which defines the various locations of the recording electrodes during an experiment. Actual recordings of slow wave activity in the regions the myenteric plexus (MyP), outer circular muscle (OCM), deep muscular plexus (DMP), and submucosal plexus (SMP) border from the same tissue strip using the same electrode show that the slow wave patterns are not homogeneous within the circular muscle layer. Figure 1A also demonstrates the apparent gradient in baseline membrane potential, being more hyperpolarized near the MyP region and about 10 mV more depolarized near the DMP region. Figure 1B, an expanded recording near the MyP region from a different animal, shows the method for measuring the different parameters associated with slow wave activity and responses to electrical field stimulation or EFS (a=slowwave amplitude; b=slow wave duration; c=amplitude of slow wave triggered by an IJP. These often occurred prematurely, but could also occur after the IJP delayed relative to the expected timing of the next slow wave. In addition, they frequently reset the timing of subsequent slow waves (Figures 2A and 2C). Therefore, they were designated as triggered slow waves (TSWs); d=TSW duration; e=IJP amplitude; f=IJP duration; and g=TSWdelay).

Figure 2 illustrates the characteristic slow wave patterns, responses to neural stimulations after inhibition of adrenergic and cholinergic effects, and their mechanical counterparts in whole-thickness preparations. Atropine, guanethidine, propranolol and

phentolamine (all at 10^{-6} M) did not significantly affect the membrane potentials or any of the parameters of spontaneous slow waves, TSWs, or IJPs (see Table 1). Note that Figure 2A and 2B are from the same tissue strip while 2C and 2D are from a single strip from a different animal. The polarity of EFS in Figure 2C was reversed, a procedure which did not influence IJPs in any way. Slow waves recorded near the MyP exhibited a fast upstroke followed by a plateau and repolarisation (Figure 2A, 3Ai-iii). However, near the DMP and SMP regions slow waves were triangular and showed a sigmoidal onset (Figure 2C and 2D, Figure 3Bi). Neither the fast upstroke nor the plateau was present in these regions. Intermediate forms were found between the two plexuses (*i.e.*, recordings in OCM region as shown in Figure 2B) and sometimes close to them (Figures 3Aii and 3Bii). Close to the submucosal border the slow waves were less regular compared to the rest of the muscle (Figure 1 A). We never found any spike burst superimposed on the slow waves either in this area or in any other area. The slow wave amplitude was maximal near the MyP region and decayed toward the SMP region (Table 2). The frequencies of slow waves recorded near the MyP and the DMP were not statistically different (Table 2). We did not simultaneously record the slow waves from near these two regions, so we compared frequencies of slow waves recorded at different times and made statistical comparisons as summarized in the tables. The membrane potentials were also more hyperpolarized near the MyP than in other areas (Figure 2A-D), and the peak depolarization during the slow wave was near -40 mV in this region (Figure 2A). Near the DMP the peak depolarization was near -35 mV (Figure 2C). When the mechanical activity was recorded simultaneously with the electrical activity, the slow

waves were temporally associated with phasic contractions. High frequency EFS (30 pps) elicited maximal IJPs mediated by nitric oxide, (Cayabyab, F.S., M. Jiménez, P. Vergara, H. deBruin, and E.E. Daniel, submitted) released from nerves (see Figures 2 A to D, top panels). The ending of the IJP triggered a slow wave and often reset the slow wave pattern (Figures 2A and 2C).

In addition to the TSWs following an IJP (Figure 2 and Figure 3, also Figure 4), these full-thickness preparations responded with TSWs (without a prior IJP) to a long duration, single pulse (Figure 3Aiii and 3Bii, bottom panels). This long duration pulse would be expected to activate (depolarize) a population of cells with a longer time constant (*i.e.*, non-neural) than nerves. These TSWs were unaffected by the presence or absence of tetrodotoxin (data not shown). Figure 3 also shows the different patterns of slow waves and their associated contractions recorded from the MyP and DMP regions and demonstrates that, on occasion, slow waves with unusually large amplitudes (30-40 mV) were recorded from cells with very hyperpolarized baseline membrane potential near the MyP (n=5) and DMP (n=4) regions (Figure 3Ai, 3Bi) but never near the OCM or SMP regions. This suggested that the recording electrode impaled a smooth muscle cell which was located close to the pacemaker network. About 90% of all the recordings from these regions showed slow waves with amplitudes of 15-25 mV like those shown in Figures 3Aiii and 3Bii (see also Figure 2, Table 2).

Inhibitory junction potentials and triggered slow waves in the full-thickness preparation.

IJPs could be recorded after EFS in all the areas of the circular muscle (Figures 2A-D). However, their amplitudes (with supramaximal stimuli) were different depending on the section studied (ANOVA, $p < 0.0001$) (Table 2). Smaller IJPs were recorded close to the myenteric or submucosal sites (10 -15 mV) whereas IJPs of greater amplitude were recorded near the DMP and in the centre of the circular muscle (15 - 20 mV). IJPs had insignificantly shorter durations near the myenteric and submucosal plexuses than in the other areas (Table 2).

A TSW was always recorded after the IJP in the whole-thickness preparation (Figures 2, 3Aiii, and 3Bii). It was everywhere, including near the DMP, characterized by a fast upstroke followed by a plateau before repolarization. Thus the TSWs were distinguishable from the slow waves by their shape and amplitude (Table 2) as well as their time of occurrence. The amplitudes of the TSWs were maximum near the MyP as were the slow wave amplitudes, and were significantly greater than those near the DMP or the SMP (Table 2, Figure 4A). The TSWs decreased progressively in amplitude with distance from the MyP (Table 2, Figure 4A). Note that the data presented in Figure 4 were those obtained from recordings wherein two or more regions of impalements from the same muscle strip were obtained. The delay between the stimulus and the induction of the TSW was shorter near the MyP, where the TSW probably originates, and becomes progressively longer toward the DMP (Figure 4B). There was a negative correlation between the TSW amplitude and induction delay within the circular muscle (Figure 4C).

Isolated circular muscle with the deep muscular plexus intact

Figure 5 shows recordings made in a strip of isolated circular muscle near the DMP and close to the MyP side. The results are summarized in Table 2. The mean resting membrane potential recorded between slow waves was between -55 and -62 mV. Twenty out of 25 preparations exhibited spontaneous oscillations in the membrane potential with no spike potentials associated with them, which were therefore considered to be slow waves (Figure 5). The shape of the slow waves was triangular, both in the inner and in the outer circular muscle. However, the amplitude of the slow waves was higher (Student *t* test, $p < 0.05$) near the DMP than in the OCM (Table 2). The mean frequency, 8 cycles/min, was similar in recordings from the DMP and the OCM. However, the frequency of slow waves recorded in both regions in the isolated circular muscle preparation was slightly but significantly lower than the frequency recorded in similar regions in the whole-thickness preparation (Table 2). A monophasic contraction occurred with each slow wave (Figure 5). Supramaximal field stimulation produced IJPs with a prominent hyperpolarization of 18 to 20 mV (Figure 5). The IJP repolarization showed two components. The repolarization began with a fast slope (fast component) which was followed by a significantly slower slope (slow component). These two components were found in both the DMP and the OCM. The total duration of the IJP in the isolated circular muscle was 5 seconds, which was significantly greater than the duration of IJP recorded in similar areas in the full-thickness preparation (Table 2). Field stimulation never elicited a TSW in these preparations and did not modify the frequency of the slow waves (Figure 5A) although oscillations were usually reset (Figure 5B) or one

slow wave was lost (Figure 5A). In Figure 5B, the IJP did reset the slow waves.

Figure 6 shows two recordings near the DMP from two different isolated circular muscle strips. Figure 6A shows regular spontaneous slow waves accompanied by phasic contractions. Field stimulation using 30 pps (short pulses) produced IJPs but no apparent TSWs (Figure 6A, top). Using a longer duration, single pulse (50-100 msec, 10-20 V) sufficient to electrically drive the pacemaker(s) in the full-thickness preparations (see previously, Figures 3Aiii and 3Bii, bottom panels), no TSW could be elicited (Figure 6A, bottom). In a few cases (n=5) illustrated in Figure 6B (top panel), the absence of slow waves in cells with a slightly depolarized membrane potential, attributed to damage to pacemaker cells or uncoupling of these pacemakers, produced irregular mechanical activity. IJP could be induced by high frequency (30 pps) EFS in such preparations, but the long duration pulse stimulations did not elicit TSWs (Figure 6B, bottom). These results suggest that an inhibitory neural input and a network of pacemaker cells in the DMP region can control the electrical and mechanical activities independently of the neural input and pacemaker cell network from the MyP region. They also suggest that any TSW must originate from the MyP and propagate to other regions in the circular muscle.

DISCUSSION

Heterogeneity in spontaneous slow waves in the circular muscle

These studies provide a body of evidence consistent with the hypothesis that there are two networks of pacemakers capable of independent pacemaking. Both the whole thickness of muscularis externa and the isolated circular muscle produced regular slow waves of different configurations. One set of pacemakers was located near the MyP. Its activity resulted in slow waves with plateaus following a fast upstroke and without a noticeable slow initial depolarization. This set of pacemakers was also the apparent source of triggered slow waves under our conditions, triggered by the ending of an IJP evoked by high frequency stimulation with brief pulses or by a single, long duration electrical pulse which did not produce an IJP.

The other set of pacemakers was located near or in the DMP. The slow waves it initiated were triangular in shape, lacking a plateau and a fast upstroke, and began with a slow, sigmoidal depolarization. The slow waves were identical in configuration near the DMP whether the circular muscle was detached from the longitudinal muscle and MyP or not. In the region between the two sets of pacemakers, the slow waves were intermediate in character, and regions which had triangular slow waves when circular muscle was isolated usually had plateau-type slow waves when they were connected to the MyP. This last observation suggests that the two slow waves interact and can become phase-locked and that the response of circular muscle to pacemaker inputs can be determined by dual inputs.

However, the nature of coupling of the two pacemaker networks remains unclear. In each region from which pacemaker activity originates, a network of ICC (putative pacemakers) exists (6). How the slow waves paced from the DMP region get coupled to and become phase-locked with the slow waves paced from the MyP region is still unresolved. The ICC of the MyP, in contrast to those of the DMP, have been reported not to be connected by visible gap junctions to one another and to the two muscle layers (6). Neither have chains of ICC been shown to couple the two regions of pacemakers. An alternate morphological basis to provide for coupling the two networks of pacemakers can be proposed (7, 9, 22). There are numerous gap junctions between outer circular smooth muscle cells and between the ICC of the DMP and the surrounding outer circular smooth muscle layer. This may allow the formation of a three-dimensional syncytium of smooth muscle capable of coupling the inputs of the two pacemakers. Although ICC have been shown to be present in regions between circular muscle bundles (21), the lack of evidence for a continuous connected array of ICC between the two plexuses adds uncertainty to coupling by such ICC. The much larger slow waves which were occasionally recorded near the ICC networks (Figure 3) may result from the uncommon penetration of circular smooth muscle cells closely coupled to ICC, as originally suggested by Taylor *et al.* (20) from studies in rabbit intestine. Our data does not show a clear gradient in slow wave amplitudes declining away from presumed sites of origin of pacemaking activity. Thus it is possible that circular smooth muscle cells participate actively in propagation of pacemaking activity between the two sites.

Observations made earlier in canine duodenum (1) suggested that the plateau-type

slow wave was found throughout the intact circular muscle layer. Isolated circular muscle from the canine duodenum has not been studied, however, so we cannot be sure whether that finding was the result of a greater dominance (spread) of plateau-type slow waves from the MyP or of a difference in the character of pacemaking in the isolated circular muscle. Hara *et al.* (8) also found different results about the nature of slow waves in the isolated circular muscle of canine jejunum; *i.e.*, irregular and intermittent slow wave activity in 74% of their comparable preparations (see their Tables 1 and 2). However, it is possible that this resulted from their dissection procedures. If there is a fundamental difference between the character of slow waves activated from the region of the DMP in the ileum, or in the ability of those activated in the MyP to dominate the entire circular muscle, this may relate to the inability of the ileum in contrast to the duodenum and upper jejunum to undergo phase-locking in the longitudinal axis of the organ (6). Phase-locking may require a slow wave with a fast upstroke throughout the circular muscle. In addition, it is noteworthy that the frequencies of slow waves from the MyP and the DMP were not different in the whole-thickness preparation. However, in the isolated circular muscle the frequency of slow waves recorded near the DMP was significantly lower compared to the frequency recorded near either the DMP or MyP in the whole-thickness preparation (Table 2). This suggests that the slow waves from the DMP become entrained by the higher frequency slow waves from the MyP.

It is important to compare our findings with those of Hara *et al.* (8) made in the canine jejunum in some detail. Among several similarities there are some important differences. One important difference, already mentioned, was that nearly all our isolated

circular muscle preparations showed regular triangular slow waves with associated contractions occurring at a frequency slightly, but significantly lower than that in whole thickness preparations. Even when slow waves and contractions were irregular in amplitude, they could be increased in amplitude and regularized by blocking NO-synthase (3; see also Cayabyab, F.S., M. Jiménez, P. Vergara, H. deBruin, and E.E. Daniel, submitted).

Another difference was that Hara *et al.* (8) found no gradient of membrane potential within the circular muscle. Only the innermost circular muscle layer (presumably inside the DMP) had a significantly lower membrane potential (see their Tables 1 and 2). In contrast, a gradient of membrane potentials, most negative near the MyP, and least negative near the DMP (see Table 2), was present in our preparation.

Hara *et al.* (8) did not report the consistent occurrence of a slow depolarization preceding slow waves when triangular slow waves were produced in the region near the DMP as we did, nor the absence of such depolarizations when slow waves were of the type with plateaus. Also, they observed spike potentials on slow waves recorded from the submucosal surface of the circular muscle, but we never recorded spikes from any region. However, our technique may not have allowed us to record from the innermost muscle cells. Frequencies of slow waves were less in our recordings in the ileum than in the jejunum (10 vs. 13 cycles/min.) as expected from the known intrinsic frequencies of these regions (6).

However, membrane potentials and slow wave configurations were similar in outer circular muscle of jejunum and ileum. Also IIPs, at least in the isolated circular muscle

strip, were similar to those recorded in the same preparation by Christinck *et al.* (5) and by Stark *et al.* (18). No other authors have reported on triggered slow waves in canine intestine.

Origin of triggered slow waves

The different (triangular) configuration of slow waves in the inner circular muscle of ileum may not be a property imposed by the muscle itself in this region. This is suggested by the fact that triggered slow waves, which cannot be initiated in isolated circular muscle, always have a fast upstroke wherever they occur. These triggered slow waves may appear first at the MyP and spread to the DMP without changing their configuration, though they do decrease in amplitude with distance from the MyP. If TSWs can spread from the MyP to the inner circular muscle, then the failure of slow waves spontaneously paced from the region of the MyP to determine the character of slow waves except nearby their origin, cannot be attributed to the characteristics of the circular muscle. Instead, there must be a dominance of the DMP pacemaking activity over nearby regions of muscle which is turned off or overcome when triggered activity occurs in the MyP network of pacemakers.

The TSWs can occur in response to a preceding IJP or to a single, long stimulating pulse or various stimulus parameters unable to initiate IJPs. In another report (Cayabyab, F.S., M. Jiménez, P. Vergara, H. deBruin, and E.E. Daniel, submitted), it was shown that these TSWs in response to high frequency EFS and to the long duration, single pulse were evoked even after neural function was blocked by tetrodotoxin or omega conotoxin GVIA. These plateau-type TSWs are larger near the MyP and occur with

increasing delay and decreasing amplitude at sites deeper in the circular muscle. As noted above, they cannot be initiated by similar stimuli in isolated circular muscle even though regular slow waves and large IJPs occur. These facts suggest that in the whole-thickness preparations under our conditions the TSWs originate only from the MyP. If so the pacemaker network in the MyP but not that in the DMP appears to be driven easily by electrical pulses. Circular smooth muscle cells, when isolated from the MyP, also appeared to be unable to respond to the same electrical stimuli which triggered slow waves near the MyP by initiating slow waves. This does not imply that they are electrically inexcitable; only that a single 50-100 msec pulse or electrical field stimulation to trigger an IJP cannot excite them. If the network of pacemakers in the DMP and the connecting smooth muscle cannot be driven by depolarizing square waves or hyperpolarizing IJPs, the basis for phase-locking between the two sets of pacemakers is not clear. Indeed, it is unclear from experimental data currently available that they are always phase-locked when the intestine is intact. If they are phase-locked in the intact but not in dissected ileum, there must be a connection present in the intact circular muscle and lost on dissection. As noted earlier, Thuneberg (21) presented structural evidence suggesting the existence of ICC within the circular muscle bundles, but so far no structural or functional evidence is available to show that a chain of ICC processes connected by gap junctions joins the two pacemaking areas. Moreover, a recent study reported that no junctions could be found between the ICC networks of the human intestine (11). However, canine ileum slow wave activity triggered from the MyP pacemaker network spread to the DMP region and reset the pacemaker potentials in that

region. That this spread involved coupling between smooth muscle cells seems possible, but is not established. Thus coupling by way of outer circular muscle may be the best explanation of any phase-locking between the two sets of pacemakers.

There was a gradient of circular muscle cell membrane potential (see Table 2) from the MyP to the submucosa (from -67 to -70 mV to -55 to -58 mV). This gradient might make it easier to propagate slow waves from the MyP to the DMP than in the reverse direction. If a depolarizing pulse derived from a network of pacemakers must depolarize coupled cells to reach a threshold for excitation, then the spread of activity will be facilitated by coupling to less polarized cells and inhibited by coupling to more polarized cells. However, isolated circular muscle strips (Table 2) had no significant gradient of membrane potential but slow waves could be triggered by the biological pacemaker but not by an electrical one with the stimuli applied. We must conclude that the MyP pacemaker can easily be electrically stimulated, but the DMP one and the circular muscle itself cannot. One possible explanation is that ICC near the DMP are very tightly coupled by many visible gap junctions and behave as a syncytium requiring a much larger stimulus to depolarize to threshold. The basis for this difference in electrical excitability of the two sets of pacemakers requires further investigation.

Distribution of IJPs in the circular muscle

We observed some heterogeneity in the IJPs across the circular muscle in the whole-thickness preparation of the canine ileum. Those recorded near the MyP were smaller in amplitude and shorter in duration as compared to those from the DMP regions. Our previous studies with the isolated circular muscle preparation suggested that the IJP

reversed near the K^+ equilibrium potential and was partially blocked by apamin (5). Hence, the difference in amplitude likely reflects the difference in the driving potential from K^+ -channel opening since the membranes of muscle cells were more depolarized near the DMP. All IJPs in all regions reached a maximum hyperpolarization near -80 to -90 mV (see Table 2). However, the difference in duration may relate to the differences in ultrastructural organizations of ICC and nerves. Both ICC types from the MyP and DMP regions were closely associated with nerve fibres (<20nm), but only the DMP ICC network formed many visible gap junctions with one another and with outer circular smooth muscle (7, 11, 22; reviewed in 6). Thus the prolonged duration of IJPs and even their higher amplitudes in the DMP region would be consistent with greater ICC-smooth muscle coupling if ICC play a special role in IJP generation.

In the isolated circular muscle, the IJPs did not trigger slow waves. Moreover the IJPs had a second slower phase of repolarization in addition to the initial fast repolarization. These IJPs abolished or delayed slow waves which should have occurred during their period of hyperpolarization. This suggests that the pacemaking network of the DMP or the spread of activity from it was sensitive to hyperpolarization *per se* or to the mediator of the IJP. Both phases of the IJP in this region were abolished by inhibition of NO synthase and therefore depended on NO production (3; see also the next report by Cayabyab, F.S., M. Jiménez, P. Vergara, H. deBruin, and E.E. Daniel, submitted). It is possible that these two phases of the IJP resulted from activation of different cell types; *e.g.*, from NO action on ICC and on smooth muscle.

The results of this study bear on the nature of pacemaking in canine ileum muscle

and their relationship to contraction. This study presented a body of evidence in support of the hypothesis that there are two sources of pacemaking activity in the canine ileum, each source producing slow waves of different configuration but of similar frequency as recorded in the whole-thickness preparations and each source capable of independently coupling the slow wave excitation to contraction. The two distinct types of slow waves have been described in relation to the presence of two pacemaker networks found near the MyP and DMP regions. In the isolated preparation, the intrinsic frequency of slow waves generated from the DMP pacemaker network was less than when this network was connected to the MyP pacemaker network. Thus the higher frequency, plateau-type slow waves paced from the MyP region may be able to entrain and are responsible for phase-locking the lower frequency, triangular slow waves transmitted from the DMP region. A plateau-type TSW activity appeared to originate from the MyP region. The absence of this TSW in isolated circular muscle implies that the pacemaking activity of the DMP ICC network is more difficult to trigger electrically. The nature of coupling between the two regions remains to be elucidated. Slow waves and TSWs occurred without spikes but were associated with contractions. Finally, the ionic mechanisms that determine a triangular or sigmoidal mechanism for slow waves near the DMP in contrast to the more common plateau-type slow waves near the MyP were not established in this study.

ACKNOWLEDGEMENT

M.J. was supported by Personal Investigator Visiting Grant from the Comissió Interdepartamental de Recerca i Innovació Tecnològica (CIRIT, Ref. EE92/2-369), Catalonia, Spain. P.V. was supported by Personal Investigator Visiting Grant from the Dirección General de Investigación Científica y Técnica, Spain. This research was supported by MRC of Canada.

REFERENCES

1. Bayguinov, O., F. Vogalis, B. Morris, and K.M. Sanders. Patterns of electrical activity and neural responses in canine proximal duodenum. *Am. J. Physiol.* 263: G887-G894, 1992.
2. Berezin, I., J. D. Huizinga, and E. E. Daniel. Interstitial cells of Cajal in canine colon: A special communication network at the inner border of the circular muscle. *J. Comp. Neurol.* 273: 42-51, 1988.
3. Cayabyab, F.S., H. deBruin, and E. E. Daniel. NO and NANC inhibitory mediation in the canine ileum (Abstract). *Can. J. Physiol. Pharmacol.* 72: 234, 1994.
4. Cayabyab, F.S., M. Jiménez, P. Vergara, and E.E. Daniel. Two independent pacemakers drive the electrical and mechanical activities of the canine ileum (Abstract). *Neurogastroenterology and Motility.* 6: 152, 1994.
5. Christinck, F., J. Jury, F. Cayabyab, and E.E. Daniel. Nitric oxide may be the final mediator of nonadrenergic, noncholinergic inhibitory junction potentials in the gut. *Can. J. Physiol. Pharmacol.* 69: 1448-1458, 1991.
6. Daniel, E.E., and I. Berezin. Interstitial cells of Cajal: are they major players in control of gastrointestinal motility? *J. Gastrointestinal Motility.* 4: 1-24, 1992.
7. Duchon, G., R. Henderson, and E.E. Daniel. Circular muscle layers in the small intestine. In: *Proceedings of the international Symposium of Gastrointestinal Motility.* edited by E.E. Daniel. Vancouver: Mitchell Press 1974, p. 635-646.
8. Hara, Y., M. Kubota, and J.H. Szurszewski. Electrophysiology of smooth muscle of the small intestine of some mammals. *J. Physiol.* 372: 501-520, 1986.
9. Henderson, R.M., G. Duchon, and E.E. Daniel. Cell contacts in duodenal smooth muscle layers. *Am. J. Physiol.* 221: 793-799, 1971.
10. JIMÉNEZ, M., P. Vergara, and E.E. Daniel. Origin of the "off"-response after field stimulation in the canine ileum (Abstract). *J. Gastrointestinal Motility.* 5: 197, 1993.
11. Rumessen, J.J., H.B. Mikkelsen, K. Qvortrup, and L. Thuneberg. Ultrastructure of interstitial cells of Cajal in circular muscle of human intestine. *Gastroenterology.* 104: 343-350, 1993.
12. Rumessen, J.J., H.B. Mikkelsen, and L. Thuneberg. Ultrastructure of interstitial cells of Cajal associated with deep muscular plexus of the human small intestine.

Gastroenterology. 102: 56-68, 1992.

13. **Rumessen, J.J., and L. Thuneberg.** Interstitial cells of Cajal in human small intestine. Ultrastructural identification and organization between the main smooth muscle layers. *Gastroenterology*. 100: 1417-1431, 1991.
14. **Rumessen, J.J., L. Thuneberg, and H.B. Mikkelsen.** Plexus muscularis profundus and associated interstitial cells. II. Ultrastructural studies of mouse small intestine. *Anat. Rec.* 203: 129-146, 1982.
15. **Sanders, K.M.** Excitation-contraction coupling without Ca^{2+} action potentials in small intestine. *Am. J. Physiol.* 224: C356-C361, 1983.
16. **Sanders, K.M.** Ionic mechanisms of electrical rhythmicity in gastrointestinal smooth muscles. *Annu. Rev. Physiol.* 54: 439-453, 1992.
17. **Smith, T.K., J.B. Reed, and K.M. Sanders.** Interaction of two electrical pacemakers in muscularis of canine colon. *Am. J. Physiol.* 252: C290-C299, 1987.
18. **Stark, M.E., A.J. Bauer, and J.H. Szurszewski.** Effect of nitric oxide on circular muscle of the canine small intestine. *J. Physiol.* 444: 743-761, 1991.
19. **Szurszewski, J.H.** Electrical basis for gastrointestinal motility. In: *Physiology of the Gastrointestinal Tract* (2nd ed.) edited by L.R. Johnson. New York: Raven Press. 1987. p. 383-423.
20. **Taylor, G.S., E.E. Daniel, and T. Tomita.** Origin and mechanism of intestinal slow waves. In: *Proceedings of the Fifth International Symposium on Gastrointestinal Motility*. edited by G. Van-Trappen. Belgium: Typoff Press. 1975. p.102-106.
21. **Thuneberg, L.** Interstitial cells of Cajal: intestinal pacemakers? *Adv. Anatomy, Embryology and Cell Biol.* 71: 1-130, 1982.
22. **Torihashi, S., S. Kobayashi, W.T. Gerthoffer, and K.M. Sanders.** Interstitial cells in deep muscular plexus of canine small intestine may be specialized smooth muscle cells. *Am. J. Physiol.* 265: G638-G645, 1993.

FIGURE LEGENDS

Figure 1. *A.* A schematic of the intact cross-sectioned slab preparation showing the various regions and sites of recording electrode within the circular muscle layer (left). Actual recordings from a single muscle strip of spontaneous slow waves near the myenteric plexus (MyP), the outer circular muscle (OCM), the deep muscular plexus (DMP), and the submucosal plexus (SMP) are shown (right). Note the gradient in resting membrane potentials. *B.* A recording with expanded time scale showing the method for determining the various parameters associated with the spontaneous slow waves and responses to electrical field stimulation.

Figure 2. Characteristic patterns of electrical activity (spontaneous slow waves, monophasic inhibitory junction potentials (IJPs), and triggered slow waves (TSWs)) and their mechanical counterparts recorded in the various regions in the circular muscle layer of the full-thickness preparation. The recordings are shown 30 minutes after superfusion with adrenergic and cholinergic blockers which themselves did not affect the electrical properties of the muscle preparation (Table 1). Square shaped slow waves with plateaus having rounded or triangular profile were recorded near the MyP and OCM regions while triangular or sigmoidal slow waves were recorded near the DMP and SMP regions. Monophasic IJPs and TSWs with a fast upstroke could be evoked everywhere in the circular muscle bundle (Table 2). A gradient in membrane potential (Table 2) and the lack of spike action potentials in any region were recorded.

Figure 3. Recordings of intracellular electrical and mechanical activity from whole-thickness preparations. Figures 3Ai-iii were from three different preparations and 3Bi-ii from two different preparations. Large amplitude slow waves were seldom recorded in both pacemaker regions (Figures 3Ai-ii, 40-45 mV; Figure 3Bi, 30 mV) from cells with a more hyperpolarized baseline membrane potential. The majority of recordings showed slow waves with amplitudes ranging from 15-25 mV from either the MyP or DMP region (Figures 3Aiii and 3Bii), where TSWs were evoked by the ending of IJPs or by long duration, single pulse.

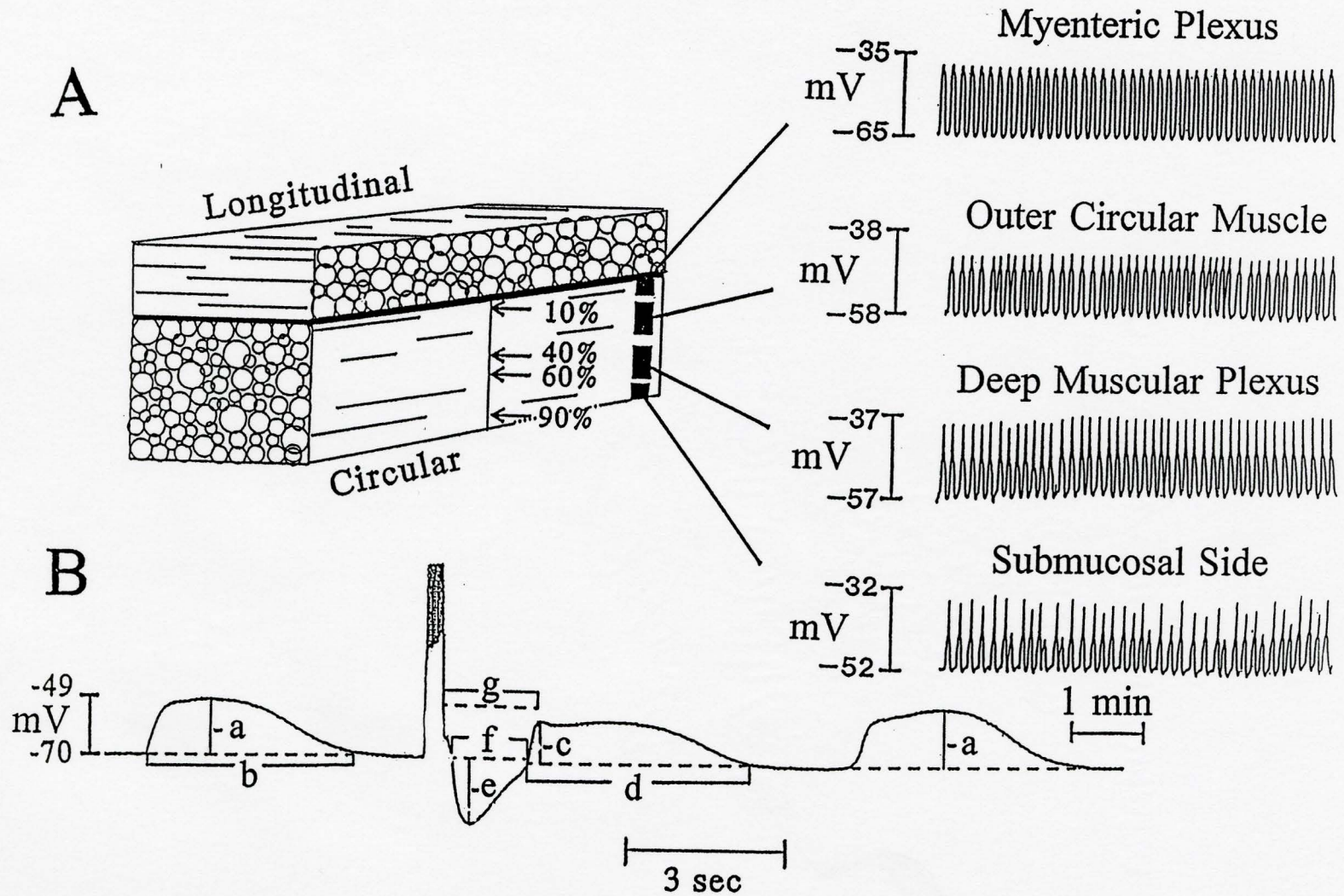
Figure 4. The gradation of amplitudes and induction delays of TSWs (triggered by the ending of IJPs evoked by high frequency EFS) with distance from the MyP-longitudinal muscle border. *A.* The amplitudes of the TSW were maximum near the MyP and were significantly greater than those recorded from the DMP and SMP regions. Note that the data from Table 2 was truncated and the data presented above include only those recordings where at least two regions of impalements were obtained (MyP, n =35; OCM, n =16; DMP, n =35; SMP, n=10). *B.* In contrast, the durations of the delay in the occurrence of TSWs were progressively prolonged with distance from the MyP. *C.* An inverse correlation between the amplitudes of TSWs and induction delays was obtained.

Figure 5. Spontaneous slow waves and biphasic IJPs recorded in the isolated circular muscle were less regular in amplitude at recording sites near the MyP side (*A*, outer area) while those recorded near the DMP (*B*, inner area) were more regular. Only triangular

slow waves which lacked plateaus and spike action potentials were recorded. Note that the frequencies of slow waves in A and B were significantly lower compared to the frequency recorded in similar areas in the full-thickness preparation (Table 2).

Figure 6. Recordings near the DMP from different isolated circular muscle preparations. *A.* Spontaneous slow waves, phasic contractions, and biphasic IJPs evoked by high frequency (30 pps) EFS were apparent (top). Long duration, single pulses (50-100 msec, 10-20 V) did not evoke TSWs (bottom). *B.* Lack of spontaneous slow waves resulted in irregular circular muscle contractions (top). Note the depolarized membrane potentials and the different time scale. This preparation responded with biphasic IJPs when high frequency EFS was used and with no TSW when long pulse stimulation was used (bottom).

Fig. 1. Heterogeneity in electrical slow waves in canine ileum circular muscle



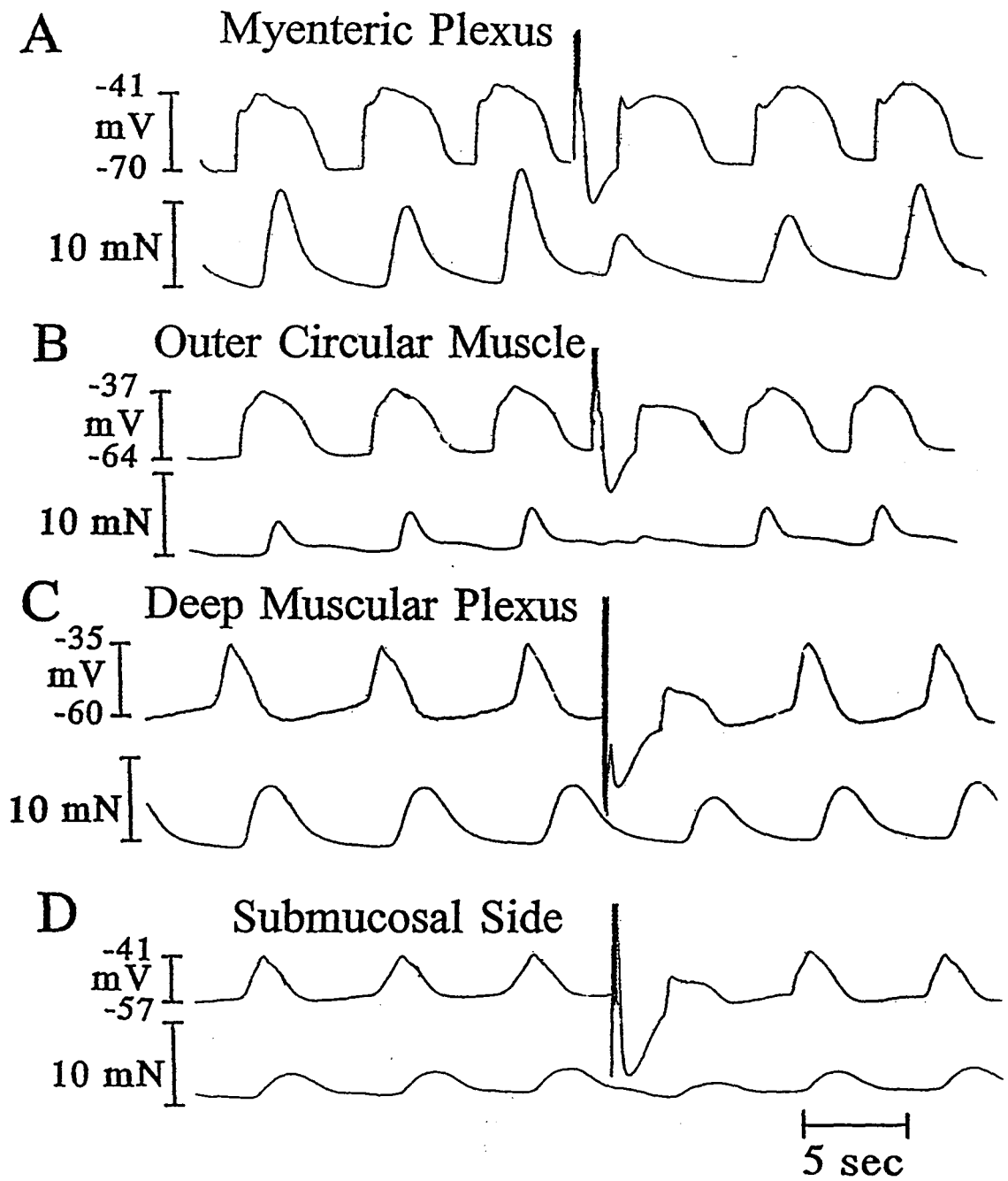


Fig. 2. Gradient in IJPs and resting potentials in canine ileum circular muscle

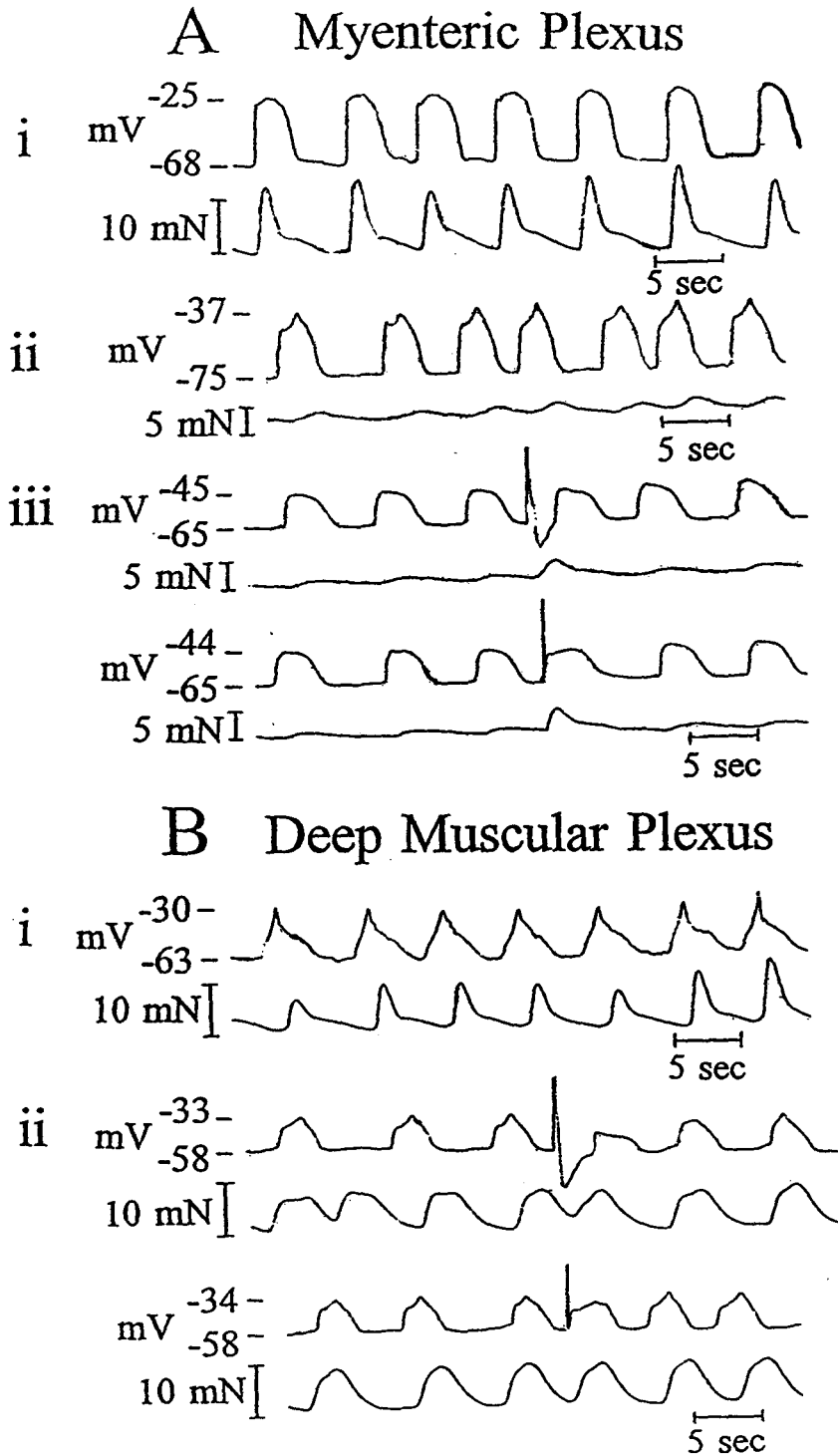


Fig. 3. Spontaneous slow waves and triggered activity near the pacemaking regions

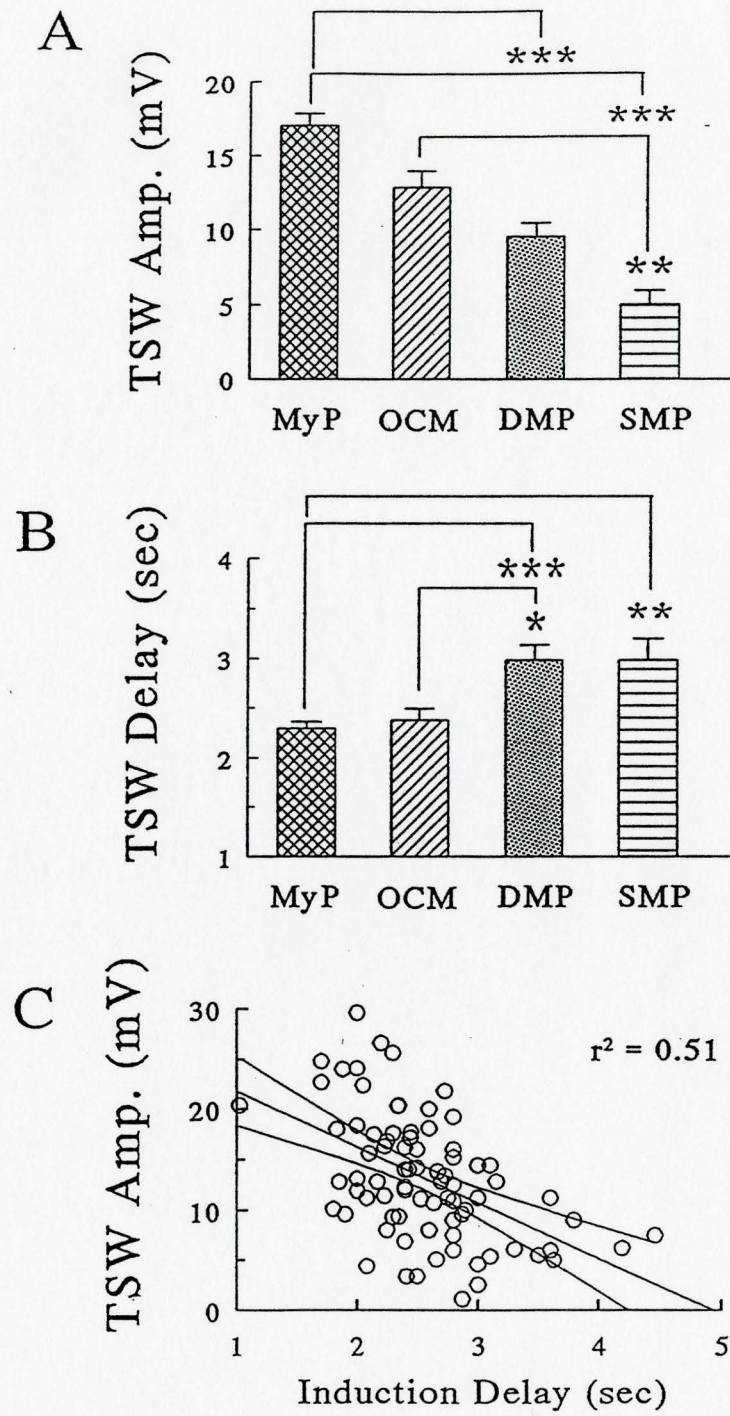
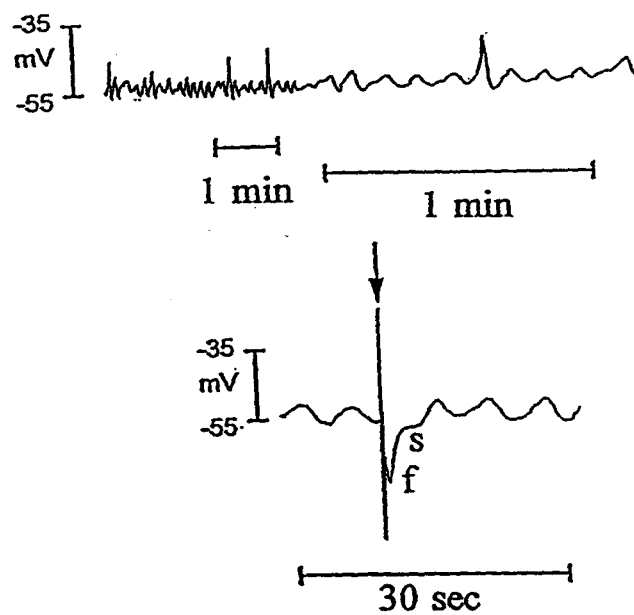


Fig. 4. Origin of triggered slow waves in canine ileum circular muscle

Isolated Circular Muscle

A Outer Area



B Inner Area

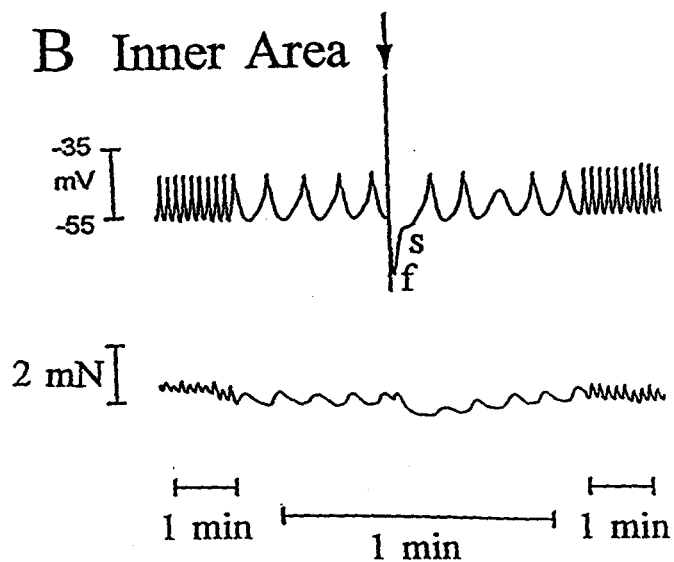


Fig. 5. Slow waves and IJPs in isolated circular muscle preparations

Isolated Circular Muscle - Deep Muscular Plexus

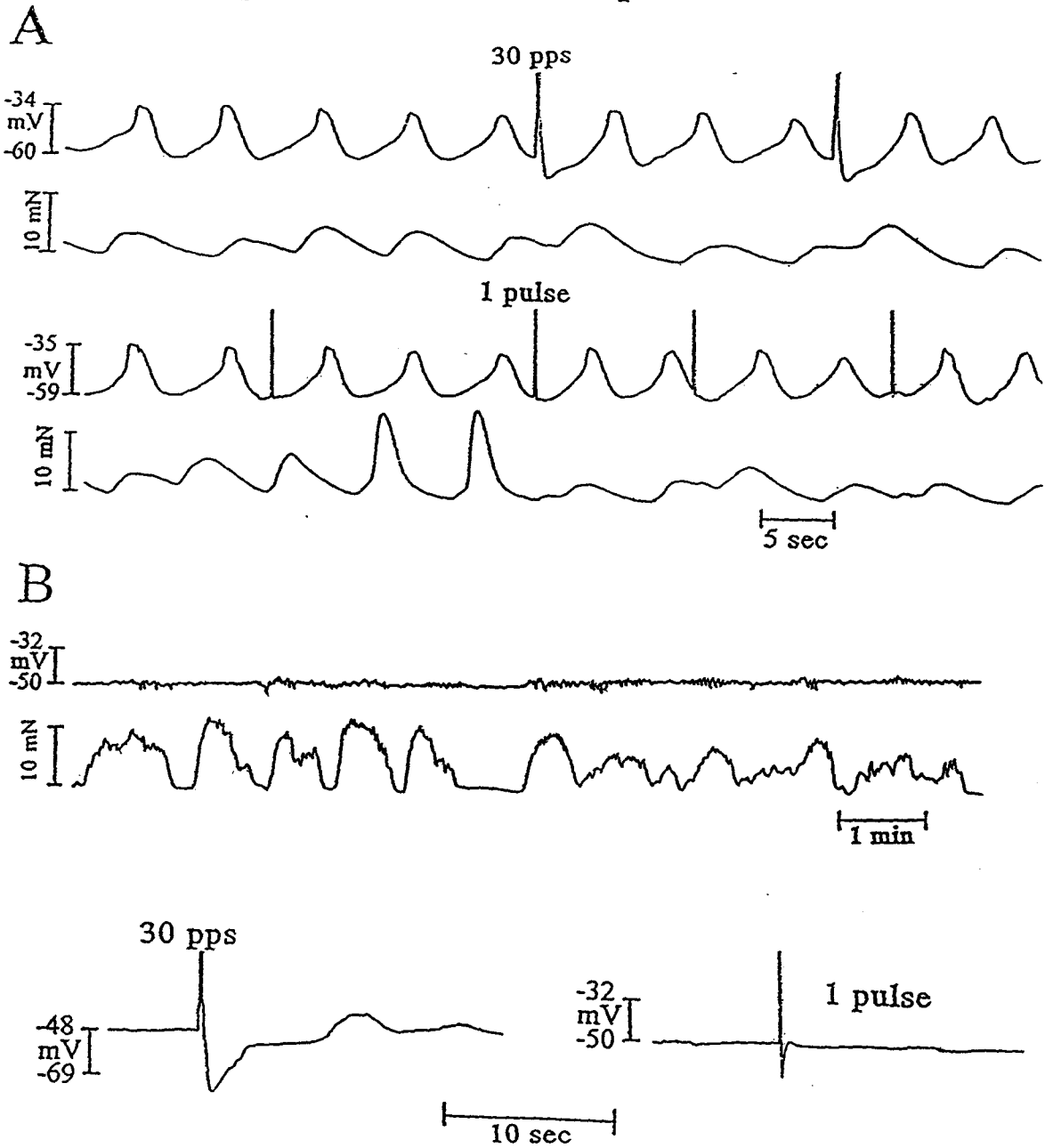


Fig. 6. Lack of triggered activity in isolated circular muscle preparations

Table 1. Electrophysiological effects of NANC blockers (all at 10^{-6} M) on cells near the regions of the myenteric plexus (MyP) (A) and deep muscular plexus (DMP) (B).

TREATMENT	Slow Wave Frequency (cycles/min)	Slow Wave Amplitude (mV)	Slow Wave Duration (sec)	Resting Membrane Potential (mV)	TSW _{30pps} Amplitude (mV)	TSW _{30pps} Duration (sec)	IJP Amplitude (mV)	IJP Duration (sec)	TSW _{30pps} Induction Delay (sec)
A. Control near MyP	10.25 ± 0.22 (n=13)	21.89 ± 1.85 (n=13)	4.10 ± 0.09 (n=13)	-69.09 ± 1.64 (n=13)	14.03 ± 1.19 (n=12)	3.76 ± 0.32 (n=12)	16.44 ± 1.02 (n=12)	1.30 ± 0.09 (n=12)	2.29 ± 0.11 (n=12)
+ Atropine + Guanethidine	10.53 ± 0.26 (n=6) NS	22.42 ± 1.69 (n=6) NS	4.07 ± 0.15 (n=6) NS	-69.17 ± 2.96 (n=6) NS	11.75 ± 0.25 (n=4) NS	4.30 ± 0.20 (n=4) NS	19.83 ± 1.08 (n=4) NS	1.52 ± 0.14 (n=4) NS	2.62 ± 0.43 (n=4) NS
+ Propranolol + Phentolamine	10.00 ± 0.22 (n=13) NS	22.38 ± 1.72 (n=13) NS	4.19 ± 0.09 (n=13) NS	-70.27 ± 1.87 (n=13) NS	13.73 ± 1.45 (n=12) NS	4.15 ± 0.13 (n=12) NS	16.23 ± 1.59 (n=12)	1.46 ± 0.12 (n=12) NS	2.45 ± 0.16 (n=12) NS
B. Control near DMP	9.58 ± 0.31 (n=5)	19.7 ± 2.86 (n=5)	5.34 ± 0.22 (n=5)	-58.40 ± 2.14 (n=5)	7.82 ± 0.89 (n=5)	3.81 ± 0.36 (n=5)	21.70 ± 3.62 (n=5)	1.76 ± 0.15 (n=5)	3.04 ± 0.36 (n=5)
+ Atropine + Guanethidine	9.13 ± 0.13 (n=4) NS	18.5 ± 3.40 (n=4) NS	4.98 ± 0.47 (n=4) NS	-59.75 ± 2.84 (n=4) NS	6.80 ± 1.59 (n=4) NS	3.34 ± 0.24 (n=4) NS	21.25 ± 4.04 (n=4) NS	2.06 ± 0.19 (n=4) NS	2.63 ± 0.09 (n=4) NS
+ Propranolol + Phentolamine	8.84 ± 0.10 (n=5) NS	19.68 ± 2.90 (n=5) NS	5.5 ± 0.41 (n=5) NS	-57.80 ± 1.99 (n=5) NS	7.24 ± 1.38 (n=5) NS	3.73 ± 0.27 (n=5) NS	22.54 ± 2.81 (n=5) NS	2.01 ± 0.12 (n=5) NS	2.80 ± 0.22 (n=5) NS

No significance was denoted by NS = $P > 0.05$, and treatments were compared to relevant controls.

Table 2. Characteristics of the resting membrane potentials, slow waves and responses to electrical field stimulations in the different regions of the circular muscle layer of the canine ileum.

Site of Recording	Resting Membrane Potential (mV)	Slow Wave Frequency (cycles/min)	Slow Wave Amplitude (mV)	Inhibitory Junction Potential Amplitude (mV)	Inhibitory Junction Potential Duration (sec)	Triggered Slow Wave Amplitude (mV)	Delay in Induction of Triggered Slow Wave (sec)
A. Full Thickness Preparation							
Near Myenteric Plexus (MyP)	-67.30 ± 0.72 (49)	9.80 ± 0.17 (n=49)	22.68 ± 1.01 (n=50)	14.14 ± 0.58 (n=43)	1.44 ± 0.07 (43)	16.01 ± 0.70 (n=45)	2.04 ± 0.10 (43)
In Outer Circular Muscle (OCM)	-61.45 ± 1.20 (18) ***	8.78 ± 0.32 (n=17) *	18.99 ± 1.20 (n=17) NS	16.14 ± 0.61 (n=16) NS	1.56 ± 0.10 (n=16) NS	13.11 ± 0.71 (n=16) NS	1.94 ± 0.13 (n=16)
Near Deep Muscular Plexus (DMP)	-59.11 ± 0.82 (n=35) ***	9.40 ± 0.19 (n=38) NS	18.21 ± 1.11 (n=38) *	18.81 ± 0.87 (n=36) ***	2.28 ± 0.57 (n=36) NS	8.15 ± 0.69 (n=36) *** *** wrt OCM	2.54 ± 0.14 (n=36) * * wrt OCM
Near Submucosal Plexus (SMP)	-54.83 ± 1.87 (n=9) *** * wrt OCM	8.06 ± 0.45 (n=9) *** * wrt DMP	14.8 ± 2.12 (n=9) **	11.21 ± 1.06 (n=8) NS * wrt OCM *** wrt DMP	1.31 ± 0.13 (n=8) NS	4.47 ± 1.14 (n=8) *** *** wrt OCM	2.86 ± 0.23 (n=9) ** ** wrt OCM
B. Isolated Circular Muscle							
Near Outer Circular Muscle (OCM)	-59.4 ± 1.8 (n=5) NS wrt OCM in A	8.3 ± 0.4 (n=5) NS wrt OCM in A	6.1 ± 1.0 (n=5) **** wrt OCM in A	21.1 ± 1.1 (n=5) *** wrt OCM in A	5.12 ± 0.49 (n=5) **** wrt OCM in A	0.0 ± 0.0 (n=5)	not measured
Near Deep Muscular Plexus (DMP)	-57.1 ± 1.0 (n=20) NS wrt OCM in B or DMP in A	8.5 ± 0.4 (n=20) NS wrt OCM in B * wrt DMP in A	10.5 ± 1.8 (n=20) * wrt OCM in B *** wrt DMP in A	19.7 ± 2.0 (n=20) NS wrt OCM in B NS wrt DMP in A	5.10 ± 0.43 (n=20) NS wrt OCM in B ** wrt DMP in A	0.0 ± 0.0 (n=20)	not measured

Significances in the full-thickness preparation are with respect to (wrt) the MyP unless otherwise stated and significances in the isolated circular muscle are with respect to the region near outer circular muscle unless otherwise stated. Bonferroni correction was used regarding multiple comparisons in ANOVA.

CHAPTER 3.2

PAPER No. 2

INFLUENCE OF NITRIC OXIDE ON THE SPONTANEOUS AND TRIGGERED ELECTRICAL AND MECHANICAL ACTIVITIES OF THE CANINE ILEUM

Submitted March, 1995 to *American Journal of Physiology (Gastrointestinal and Liver Physiology)*, in revision

Francisco Cayabyab's contribution:

- (i) performance of all electrophysiological experiments except for those involving L-NAME and apamin
- (ii) data presentation and statistical analysis
- (iii) writing, revising, and preparing manuscript for submission to *American Journal of Physiology*

INFLUENCE OF NITRIC OXIDE ON THE SPONTANEOUS AND TRIGGERED ELECTRICAL AND MECHANICAL ACTIVITIES OF THE CANINE ILEUM

Francisco S. Cayabyab^{1,2}, Marcel Jiménez³, Patri Vergara³, Hubert deBruin², and Edwin E. Daniel¹. Departments of Biomedical Sciences¹ and Electrical & Computer Engineering², McMaster University, 1200 Main Street West, Hamilton, Ontario L8N 3Z5; and Department of Cell Biology and Physiology³. Universitat Autònoma de Barcelona, Bellaterra 08193 Barcelona, Spain.

Running title: Nitrgergic neural modulation of intestinal slow waves

Address for correspondence: E.E. Daniel, PhD

Division of Physiology and Pharmacology

Department of Biomedical Sciences

Faculty of Health Sciences

McMaster University

1200 Main Street West

Hamilton, Ontario, Canada L8N 3Z5

Telephone no: 1-905-525-9140 ext. 22250. Fax no. 1-905-524-3795

ABBREVIATIONS

D-ARG - D-arginine

DMP - deep muscular plexus

EFS - electrical field stimulation

ICC - interstitial cells of Cajal

IJPs - inhibitory junction potentials

L-ARG - L-arginine

L-NAME - N^ω nitro L-arginine methyl ester

L-NNA - N^ω nitro L-arginine

MyP - myenteric plexus

NANC - nonadrenergic noncholinergic

NOS - nitric oxide synthase

OCM - outer circular muscle

ω-CTX - ω-conotoxin GVIA

SIN-1 - 3-morpholino-sydnonimine-hydrochloride

SMP - submucosal plexus

TSWs - triggered slow waves

TTX - tetrodotoxin

VIP - vasoactive intestinal polypeptide

ABSTRACT

Nitroergic neural modulation of canine ileal pacemaker activity for motility was studied by simultaneously recording the intracellular electrical and mechanical activity from a cross-sectioned preparation of the entire muscularis externa and from an isolated muscle preparation devoid of longitudinal muscle and myenteric plexus (MyP) but with deep muscular plexus (DMP) intact. In the whole-thickness preparation previously treated with atropine, guanethidine, propranolol, and phentolamine (all at μM), the inhibitory junction potentials (IJP) recorded near the MyP or DMP were prolonged by L-arginine (1mM), abolished by tetrodotoxin (TTX, 1 μM) alone or by the NO-synthase (NOS) inhibitor, N^o nitro L-arginine (L-NNA at 50 μM). Triggered slow wave (TSW) in response to electrical field stimulation (EFS) using brief pulses occurred advanced in time and increased in amplitude after the abolition of IJP by TTX. The effects of L-NNA were partially reversed by L- but not D-arginine (both 1 mM). TTX or L-NNA did not alter the resting membrane potentials or the characteristics of spontaneous slow waves and TSWs evoked by a long stimulating pulse. L-NNA at 100 μM enhanced the amplitude but not the frequency of spontaneous slow waves. ω -conotoxin GVIA (ω -CTX, 1-3 $\times 10^{-7}$ M), abolished the IJP but when EFS still produced a TSW it occurred only after a delay. Subsequent addition of TTX or L-NNA advanced the onset of the TSW. ω -CTX did not modify the resting membrane potentials, spontaneous slow waves, or TSWs elicited by long single pulses. In isolated circular muscle preparations, the NOS inhibitors, N^o nitro L-arginine methyl ester (L-NAME at 300 μM) or L-NNA at 100 μM , abolished the IJP and increased the regularity and amplitude of spontaneous slow waves, but TSWs could

not be evoked before or after NOS inhibition. L-arginine (1 mM) partially reversed the effects of L-NAME. Apamin (10^{-6} M) did not affect the resting membrane potentials or spontaneous slow waves but inhibited the IJP amplitude by up to 70% in both preparations and slightly but significantly enhanced the TSW amplitude in whole thickness preparations. Apamin, TTX, ω -CTX, and NOS blockers all increased circular muscle contractions associated with the spontaneous slow waves and TSWs. SIN-1 (200 μ M) produced TTX-insensitive hyperpolarizations of amplitudes (15 to 20 mV) similar to those of IJPs near both pacemaking regions of the full-thickness preparation. It attenuated the IJPs and abolished all mechanical activities. SIN-1 increased the slow wave frequency but decreased the amplitude and duration of spontaneous slow waves and TSWs. We conclude that spontaneous slow waves initiated near the MyP and DMP regions and TSWs generated from the MyP region originate independently of neural activity. Each pacemaking region possesses an inhibitory neural input which releases NO to mediate apamin-sensitive IJPs and relaxation and influence the delay before a TSW. NO release from nerves affects the ability of the pacemaker cells to initiate spontaneous or triggered slow waves near the MyP, and NO release not requiring nerve stimulation also appears to amplify the NO signal from nerves and modulate pacemaking activity from the DMP region.

Key words: nitric oxide synthase, interstitial cells of Cajal, NANC inhibitory neurotransmission, inhibitory junction potential, SIN-1, K^+ channels, triggered slow waves, intercellular communication, nitrergic nerves

INTRODUCTION

Electrophysiological studies of the small and large intestinal musculature suggest that the interstitial cells of Cajal (ICC) are the putative pacemakers or provide clocks for the pacemaking activity of the gut. They are closely innervated and may also facilitate communication between the enteric nervous system and the smooth muscle to which they are electrically coupled (22, 38, 41; see reviews 14 and 15). ICC have also been postulated to play a role in the neurotransmission of non-adrenergic, non-cholinergic (NANC) inhibitory activity (see 15). In several small intestinal muscles, the ICC from the myenteric plexus (MyP) were near nerve profiles and made close contact with one another and with longitudinal and circular smooth muscle (32, 34, 40), while the ICC from the deep muscular plexus (DMP) made gap junction contact with one another and with circular muscle cells (18, 19, 32, 33, 42) and are in close (< 100nm) contact with nerve axons and varicosities. Thus if ICC networks provide for pacemaking activity, the slow waves they generate may be modulated by neural inputs. In fact, ICC observed in the circular muscle of esophagus, small intestine and colon have been found close to nerve endings often containing large granular vesicles (4, 5, 6, 7). The neuropeptide in these nerves has often been identified as vasoactive intestinal polypeptide (VIP). However, VIP had no discernible effect on electrical and mechanical activities of canine intestinal circular muscle (12) and no VIP receptors could be found on circular muscle membranes (29).

Nitric oxide (NO), another putative NANC mediator, has been shown to be present in nerves with NO-synthase (NOS) in the MyP of the guinea pig intestine and canine

colon (8, 20, 30, 45) and in the synaptosomes of the DMP of the canine ileum (28). Recently, NOS and VIP have been shown to be found in the same nerve varicosities from both plexuses in the canine ileum and colon (7). Moreover, inhibitory responses mediated by NO have been reported in several areas of the gastrointestinal tract such as the opossum lower esophageal sphincter and body circular muscle (12, 25, 43), the canine pylorus (2), proximal duodenum, jejunum and ileum (3, 12, 35, 36) and colon (13, 26, 44). Controversy exists regarding the origin of NO in the gastrointestinal tract. The fact that inhibitory junction potentials (IJPs) were abolished by tetrodotoxin (35) suggested that NO was released from nerves to the smooth muscle either directly or by an intermediate cell. Interstitial cells isolated from the canine colon have been shown to respond to NO by increasing cytosolic Ca^{2+} concentration leading to the production and release of NO by a positive feedback mechanism (31). However the mechanism of storage and release of NO is not yet well understood (7, 15, 37) and how NO-mediated effects might influence spontaneous slow waves or triggered slow waves (TSWs) remains to be elucidated. Indeed, IJPs were shown to be able to drive slow waves in rabbit intestine (11, 39) and canine antral circular muscle (27).

As the structural or cellular organization in the circular muscle of the canine ileum has been well established, experiments were undertaken to investigate the hypothesis that inhibitory nitrenergic neural inputs modulate pacemaking function of ICC of MyP and DMP in the small intestine. To test this hypothesis, simultaneous recordings of mechanical and intracellular electrical activity from a cross-sectioned preparation of the entire muscularis externa were compared to those from an isolated circular muscle preparation devoid of

longitudinal muscle and MyP. The inhibitory neural input influenced the pacemaker cell network from the DMP region and the electrical and mechanical activity of the isolated circular muscle strip, and the inhibitory neural input near the pacemaker cell network from the MyP region influenced that of the whole circular muscle. Production of NO mediated the apamin-sensitive IJPs elicited near both pacemaker regions. NO from the NO-liberating organic compound, SIN-1, mimicked the hyperpolarization and relaxation induced by the endogenous NO released from NANC nerves. Finally, the spontaneous slow waves or TSWs (triggered by the ending of an IJP, or by various stimulation parameters that did not induce an IJP) and accompanying circular muscle contractions were modulated by using pharmacological neural toxins or by changing the availability of endogenous NO using NOS inhibitors, suggesting that ongoing release of NO from nerves may be occurring *in vitro*. Preliminary accounts of some of this work have been published (9, 10).

MATERIALS AND METHODS

Preparation of ileal circular muscle.

Healthy adult mongrel dogs of either sex, ranging from 10 to 25 Kg, were euthanized using intravenous sodium pentobarbitone (65 mg/kg). This procedure was approved by the McMaster University Animal Care Committee. The abdomen was immediately opened along the midline and a segment of ileum (10 cm) was removed from a position about 10 cm oral to the ileocaecal junction. The dissection was made at room temperature in normal oxygenated Krebs solution. The segment of ileum was cleaned of external fat and connective tissue and opened along the mesenteric border. The mucosa and submucosa were removed taking care not to damage the circular muscle. In some cases, the longitudinal muscle was also removed in the isolated circular muscle strips using the same technique already described (12). Electron micrographs of this preparation confirmed that the longitudinal muscle and the MyP were completely removed and the DMP was intact. Tissue strips (1 x 10 mm) were cut parallel with the circular muscle fibres and placed in a 5 ml organ chamber for electrophysiological recordings. The strips were pinned to the floor of the chamber to immobilize regions selected to record the intracellular electrical activity. About 1 cm of unpinned region was connected to a force transducer for recording of mechanical activity. This unpinned region was stretched by 2 g once, and the whole preparation was allowed to equilibrate for two to three hours before impalements were attempted. The tissue was superfused constantly by Krebs solution at a rate of 3 ml/min (37 ± 2 °C). Glass electrodes filled with 3 M KCl with resistances ranging from 30 to 80 M Ω were used to impale the cells. Membrane potential

changes were measured using a standard electrometer (World Precision Instruments KS-700). The signal was monitored on a dual beam oscilloscope (Tektronix D13; 5A22N differential amplifier; 5B12N dual time base) and recorded on 1/4 inch magnetic tape with a Hewlett-Packard instrumentation recorder and on chart paper (Gould 2200). A microscope (M3C, Wild Leitz) with calibrated eyepiece graticule was used to select accurately the position of the recording electrode. The electrical activity was studied in the following areas of the circular muscle (see Figure 1A): 1) near the MyP (0-10% of the total width close to the longitudinal muscle, n =50) and 2) near the DMP (60-90% from the MyP, n =38). The isolated circular muscle was also studied near the DMP (n=20). The number of strips from at least three different animals used from each type of experiment is indicated by n, and a total of 64 animals were used in this study.

Simultaneous recordings of the intracellular electrical and mechanical responses to apamin were not made during some early stages of the study. Instead the effects of apamin on the mechanical activity were obtained by recording tension changes in the organ bath. Circular muscle strips (2 cm x 1 mm) were suspended in a 15 ml organ bath (37 ± 2 °C) containing Krebs solution bubbled with 95% O₂ - 5% CO₂. Each strip was fixed at one end of an electrode holder by a silk ligature, and the other end of the tissue was fixed with another ligature to a force displacement transducer (Grass FTOC3). Initial tension (2.5 grams) was applied to each muscle strip which was then allowed to equilibrate for 2 hours. The changes in tension were recorded on a Beckman R611 dynograph.

Electrical field stimulation

Electrical field stimulation was achieved using a pore-type silver electrode in contact with the tissue on one side of the strip, and a silver ground electrode on the other side. Stimuli were provided by a Grass S88 stimulator through a stimulus isolation unit (Grass SIU5). A range of parameters was used to obtain the supramaximal IJPs in each strip. The pulse rate was 25-30 pps, the train duration 300 msec, supramaximal voltage 120 - 150 V, 0.3-0.4 msec pulses. Single pulse stimulation was achieved by using 50-100 msec square wave (10-20 V).

Solutions and drugs

The Krebs solution (in mM: NaCl, 115.5; NaH₂PO₄, 1.6; NaHCO₃, 21.9; KCl, 4.2; CaCl₂, 2.5; MgSO₄, 1.2 and glucose, 11.1) was continuously aerated with 95% O₂ - 5% CO₂ to maintain pH of approximately 7.4. Drugs were introduced to the Krebs reservoir and superfused (3 ml/min) for at least 25-30 minutes. Two concentrations (10⁻⁷ and 3 x 10⁻⁷ M) were used for ω-Conotoxin (GVIA) (ω-CTX) (from Peninsula, CA, U.S.A.). Atropine, guanethidine, propranolol, phentolamine, tetrodotoxin (TTX), and apamin were used at 10⁻⁶ M. N^ω nitro L-arginine (L-NNA) and N^ω nitro L-arginine methyl ester (L-NAME) were superfused at concentrations of 50 μM and 300 μM, respectively. L-Arginine (L-ARG) and D-Arginine (D-ARG) were used at 10⁻³ M. All these drugs were from Sigma (CA, U.S.A.). The sydnonimine SIN-1 (3-morpholino-sydnonimine-hydrochloride) was a generous gift from Dr. Rudolf Kunstmann (Cassella AG). It was dissolved in dimethyl sulfoxide to give 10⁻¹ M stock solutions and was stored in the dark at -22 °C at all times.

Recordings and statistical analysis.

The resting membrane potential, frequency, duration and amplitude of slow waves, and the durations and amplitudes of IJPs and TSWs were analysed for each record. TSWs were distinguished from spontaneous slow waves by their occurrence advanced or delayed in time relative to the expected occurrence of the next spontaneous slow wave. These parameters were analysed during the control period (20 minutes) and every 5 minutes following the drug infusion (30 minutes). Frequencies of slow waves were determined by averaging the number of slow waves occurring over a period of 3 minutes. The motility index was calculated by multiplying the mean contraction amplitude in a 1-min interval with the number of contractions occurring during this interval. Spontaneous phasic contractions were measured immediately before and 20 to 30 minutes after onset of each treatment. Data are presented as mean \pm S.E.M. Ordinary ANOVA (analysis of variance, with Bonferroni correction) or Student *t*-tests, as appropriate, were performed to check for statistical significance. Mean values were considered significantly different when $p < 0.05$. Significances are denoted as follows: * = $P < 0.05$, ** = $P < 0.01$, *** = $P < 0.001$, **** = $P < 0.0001$.

RESULTS

Resting membrane potentials and spontaneous slow waves in the full thickness preparation

Figure 1A shows a schematic of the full-thickness preparation which defines the various locations of the recording electrodes during an experiment. The heterogeneity in slow wave activity and the distribution of IJPs in the regions of the myenteric plexus (MyP), outer circular muscle (OCM), deep muscular plexus (DMP), and submucosal plexus (SMP) of the circular muscle layer were investigated in a previous study (Jiménez, M., F.S. Cayabyab, P. Vergara, and E.E. Daniel, submitted). It was also established in that study that two networks of pacemakers located near the MyP and DMP could interact but could also function independently, and that triggered slow wave (TSW) activity appeared to originate from the MyP region under our conditions. Figures 1B and 1C demonstrate the observed gradient in baseline membrane potential, with cells near the MyP having membrane potentials between slow waves about 10 mV more hyperpolarized than cells from the DMP region. The slow waves from the MyP were plateau-type in shape (with plateaus which were rounded, flat, or occasionally triangular in profile), preceded by a fast upstroke, and oscillated at about 9-10 cycles/minute. The slow waves recorded near the DMP region were triangular in shape, usually following a sigmoidal depolarization, and lacking a plateau region. The slow waves originating near these pacemaking regions oscillated at nearly the same frequency. The different parameters associated with slow wave activity and responses to electrical field stimulation or EFS were determined as labelled in Figures 1B and 1C (a=slowwave amplitude; b=slow wave

duration; c=amplitude of slow wave triggered by IJP. These often occurred prematurely, but could also occur after the IJP delayed relative to the expected timing of the next slow wave. Therefore, they were designated as triggered slow waves (TSWs); d= TSW duration; e=IJP amplitude; f=IJP duration; and g=TSWdelay).

Effects of neural blockers on IJPs, spontaneous slow waves, and TSWs

Figure 2 shows that in whole-thickness preparations TTX abolished the IJP in the MyP (Figure 2A) and the DMP (Figure 2B) regions, but significantly enhanced the TSW amplitude when triggered by a high frequency (30 pps, supramaximal voltage) stimulus (Table 1). TTX did not modify the slow wave frequency or amplitude. The TSW elicited by long duration pulse (50-100 msec , 10- 20 V) was unaffected by TTX shown in Figures 2A and B (bottom traces), as expected if this stimulus evoked little or no neural activation. The mechanical counterparts of the spontaneous slow waves and the TSWs elicited by short pulses or a long pulse were significantly increased in amplitude during superfusion with TTX (Figure 2 and Figure 8).

The presence of atropine, guanethidine, propranolol, and phentolamine (all at 10^{-6} M) did not affect the slow waves from the MyP and DMP regions (see preceding report by Jiménez, M., F.S. Cayabyab, P. Vergara, and E.E. Daniel, submitted). After block of adrenergic and cholinergic nerves, subsequent addition of the NOS inhibitor L-NNA (50 μ M) abolished the IJP and increased the TSW amplitude in both regions (Figures 3A, 3B). L-NNA effects were partially reversed by L- but not D-ARG (Figures 3A and 3B, Tables 2A and 2B). Note that despite the incomplete recovery of the IJP amplitude

during superfusion with L-ARG before washout, the IJP duration and the delay before triggering of a slow wave were significantly prolonged (Tables 2A and 2B).

Figure 4 shows recordings from the MyP region (4A) and the DMP region (4B) illustrating the effects of NANC blockers and L-NNA on the responses to EFS administered at varying intervals after a preceding slow wave. EFS was delivered between slow waves (MIDDLE), right after a slow wave (EARLY), and just before the onset of another slow wave (LATE). In Figures 4A and 4B (left panels), EFS at every interval elicited an IJP which triggered a slow wave (sometimes early, sometimes delayed). Subsequent addition of 50 μ M L-NNA abolished the IJPs but enhanced the amplitudes of the TSWs (Figure 4A and 4B, right panels). A TSW was always evoked near the MyP region at the "early" and "middle" intervals between slow waves, whereas near the DMP a TSW could be evoked only during the "middle" interval but never at the "early" interval. In both recordings, EFS during the "late" interval evoked a delayed TSW (Figure 4A) or the next spontaneous slow wave intervened (Figure 4B).

Spontaneous slow waves and IJPs after NOS inhibition: isolated circular muscle vs. full-thickness preparations

In isolated circular muscle, the IJP repolarized in two steps, a fast hyperpolarization reaching a maximum amplitude of 14 ± 2.1 mV followed by a slow hyperpolarization of 5.14 ± 0.75 mV ($n = 18$). The IJP was abolished by 300 μ M L-NAME ($n=6$) in the isolated circular muscle preparation (Figure 5A) and a reversal of L-NAME effects by L-ARG ($n=5$) (Figure 5A) but not by D-ARG ($n=3$) (data not shown)

was observed as expected in this preparation. Whenever slow waves were irregular in this preparation, the addition of L-NAME produced a more regular slow waves of higher amplitudes (Figure 5B). In preliminary studies using the isolated circular muscle (Figure 6A) and full-thickness (Figure 6B) preparations, superfusion of a higher concentration of L-NNA (100 μ M vs. 50 μ M) after prior treatment with the NANC blockers increased the amplitude of slow waves and circular muscle contractions (Figure 6A and 6B). We subsequently used a lower concentration of L-NNA (50 μ M), which was sufficient to abolish the IJPs, in order to facilitate recovery of IJPs and spontaneous circular muscle contractions with or without L-ARG.

Effects of omega conotoxin GVIA (ω -CTX) and apamin in the full thickness preparation

Since neural mediators may modulate pacemaking activity, we evaluated changes induced by blocking neural function. ω -CTX is a selective neuronal N-type Ca^{2+} channel antagonist (23). This blocker did not affect the frequency, amplitude, or shape of the slow waves (Figure 7). However, ω -CTX inhibited the IJP in a dose dependent manner. ω -CTX at 10^{-7} M gradually inhibited the amplitude of IJP (data not shown, maximum inhibitory effect observed at 30-40 minutes), but at 3×10^{-7} M the IJPs were rapidly abolished (Figures 7A and 7B). The inhibition started 5 minutes after the beginning of the infusion with a full abolition after 15-20 minutes. The effect was partly reversible after 40-60 minutes of washing. The abolition of the IJP by ω -CTX was accompanied by an increased delay before the next TSW in both regions (Figures 7 A and B middle panels). Subsequent addition of either L-NNA (Figures 7 A and B, bottom panels) or

TTX (data not shown, $n=4$ from MyP and $n=3$ from DMP) abolished the delay in induction of a TSW and enhanced the TSW amplitudes. Long duration, single pulse-induced TSWs were unaffected by ω -CTX (data not shown), which was similar to the lack of effect of TTX as shown earlier in Figure 2.

Apamin 10^{-6} M ($n=5$) did not modify the shape of the slow waves or the resting membrane potential, but reduced the IJP amplitude by 70% (paired Student t -test; $p < 0.05$) and increased slightly (30%) the amplitude of the TSWs (paired Student t -test; $p < 0.05$) (Figure 8A). No differences were found between the studied areas (3 recordings from the DMP region and 2 from the OCM). The effect of apamin was still present 30 minutes after washout. Note that apamin along with TTX, ω -CTX, and L-NNA each significantly increased circular muscle contractions and the motility index (Figure 8B and Figures 9A and 9B). Apamin also inhibited the IJP by 60% in the isolated circular muscle preparation as previously reported (12).

Effects of the NO-donor, SIN-1, in the full thickness preparations.

SIN-1 at 200 μ M hyperpolarized the membrane potentials by 10-15 mV from recordings near the MyP ($n=4$) and the DMP ($n=3$) (Figures 10A and 10B, respectively). The amplitudes of these hyperpolarizations were similar to those of the IJPs elicited by EFS. SIN-1 (200 μ M) attenuated the IJP amplitude and duration (Amplitude: control 14.9 ± 1.3 mV vs. treated 4.0 ± 1.1 mV, $n=7$ (**); Duration: control 1.7 ± 0.2 sec vs. treated 0.6 ± 0.2 sec, $n=7$ (**)). As shown in Figures 10A, 10B and 10C, SIN-1 slightly but significantly increased the slow wave frequency (control 10.0 ± 0.6 cycles/min vs. treated 10.9 ± 0.6 cycles/min, $n=7$ (*)), reduced the slow wave durations (control 4.4 ± 0.1 sec

vs. treated 3.7 ± 0.1 sec, $n=7$, (**)), and attenuated its amplitude (control 21.7 ± 1.8 mV vs. treated 15.6 ± 2.4 mV (***)). TTX at 10^{-6} M did not affect SIN-1 hyperpolarizations ($n=3$, data not shown). Application of SIN-1 ($200 \mu\text{M}$) in the presence of TTX showed that the muscle preparations still responded with a TSW to a long duration, single pulse stimulation (Figure 10C).

DISCUSSION

The results of the present study are consistent with the hypothesis that the functioning of both sets of ileal pacemakers (in the MyP and the DMP) can be modulated by the activity of nitrenergic nerves or by the spontaneous release of NO. The availability of NO apparently affected the response of the muscle to the pacemaking function since the amplitudes of the spontaneous and triggered slow waves and the accompanying contractions of the circular muscle were enhanced by block of NOS. The effect was most marked in isolated circular muscle preparations. Other electrophysiological studies of various regions of the canine gut reported no effects of inhibition of NO synthesis on the spontaneous slow waves, possibly because the concentration of NOS blocker used was not sufficiently high to block NO release from all sources (3, 44) or the activity of NO sources differed in jejunum from those in ileum (35, 36).

Triggered slow wave activity was initiated by IJPs as well as by single, long pulse stimulation. Under our condition, removal of the MyP eliminated TSWs in response to IJPs or single pulses; thus likely site of triggering is the MyP pacemaking network. After an IJP but not after a single pulse stimulus, the TSW occurred following a delay. This implies that the hyperpolarization during the IJP delayed the onset of the TSW. The triggering may have resulted from the "off" depolarization or rebound following the IJP. However, when the IJP was abolished by block of NOS or by TTX, TSWs still occurred but with no delay. Thus the burst of 30 pps stimuli, which may cause persistent depolarization in structures with a long time constant (18), was itself able to trigger a slow wave from the MyP pacemaker network when no IJP occurred. This observation

is consistent with the possibility that the mediator of hyperpolarization delayed the TSWs by affecting the pacemakers directly. Such a delay could also result from an effect of hyperpolarization or its mediator on the electrical coupling of the pacemaker network to the circular muscle which produced an IJP.

Surprisingly when IJPs were abolished by ω -CTX, a delay still occurred before the TSW. Subsequent treatment with a NOS blocker abolished the delay. One explanation of these observations is that when release of NO from nerves was abolished by ω -CTX, there was still a source of NO not requiring neural excitation but affecting the ability of the MyP pacemaker network to respond to electrical stimulation. A recent study by Berezin *et al.* (7), employing immunoelectron microscopy combined with immunogold staining technique, showed the presence of NOS immunoreactivity in nerves of the MyP as well as in the nerves of the circular muscle layer of the canine ileum and colon. This study was consistent with previous work employing a variety of immunocytochemical techniques for localization of NOS activity (20, 45). NOS immunoreactivity was also detected occasionally in circular smooth muscle cells and ICC in the DMP of ileum (7). A recent report in guinea pig intestine suggests that VIP releases NO from isolated muscle cells (21). Another report in proximal colon, using light-microscopic immunocytochemical technique, revealed NOS-immunopositive nerve fibers along with NOS-immunopositive cell bodies (possibly ICC) near the submucosal border of the circular muscle layer (45). If ICC or other cells contain a different NO-synthase from nerves, it may be less susceptible to inhibition by ω -CTX or L-NNA.

An alternative explanation for the delay in TSW after ω -CTX block of IJPs is that

another type of voltage-activated Ca^{2+} channels in nerves may allow Ca^{2+} influx and sufficiently raise $[\text{Ca}^{2+}]_i$ to activate NOS to release some NO. Indeed, there are new "P" type as well as "Q" type voltage activated Ca^{2+} channels that have been shown to participate in synaptic transmission in the central nervous system (46). ω -CTX-insensitive "P"-type Ca^{2+} channels may contribute to Ca^{2+} influx to activate NOS and release of NO from nerves as has been recently reported (1). The fact that TTX, like inhibition of NOS, abolished the delay in induction of the TSW after ω -CTX pretreatment (data not shown) suggests that an ω -CTX-insensitive Ca^{2+} influx in nerves contributes to NO release and inhibits the initiation of a TSW. However, this NO release is insufficient to initiate an IJP. It is also possible that another mediator is released from a TTX-sensitive nerve, not sensitive to the conotoxin, to act indirectly to release NO.

Structural studies of localization of NOS in canine intestine (7; Wang, Mao, and Daniel, unpublished) show that there is a NADPH-diaphorase activity, not recognized by all neural NOS antibodies, in ICC in the MyP and DMP. NOS activity may be able to affect the activity of pacemaking cells. However, it does not seem to be required for the normal occurrence of pacemaking activity or polarization of nearby smooth muscle cells; *i.e.*, after L-NNA or L-NAME slow waves of normal configuration and frequency persisted without any change in resting membrane potential. On occasion, the amplitudes of slow waves were increased by L-NNA (100 μM) in recordings near the MyP in the full-thickness preparation (Figure 6B), while slow waves with less regular amplitudes as recorded near the DMP in the isolated circular muscle were clearly increased in amplitude and regularity (Figure 5B and Figure 6A). Thus inhibition of NOS may remove a

modulatory control over slow wave amplitude either in the pacemaker networks or in the muscle cells coupled to them. In contrast, superfusion with the NO-donor, SIN-1, hyperpolarized the membrane and caused a small increase in slow wave frequency. SIN-1 also reduced the amplitude and duration of spontaneous slow waves, which is consistent with other studies on the effects of authentic NO solution on electrical properties of the colon (44). It is unclear from these data whether exogenous application of NO has a direct effect on the ICC networks. Recording directly from the pacemaker networks would clarify how NOS activity might influence pacemaking but may not be possible. If pacemaking cells of the intestine have a constitutive NOS, they might respond to an increase in intracellular Ca^{2+} by releasing NO and modulating Ca_i^{2+} as reported recently by Publicover *et al.* (31) in their studies of isolated interstitial cells from the canine colon.

In the isolated circular muscle, IJPs did not trigger slow waves. Moreover the IJPs had a second slower phase of repolarization in addition to the initial fast repolarization. The absence of the second phase of persistent hyperpolarization in full thickness preparations probably resulted from the onset of a TSW as soon as the fast repolarization was complete. In isolated circular muscle preparations, IJPs often abolished or delayed slow waves which should have occurred during their period of hyperpolarization. This suggests that the pacemaking network of the DMP or the spread of activity from it was sensitive to NO or to hyperpolarization *per se*, perhaps more so than MyP pacemakers. Both phases of the IJPs in this region were abolished by inhibition of NOS and therefore depended on NO production. It is possible that these two phases of the IJP resulted from activation by NO of different cell types; *e.g.*, from NO action on ICC and on smooth

muscle. This possibility is consistent with the observation that apamin inhibited IJPs only partially and primarily by abolishing the fast component (24). The DMP nerves and its ICC both have NOS activity as judged by NADPH diaphorase histochemistry (Wang, Mao, & Daniel, unpublished) and by using polyclonal antisera raised against cerebellar NOS for immunogold staining and for immunoelectron microscopy immunostaining (7). Also the DMP synaptosomes carry out the biochemical conversion of tritiated L-arginine to L-citrulline (28) but circular muscle cells do not. Both *in vivo* and *in vitro* functional studies of canine ileum demonstrate the inhibition by NOS inhibitors of IJPs and relaxations induced by EFS (12, 17). There are also many VIP-immunoreactive nerves in this region (7, 16). Earlier we found VIP binding to a fraction of membranes from circular muscle tissues which were non-neural and not typical of smooth muscle (29). In addition VIP bound to synaptosomes from the DMP but not to muscle membranes. Thus it is possible that the delayed repolarization of IJPs reflects an action of VIP on ICC to activate NOS and hyperpolarize these and coupled smooth muscle cells.

In the whole thickness preparation, the slow wave triggered from the MyP after the IJP spread into the DMP region and accelerated repolarization. This would have obscured these responses to VIP. When VIP was applied to isolated circular muscle strips (12) it had no clear effects on membrane potentials, IJPs or contractions recorded in the double sucrose gap. However these experiments need to be repeated with the isolated slab used in this study, since slow waves were not recorded under the conditions of the earlier experiments.

The configuration of the IJPs in the canine ileal circular muscle was different when

recorded in the whole thickness preparation with the MyP and in isolated circular muscle (as discussed in the preceeding report by Jiménez *et al.*, in press). The observed gradient in resting membrane potentials across the circular muscle bundle should create a difference in the driving potential from K⁺-channel opening, which is consistent with earlier studies (12) which suggested the IJP reversed near the K⁺ equilibrium potential (reviewed in 37). The fast and slow components of the IJP in isolated circular muscle were both totally sensitive to L-NNA, and the fast component was partially sensitive to apamin. These results differed from recent reports in human colonic (26) and intestinal tissues (36) in which the slow component of IJPs was shown to be apamin-sensitive but the fast component was resistant to the NOS inhibitors, L-NNA or L-NAME. These investigators suggested that another inhibitory mediator, possibly VIP or adenosine triphosphate, may have had effects not mediated by NO. However, in our studies using both the isolated and full-thickness preparations of canine ileum the IJPs were fully inhibited by L-NNA, consistent with findings in other studies which used various regions of the canine gut (35, 36, 44).

In conclusion, this study presented a body of evidence providing additional support for the hypothesis that there are two distinct types of slow waves spontaneously generated by two different sources located near the MyP and DMP regions respectively. Slow wave activity could be triggered after an IJP and originated only from the MyP region from which it spread to the DMP region. The amplitude of TSWs was modulated in both regions by the presence of nitrergic nerves which released NO upon nerve stimulation to mediate the apamin-sensitive IJPs and relaxations. Inhibition of NOS increased slow

wave amplitude while exogenous application of NO from the NO-donor, SIN-1, reduced its amplitude and duration. NOS inhibition and other treatments which abolished or diminished the IJPs increased spontaneous circular muscle contractions. These results suggested that neural release of NO in or near the pacemaker networks may affect slow wave generation and propagation by acting on either the ICC (the putative pacemakers) or the muscle cells coupled to them or both. However, they do not rule out the possibility that NO release occurring spontaneously; possibly from ICC or from nerves, modulates pacemaking activity.

ACKNOWLEDGEMENT

M.J. was supported by Personal Investigator Visiting Grant from the Comissió Interdepartamental de Recerca i Innovació Tecnològica (CIRIT, Ref. EE92/2-369), Catalonia, Spain. P.V. was supported by Personal Investigator Visiting Grant from the Dirección General de Investigación Científica y Técnica, Spain. This research was supported by MRC and NSERC of Canada. The authors wish to thank Dr. Rudolf Kunstmann (Cassella AG) for the generous gift of SIN-1.

REFERENCES

1. **Alagarsamy, S., G. Lonart, and K.M. Johnson.** The role of P-type calcium channels in the depolarization-induced activation of NOS in frontal cortex. *J. Neurochem.* 62: 400-403, 1994.
2. **Allescher, H.D., G. Tougas, P. Vergara, S. Lu, and E.E. Daniel.** Nitric Oxide as a putative nonadrenergic, noncholinergic inhibitory transmitter in the canine pylorus. *Am. J. Physiol.* 262: G695-G702, 1992.
3. **Bayguinov, O., F. Vogalis, B. Morris, and K.M. Sanders.** Patterns of electrical activity and neural responses in canine proximal duodenum. *Am. J. Physiol.* 263: G887-G894, 1992.
4. **Berezin, I., H.D. Allescher, and E.E. Daniel.** Ultra-structural localization of VIP-immunoreactivity in canine distal esophagus. *J. Neurocytology* 16: 749-757, 1987.
5. **Berezin, I., J.D. Huizinga, L. Farroway, and E.E. Daniel.** Innervation of interstitial cells of Cajal by VIP-containing nerves in canine colon. *Can. J. Physiol. Pharmacol.* 68: 922-932, 1990.
6. **Berezin, I., S. Sheppard, E.E. Daniel, and N. Yanaihara.** Ultrastructural immunocytochemical distribution of VIP-like immunoreactivity in dog ileum. *Regulatory Peptides* 11: 287-298, 1985.
7. **Berezin, I., S.H. Snyder, D.S. Bredt, and E.E. Daniel.** Ultrastructural localization of NOS in canine small intestine and colon. *Am. J. Physiol.* 266: C981-C989, 1994.
8. **Bredt, D.S., P.M. Hwang, and S.H. Snyder.** Localization of nitric oxide synthetase indicating a neural role for nitric oxide. *Nature* 347: 768-770, 1990.
9. **Cayabyab, F.S., H. deBruin, and E.E. Daniel.** NO and NANC inhibitory mediation in the canine ileum (Abstract). *Can. J. Physiol. Pharmacol.* 72: 234, 1994.
10. **Cayabyab, F.S., M. Jiménez, P. Vergara, and E.E. Daniel.** Two independent pacemakers drive the electrical and mechanical activities of the canine ileum (Abstract). *Neurogastroenterology and Motility* 6: 152, 1994.
11. **Cheung, D.W., and E.E. Daniel.** Comparative study of the smooth muscle layers of the rabbit duodenum. *J. Physiol.* 309: 13-27, 1980.
12. **Christinck, F., J. Jury, F. Cayabyab, and E.E. Daniel.** Nitric oxide may be the final mediator of nonadrenergic, noncholinergic inhibitory junction potentials in

the gut. *Can. J. Physiol. Pharmacol.* 69: 1448-1458, 1991.

13. Dalziel, H.H., K.D. Thornbury, S.M. Ward, and K.M. Sanders. Involvement of nitric oxide synthetic pathway in inhibitory junction potentials in canine proximal colon. *Am. J. Physiol.* 260: G789-G792, 1991.
14. Daniel, E.E., B.L. Bardakjian, J.D. Huizinga, and N.E. Diamant. Relaxation oscillator and core conductor models are needed for understanding of GI electrical activities. *Am. J. Physiol.* 266: G339-G349, 1994.
15. Daniel, E.E., and I. Berezin. Interstitial cells of Cajal: are they major players in control of gastrointestinal motility? *J. Gastrointestinal Motility* 4: 1-24, 1992.
16. Daniel, E.E., J.B. Furness, M. Costa, and L. Belbeck. The projections of chemically identified nerve fibers in canine ileum. *Cell Tissue Res.* 247: 377-384, 1987.
17. Daniel, E.E., C. Haugh, Z. Woskowska, S. Cipris, J. Jury, and J.E.T. Fox-Threlkeld. Role of nitric oxide-related inhibition in intestinal function: relation to vasoactive intestinal polypeptide. *Am. J. Physiol.* 266: G31-G39, 1994.
18. Daniel, E.E., and V. Posey-Daniel. Neuromuscular structures in opossum esophagus: role of interstitial cells of Cajal. *J. Physiol.* 246: G305-G315, 1984.
19. Duchon, G., R. Henderson, and E.E. Daniel. Circular muscle layers in the small intestine. In: *Proceedings of the international Symposium of Gastrointestinal Motility*, edited by Daniel E.E., Vancouver: Mitchell Press, pp 635-646, 1974.
20. Furness, J.B., S. Pompolo, C.W.D. Shuttleworth, and D.E. Burleigh. Light and electron microscopic immunohistochemical analysis of nerve fiber types innervating the taenia of the guinea pig caecum. *Cell Tissue Res.* 270: 125-137, 1992.
21. Grider, J.R., K.S. Murthy, J.G. Jin, and G.M. Makhlof. Stimulation of nitric oxide from muscle cells by VIP: prejunctional enhancement of VIP release. *Am. J. Physiol.* 262: G774-G777, 1992.
22. Hara, Y., M. Kubota, and J.H. Szurszewski. Electrophysiology of smooth muscle of the small intestine of some mammals. *J. Physiol.* 372: 501-520, 1986.
23. Hirning, L.D., A.P. Fox, E.W. McCleskey, B.M. Olivera, S.A. Thayer, R.J. Miller, and R.W. Tsien. Dominant role of N-type Ca^{2+} channels in evoked release of norepinephrine from sympathetic neurons. *Science* 239:57-60, 1988.

24. **JIMÉNEZ, M., P. Vergara, F. Christinck, and E.E. Daniel.** Mechanism of action of somatostatin on the canine ileal circular muscle. *Am. J. Physiol.*, 1995 (accepted).
25. **Jury, J., N. Ahmedzadeh, and E.E. Daniel.** A mediator derived from arginine is released from sphincteric intrinsic nerves to mediate inhibitory junction potentials and relaxations. *Can. J. Physiol. Pharmacol.* 70: 1182-1189, 1993.
26. **Keef, K.D., C. Du, S.M. Ward, B. McGregor, and K.M. Sanders.** Enteric inhibitory neural regulation of human colonic circular muscle: role of nitric oxide. *Gastroenterology* 105: 1009-1016, 1993.
27. **King, B.F.** Excitatory and inhibitory junction potentials in canine antral circular muscle. *Neurogastroenterology and Motility* 6: 59-65, 1994.
28. **Kostka, P., E. Jang, E.G. Watson, J.L. Stewart, and E.E. Daniel.** NOS in the autonomic nervous system of the canine ileum. *J. Pharmacol. Exp. Therap.* 264(1): 234-239., 1993
29. **Mao, Y.K., W. Barnett, D.H. Coy, G. Tougas, and E.E. Daniel.** Distribution and characterization of vasoactive intestinal polypeptide (VIP)-binding in circular muscle and characterization of VIP-binding in canine small intestinal mucosa. *J. Pharmacol. Exp. Therap.* 258: 986-991, 1991.
30. **Nichols, K., A. Krantis, and W. Staines.** Histochemical localization of nitric oxide-synthesizing neurons and vascular sites in the guinea-pig intestine. *Neurosci.* 51(4): 791-799, 1992.
31. **Publicover, N.G., E.M. Hammond, and K.M. Sanders.** Amplification of nitric oxide signaling by interstitial cells isolated from canine colon. *Proc. Nat. Acad. Sci. (U.S.A.)* 90: 2087-2091, 1993.
32. **Rumessen, J.J., J.B. Mikkelsen, K. Qvortrup, and L. Thuneberg.** Ultrastructure of interstitial cells of Cajal in circular muscle of human intestine. *Gastroenterology* 104: 343-350, 1993.
33. **Rumessen, J.J., H.B. Mikkelsen, and L. Thuneberg.** Ultrastructure of interstitial cells of Cajal associated with deep muscular plexus of the human small intestine. *Gastroenterology* 102: 56-68, 1992.
34. **Rumessen, J.J., L. Thuneberg, and H.B. Mikkelsen.** Plexus muscularis profundus and associated interstitial cells. II. Ultrastructural studies of mouse small intestine. *Anat. Rec.* 203: 129-146, 1982.

35. Stark, M.E., A.J. Bauer, and J.H. Szurszewski. Effect of nitric oxide on circular muscle of the canine small intestine. *J. Physiol.* 444: 743-761, 1991.
36. Stark, M.E., A.J. Bauer, M.G. Sarr, and J.H. Szurszewski. Nitric Oxide mediates inhibitory nerve input in human and canine jejunum. *Gastroenterology* 104: 398-409, 1993.
37. Stark, M.E., and J.H. Szurszewski. Role of nitric Oxide in gastrointestinal and hepatic function and disease. *Gastroenterology* 103: 1928-1949, 1992.
38. Suzuki, N., C.L. Prosser, and V. Dahms. Boundary cells between longitudinal and circular layers: essential for electrical slow waves in cat intestine. *Am. J. Physiol.* 250: G287-G294, 1986.
39. Taylor, G.S., E.E. Daniel, and T. Tomita. Origin and mechanism of intestinal slow waves. In: *Proceedings of the Fifth International Symposium on Gastrointestinal Motility*, edited by Van-Trappen, G., Belgium: Typoff Press, pp. 102-106, 1975.
40. Thuneberg, L. Interstitial cells of Cajal: intestinal pacemakers? *Advances in Anatomy, Embryology and Cell Biology* 71: 1- 130, 1982.
41. Thuneberg, L., V. Johansen, J.J. Rumessen, and B.G. Anderson. Interstitial cells of Cajal: selective uptake of methylene blue inhibits slow wave activity. In: *Gastrointestinal Motility*, edited by Roman, C. pp. 495-502. Lancaster, England: MTP Press, pp. 495-502, 1984.
42. Torihashi, S., S. Kobayashi, W.T. Gerthoffer, and K.M. Sanders. Interstitial cells in deep muscular plexus of canine small intestine may be specialized smooth muscle cells. *Am. J. Physiol.* 265: G638-G645, 1993.
43. Töttrup, A., D. Svane, and A. Forman. Nitric oxide mediating NANC inhibition on opossum lower esophageal sphincter. *Am. J. Physiol.* 260: G385-G389, 1991.
44. Ward, S.M., H.H. Dalziel, K.D. Thornbury, D.P. Westfall, and K.M. Sanders. Nonadrenergic, noncholinergic inhibition and rebound excitation in canine colon depend on nitric oxide. *Am. J. Physiol.* 262: G237-G243, 1992.
45. Ward, S.M., C. Xue, W. Shuttleworth, D.S. Bredt, S.H. Snyder, and K.M. Sanders. NADPH diaphorase and NOS colocalization in enteric nerves of canine colon *Am. J. Physiol.* 263: G277-G248, 1992.
46. Wheeler, D.B., A. Randall, and R.W. Tsien. Roles of N-type and Q-type Ca^{2+}

channels in supporting hippocampal synaptic transmission. *Science* 264: 107-111, 1994.

FIGURE LEGENDS

Figure 1. *A.* A schematic of the intact cross-sectioned slab preparation showing the various regions and sites of recording electrode within the circular muscle layer. Actual recordings from two different muscle strips showing the spontaneous slow waves, IJPs and TSWs (evoked by the ending of the IJP) characteristic of those recorded from the myenteric plexus (MyP) (*B*) and the deep muscular plexus (DMP) (*C*). The methods for determining the various parameters associated with the spontaneous slow waves and responses to electrical field stimulation are indicated by lower case letters a to g (see text for details).

Figure 2. Effects of tetrodotoxin (TTX) on spontaneous slow waves, TSWs, IJPs, and circular muscle contractions in the full-thickness preparation. TTX after superfusion for 20-30 minutes abolished the IJPs in the regions of the MyP (*A*) and the DMP (*B*). TSWs elicited by high frequency stimulations (left of panels) were enhanced in amplitude in the presence of TTX in both regions, but they were unchanged when long (50-100 msec), single pulse stimulations (right of panels) were used (Table 1). Note the increase in circular muscle contractions after TTX (see also Figure 9).

Figure 3. *A.* In whole-thickness recordings near the MyP, superfusion of atropine and guanethidine or propranolol and phentolamine (all 1 μ M) did not significantly change the spontaneous slow waves, TSWs, IJPs, or circular muscle contractions (Top panel, Table 2A, Figure 9). L-NNA (50 μ M) after 30 minutes abolished the IJP and enhanced the

amplitudes of TSWs and phasic contractions (Second panel, Table 2A, Figure 9). D-ARG (1 mM) after 40 minutes was without effect (Third panel, Table 2A), but subsequent L-ARG (1 mM) superfusion resulted in partial recovery of IJPs (Fourth panel, Table 2A) and a full recovery of circular muscle contractions (Figure 9). All L-NNA effects were removed after 30 minutes of restoration of normal Krebs (Fifth panel). All panels were from a continuous recording from the same impalement. *B*. A full-thickness recording near the DMP showing the effects of neural blockers under the same conditions as in *A* but from a different preparation. The IJPs were abolished by L-NNA, partially reversed by L- but not D-ARG (Table 2B). All recordings were from the same cell. The amplitudes of TSWs were also significantly enhanced after L-NNA (Table 2B).

Figure 4. Effects of NANC blockers (atropine, guanethidine, phentolamine, and propranolol, all at 1 μ M) and L-NNA (50 μ M) on IJPs and TSWs evoked by high frequency (30 pps) electrical field stimulation delivered at different periods between slow waves (middle, early, and late phase). Notice that after blockade of IJP by L-NNA, TSW could be evoked without any delay at all periods of stimulation in the MyP region, and stimulation in the DMP region evoked a TSW during the "middle" period between slow waves but never during the "early" period. Tension calibration bars are 5 mN for *A* and 10 mN for *B*. The 5 second time scale applies to *A* and *B*.

Figure 5. *A*. Recordings near the DMP from the isolated circular muscle preparation showing the full inhibition of the IJP by L-NAME after 25 minutes and the partial

recovery of the IJP by L-ARG after 40 minutes. *B.* Recordings near the DMP from a different isolated circular muscle preparation showing that L-NAME increased the regularity of slow wave amplitudes. Effects of L-NAME as shown in *A* and *B* were unaccompanied by membrane potential changes.

Figure 6. *A.* In isolated circular muscle preparations, L-NNA had effects similar to L-NAME; *i.e.*, L-NNA increased the regularity of slow wave amplitude and circular muscle contractions but did not affect membrane potentials. *B.* Recordings near the MyP from the full-thickness preparation showing that L-NNA increased slow wave amplitudes and circular muscle contractions without effect on membrane potentials. Experiments shown in *A* and *B* were performed in the presence of atropine, guanethidine, propranolol, and phentolamine (all 1 μM , NANC blockers). Note that excitatory junction potentials were never recorded after superfusion with either L-NAME (see Figure 5A) or L-NNA (Figure 6B).

Figure 7. In the whole-thickness preparations, ω -CTX (3×10^{-7} M) abolished the IJP and delayed the occurrence of a TSW in both the MyP (*A*) and the DMP (*B*) recordings (compare top and middle panels). Subsequent superfusion of L-NNA abolished this delay and increased the TSW amplitudes (bottom panels). In other studies, when TTX instead of L-NNA was superfused after ω -CTX block of the IJP, the delay in induction of a TSW was similarly abolished.

Figure 8. *A.* Apamin did not abolish the IJP recorded in the full-thickness preparation near the DMP, but caused a 70 % inhibition of the amplitude of the IJPs and a 30 % enhancement of the amplitude of the TSWs after 20 minutes of superfusion. *B.* Spontaneous circular muscle contractions recorded in the organ bath were increased by apamin during similar periods of inhibition of the IJP amplitudes.

Figure 9. Motility index (see MATERIALS AND METHODS for definition) was enhanced by all treatments which abolished or inhibited the IJP. *A.* The number of different strips from different animals used were: Control, $n = 23$; Atr (atropine) + Gua (guanethidine) both at $1 \mu\text{M}$, $n = 15$; Pro (propranolol) + Phe (phentolamine) both at $1 \mu\text{M}$, $n = 23$; L-NNA at $50 \mu\text{M}$, $n = 20$; D-ARG at 1 mM , $n = 17$; L-ARG at 1 mM , $n = 13$; and washout, $n = 8$. *B.* The number of strips used were: TTX at $1 \mu\text{M}$, $n = 8$; ω -CTX at $3 \times 10^{-7} \text{ M}$, $n = 8$; and apamin at $1 \mu\text{M}$, $n = 9$.

Figure 10. Effects of the NO-donor, SIN-1 at $200 \mu\text{M}$, on the electrical and mechanical activities of the whole thickness muscle preparation. SIN-1 caused hyperpolarizations of 10-15 mV as recorded from smooth muscle cells near the MyP (Figure 10A) and the DMP (Figure 10B), and abolished the spontaneous circular muscle contractions. In Figure 10C, a recording near the DMP shows that SIN-1, applied after pretreatment with 10^{-6} M TTX, slightly but significantly increased the slow wave frequency but reduced the amplitude and duration of spontaneous slow waves and TSWs (Figure 10C).

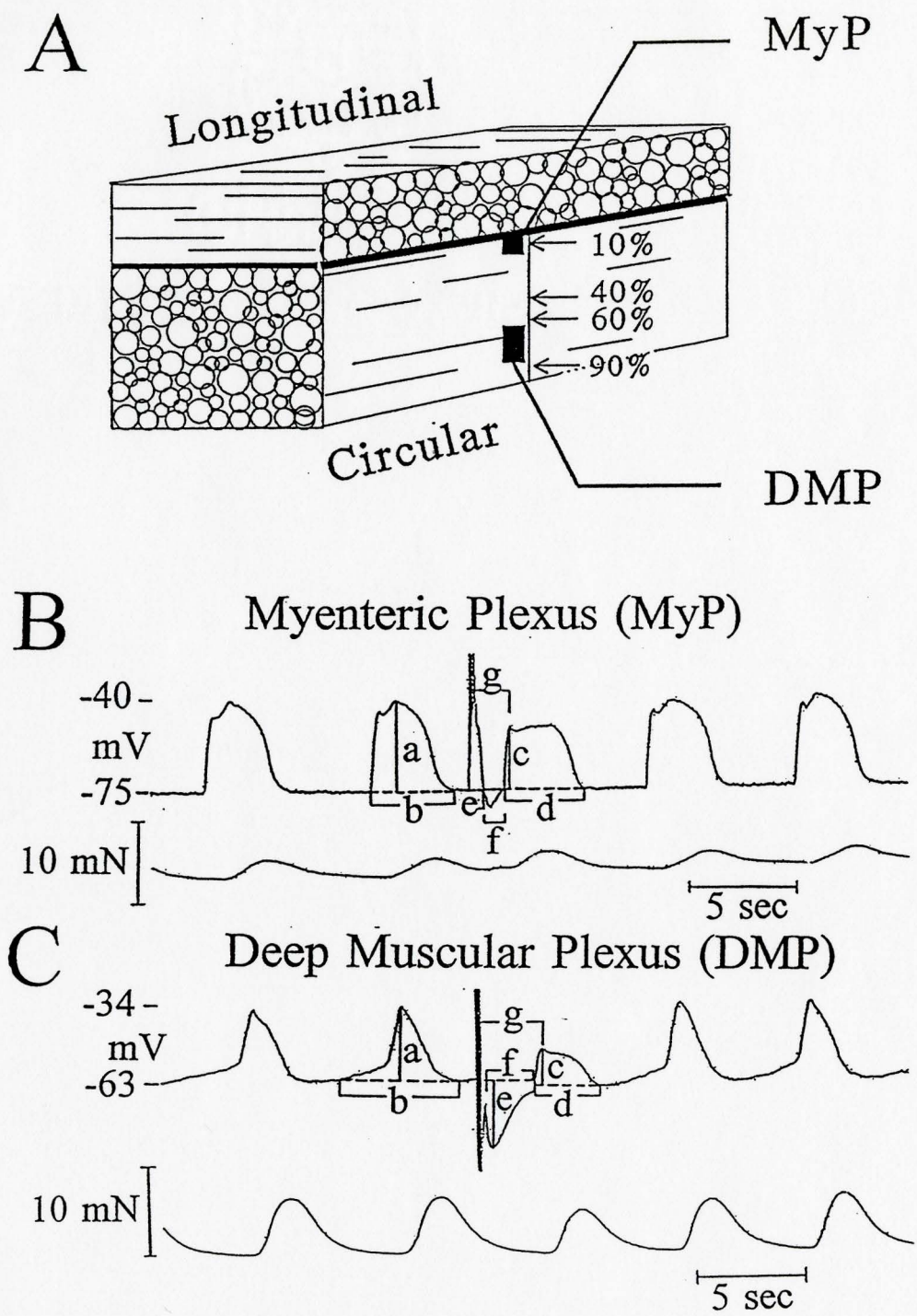


Fig. 1. Spontaneous slow waves and IJPs near pacemaking regions

Fig. 2. Blockade of nerve function with tetrodotoxin and its effects on spontaneous and triggered slow waves

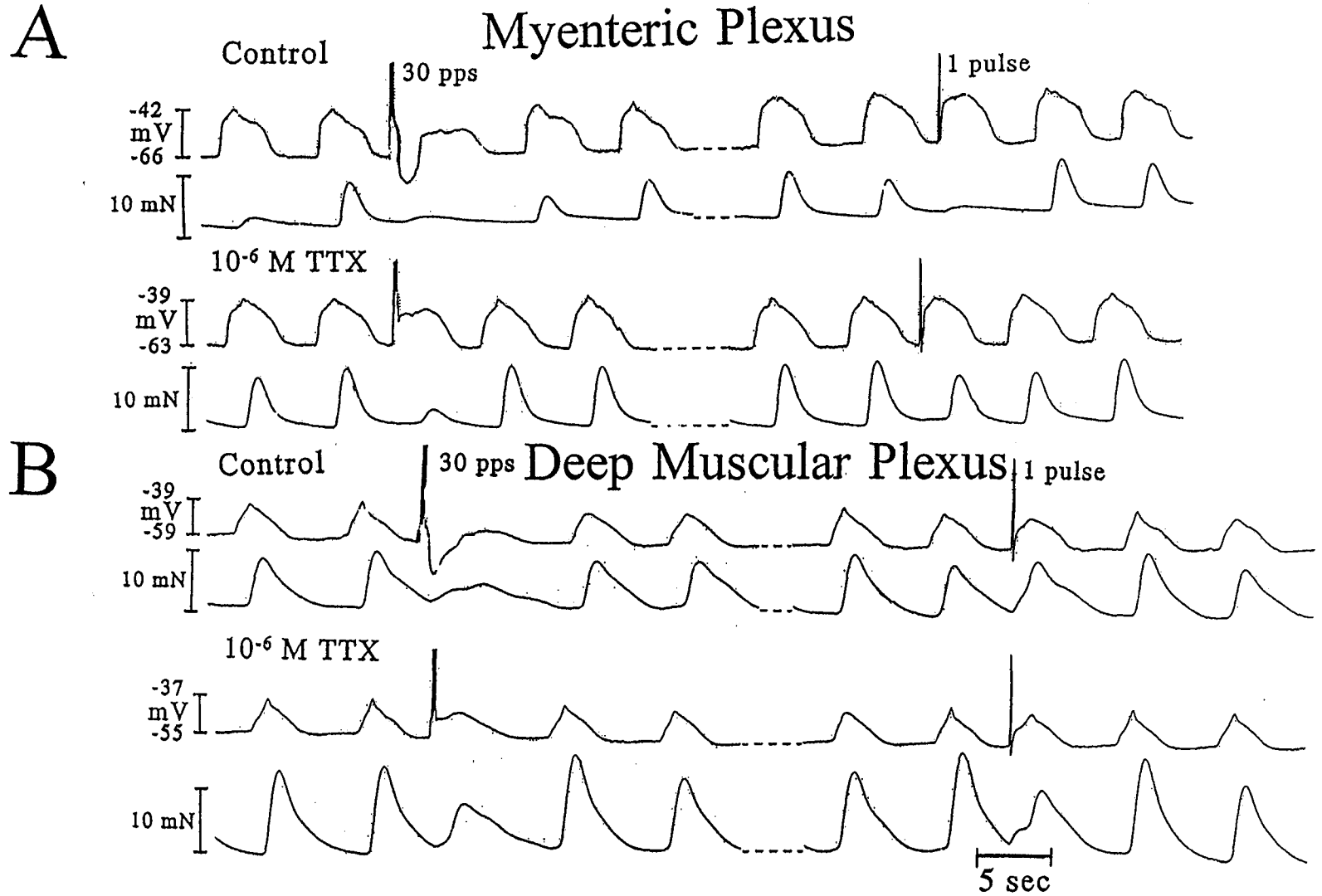


Fig. 3. Effects of nitric oxide synthesis blockers on slow waves and IJPs in different regions of circular muscle

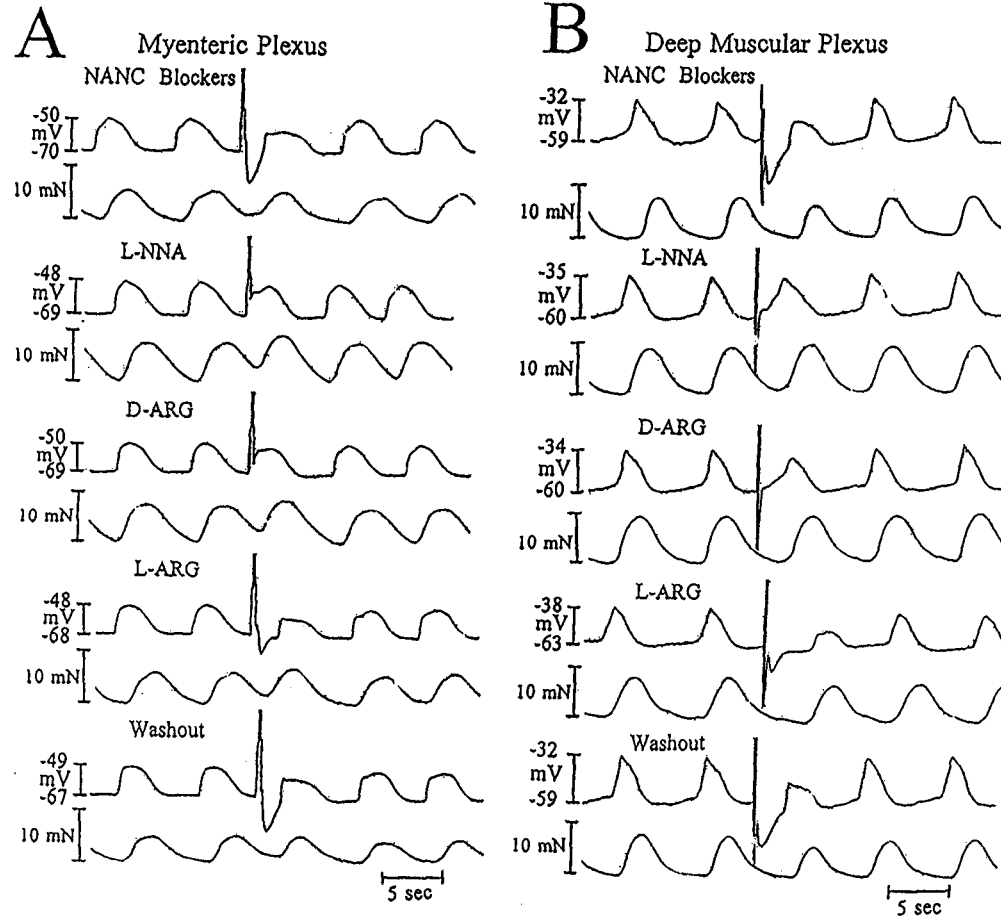


Fig. 4. Effect of nitric oxide synthesis blockers on time delays of triggered slow waves

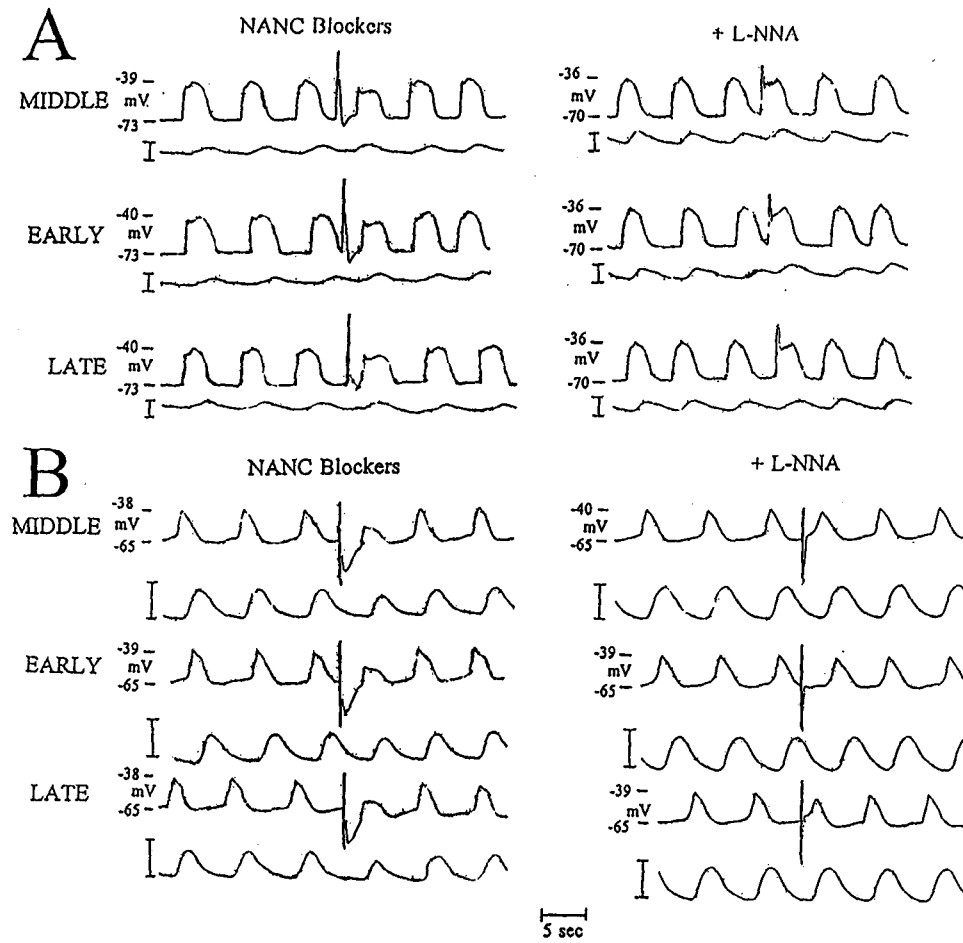
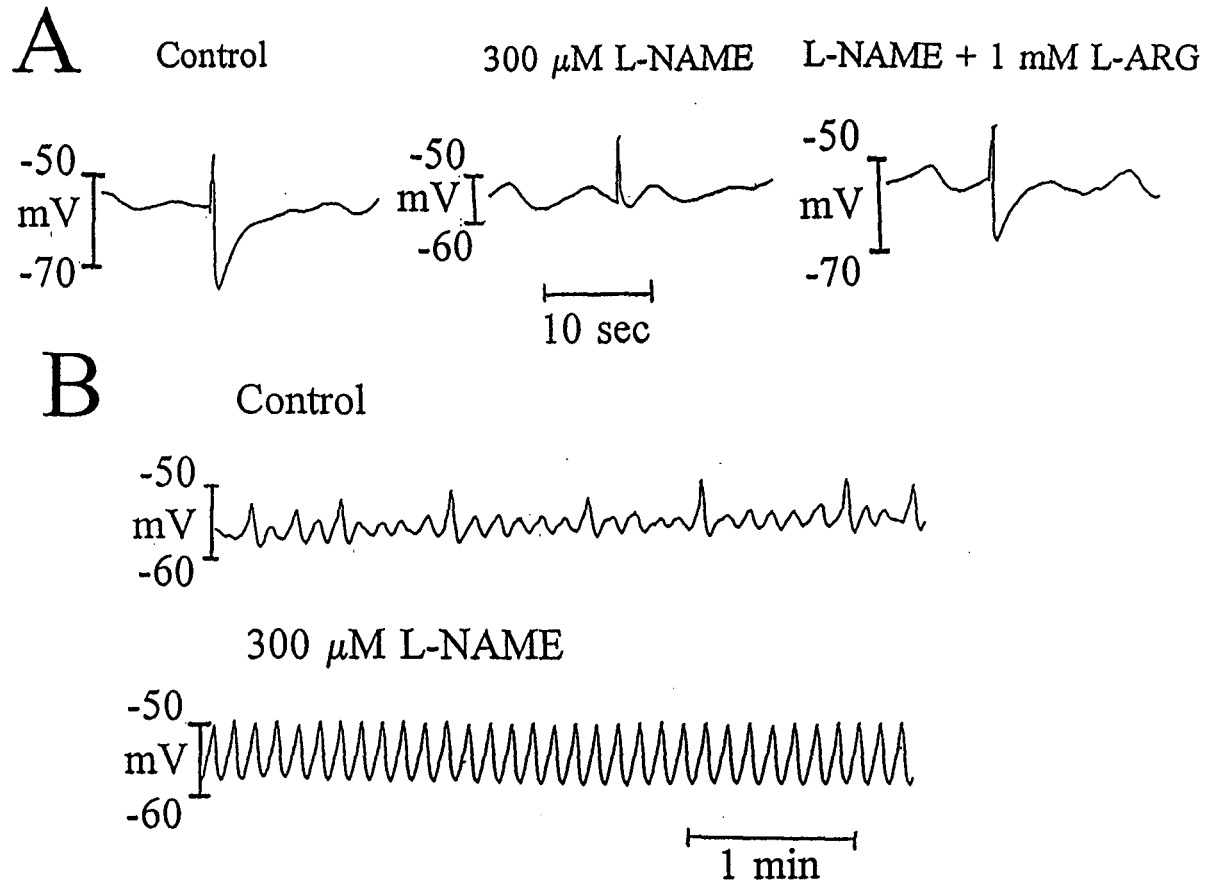


Fig. 5. Effects of nitric oxide synthesis blockers on slow waves and IJPs in isolated circular muscle



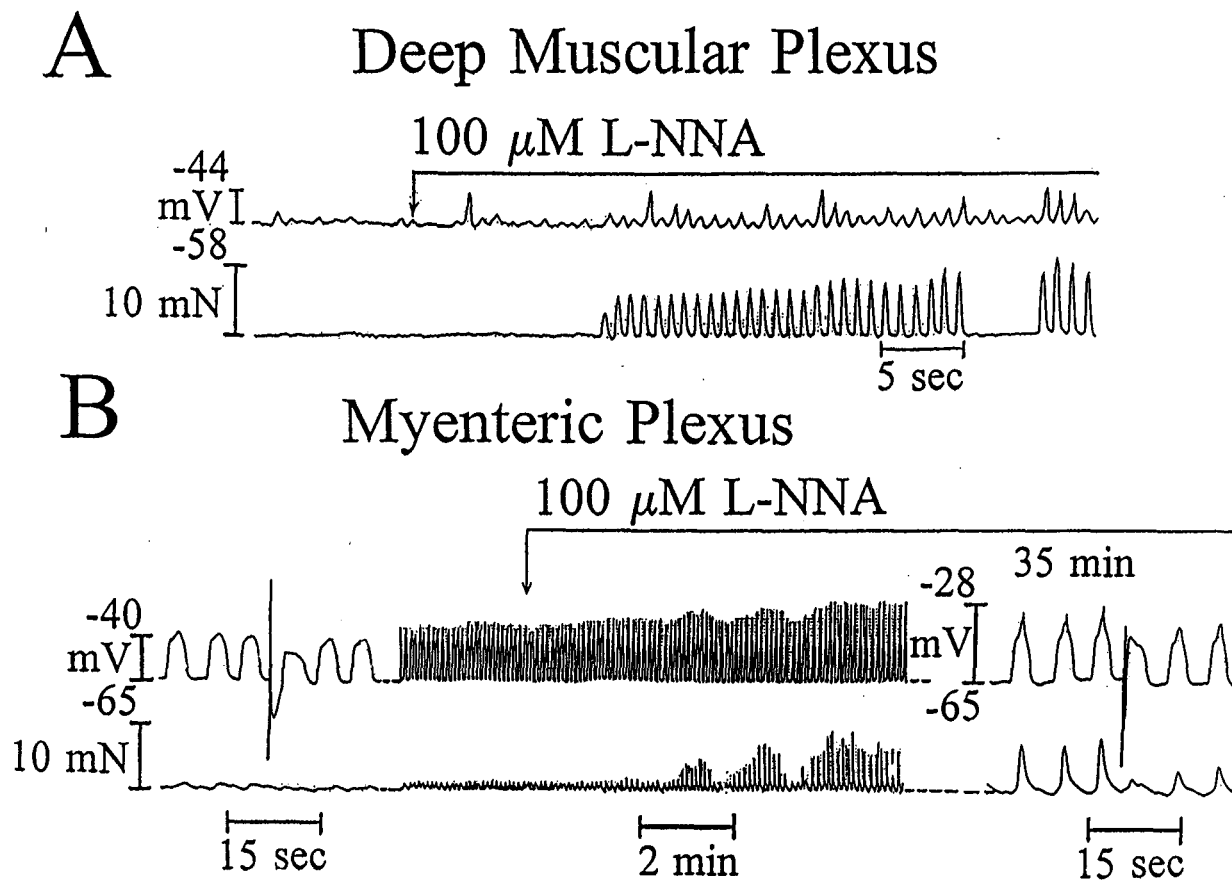
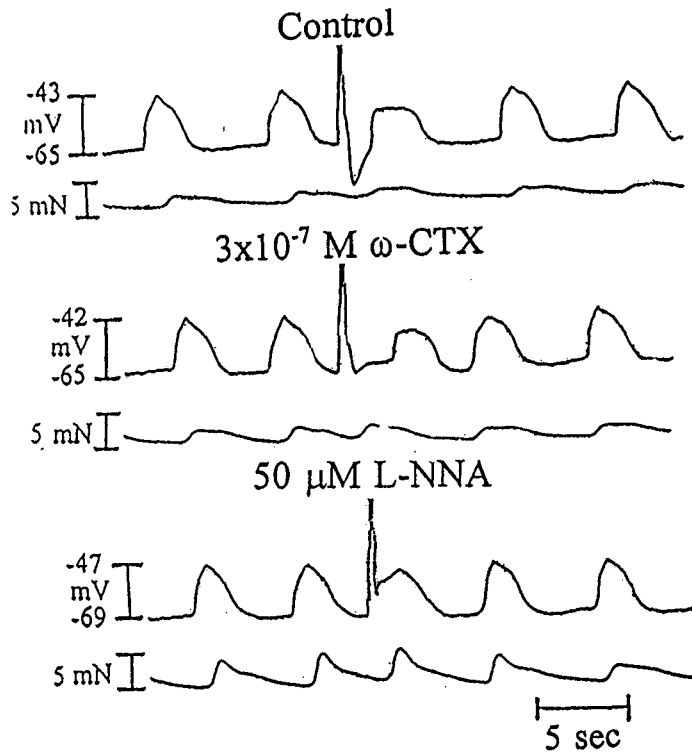


Fig. 6. Nitric oxide synthesis blockers enhance slow waves and contractions

A Myenteric Plexus



B Deep Muscular Plexus

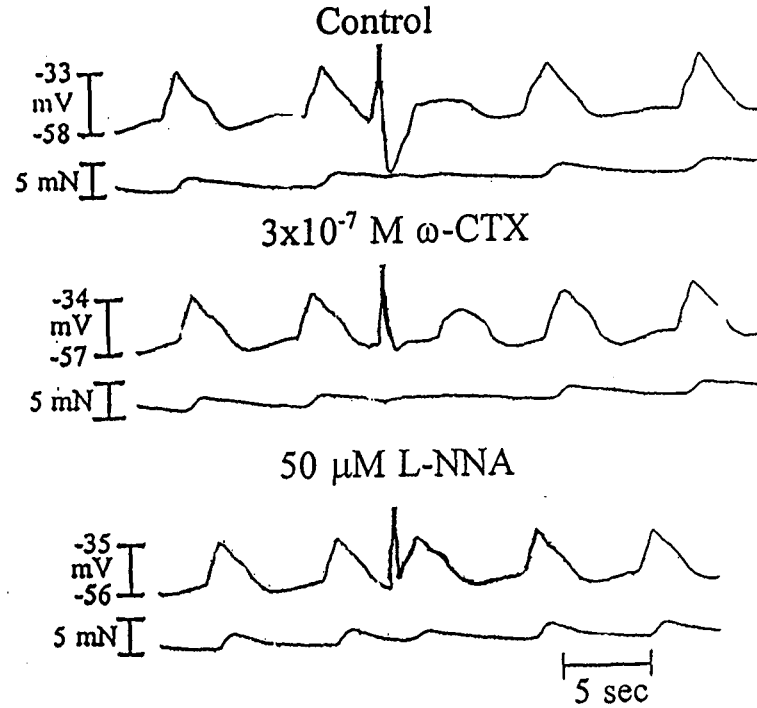
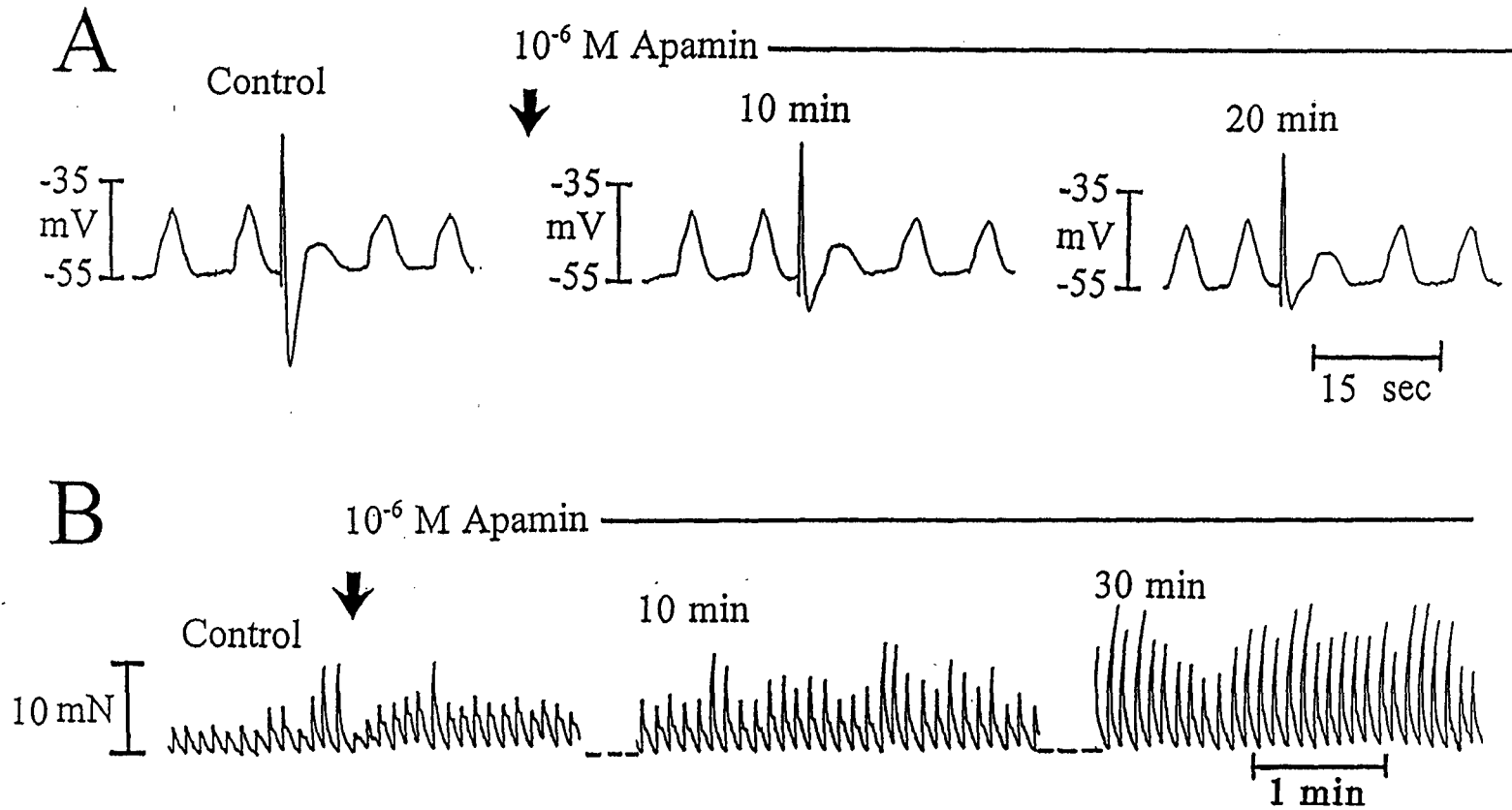


Fig. 7. Blockade of nerve function with ω -conotoxin GVIA and its effects on triggered slow wave delays

Fig. 8. Effects of K^+ channel blocker, apamin, on slow waves and contractions



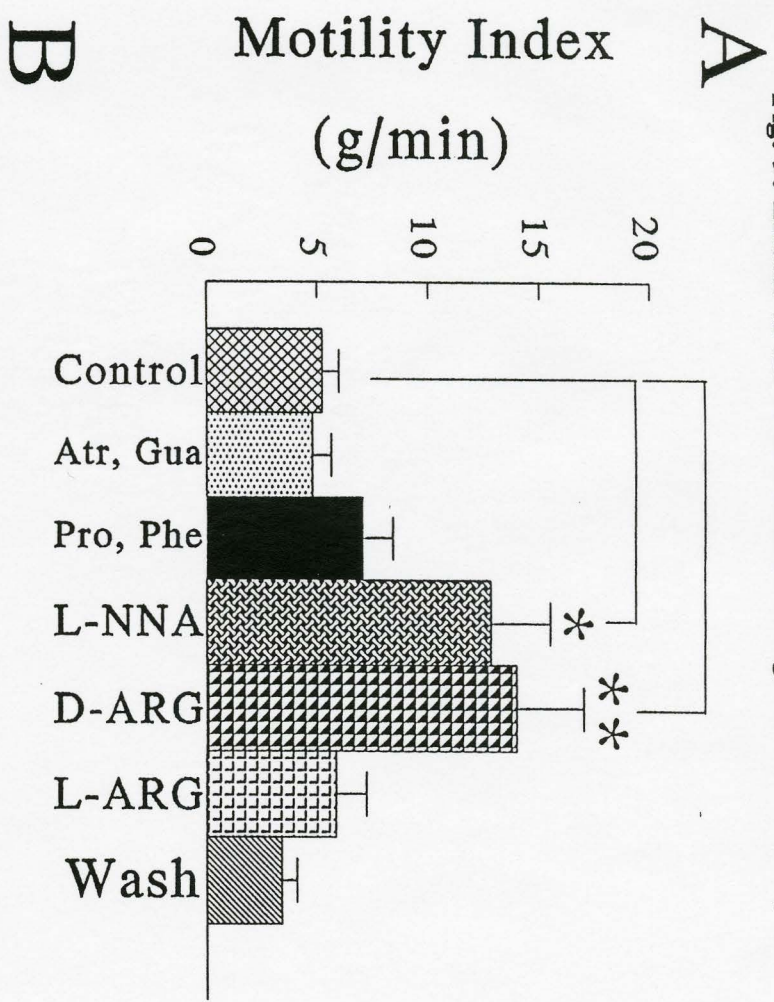
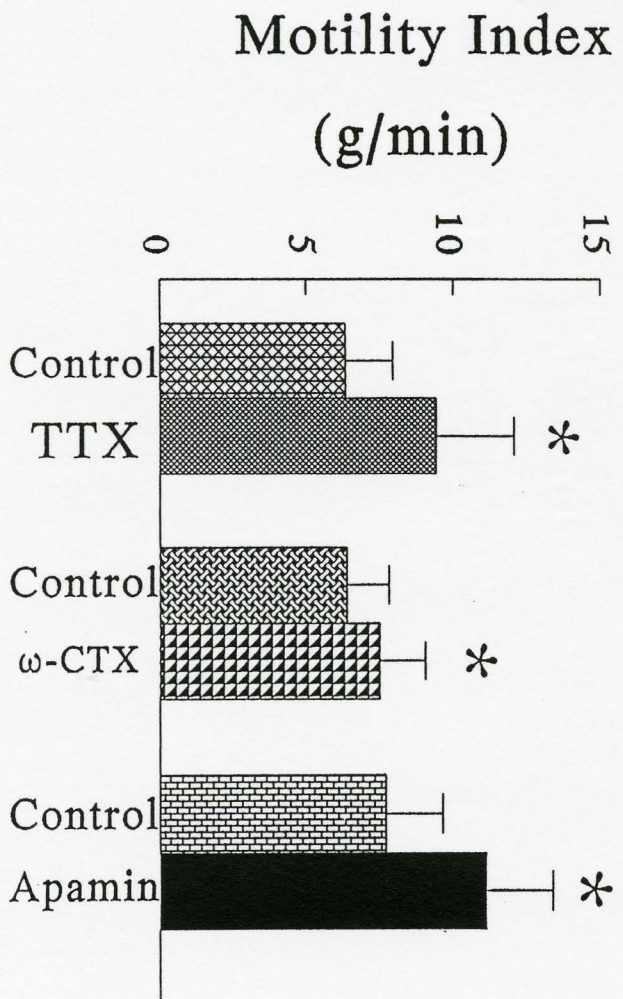


Fig. 9. Effects of nerve and muscle antagonists on motility index

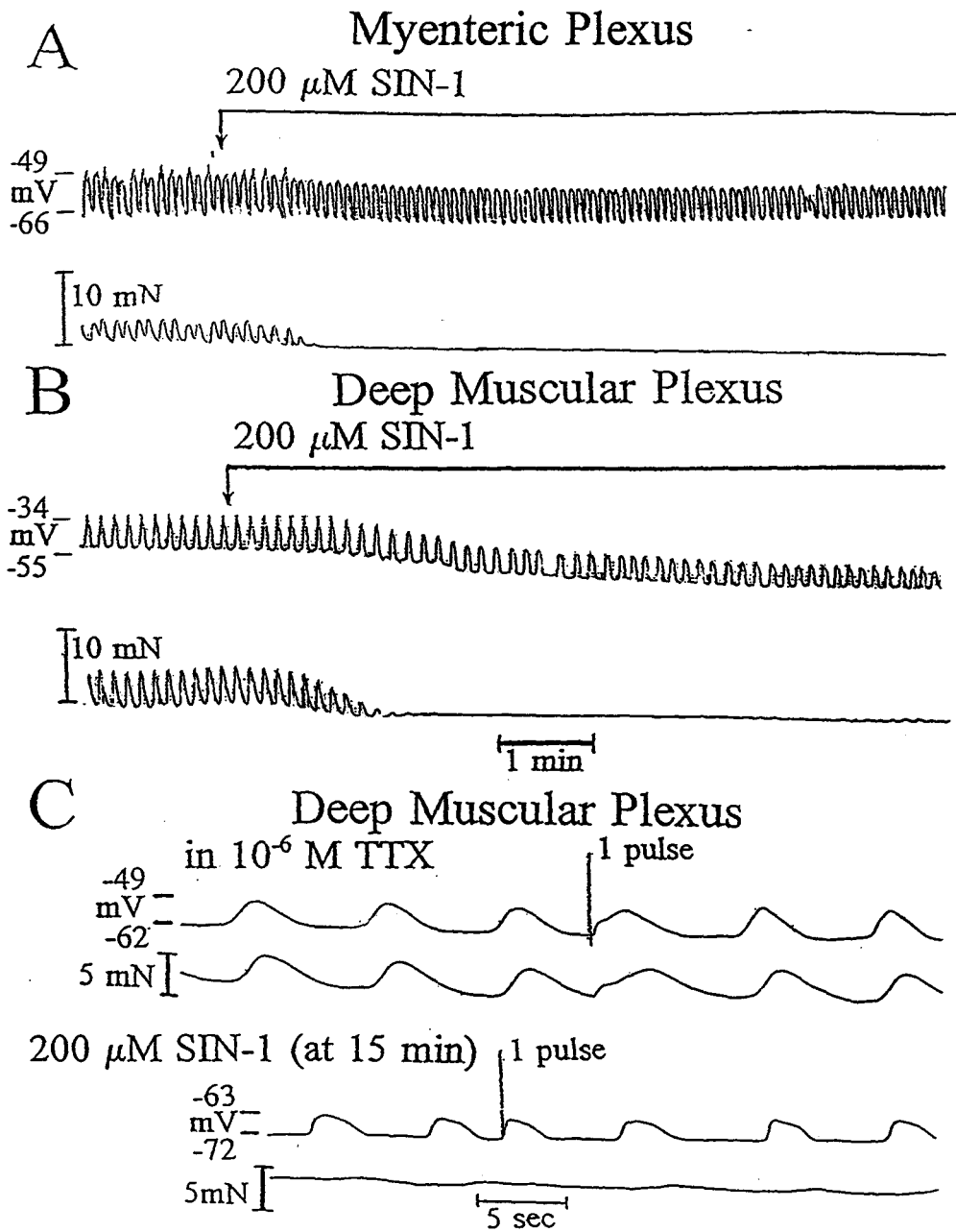


Fig. 10. Effects of nitric oxide donors on slow waves and contractions

Table 1. Electrophysiological effects of tetrodotoxin (10^{-7} M) on cells near the regions of the myenteric plexus (MyP) (A) and the deep muscular plexus (DMP) (B).

TREATMENT	SW Frequency (cpm)	SW Amplitude (mV)	SW Duration (sec)	Resting Membrane Potential (mV)	TSW _{30pps} Amplitude (mV)	TSW _{30pps} Duration (sec)	IJP Amplitude (mV)	IJP Duration (sec)	TSW _{30pps} Induction Delay (sec)
A. Control Near MyP	10.38 ± 0.31 (n=4)	24.6 ± 0.89 (n=4)	4.48 ± 0.08 (n=4)	-66.75 ± 1.93 (n=4)	15.68 ± 1.11 (n=4)	4.96 ± 0.46 (n=4)	13.73 ± 0.90 (n=4)	1.53 ± 0.07 (n=4)	2.62 ± 0.23 (n=4)
TTX Near MyP	10.50 ± 0.29 (n=4) NS	25.5 ± 0.78 (n=4) NS	4.5 ± 0.20 (n=4) NS	-63.75 ± 0.25 (n=4) NS	21.9 ± 1.90 (n=4) *	4.19 ± 0.11 (n=4) NS	0.0 ± 0.0 (n=4) **	0.0 ± 0.0 (n=4) **	0.60 ± 0.60 (n=4) **
B. Control Near DMP	9.0 ± 0.58 (n=3)	18.13 ± 2.54 (n=3)	5.10 ± 0.82 (n=3)	-59.0 ± 1.16 (n=3)	9.10 ± 2.07 (n=3)	4.69 ± 0.70 (n=3)	19.60 ± 1.31 (n=3)	1.81 ± 0.10 (n=3)	3.56 ± 0.36 (n=3)
TTX Near DMP	9.27 ± 0.43 (n=3) NS	17.33 ± 3.08 (n=3) NS	5.03 ± 0.64 (n=3) NS	-57.67 ± 2.19 (n=3) NS	14.83 ± 2.90 (n=3) *	4.99 ± 0.58 (n=3) NS	0.0 ± 0.0 (n=3) **	0.0 ± 0.0 (n=3) **	0.0 ± 0.0 (n=3) **

No significance was denoted by NS = $P > 0.05$, and significances were compared to relevant controls.

Table 2A. Electrophysiological effects of L-NNA (50 μ M), D- and L-ARG (both 1 mM) on cells near the region of the myenteric plexus (MyP).

Treatment	Slow Wave Frequency (cycles/min)	Slow Wave Amplitude (mV)	Slow Wave Duration (sec)	Resting Membrane Potential (mV)	TSW _{30pps} Amplitude (mV)	TSW _{30pps} Duration (sec)	IJP Amplitude (mV)	IJP Duration (sec)	TSW _{30pps} Induction Delay (sec)
1. NANC Control near MyP	10.00 \pm 0.22 (n=13) NS	22.38 \pm 1.72 (n=13) NS	4.19 \pm 0.09 (n=13) NS	-70.27 \pm 1.87 (n=13) NS	13.73 \pm 1.45 (n=12) NS	4.15 \pm 0.13 (n=12) NS	16.23 \pm 1.59 (n=12)	1.46 \pm 0.12 (n=12) NS	2.45 \pm 0.16 (n=12) NS
2. + L-NNA	10.30 \pm 0.18 (n=13) NS	24.96 \pm 1.82 (n=13) NS	4.07 \pm 0.12 (n=13) NS	-69.27 \pm 1.79 (n=13) NS	19.62 \pm 1.76 (n=12) ** wrt 1	3.82 \pm 0.15 (n=12) NS	0.0 \pm 0.0 (n=12) *** wrt 1	0.0 \pm 0.0 (n=12) *** wrt 1	0.0 \pm 0.0 (n=12) ***
3. + D-ARG	10.20 \pm 0.37 (n=5) NS	23.32 \pm 3.01 (n=5) NS	4.08 \pm 0.14 (n=5) NS	-70.00 \pm 3.29 (n=5) NS	17.38 \pm 1.13 (n=5) NS	4.02 \pm 0.16 (n=5) NS	0.0 \pm 0.0 (n=5) *** wrt 1	0.0 \pm 0.0 (n=5) *** wrt 1	0.0 \pm 0.0 (n=5) *** wrt 1
4. + L-ARG	9.07 \pm 0.97 (n=8) NS	21.38 \pm 1.98 (n=8) NS	3.98 \pm 0.16 (n=8) NS	-68.25 \pm 2.57 (n=8) NS	11.40 \pm 1.01 (n=8) ** wrt 2	4.52 \pm 0.34 (n=8) NS	11.1 \pm 1.94 (n=8) * wrt 1	1.79 \pm 0.22 (n=8) ** wrt 1	3.55 \pm 0.44 (n=8) ** * wrt 1
5. Washout	9.98 \pm 0.44 (n=6) NS	22.30 \pm 1.80 (n=6) NS	4.07 \pm 0.12 (n=6) NS	-71.83 \pm 2.18 (n=6) NS	11.43 \pm 1.29 (n=6) NS	3.98 \pm 0.14 (n=6) NS	17.40 \pm 1.65 (n=6) NS	1.38 \pm 0.08 (n=6) NS	3.08 \pm 0.08 (n=6) NS

No significance was denoted by NS= $P > 0.05$. Significances were with respect to (wrt) controls unless otherwise stated. NANC blockers consisted of atropine, guanethidine, propranolol, and phentolamine (all at 1 μ M). Bonferroni correction was used in ANOVA for multiple comparisons.

Table 2B. Electrophysiological effects of L-NNA (50 μ M), D- and L-ARG (both at 1mM) on cells near the region of the deep muscular plexus (DMP).

Treatment	Slow Wave Frequency (cycles/min)	Slow Wave Amplitude (mV)	Slow Wave Duration (sec)	Resting Membrane Potential (mV)	TSW _{30pps} Amplitude (mV)	TSW _{30pps} Duration (sec)	IJP Amplitude (mV)	IJP Duration (sec)	TSW _{30pps} Induction Delay (sec)
1. NANC Control near DMP	8.84 \pm 0.10 (n=5) NS	19.68 \pm 2.90 (n=5) NS	5.5 \pm 0.41 (n=5) NS	-57.80 \pm 1.99 (n=5) NS	7.24 \pm 1.38 (n=5) NS	3.73 \pm 0.27 (n=5) NS	22.54 \pm 2.81 (n=5) NS	2.01 \pm 0.12 (n=5) NS	2.80 \pm 0.22 (n=5) NS
2. + L-NNA	8.94 \pm 0.06 (n=5) NS	19.22 \pm 2.63 (n=5) NS	5.50 \pm 0.41 (n=5)	-57.80 \pm 2.22 (n=5) NS	14.3 \pm 3.68 (n=5) *	4.80 \pm .43 (n=5) NS	0.0 \pm 0.0 (n=5) ***	0.0 \pm 0.0 (n=5) **	0.96 \pm 0.96 (n=5) *
3. + D-ARG	8.88 \pm 0.13 (n=4) NS	17.25 \pm 2.74 (n=4) NS	5.13 \pm 0.55 (n=4) NS	-58.00 \pm 2.94 (n=4) NS	14.33 \pm 2.53 (n=4) *	5.40 \pm 0.26 (n=4) *	0.0 \pm 0.0 (n=5) ***	0.0 \pm 0.0 (n=4) **	1.35 \pm 1.30 (n=4) *
4. + L-ARG	8.25 \pm 0.25 (n=4) ***	16.3 \pm 2.73 (n=4) NS	5.45 \pm 0.78 (n=4) NS	-58.75 \pm 3.52 (n=4) NS	7.33 \pm 1.23 (n=4) NS	3.43 \pm 0.24 (n=4) NS	12.48 \pm 3.75 (n=4) NS	3.92 \pm 0.41 (n=4) ***	4.4 \pm 0.41 (n=4) NS
5. Washout	9.25 \pm 0.21 (n=3) NS	11.87 \pm 1.31 (n=3) NS	4.80 \pm 0.70 (n=3) NS	-55.33 \pm 0.67 (n=3) NS	7.10 \pm 1.51 (n=3) NS	3.53 \pm 0.29 (n=3) NS	13.93 \pm 6.44 (n=3) NS	3.47 \pm 0.89 (n=3) NS	3.65 \pm 1.35 (n=3) NS

No significance was denoted by NS= $P > 0.05$. Significances were with respect to (wrt) controls unless otherwise stated. NANC blockers consisted of atropine, guanethidine, propranolol, and phentolamine (all at 1 μ M). Bonferroni correction was used in ANOVA for multiple comparisons.

CHAPTER 3.3

PAPER No. 3

Ca²⁺ ROLE IN CANINE ILEUM SLOW WAVE FORMATION, NERVE ACTIVATION, AND EXCITATION-CONTRACTION COUPLING

Submitted June, 1995 to *American Journal of Physiology (Cell Physiology)*, in revision

Francisco Cayabyab's contribution:

- (i) performance of all electrophysiological studies except for those studying effects of nifedipine
- (ii) data presentation and statistical analysis
- (iii) writing and preparing manuscript for submission to *American Journal of Physiology*

**Ca²⁺ ROLE IN CANINE ILEUM SLOW WAVE FORMATION,
NERVE ACTIVATION, AND EXCITATION-CONTRACTION
COUPLING**

Francisco S. Cayabyab^{1,2}, Hubert deBruin², Marcel Jiménez³, and Edwin E. Daniel¹.

Departments of Biomedical Sciences¹ and Electrical & Computer Engineering²,

McMaster University, 1200 Main Street West, Hamilton, Ontario L8N 3Z5; and

Department of Cell Biology and Physiology³. Universitat Autònoma de Barcelona,

Bellaterra 08193 Barcelona, Spain.

Running title: **Ca²⁺ and canine ileal slow waves, contractions, and IJPs**

Address for correspondence: E.E. Daniel, PhD

Division of Physiology and Pharmacology

Department of Biomedical Sciences

Faculty of Health Sciences

McMaster University

1200 Main Street West

Hamilton, Ontario, Canada L8N 3Z5

Telephone no: 1-905-525-9140 ext. 22130.

Fax no. 1-905-524-3795 or 1-905-648-8506

ABBREVIATIONS

BK - large conductance Ca^{2+} -activated K^+ channels

Ca^{2+} -ATPase - Ca^{2+} adenosinetriphosphatase

Ca_i^{2+} - intracellular Ca^{2+}

Ca_o^{2+} - extracellular Ca^{2+}

CICR - Ca^{2+} -induced Ca^{2+} -release

CM - circular muscle

CPA - cyclopiazonic acid

E-C - excitation-contraction

EGTA - ethyleneglycol-bis(betaaminoethylether)-N,N,N,N-tetraacetic acid

DMP - deep muscular plexus

EFS - electrical field stimulation

EJP - excitatory junction potential

ICC - interstitial cells of Cajal

IJPs - inhibitory junction potentials

MyP - myenteric plexus

NANC - nonadrenergic noncholinergic

NO - nitric oxide

ω -CTX - ω -conotoxin GVIA

SR - sarcoplasmic reticulum

TSWs - triggered slow waves

ABSTRACT

The roles of Ca^{2+} in nerve activation, slow wave generation, and excitation-contraction (E-C) coupling in canine ileum circular muscle (CM) were studied. Simultaneous recordings of mechanical and intracellular electrical activity were made in cross-sectioned slabs of muscularis externa or of isolated CM with deep muscular plexus (DMP) intact. Triangular slow waves recorded near the DMP and plateau-type slow waves recorded near the myenteric plexus (MyP), oscillated with frequencies of 9-10 cycles/min in the whole-thickness preparation as did triangular slow waves found in isolated CM. CM contractions accompanied both types of slow waves. The L- Ca^{2+} channel blocker, nifedipine at $3 \times 10^{-7}\text{M}$, abolished contractions but affected neither slow waves nor inhibitory junction potentials (IJPs) (0.5 msec, 25 pps, 80-120 V, in trains of 300 msec). The ending of an IJP or a 50-100 msec pulse elicited a triggered slow wave (TSW) (maximum amplitude near MyP) throughout the CM in the whole-thickness but not in isolated CM preparations. The neuronal N- Ca^{2+} channel blocker, ω -conotoxin GVIA at $3 \times 10^{-7}\text{M}$, did not affect slow waves or TSWs, but abolished IJPs. Ni^{2+} (200 μM), a non-selective Ca^{2+} channel antagonist, did not affect IJPs but suppressed contractions and slow wave amplitudes and frequencies from both pacemaking regions. Ni^{2+} also inhibited TSW amplitude while increasing both slow wave and TSW durations. Ca^{2+} -free Krebs (100 μM EGTA) abolished IJPs and contractions prior to changes in CM membrane potentials. After 10-12 min in Ca^{2+} -free solution, TSWs evoked by a 100 msec pulse were attenuated by 50% in amplitude near MyP and abolished near DMP in the full-thickness preparation. Slow waves recorded near DMP persisted and resembled those

recorded near MyP in the full-thickness preparation but were abolished in isolated CM. The inhibitor of sarcoplasmic reticulum Ca^{2+} -ATPase, cyclopiazonic acid (CPA, 10-30 μM), increased slow wave frequency, produced spikes on slow wave plateaus, increased CM tone, but did not affect IJPs or resting membrane potentials. We conclude that Ca^{2+} influx through neither L- nor N- Ca^{2+} channels helps to initiate ileal slow waves; L- Ca^{2+} channels are involved in E-C coupling. Nerve-mediated and spontaneous release of IJP mediator requires Ca^{2+} influx into nerves through N- Ca^{2+} channels, but does not influence pacemaking. Intracellular Ca^{2+} stores modulate ileal pacemaking, which is dominated by MyP pacemakers under normal and reduced Ca_o^{2+} levels.

Key words: L- and N-type Ca^{2+} channels, interstitial cells of Cajal, Ni^{2+} , intercellular communication, inhibitory junction potentials, excitation-contraction coupling, intracellular Ca^{2+} stores, cyclopiazonic acid, intestinal pacemaking

INTRODUCTION

The innervation of the muscularis externa of canine ileum is concentrated at the myenteric plexus (MyP) and the deep muscular plexus (DMP). At each of these plexuses, the presence of interstitial cells of Cajal (ICC) has been reported in several species including mouse (37,46), dog (16), and human (34,35,36). ICC are postulated to be essential for the pacemaker function of the gut (reviewed in 13). In several intestinal muscles, slow waves paced by ICC and occurring in smooth muscle *in vitro* can directly initiate contractions with or without action potentials (21,38,45). ICC are coupled to one another and to smooth muscle cells by gap junctions and other junctions (16). These networks of ICC at each of the plexuses may determine the homogeneity or heterogeneity in slow wave configurations in various regions of the canine gut (3,4,9,21,39).

Based on morphological evidence, the networks of ICC have also been postulated to play an important role in the neurotransmission of nonadrenergic, noncholinergic (NANC) inhibitory activity (13). That ICC are often found in close proximity to nerve profiles (16) containing vasoactive intestinal polypeptide and nitric oxide (NO) synthase (6) has led to the hypothesis that the slow waves they generate are likely to be modulated by release of various neurotransmitters. NO or a NO-related compound has recently been suggested to be the primary NANC neurotransmitter mediating inhibitory responses in canine ileum (8,12), proximal duodenum (4), jejunum (40,41), pylorus (2), and other regions of the gut (see review in 42). NO has been shown through blockade of neuronal function with tetrodotoxin or the N-Ca²⁺ channel antagonist, ω -conotoxin GVIA (ω -CTX), to be tonically released from nerves of the *ex vivo* perfused canine ileum (14) and from

in vitro preparations of the ileal muscularis externa (8; Cayabyab, F.S., M. Jiménez, P. Vergara, H. deBruin, and E.E. Daniel, unpublished observations). However, whether tonic NO-release occurs *in vitro* and requires Ca^{2+} entry to influence spontaneous slow waves and triggered slow waves (TSWs) and their associated contractions, remains to be elucidated.

Studies done using tissues of rabbit jejunum and duodenum (10,17) showed marked temperature dependence of the slow wave frequency, suggesting that the conductance of ionic currents mediating the slow waves or their pacemakers was metabolically regulated. The ionic mechanism involved in the regulation of slow waves remains unclear and most of the studies have been undertaken using colonic and gastric slow waves. The amplitude of the plateau phase is reduced by L- Ca^{2+} channel blockers in cat antral slow waves (33). A recent study in canine antral smooth muscle (31) showed that the two products of phosphatidylinositol hydrolysis, inositol 1,4,5-triphosphate and diacylglycerol, as well as ATP inhibited the slow waves, phasic contractions, and associated intracellular Ca^{2+} (Ca_i^{2+}) elevation mediated by Ca^{2+} influx. In canine colon, blockers of L- Ca^{2+} channels slowed the upstroke and diminished the plateau amplitude and duration in the circular muscle (CM) slow waves (25). However the upstroke persists and the slow wave frequency is insensitive to L- Ca^{2+} channel blockers (25). In rabbit jejunal longitudinal muscle, L- Ca^{2+} channel blockers did not affect slow waves but abolished spike potentials and phasic contractions (18). However, removal of extracellular Ca^{2+} (Ca_o^{2+}) reduced slow wave amplitude and its rate of rise (18).

In the canine colon it is clear that there are two sets of pacemakers, one associated

with the ICC network at the inner border of CM and another associated with the ICC network of the MyP (5,39). In contrast, it is less clear that two such networks exist in the canine small intestine. Hara *et al.* (21) suggested that one near the MyP was predominant in canine jejunum while one located near the DMP was unable to induce regular slow waves. Bayguinov *et al.* (4) found a uniformity of slow waves throughout the canine proximal duodenum but did not determine their origin. Recently, we found evidence of heterogeneity in slow wave configurations across the CM layer of the canine ileum (9; Jiménez, M., F.S. Cayabyab, P. Vergara, and E.E. Daniel, unpublished observations) which has been described in relation to the clear presence of two distinct ICC networks found in these two plexuses in the small intestine (16,34,35,36,37,46). However, our data suggested that each of the two potential gut pacemakers, located in the MyP and DMP regions, could function independently, but the nature of their coupling in the intact system remains unclear (13).

The present study evaluated the roles of Ca^{2+} channel conductance in the neurotransmitter release and in the generation of electrical slow waves and their coupling to CM contraction. Simultaneous recordings of mechanical and intracellular electrical activity were undertaken from cells located near the MyP and DMP regions in the CM layer of the canine ileum. A variety of Ca^{2+} channel antagonists (L-type blocker, nifedipine, N-type blocker, ω -CTX, and non-selective voltage-gated and receptor operated Ca^{2+} channel antagonist, Ni^{2+}) as well as removal of external Ca^{2+} were tested to provide information on the role of Ca^{2+} in the mechanisms underlying the different configurations of slow waves recorded near the MyP and the DMP. We also evaluated whether

prevention of Ca^{2+} uptake by sarcoplasmic reticulum (SR) affected pacemaking and E-C coupling, by using cyclopiazonic acid (CPA) as a tool for selectively inhibiting the SR Ca^{2+} -ATPase (15,28). Preliminary accounts of this work have been published (8,9).

MATERIALS AND METHODS

Preparation of ileal circular muscle or whole-thickness preparation. Healthy adult mongrel dogs of either sex, ranging from 10 to 25 Kg, were euthanized using intravenous sodium pentobarbitone (65 mg/kg). This procedure was approved by the McMaster University Animal Care Committee. The abdomen was immediately opened along the midline and a segment of ileum (10 cm) was removed from a position about 10 cm oral to the ileocecal junction. The dissection was made at room temperature in normal oxygenated Krebs solution. The segment of ileum was cleaned of external fat and connective tissue and opened along the mesenteric border. The mucosa and submucosa were removed taking care not to damage the CM. In some cases, the longitudinal muscle and myenteric plexus were also removed in the isolated CM strips using the technique already described (12). Electron micrographs of this preparation confirmed that the longitudinal muscle and the MyP were completely removed and the DMP intact. Tissue strips (1 x 10 mm) of the whole-thickness or isolated CM preparations were cut parallel with the CM fibres and placed in a 5 ml organ chamber for electrophysiological recordings. The strips were pinned to the sylgard floor of the chamber to facilitate recordings of intracellular electrical activity. A region of about 1 mm² area with circular and longitudinal muscles was isolated using fine pins to ensure prolonging and maintaining impalements of CM cells by the same recording electrode during an experiment. About 1 cm of unpinned region was connected to a force transducer for recording of mechanical activity. This unpinned region was stretched by 2 g once, and the whole preparation was allowed to equilibrate for two to three hours before

impalements were attempted. The tissue was superfused constantly by Krebs solution at a rate of 3 ml/min (37°C). Glass electrodes filled with 3 M KCl with resistances ranging from 30 to 80 M Ω were used to impale the cells. Membrane potential changes were measured using a standard electrometer (World Precision Instruments KS-700). The signal was monitored on a dual beam oscilloscope (Tektronix D13; 5A22N differential amplifier; 5B12N dual time base) and recorded on 1/4 inch magnetic tape with a Hewlett-Packard instrumentation recorder and on chart paper (Gould 2200). A microscope (M3C, Wild Leitz) with calibrated eyepiece graticule was used to select accurately the position of the recording electrode. The electrical activity was studied in the following areas of the CM in whole-thickness preparations and isolated circular muscle preparation (see Figure 1A): 1) near the MyP (0-10% of the total CM width close to the MyP, n = 50); 2) near the DMP (60-90% of the CM width from the MyP, n = 38); and 3) near the DMP region in the isolated CM preparation (n = 25). The number of strips from at least three different animals used from each type of experiment is indicated by n, and a total of 48 animals were used in this study.

The effects of nifedipine on the mechanical activity were not recorded simultaneously with the intracellular electrical activities in the early stages of the study, but were later also studied by recording tension changes without electrical recordings in the organ bath. CM strips (2 cm x 1 mm) were suspended in a 15 ml organ bath (37 \pm 2 °C) containing Krebs solution bubbled with 95% O₂ - 5% CO₂. Each strip was fixed at one end of an electrode holder by a silk ligature, and the other end of the tissue was fixed with another ligature to a force displacement transducer (Grass FTOC3). Initial

tension (2.5 grams) was applied to each muscle strip which was then allowed to equilibrate for 2 hours. The changes in tension were recorded on a Beckman R611 dynograph.

Electrical field stimulation. Electrical field stimulation was achieved using a pore-type silver electrode in contact with the tissue on one side of the strip, and a silver ground electrode on the other side. Stimuli were provided by a Grass S88 stimulator through a stimulus isolation unit (Grass SIU5). A range of parameters was used to obtain the supramaximal IJPs in each strip. Usually these occurred when the pulse rate was 25-30 pps, the train duration 300 msec, at a supramaximal voltage of 120 - 150 V, with 0.3-0.4 msec pulses. Single pulse stimulation was achieved by using a 50-100 msec square wave (10-20 V).

Solutions and drugs. The Krebs solution (in mM: NaCl, 115.5; NaH₂PO₄, 1.6; NaHCO₃, 21.9; KCl, 4.2; CaCl₂, 2.5; MgSO₄, 1.2 and glucose, 11.1) was continuously aerated with 95% O₂ - 5% CO₂ to maintain pH of approximately 7.4. Drugs were introduced to the Krebs reservoir and superfused (3 ml/min) for at least 25-30 minutes. Two concentrations (10⁻⁷ and 3 x 10⁻⁷ M) were used for ω -conotoxin GVIA (ω -CTX) (from Peninsula) and nifedipine (from Sigma). Calcium free Krebs was prepared using the same composition as described before but omitting CaCl₂ and adding 100 μ M of EGTA (ethyleneglycol-bis(betaaminoethylether)-N,N,N,N-tetraacetic acid) from Sigma. Studies of free Ca²⁺ in this solution with Fura-2 acid showed the levels to be less than 2 nM. Cyclopiazonic acid (CPA) and NiCl₂ were obtained from Sigma.

Recordings and statistical analysis. The resting membrane potential, frequency,

duration and amplitude of slow waves, and the durations and amplitudes of IJPs and TSWs were analyzed for each record. These parameters were analyzed during the control period (20 minutes) and every 5 minutes following the drug infusion (30 minutes). A TSW, triggered only in the full-thickness preparations, was distinguished from a spontaneous slow wave in this manner: when EFS using short pulses or a single long pulse was applied at any time between spontaneous slow waves, a TSW characterized by a fast upstroke occurred prematurely or late relative to the expected timing of the next spontaneous slow wave. TSW was often able to reset the slow wave frequency. Frequencies of slow waves were determined by averaging the number of slow waves occurring over a period of 3 minutes. The motility index was calculated by multiplying the mean contraction amplitude in a 1-min interval with the number of contractions occurring during this interval. Spontaneous phasic contractions were measured immediately before and 20 to 30 minutes after onset of each treatment. Data are presented as mean \pm S.E.M. Ordinary ANOVA (analysis of variance, with Bonferroni correction) or Student *t*-tests, as appropriate, were performed to check for statistical significance. Mean values were considered significantly different when $P < 0.05$.

The amplitudes of slow waves in Ca^{2+} -free solution versus time were analyzed by simultaneous non-linear curve fitting. The experimental data points were fitted into the sigmoidal function:

$$y = a_0 + a_1 / (1 + \exp(-(x-a_2)/a_3))$$

by means of non-linear least square regression using the Levenberg-Marquardt algorithm for least square regression available in the Slidewrite Plus version 6.0 (Advanced Graphics

Software, Sunnyvale, CA) graphics and statistical package. In the equation y is the slow wave amplitude; x is time in minutes; a_0 the slow wave amplitude at time zero; a_1 the amplitude at 'infinite' time; a_2 and a_3 are slope factors that determine the steepness of the curve.

RESULTS

Resting membrane potentials and spontaneous slow waves in the full thickness preparation

Figure 1A shows a schematic of the full-thickness preparation which defines the various locations of the recording electrodes in the CM layer during an experiment. Actual recordings from two different preparations of slow wave activity in the regions near the myenteric plexus (MyP) (Figure 1B) and the deep muscular plexus (DMP) (Figure 1C) show that the slow wave patterns are not homogeneous within the CM layer. Figures 1B and 1C also demonstrate the apparent gradient in baseline membrane potential, being more hyperpolarized near the MyP region and about 10 mV more depolarized near the DMP region. Figures 1B and 1C also show the method for measuring the different parameters associated with slow wave activity and responses to electrical field stimulation or EFS (a= slow wave amplitude; b= slow wave duration; c= IJP amplitude; d= IJP duration; e= amplitude of slow wave triggered by IJP. These often occurred prematurely, but could also occur after the IJP delayed relative to the expected timing of the next slow wave. Therefore, they were designated as triggered slow waves (TSWs); f= TSW duration; and g= TSW delay). Slow waves recorded near the MyP exhibited a fast upstroke from a stable baseline followed by a plateau which was flat, rounded or sometimes with a second peak (Figure 1B). In contrast, slow waves recorded from the DMP region were triangular without a plateau and usually showed a sigmoidal onset (Figure 1C). Triangular or sigmoidal slow waves accompanied by phasic contractions were also recorded throughout the CM layer in isolated CM preparations (Figure 1D).

IJPs elicited by EFS using supramaximal stimuli were smaller when recorded close to the MyP (10 -15 mV) compared to those recorded near the DMP (15 - 20 mV). A TSW, triggered by the ending of an IJP, was recorded everywhere in the whole-thickness preparation (Figures 1B and 1C) including near the DMP, but never in isolated CM preparations (Figure 1D). It was characterized by a fast upstroke followed by a plateau before repolarization. The TSW amplitudes were significantly greater near the MyP region than near the DMP region (Tables 1 and 3, compared the control TSW amplitudes from MyP and DMP). Thus the TSWs were distinguishable from the spontaneous slow waves by their shape and amplitude; *i.e.*, everywhere in the CM of the whole-thickness preparation, the TSWs occurring after IJPs or evoked by a long duration, single pulse resembled the plateau-type shape of the spontaneous slow waves with a fast upstroke recorded near the MyP (Figure 2). They were also longer in duration and frequently occurred at a time advanced or delayed compared to other spontaneous slow waves. Elsewhere the possibility that they originate from the MyP pacemakers has been considered (9; Jiménez, *et al.*, unpublished observations).

Effect of calcium channel blockers in the full thickness preparation

We evaluated whether Ca^{2+} entrance played a role in slow wave formation by blocking entry of Ca^{2+} or by removal of Ca^{2+} from the extracellular space. Transmitter release from nerve terminals of the central nervous system depends on calcium influx via voltage activated calcium channels of the N-type but usually not L-type (23), although L- Ca^{2+} channel as well as N- Ca^{2+} channel binding occurs in DMP synaptosomes (1). We investigated the effects of L- and N- Ca^{2+} channel blockers on IJPs, slow waves and TSWs

in all regions of the CM in the full-thickness preparation.

Neither of the calcium channel blockers tested (L and N type) modified the resting membrane potential. Neither ω -CTX (Figure 2) nor nifedipine (Figure 3) affected the frequency, amplitude or shape of slow waves in any area (Table 1). In particular, the plateau of the slow waves recorded near the MyP was unchanged after superfusion of nifedipine (10^{-7} or 3×10^{-7} M) although CM contractions were significantly reduced at 10^{-7} M and abolished at 3×10^{-7} M (Figure 3B). Recordings of the slow waves and IJPs from the DMP region were also unaffected by nifedipine (3×10^{-7} M) (Table 1). However, ω -CTX (3×10^{-7} M) inhibited the IJP (Figure 2A and 2B) and sometimes enhanced CM contractions in other recordings (data not shown). The inhibition of IJPs started 5 minutes after the beginning of the infusion with full abolition occurring after 15-20 minutes. The effect was partly reversible after 40-60 minutes of washing. The response to EFS which usually elicited an IJP was accompanied after abolition of the IJP by ω -CTX by an increased delay before the next TSW (Table 1; Figures 2A and 2B, bottom panels). Subsequent addition of tetrodotoxin or NO synthase inhibitors (8; Cayabyab *et al.*, unpublished observations) abolished the delay in induction of a TSW and enhanced the TSW amplitudes, suggesting that an ω -CTX-insensitive neural release of NO was still occurring to delay the onset of TSWs.

Ni²⁺ effects on spontaneous and triggered slow waves and contractions in full-thickness preparations

Ni^{2+} , a non-selective Ca^{2+} channel antagonist (27), significantly decreased the frequency and amplitude of slow waves recorded near the MyP and DMP, and decreased

their rate of rise but prolonged their duration (Figures 4A and 4B, Table 2). Similarly, Ni^{2+} inhibited the amplitudes but enhanced the durations of the TSWs (Figures 4A and 4B, Table 2). Ni^{2+} also diminished the spontaneous CM contractions associated with the spontaneous slow waves and TSWs (Figure 5), as did nifedipine but not ω -CTX (see Figure 2). Ni^{2+} caused an uncoupling of slow waves from contractions in some recordings (Figure 4B). Ni^{2+} had no significant effects on the IJPs (Figures 4A and 4B, Table 2).

Effect of Ca^{2+} -free Krebs in the full thickness and isolated CM preparations.

In the whole-thickness slab preparation, Ca^{2+} -free Krebs (100 μM EGTA) gradually decreased the amplitude and frequency of slow waves from the MyP and DMP regions (Figures 6A and 6B, Table 3). The recordings shown in Figures 6A and 6B were from the same muscle strip. All the parameters of the IJPs, TSWs and spontaneous slow waves returned to their control values 10 to 15 minutes after restoration of normal Krebs. The IJPs and TSWs previously elicited by trains of short pulse stimulation (30 pps) were abolished 10 - 15 minutes after the beginning of the infusion. At that time, the mean slow wave frequency was significantly reduced by 40% in both the MyP and DMP regions (Figure 7A, Table 3). Also the amplitudes of slow waves were markedly reduced by 60% in both regions (Figure 7B, Table 3). In Ca^{2+} -free Krebs for 10-12 minutes, the TSWs elicited by long pulse stimulation were not abolished in the MyP region (Figure 6A) but disappeared in the DMP region (Figure 6B). At that time, membrane potentials were not significantly reduced (Figure 7C). However, TSWs elicited by high frequency EFS (30 pps) could not be evoked (Figure 6A and 6B, bottom panels). Also, slow waves recorded near the DMP had acquired the shape of those normally found near the MyP;

i.e., they had plateaus (compare Figures 6A and 6B, bottom panels). In Table 3, the values of amplitude, duration, and induction delay of "TSW" recorded in Ca^{2+} -free medium and elicited at 30 pps near both pacemaking regions and at 1 pulse only at DMP region, actually refer to the next spontaneous slow waves since no TSW was produced. The amplitude and frequency of slow waves near the DMP of the isolated CM preparations were reduced more rapidly than those parameters near the MyP region (Figures 7A and 7B).

Effects of CPA, a blocker of SR Ca^{2+} -ATPase, on E-C coupling in full-thickness preparations.

CPA, shown to be a selective inhibitor of the SR pump (15,28), was used to determine whether emptying of intracellular Ca^{2+} stores as a result of disruption of the balance between SR Ca^{2+} uptake and release, affected pacemaking activity. In the full-thickness preparations, CPA similarly affected both plateau-type and triangular slow waves (Figures 8 and 9). CPA at 10 μM did not significantly depolarize the membrane potentials (control -66.0 ± 0.6 mV vs. treated -64.5 ± 0.5 mV, $n=3$, $P>0.05$) but slightly decreased slow wave amplitude (bottom to peak of slow wave: control 28.4 ± 2.5 mV vs. treated 21.9 ± 7.0 mV, $n=3$, $P>0.05$) and increased frequency (control 10.3 ± 0.3 cycles/min vs. treated 12.0 ± 0.0 cycles/min, $n=3$, $P>0.05$) (see Figures 8B and 9B). The IJPs were unaffected by CPA pretreatment (Figure 8B). Subsequent addition of CPA at 30 μM (15-25 minutes after 10 μM CPA superfusion) did not significantly affect membrane potentials or IJPs (Figures 8C and 9C), but further reduced the amplitudes of slow waves (treated 17.2 ± 3.8 mV, $n=3$, $P<0.01$ compared to control, see Figures 8C, 8E,

and 9C). These slow waves, which were plateau-type or triangular in shape before the CPA treatment, had an occasional spike potential superimposed on the slow waves in the presence of CPA. At 30 μM , CPA continued to increase significantly slow wave frequency (treated 12.3 ± 0.9 cycles/min, $n=3$, $P<0.05$ compared to control values) but reduced the plateau duration (measured at 50 % maximum slow wave amplitude: control 2.35 ± 0.06 sec vs. treated 1.84 ± 0.06 sec, $n=3$, $P<0.001$) (see Figure 8E). CPA (10-30 μM) increased tone and phasic contractions (Figures 9B and 9C). All effects of CPA on slow waves and contractile responses persisted even after more than 20 minutes of washout of CPA (Figures 8D and 9D).

DISCUSSION

We investigated the roles of Ca^{2+} in pacemaking activity, slow wave generation, nerve activation and E-C coupling in canine ileum CM. The main findings were: (1) slow waves, contraction and mediator release depended on Ca_o^{2+} and ultimately disappeared in its absence; (2) slow waves did not involve a Ca^{2+} conductance through voltage-operated channels since they were not affected by L- Ca^{2+} channel blockers and were slowly affected by removal of Ca_o^{2+} ; (3) release of IJP mediator depended on Ca^{2+} entrance into nerves through N-, not L- Ca^{2+} channels; (4) E-C coupling required Ca^{2+} entrance through L- Ca^{2+} channels, but this occurred without spike activity in association with the slow wave plateaus, which reached membrane potentials of -40 to -45 mV; (5) Ni^{2+} at 200 μM inhibited slow waves and contractions but not IJPs, implying that slow wave production and repolarization may involve Ca^{2+} entrance through voltage-insensitive Ca^{2+} channels; (6) CPA enhanced slow wave frequency but diminished slow wave amplitude while not affecting membrane potentials or IJPs. It also enhanced contractions and occasionally caused spikes on slow wave plateaus which arose from membrane potentials near -50 mV; and finally (7) pacemaking activity from the MyP and DMP regions differed in their dependence on Ca_o^{2+} .

Previous studies reported spontaneous spiking activity superimposed on slow wave activity in the longitudinal and sometimes in the CM layers of the duodenum and jejunum in rabbit (10,18) and in one area (the innermost cell layers near the submucosa) of the CM of the canine jejunum (21). In our ileum preparation, we only recorded triangular or sigmoidal slow waves lacking spikes in the latter area (Jiménez, *et al.*, unpublished

observations). The slow waves near the MyP had plateaus and were similar to those described in the duodenum and jejunum (4,21). In contrast, near the DMP, we never recorded square waves or slow waves with plateaus as reported in the duodenum and spike potentials in some regions as observed in the jejunum. However, the spike potentials on the plateau of slow waves may be primarily a property of longitudinal muscle (10,18) and innermost CM (21). Longitudinal muscle of the rabbit intestine was more depolarized by 10-12 mV than CM (10) and developed action potential bursts which were not transmitted to the underlying CM. In the present study, phasic contractions accompanied slow waves which lacked spike activity in both intact slabs and isolated CM in the absence of neural toxins. The slow waves recorded everywhere in the CM layer reached maximum depolarizations near -40 mV (Figure 1), which is close to the reported voltage threshold (22) required for coupling excitations by slow waves or action potentials to contractions. Therefore, as previously described (38), intestinal slow waves in fact serve as action potentials in the canine ileum CM.

The finding that L-Ca²⁺ channel blockade has no effect on slow waves while inhibiting contractions suggests that opening of voltage-sensitive Ca²⁺ channels played no role in slow wave formation. However, Ca²⁺ influx through L-Ca²⁺ channels activated during slow waves may be sufficient to elevate [Ca²⁺]_i to trigger contraction (26). L-Ca²⁺ channels clearly existed in these muscles based on binding studies (1) and were blocked since contractions were abolished by nifedipine (11). Nifedipine markedly reduced the motility index; this confirms earlier studies in rabbit intestine longitudinal muscle (18) that showed verapamil did not affect slow waves but abolished spikes and rhythmic

contractions. Studies of canine colon (25) reported involvement of non-L- as well as L- Ca^{2+} channels in slow waves, but in that tissue as well as in cat antrum (33) L- Ca^{2+} channels are also involved and play a major role in coupling excitation by slow waves to contraction by affecting Ca^{2+} entrance during the plateau. There is currently no evidence that "T"- Ca^{2+} channels exist in ileal CM cells and it is unlikely that their transient opening and small conductance (47) could contribute to prolong slow waves. Since in most smooth muscles, L- Ca^{2+} channels begin activating only when the cell membrane is depolarized to -40 mV or more (26,47), there must be a special modulation of Ca^{2+} channels of CM during a slow wave to allow Ca^{2+} entry at polarized membrane potentials or there is a marked Ca^{2+} release from internal stores in response to a modest Ca^{2+} entry.

The results also imply that voltage-dependent Ca^{2+} -channels have no major direct role in pacemaking since frequencies of slow waves as well as their amplitudes were unchanged. This was true of pacemaking of slow waves of the types associated with MyP and with DMP. However the effects of Ni^{2+} on slow wave amplitude and duration imply that CM slow waves require Ca^{2+} entrance through Ni^{2+} -sensitive, but non-voltage activated Ca^{2+} channels or possibly through nonselective cation channels (27). The prolonged duration of slow waves in the presence of Ni^{2+} likely reflects an inhibition of an ionic conductance responsible for repolarizations of slow waves. This increase in slow wave duration may be a consequence of Ni^{2+} -induced inhibition of Ca^{2+} influx, which is coupled to Ca^{2+} -activated K^+ channel opening as suggested by studies in colon (7,26). The K^+ channel blocker, tetrapentylammonium, blocked large-conductance Ca^{2+} -activated K^+ channels or BK channels by binding to a high-affinity site on the intracellular face of

BK channels in cell attached patches, and prolonged slow wave repolarization in intact colonic muscle (7). Moreover, Ni^{2+} at 500 μM inhibited BK channels in vascular smooth muscle by inhibiting Ca^{2+} influx through voltage-gated Ca^{2+} channels (20), while Ni^{2+} at nanomolar concentrations inhibited BK channels by interacting with the Ca^{2+} /voltage sensor located on the intracellular side of the membrane (43). Either or both of these inhibitory effects of Ni^{2+} on BK channels may prolong ileal slow wave duration, but future studies are needed to demonstrate the presence of Ni^{2+} - and charybdotoxin-sensitive BK channels in isolated ileal CM cells.

However, Ca^{2+} must play some role in pacemaking and E-C coupling. That conclusion derives from the effects of Ni^{2+} and Ca^{2+} removal on slow wave frequency, triggering of slow waves, and motility index, as well as on the effect of CPA to increase slow wave frequency and tone without causing membrane depolarization of CM. It seems likely that levels of Ca_i^{2+} in pacemaking cells in some manner set the pacemaking frequency, higher at higher levels of Ca_i^{2+} induced by CPA, and lower as Ca_i^{2+} falls during Ni^{2+} treatment and Ca^{2+} depletion. Direct confirmation of this hypothesis probably requires studies of Ca_i^{2+} and pacemaking activity in ICC.

Mediator release in ileum, at least that of inhibitory mediators such as NO (12,14), depended on Ca^{2+} entrance through N-, but not L- Ca^{2+} channels, since ω -CTX blocked IJPs and relaxations. Surprisingly, IJPs were regularly produced even without inhibition of cholinergic nerves while excitatory junction potentials (EJPs) were rarely produced even after IJPs had been abolished by NO synthase blockers (8; Cayabyab *et al.*, unpublished observations). This is in contrast to the sucrose gap observations (12) and

to the situation *in vivo* (19) in which nerve stimulation evokes EJPs and cholinergic contractions. Part of the reason may be that the major excitatory action of acetylcholine is to release Ca_i^{2+} from SR and that this may occur even if acetylcholine cannot produce EJPs because of continuous release of inhibitory mediators such as NO. In some records a contraction occurred during the IJP (*e.g.*, Figs. 1C and 6A). However, recent work from our laboratory shows that NO inhibits acetylcholine release from the isolated CM strip (24). Moreover, as previously described (8,9; Cayabyab *et al.*, unpublished), NO released from nerves or from NO-releasing compounds and NO-release independent of N- Ca^{2+} channels can influence pacemaking. Thus the failure of ω -CTX to affect slow waves implies that the spontaneous release of mediators requiring Ca^{2+} entrance into nerves through N- Ca^{2+} channels was not affecting pacemaking activity.

However, the mechanisms whereby contractions are coupled to ileal slow waves remain unclear. Ca^{2+} -induced Ca^{2+} release (CICR) from SR of CM cells or reduced Ca_i^{2+} -requirements for contraction (as when protein kinase C is activated) may be involved in E-C coupling. CICR is an unlikely explanation for the initiation of contraction by small amounts of Ca^{2+} entry. This is true because CPA, which is capable of inhibiting Ca^{2+} -pumping into smooth muscle SR and depleting Ca^{2+} stores (15), enhanced rather than inhibited contractions. Prolonged exposure to CPA would be expected to increase steady state $[\text{Ca}^{2+}]_i$ as reported in other systems (28). Consequently, elevation of $[\text{Ca}^{2+}]_i$ may activate some phospholipases (D and/or A_2) to cause hydrolysis of inositol phospholipids, which in turn, would increase diacylglycerol concentration and protein kinase C activity (30). Further studies similar to those performed in canine antrum (31) are required to

evaluate whether inhibitors and activators of protein kinase C or phorbol diesters, which mimic the effects of diacylglycerol, affect CPA-induced enhancement of CM tone.

CPA produced intermittent spike potentials on slow waves which coincided with greater CM contraction. This occurred although the membrane potentials at the peak of slow waves were only near -50 mV, which would normally not activate L-Ca²⁺ channels (26,47). CPA did not depolarize CM cells, similar to the lack of effect of thapsigargin (another SR pump inhibitor) on membrane potentials of canine antral CM (31), but it enhanced slow wave frequency. Other laboratories have shown that increases in [Ca²⁺]_i activated Ca²⁺-calmodulin and Ca²⁺-calmodulin-dependent protein kinase II, which phosphorylates and decreases the Ca²⁺ sensitivity of myosin light chain kinase (32,44). Thus the spike activity observed on slow waves during CPA treatments may arise from the Ca²⁺ current potentiation mediated by Ca²⁺-calmodulin or Ca²⁺-calmodulin-dependent protein kinase II (29), while the increased CM tone may be attributed to increased activity of Ca²⁺-calmodulin and its binding to myosin light chain kinase (32,44).

Finally, we showed in previous studies (9; Jiménez *et al.*, unpublished) that in canine ileum CM the pacemaking cells from the MyP and DMP regions were capable independently of driving spontaneous slow waves of different configurations and that TSWs originated exclusively from the MyP region. In the present study, Ca²⁺-free solution rapidly eliminated IJPs before eliminating slow waves. Decreased amplitudes of slow waves without significant CM membrane depolarization accompanied these changes. After the disappearance of IJPs, the slow waves recorded throughout the CM layer, including those from DMP region, had plateaus like those initiated in the MyP region,

where they may have originated. The changed shape of slow waves recorded from the DMP region may also reflect loss of pacemaking activity from that region. However, since we are not recording directly from the pacemaker cells, the possibility exists that pacemaking continues in Ca^{2+} -free solutions but that their ability to drive CM cells is lost. Also removal of Ca_o^{2+} more rapidly inhibited slow waves recorded from the DMP region in the isolated CM preparations. Thus these results suggest the MyP pacemakers dominate pacemaking under normal and reduced $[\text{Ca}^{2+}]_o$, while the DMP pacemakers are highly sensitive to removal of Ca_o^{2+} and unable to respond with a TSW to a long duration pulse even when cells near the MyP do.

ACKNOWLEDGEMENT

F.S. Cayabyab was a recipient of a Student Abstract Prize sponsored by the American Gastroenterological Association (AGA) Foundation (F.S. Cayabyab, H. deBruin, M. Jiménez, and E.E. Daniel. Differential Ca^{2+} sensitivity of two pacemaking networks in the canine ileum. *Gastroenterology* 108:A579, 1995. AGA Meeting, San Diego, CA, 1995). M. Jiménez was supported by Personal Investigator Visiting Grant from the Comissió Interdepartamental de Recerca i Innovació Tecnològica (CIRIT, Ref. EE92/2-369), Catalonia, Spain. P. Vergara was supported by Personal Investigator Visiting Grant from the Dirección General de Investigación Científica y Técnica, Spain. This investigation was funded by MRC and NSERC of Canada.

REFERENCES

1. **Ahmad, S., J. Rausa, E. Jang, and E.E. Daniel.** Calcium channel binding in nerves and muscle of canine small intestine. *Biochem. Biophys. Res. Comm.* 159(1):119-125, 1989.
2. **Allescher, H.D., G. Tougas, P. Vergara, S. Lu, and E.E. Daniel.** Nitric oxide as a putative nonadrenergic, noncholinergic inhibitory transmitter in the canine pylorus. *Am. J. Physiol.* 262:G695-G702, 1992.
3. **Bauer, A.J., J.B. Reed, and K.M. Sanders.** Slow wave heterogeneity within the circular muscle of the canine gastric antrum. *J. Physiol. (London)* 366:221-232, 1985.
4. **Bayguinov, O., F. Vogalis, B. Morris, and K.M. Sanders.** Patterns of electrical activity and neural responses in canine proximal duodenum. *Am. J. Physiol.* 263:G887-G894, 1992.
5. **Berezin, I., J.D. Huizinga, and E.E. Daniel.** Interstitial cells of Cajal in canine colon: A special communication network at the inner border of the circular muscle. *J. Comp. Neurocyt.* 273:42-51, 1988.
6. **Berezin, I., S.H. Snyder, D.S. Bredt, and E.E. Daniel.** Ultrastructural localization of NOS in canine small intestine and colon. *Am. J. Physiol.* 266:C981-C989, 1994.
7. **Carl, A., B.W. Frey, S.M. Ward, K.M. Sanders, and J.L. Kenyon.** Inhibition of slow-wave repolarization and Ca^{2+} -activated K^+ channels by quaternary ammonium ions. *Am. J. Physiol.* 264:C625-C631, 1993.
8. **Cayabyab, F.S., H. deBruin, and E.E. Daniel.** NO and NANC inhibitory mediation in the canine ileum (Abstract). *Can. J. Physiol. Pharmacol.* 72:234, 1994.
9. **Cayabyab, F.S., M. Jiménez, P. Vergara, and E.E. Daniel.** Two independent pacemakers drive the electrical and mechanical activities of the canine ileum (Abstract). *Neurogastroenterology and Motility* 6:152, 1994.
10. **Cheung, D.W., and E.E. Daniel.** Comparative study of the smooth muscle layers of the rabbit duodenum. *J. Physiol. (London)* 309:13-27, 1980.
11. **Christinck, F., E.E. Daniel, and J.E.T. Fox-Threlkeld.** Inhibitory and excitatory mechanisms of neurotensin action in canine intestinal circular muscle *in vitro*. *Can. J. Physiol. Pharmacol.* 70:1423-1431, 1992.

12. **Christinck, F., J. Jury, F. Cayabyab, and E.E. Daniel.** Nitric oxide may be the final mediator of nonadrenergic, noncholinergic inhibitory junction potentials in the gut. *Can. J. Physiol. Pharmacol.* 69:1448-1458, 1991.
13. **Daniel, E.E., and I. Berezin.** Interstitial cells of Cajal: are they major players in control of gastrointestinal motility? *J. Gastrointest. Mot.* 4:1-24, 1992.
14. **Daniel, E.E., C. Haugh, Z. Woskowska, S. Cipris, J. Jury, and J.E.T. Fox-Threlkeld.** Role of nitric oxide-related inhibition in intestinal function: relation to vasoactive intestinal polypeptide. *Am. J. Physiol.* 266:G31-G39, 1994.
15. **Darby, P.J., C.Y. Kwan, and E.E. Daniel.** Use of calcium pump inhibitors in the study of calcium regulation in smooth muscle. *Biol. Signals* 2:293-304, 1993.
16. **Duchon, G., R. Henderson, and E.E. Daniel.** Circular muscle layers in the small intestine. In: *Proceedings of the international Symposium of Gastrointestinal Motility.* ed. Daniel E.E., pp 635- 646. Vancouver: Mitchell Press, 1974.
17. **El-Sharkawy, T.Y. and E.E. Daniel.** Electrical activity of small intestine smooth muscle and its temperature dependence. *Am. J. Physiol.* 229:1268-1276, 1975.
18. **El-Sharkawy, T.Y. and E.E. Daniel.** Ionic mechanisms of intestinal electrical control activity. *Am. J. Physiol.* 229:1287-1298, 1975.
19. **Fox, J.E.T., E.E. Daniel, J. Jury, and H. Robotham.** Muscarinic inhibition of canine small intestinal motility *in vivo*. *Am. J. Physiol.* 248:G526-G531, 1985.
20. **Gelband, C.H. and J.R. Hume.** Ionic currents in single smooth muscle cells of the canine renal artery. *Circ. Res.* 71:745-758, 1992.
21. **Hara, Y., M. Kubota, and J.H. Szurszewski.** Electrophysiology of smooth muscle of the small intestine of some mammals. *J. Physiol. (London)* 372:501-520, 1986.
22. **Hara, Y., and J.H. Szurszewski.** Effect of potassium and acetylcholine on canine intestinal smooth muscle. *J. Physiol. (London)* 372:521-537, 1986.
23. **Hirning, L.D., A.P. Fox, E.W. McCleskey, B.M. Olivera, S.A. Thayer, R.J. Miller, and R.W. Tsien.** Dominant role of N-type Ca^{2+} channels in evoked release of norepinephrine from sympathetic neurons. *Science* 239:57-60, 1988.
24. **Hryhorenko, L.M., Z. Woskowska, and J.E.T. Fox-Threlkeld.** Nitric oxide (NO) inhibits release of acetylcholine from nerves of isolated circular muscle of

- the canine ileum: Relationship to motility and release of nitric oxide. *J. Pharmacol. Exp. Ther.* 271(2):918-926, 1994.
25. **Huizinga, J.D., L. Farraway, and A. Den Hertog.** Generation of slow-wave-type action potentials in canine colon smooth muscle involves a non-L-type Ca^{2+} conductance. *J. Physiol. (London)* 442:15-29, 1991.
 26. **Langton, P.D., E.P. Burke, and K.M. Sanders.** Participation of Ca currents in colonic electrical activity. *Am. J. Physiol.* 257:C451-C460, 1989.
 27. **Lee, H.K., O. Bayguinov, and K.M. Sanders.** Role of nonselective cation current in muscarinic responses of canine colonic muscle. *Am. J. Physiol.* 265:C1463-C1471, 1993.
 28. **Mason, M.J., C. Garcia-Rodriguez, and S. Grinstein.** Coupling between intracellular Ca^{2+} stores and the Ca^{2+} permeability of the plasma membrane: comparison of the effects of thapsigargin, 2,5-di-(tert-butyl)-1,4-hydroquinone, and cyclopiazonic acid in rat thymic lymphocytes. *J. Biol. Chem.* 266:20856-20862, 1991.
 29. **McCarron, J.G., J.G. McGeown, S. Reardon, M. Ikebe, F.S. Fay, and J.V. Walsh Jr.** Calcium-dependent enhancement of calcium current in smooth muscle by calmodulin-dependent protein kinase II. *Nature* 357:74-77, 1992.
 30. **Nishizuka, Y.** Intracellular signalling by hydrolysis of phospholipids and activation of protein kinase C. *Science* 258:607-614, 1992.
 31. **Ozaki, H., L. Zhang, I.L.O. Buxton, K.M. Sanders, and N.G. Publicover.** Negative-feedback regulation of excitation-contraction coupling in gastric smooth muscle. *Am. J. Physiol.* 263:C1160-C1171, 1992.
 32. **Rembold, C.M.** Regulation of contraction and relaxation in arterial smooth muscle. *Hypertension* 20:129-137, 1992.
 33. **Renzetti, L.M., M.B. Wang, and J.P. Ryan.** Modulation of cat antral slow waves by ion substitution, Ca^{2+} and K^{+} channel blockade, and acetylcholine stimulation. *Am. J. Physiol.* 263:G880-G886, 1992.
 34. **Rumessen, J.J., H.B. Mikkelsen, K. Qvortrup, and L. Thuneberg.** Ultrastructure of interstitial cells of Cajal in circular muscle of human intestine. *Gastroenterology* 104:343-350, 1993.
 35. **Rumessen, J.J., H.B. Mikkelsen, and L. Thuneberg.** Ultrastructure of interstitial cells of Cajal associated with deep muscular plexus of the human small

- intestine. *Gastroenterology* 102:56-68, 1992.
36. **Rumessen, J.J., and L. Thuneberg.** Interstitial cells of Cajal in human small intestine. Ultrastructural identification and organization between the main smooth muscle layers. *Gastroenterology* 100:1417-1431, 1991.
 37. **Rumessen, J.J., and L. Thuneberg.** Plexus muscularis profundus and associated interstitial cells. I. Light microscopical studies of mouse small intestine. *Anat. Rec.* 203:115-127, 1982.
 38. **Sanders, K.M.** Excitation-contraction coupling without Ca^{2+} action potentials in small intestine. *Am. J. Physiol.* 224:C356-C361, 1983.
 39. **Smith, T.K., J.B. Reed, and K.M. Sanders.** Interaction of two electrical pacemakers in muscularis of canine colon. *Am. J. Physiol.* 252:C290-C299, 1987.
 40. **Stark, M.E., A.J. Bauer, M.G. Sarr, and J.H. Szurszewski.** Nitric oxide mediates inhibitory nerve input in human and canine jejunum. *Gastroenterology* 104:398-409, 1993.
 41. **Stark, M.E., A.J. Bauer, and J.H. Szurszewski.** Effect of nitric oxide on circular muscle of the canine small intestine. *J. Physiol. (London)* 444:743-761, 1991.
 42. **Stark, M.E., and J.H. Szurszewski.** Role of nitric oxide in gastrointestinal and hepatic function and disease. *Gastroenterology* 103:1928-1949, 1992.
 43. **Stockland, J., A. Sultan, D. Molony, T. DuBose Jr., and S. Sansom.** Interactions of cadmium and nickel with K channels of vascular smooth muscle. *Toxicol. Appl. Pharmacol.* 121:30-35, 1993.
 44. **Stull, J.T., L.-C. Hsu, M.G. Tansey, and K.E. Kamm.** Myosin light chain kinase phosphorylation in tracheal smooth muscle. *J. Biol. Chem.* 265:16683-16690, 1990.
 45. **Szurszewski, J.H.** Electrical basis for gastrointestinal motility. In: *Physiology of the Gastrointestinal Tract*. ed. Johnson, L.R. 2nd ed. New York: Raven Press, pp. 383-423, 1987.
 46. **Thuneberg, L.** Interstitial cells of Cajal: intestinal pacemakers? *Adv. Anat. Embryol. Cell Biol.* 71:1-130, 1982.
 47. **Yoshino, M., T. Someya, A. Nishio, K. Yazawa, T. Usuki, and H. Yabu.** Multiple types of voltage-dependent Ca channels in mammalian intestinal smooth muscle cells. *Pflügers Arch.* 414:401-409, 1989.

FIGURE LEGENDS

Figure 1. *A.* A schematic of the intact cross-sectioned slab preparation showing the various regions and placement of recording electrodes near the myenteric plexus (MyP) and deep muscular plexus (DMP) within the circular muscle layer (see *Materials and Methods* for details). Actual recordings near the MyP (*B*) and DMP (*C*) of spontaneous slow waves and triggered slow waves (TSWs), triggered after an IJP and characterized by a fast upstroke depolarization, from two different full-thickness preparations are shown. The various parameters associated with the spontaneous slow waves and responses to electrical field stimulation are denoted by the lower case letters (see text for details). Stimulus parameters used in panels *B-D* are 100-120 V, .3 msec duration, 25 pps, and 300 msec trains. In isolated CM preparations (*D*), the IJP recorded near the DMP region did not trigger a TSW; a slow IJP was observed instead. Note that in *D*, the post-IJP slow wave was not considered a TSW since its shape resembled the spontaneous slow waves and its onset lacked the fast-upstroke depolarization characteristic of a TSW or a spontaneous slow wave paced from the MyP region. Note a contraction occurring sometimes during an IJP as seen in *C*. Time calibration bar at bottom applies to all panels.

Figure 2. In the whole-thickness preparations ω -CTX (3×10^{-7} M) abolished the IJP and delayed the occurrence of a TSW (see curved arrows) in both the DMP (*A*) and the MyP (*B*) recordings. Everywhere in the circular muscle layer, the full-thickness preparation responded with a TSW without a delay (see *B*, for example, at vertical arrows) to a long

duration (100 msec), single pulse stimulation in the presence or absence of ω -CTX (3×10^{-7} M). Spontaneous slow waves and resting membrane potentials were unaffected after 20-30 min of superfusion.

Figure 3. *A.* A whole-thickness recording showing the lack of effect of nifedipine (20 minutes at 10^{-7} M and 20 minutes at 3×10^{-7} M) on any of the parameters of the spontaneous slow waves (Table 2). *B.* Spontaneous circular muscle contractions were rapidly reduced by nifedipine at 10^{-7} M and nearly abolished by 3×10^{-7} M nifedipine (see also Figure 5).

Figure 4. Effects of Ni^{2+} (200 μM) on spontaneous and triggered slow waves, IJPs and circular muscle contractions in the whole-thickness preparations. Two recordings near the MyP (*A*) and the DMP (*B*) show that Ni^{2+} decreased the amplitudes of the spontaneous and triggered slow waves (see also Table 2) and inhibited the accompanying circular muscle contractions. Note that sometimes Ni^{2+} uncoupled the contractions from the slow waves (*B*).

Figure 5. Motility index (defined in Materials and Methods) was reduced by treatments involving blockade of L- Ca^{2+} channels or removal of extracellular Ca^{2+} . The number of different strips from different animals used were: nifed (nifedipine) at 3×10^{-7} M, $n = 12$; Ni^{2+} -containing Krebs solution, $n = 8$; and Ca^{2+} -free solution, $n = 15$.

Figure 6. *A.* Top panel shows whole-thickness recording of spontaneous slow waves, TSWs evoked by 30 pps and long duration, single pulse, and their mechanical counterparts. Bottom panel shows the disappearance of the IJPs and mechanical activity in 0 Ca²⁺ (100 μM EGTA added) after 10 to 12 minutes of superfusion in this medium. Note the decrease in amplitude and duration of slow waves as well as a decrease in their frequency (Table 3A). TSWs could be evoked by long pulse stimulation (bottom panel). *B.* Ca²⁺-free Krebs also significantly reduced the amplitude, duration, and frequency of slow waves in recordings near the DMP region in the full-thickness preparation (Table 3B). In contrast, under the same condition as in *A* the circular muscle did not respond with a TSW when stimulated by a long duration pulse (bottom panel). Note that the recordings shown in *A* and *B* were from the same muscle strip separated by 1 hour of washing in normal Krebs. The slow waves persisted but their amplitudes were more rapidly inhibited in recordings near the DMP than in recordings near the MyP. In the isolated CM preparations, the slow waves were reversibly abolished after about 10 minutes in Ca²⁺-free solutions (see Figure 7A; Table 3C).

Figure 7. Time-dependent effects of Ca²⁺-free Krebs on slow wave amplitudes (*A*), frequencies (*B*), and membrane potentials (*C*) in the full-thickness and isolated circular muscle preparations. Only experiments where the microelectrode impaled the same cell before and during the entire superfusion with Ca²⁺-free Krebs were used in the analysis. The number of observations represented by the different symbols are: ○= impalements near MyP region from full-thickness preparations, n = 4; ▲= impalements near DMP

region from full-thickness preparations, $n = 7$; and \square = impalements near DMP region from isolated circular muscle preparations, $n = 5$. The slow waves from the isolated preparations were abolished within 10 minutes. In *C*, membrane potentials at about 10-12 minutes in Ca^{2+} -free Krebs were not significantly depolarized near the DMP of the full-thickness preparations, suggesting that the effects shown in Figure 6*B* were not due to depolarization. Significances are with respect to relevant controls at 0 minute. *A* and *C* were fitted using an equation for a sigmoidal curve (see Materials and Methods). The coefficients of determination, r^2 , of both curves were ≈ 1 . Units for slow wave frequency (*B*) are cycles per min (cpm).

Figure 8. *A*. Effects of 10 and 30 μM CPA on slow waves and IJPs recorded near the DMP of the full-thickness preparation. Intermittent spike potentials occurring during the plateau phase of slow waves (at around -45 mV) and a lack of effect on IJP are shown in *B*. Subsequent superfusion of 30 μM CPA enhanced slow wave frequency but decreased its amplitude (*C*) (we compared amplitudes of slow waves occurring without spikes during a two minute interval). CPA at 30 μM also did not affect IJPs. Production of spikes on slow waves persisted even after prolonged washout of CPA (*D*). CPA reduced the slow wave durations (compare *a* vs. *b* and *a* vs. *c*) as shown in *E*, where the two slow waves before the IJPs were expanded in time scale. Voltage and time calibrations at upper left of *A* also apply to panels *B-D*.

Figure 9. Effects of 10 and 30 μM CPA on slow waves and contractions recorded near

the MyP of the full-thickness preparations. CPA (10 and 30 μM), after 15 min of superfusion, increased slow wave frequencies and produced intermittent spikes during the slow wave plateaus. CPA increased basal tone and enhanced the amplitudes of phasic contractions associated with spontaneous slow waves (*B* and *C*). Effects of CPA on slow waves and tone persisted after 20 min of superfusion with normal Krebs solution (*D*). Notice that recovery in *D* was incomplete. Solid lines under contractility traces represent the baseline of tone. Voltage and time calibrations at upper left apply to all panels.

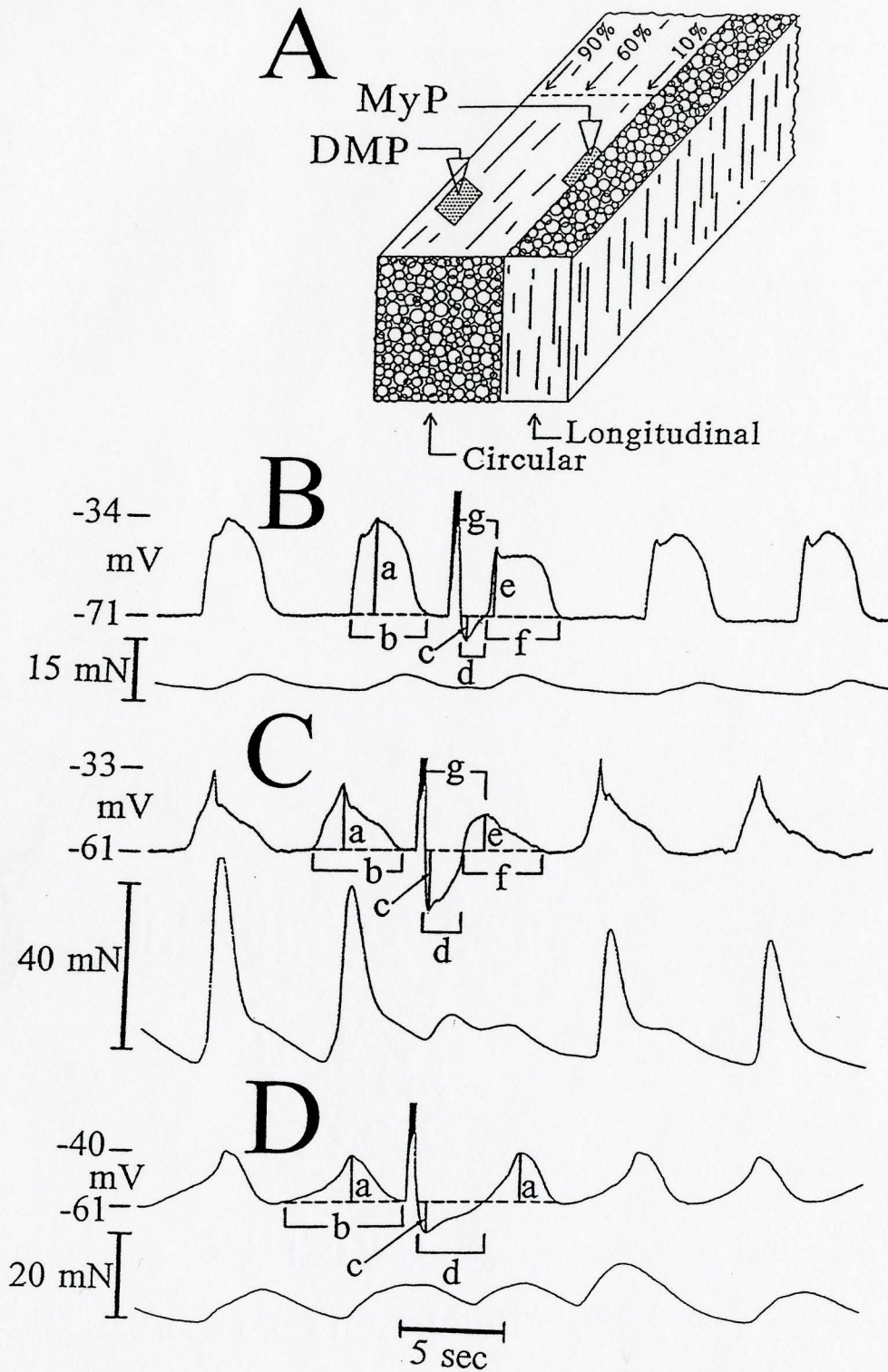


Fig. 1. Slow waves and IJPs in whole thickness and isolated circular muscle preparations

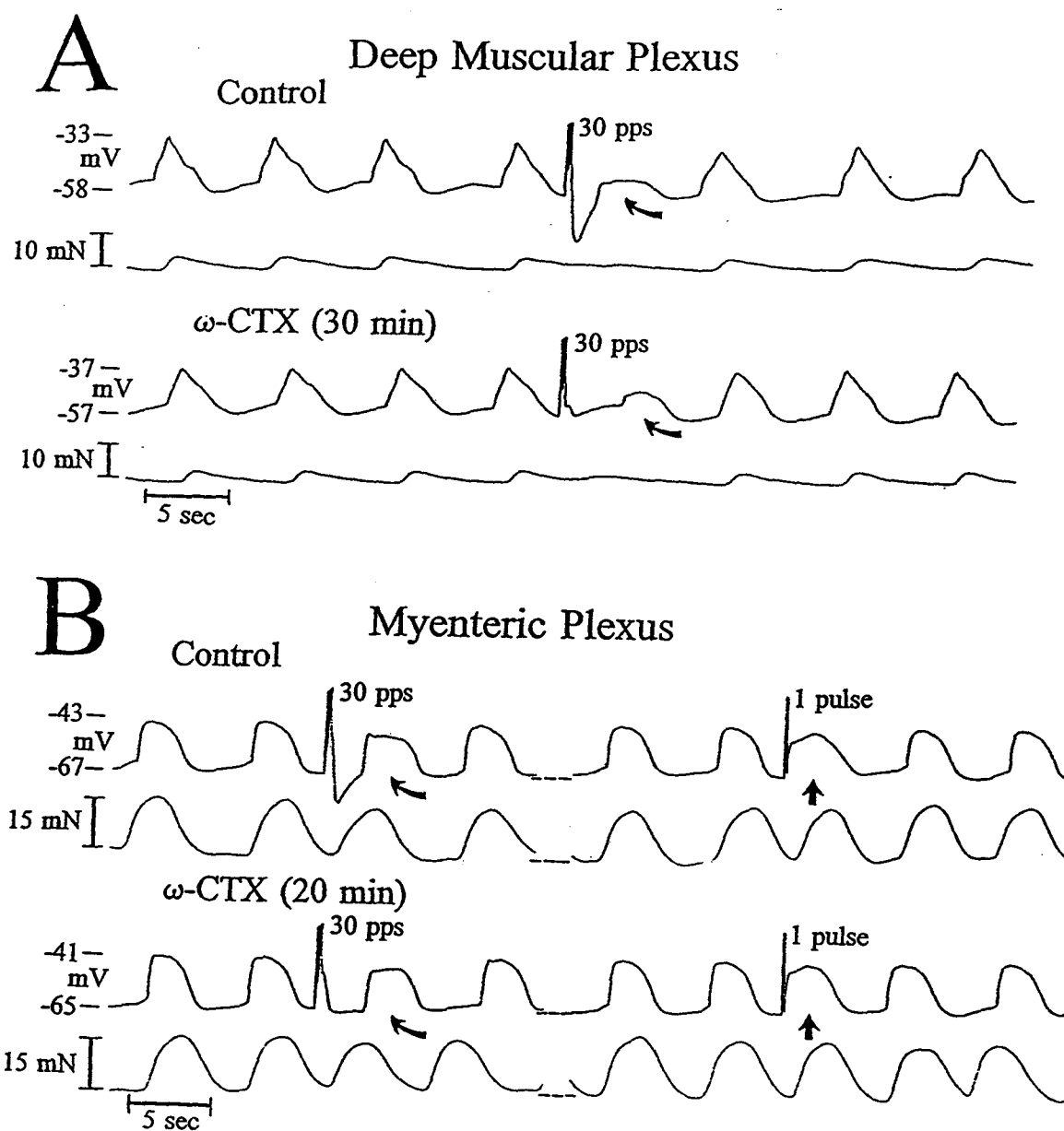
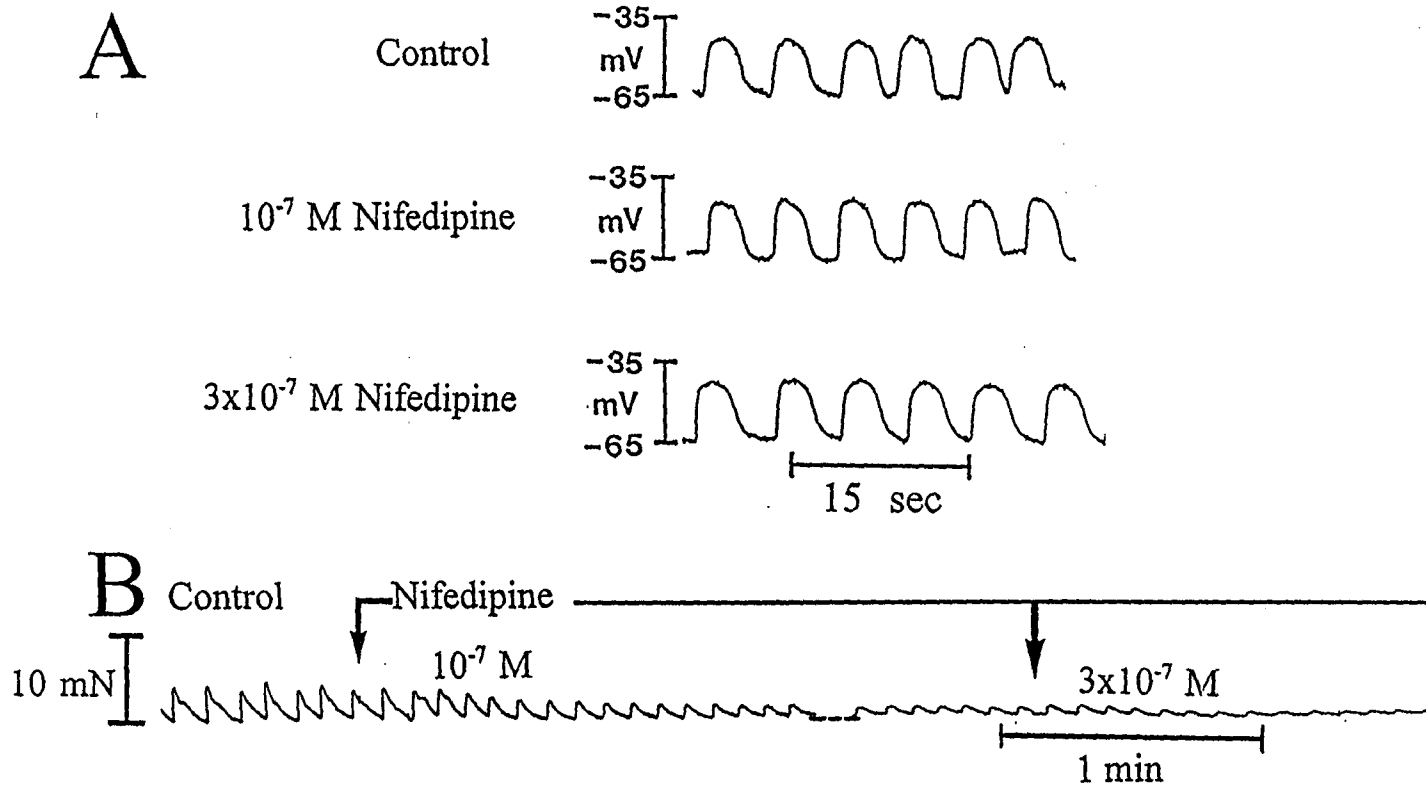


Fig. 2. Effects of ω -conotoxin GVIA on IJPs and triggered slow waves

Fig. 3 Effects of L-type Ca^{2+} channel blocker, nifedipine, on slow waves and contractions



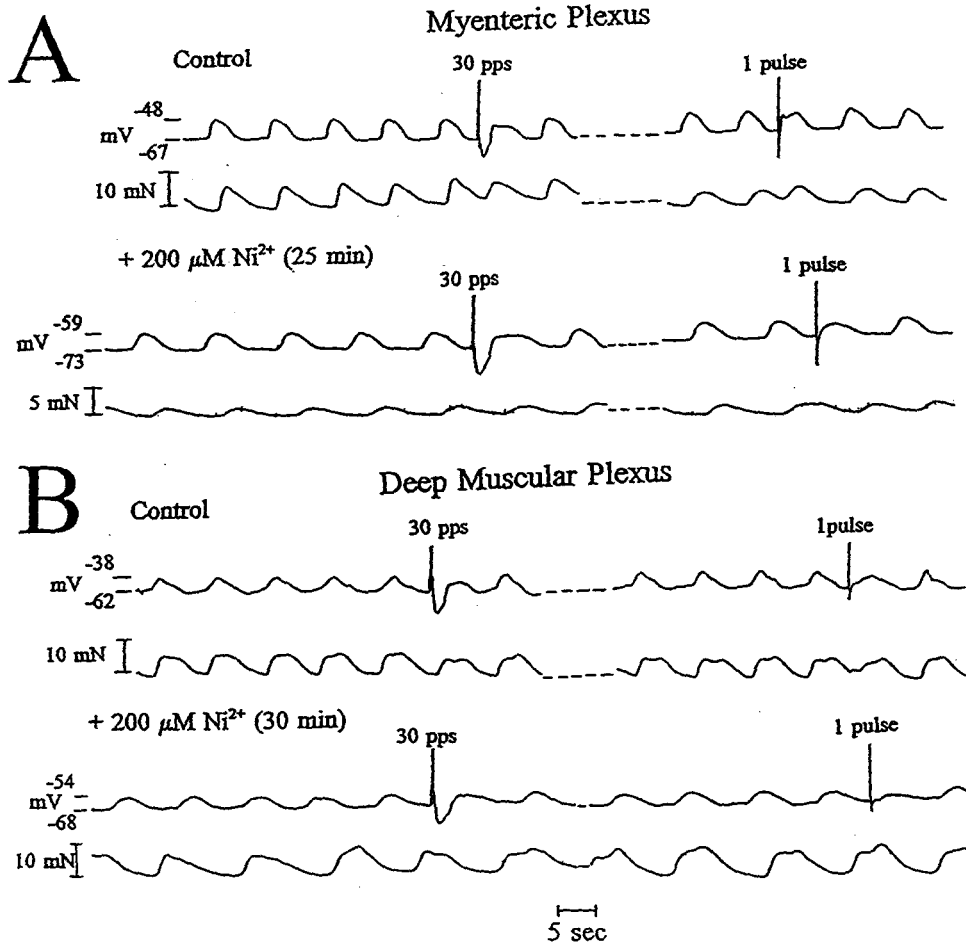


Fig. 4. Effects of Ca²⁺ influx blocker, Ni²⁺, on slow waves and contractions

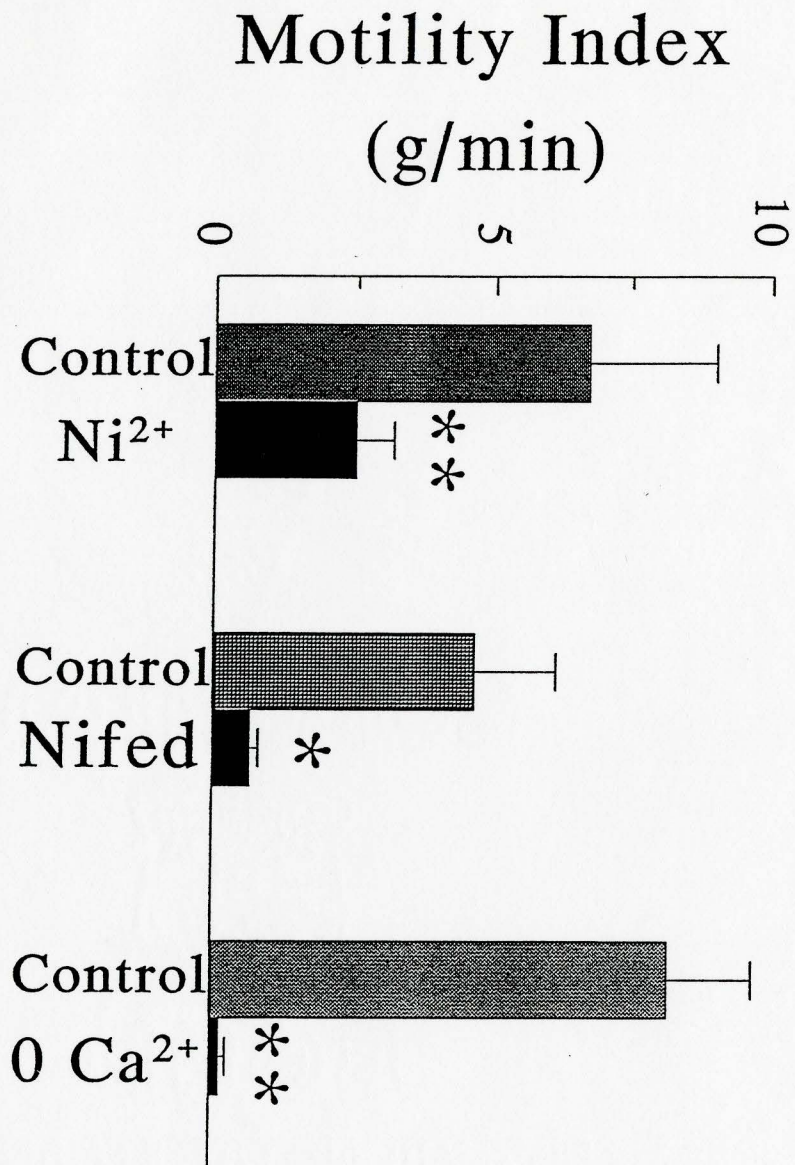
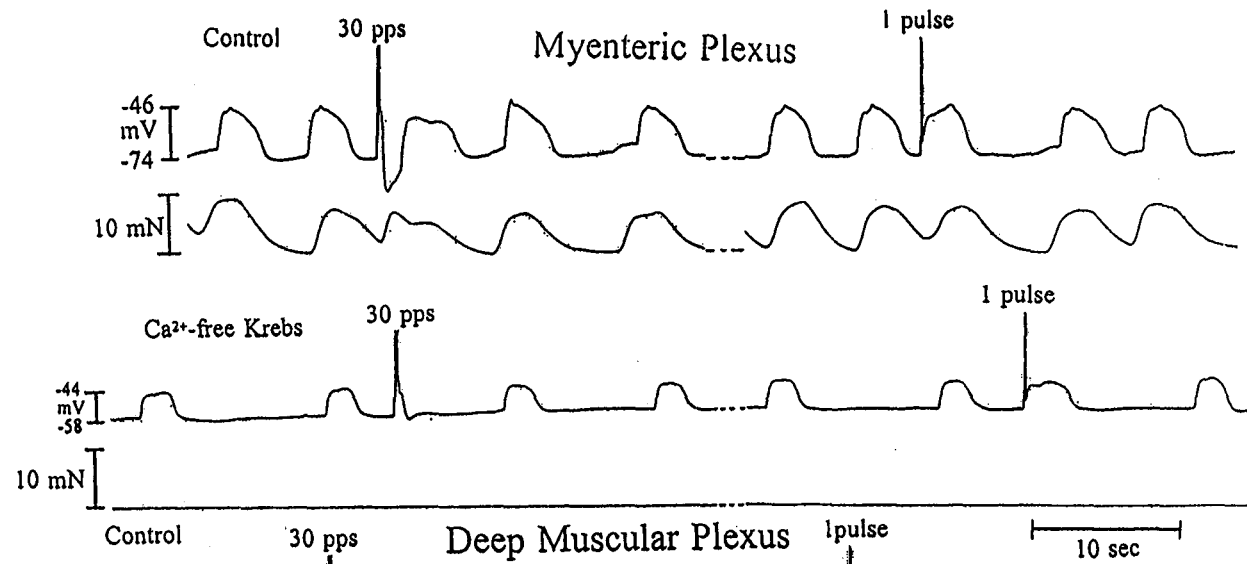
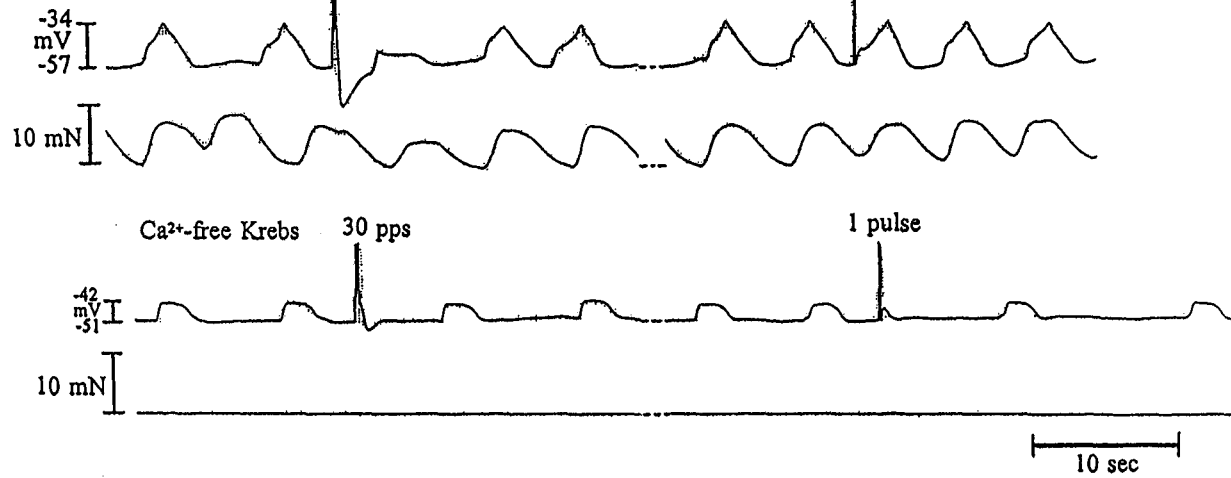


Fig. 5. Inhibitory effects of Ni²⁺, nifedipine, and Ca²⁺ removal on contractions

Fig. 6. Differential effects of Ca^{2+} removal on slow waves and triggered activity

A**B**

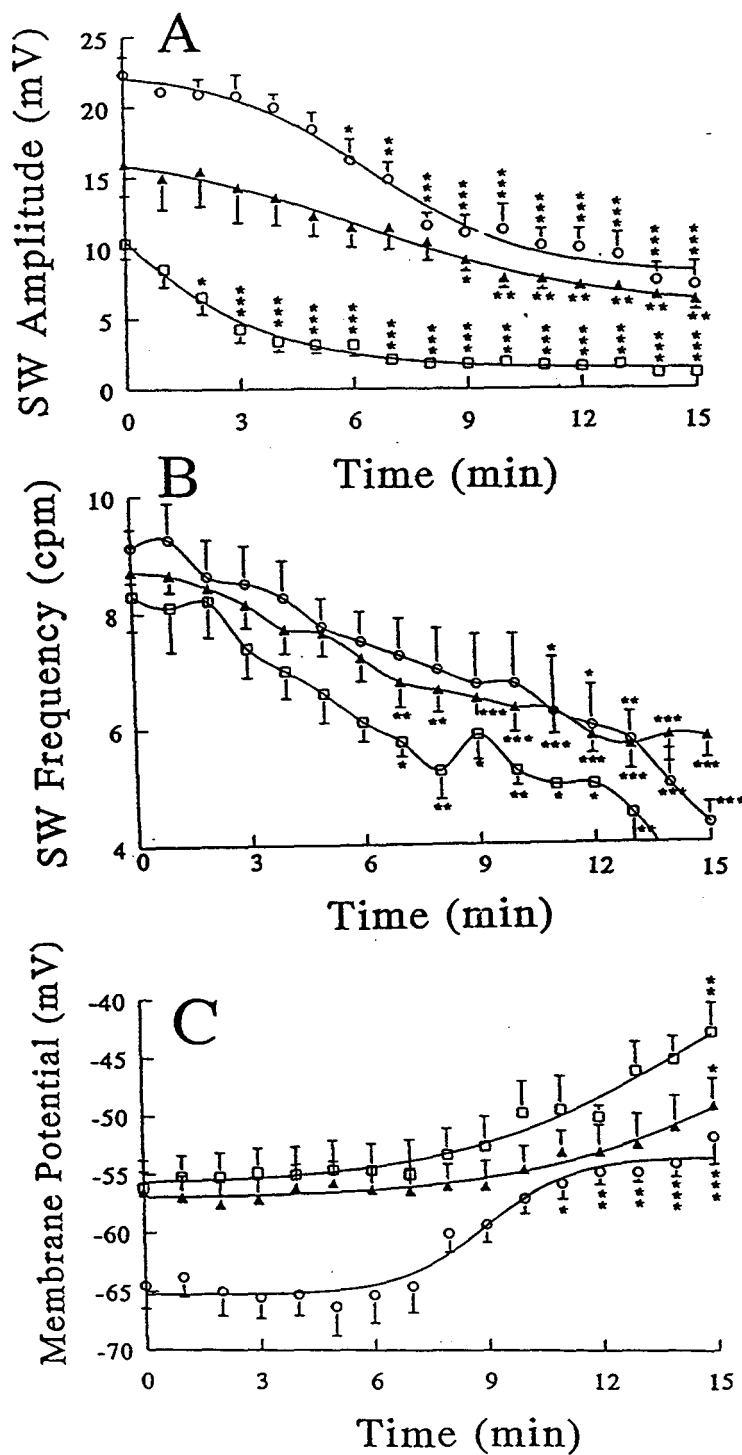


Fig. 7. Summary of inhibitory effects of Ca^{2+} removal on slow waves and membrane potentials

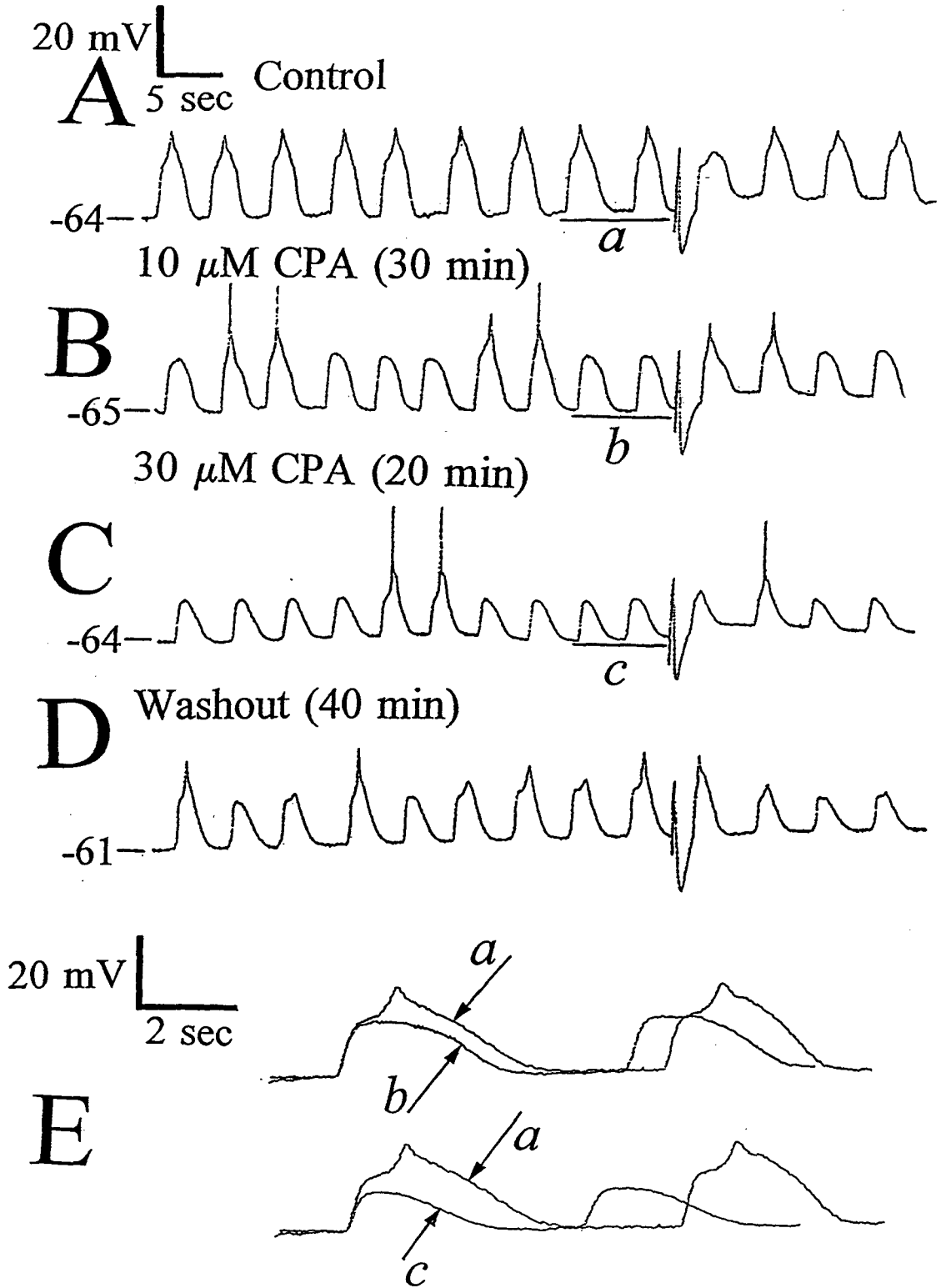


Fig. 8. Electromechanical effects of cyclopiazonic acid near the deep muscular plexus

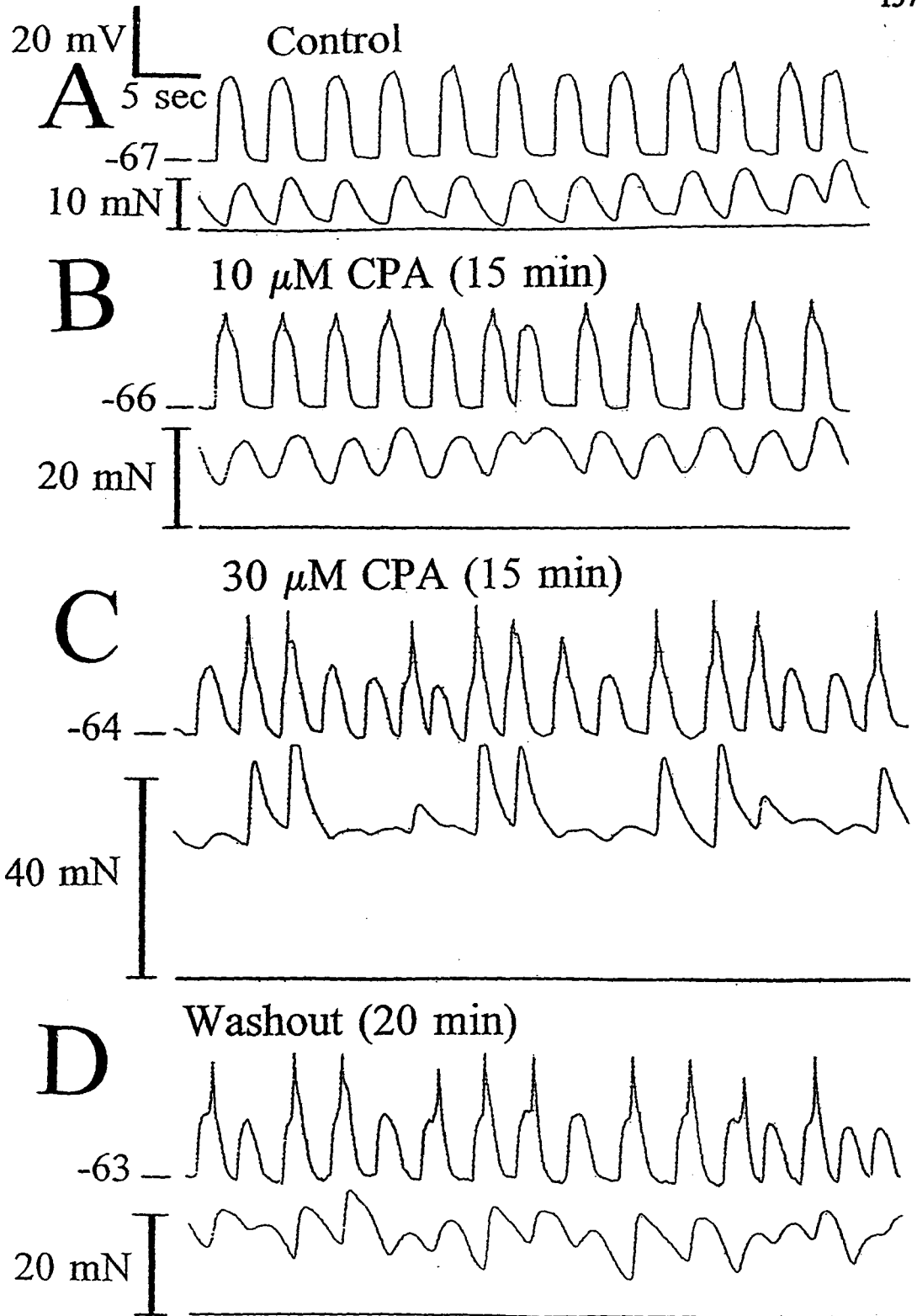


Fig. 9. Electromechanical effects of cyclopiazonic acid near the myenteric plexus

Table 1. Electrophysiological effects of the N-type Ca²⁺ channel blocker, ω -conotoxin GVIA (ω -CTX) at 10⁻⁷-3x10⁻⁷ M, and the L-type Ca²⁺ channel antagonist, nifedipine at 10⁻⁷-3x10⁻⁷ M, on cells near the regions of the myenteric plexus (MyP) (A) and the deep muscular plexus (DMP) (B) in the full-thickness preparations.

TREATMENT	SW Frequency (cycles/min)	SW Amplitude (mV)	SW Duration (sec)	Resting Membrane Potential (mV)	TSW _{30pps} Amplitude (mV)	TSW _{30pps} Duration (sec)	IJP Amplitude (mV)	IJP Duration (sec)	TSW _{30pps} Induction Delay (sec)
A. Control Near MyP	9.42 ± 0.26 (n=12)	23.82 ± 1.60 (n=12)	4.56 ± 0.20 (n=12)	-71.08 ± 2.11 (n=12)	16.73 ± 1.36 (n=12)	4.16 ± 0.16 (n=8)	14.48 ± 1.23 (n=11)	1.39 ± 0.09 (n=11)	2.23 ± 0.16 (n=11)
A. ω -CTX Near MyP	9.43 ± 0.32 (n=12) NS	24.05 ± 1.75 (n=12) NS	4.45 ± 0.23 (n=12) NS	-70.14 ± 2.41 (n=12) NS	18.3 ± 1.61 (n=12) NS	4.10 ± 0.33 (n=8) NS	2.17 ± 1.21 (n=11) ****	0.44 ± 0.23 (n=11) **	2.54 ± 0.55 (n=11) NS
B. Control Near DMP	8.87 ± 0.69 (n=4)	18.30 ± 3.77 (n=4)	4.95 ± 0.63 (n=4)	-59.25 ± 1.97 (n=4)	10.65 ± 2.14 (n=4) †	4.62 ± 0.19 (n=4)	20.25 ± 1.35 (n=4)	2.37 ± 0.57 (n=4)	3.27 ± 0.63 (n=4)
B. ω -CTX Near DMP	8.38 ± 0.80 (n=4) NS	17.48 ± 3.55 (n=4) NS	5.03 ± 0.61 (n=4) NS	-59.50 ± 2.75 (n=4) NS	12.88 ± 2.31 (n=4) NS	6.19 ± 0.12 (n=4) *	4.95 ± 4.95 (n=4) *	1.85 ± 0.05 (n=4) *	4.22 ± 0.48 (n=4) *
A. Control Near MyP	9.08 ± 1.02 (n=4)	24.1 ± 4.35 (n=4)	4.45 ± 0.17 (n=4)	-61.50 ± 1.71 (n=4)	16.88 ± 1.68 (n=4)	not measured	16.77 ± 1.73 (n=3)	2.2 ± 0.40 (n=3)	2.45 ± 0.64 (n=3)
A. Nifedipine Near MyP	8.75 ± 0.43 (n=4) NS	22.35 ± 3.75 (n=4) NS	4.45 ± 0.21 (n=4) NS	-60.8 ± 1.55 (n=4) NS	17.2 ± 0.60 (n=4) NS	not measured	18.0 ± 1.80 (n=3) NS	2.2 ± 0.30 (n=3) NS	2.25 ± 0.05 (n=3) NS
B. Control Near DMP	10.26 ± 0.63 (n=5)	15.39 ± 3.1 (n=5)	4.54 ± 0.13 (n=5)	-58.80 ± 1.83 (n=5)	6.99 ± 0.83 (n=4) ‡	not measured	17.53 ± 2.68 (n=5)	1.74 ± 0.12 (n=5)	2.38 ± 0.20 (n=5)
B. Nifedipine Near DMP	9.98 ± 0.58 (n=5) NS	15.37 ± 2.96 (n=5) NS	4.60 ± 0.15 (n=5) NS	-55.64 ± 2.54 (n=5) NS	8.0 ± 1.43 (n=4) NS	not measured	17.07 ± 1.89 (n=5) NS	1.85 ± 0.05 (n=5) NS	2.48 ± 0.27 (n=5) NS

Values (means ± SE) represent maximal effect of antagonists at 30 min postinfusion; (n) = number of animals. NS = P>0.05; *, P<0.05; **, P<0.01; ***, P<0.001; ****, P<0.0001. Significances are with respect to controls in both treatments. † P<0.05, DMP vs. MyP TSW amplitude controls in ω -CTX treatments. ‡ P<0.01, DMP vs. MyP TSW amplitude controls in nifedipine treatments.

Table 2. Electrophysiological effects of 200 μM Ni^{2+} on cells near the regions of the myenteric plexus (MyP) (A) and the deep muscular plexus (DMP) (B) in the full-thickness preparations.

TREATMENT	SW Frequency (cycles/min)	SW Amplitude (mV)	SW Duration (sec)	Resting Membrane Potential (mV)	TSW Amplitude (mV)	TSW Duration (sec)	IJP Amplitude (mV)	IJP Duration (sec)	TSW _{30pps} Induction Delay (sec)
A. Control Near MyP	8.82 \pm 0.74 (n=6)	18.53 \pm 13.68 (n=6)	4.33 \pm 0.34 (n=6)	-66.67 \pm 2.29 (n=6)	30 pps 13.78 \pm 1.87 (n=6) 1 pulse 20.25 \pm 2.25 (n=4)	30 pps 4.22 \pm 0.24 (n=6) 1 pulse 4.65 \pm 0.46 (n=4)	16.08 \pm 1.57 (n=6)	1.70 \pm 0.07 (n=6)	3.0 \pm 0.58 (n=6)
A. Nickel Near MyP	5.97 \pm 0.53 (n=6) **	13.68 \pm 1.56 (n=6) **	6.38 \pm 0.37 (n=6) **	-72.83 \pm 3.93 (n=6) NS	30 pps 13.43 \pm 2.09 (n=6) NS 1 pulse 13.9 \pm 1.34 (n=4) *	30 pps 6.16 \pm 0.39 (n=6) ** 1 pulse 6.05 \pm 0.41 (n=4) *	17.75 \pm 1.48 (n=6) NS	2.36 \pm 0.20 (n=6) NS	4.23 \pm 0.31 (n=6) **
B. Control Near DMP	8.88 \pm 0.52 (n=4)	23.93 \pm 2.77 (n=4)	4.84 \pm 0.46 (n=4)	-62.5 \pm 2.40 (n=4)	30 pps 14.95 \pm 2.02 (n=4) § 1 pulse 15.05 \pm 1.62 (n=4) §	30 pps 3.98 \pm 0.12 (n=4) 1 pulse 5.01 \pm 0.36 (n=4)	19.5 \pm 1.59 (n=4)	1.74 \pm 0.13 (n=4)	3.14 \pm .58 (n=4)
B. Nickel Near DMP	6.5 \pm 0.71 (n=4) *	13.98 \pm 1.05 (n=4) *	6.63 \pm 0.55 (n=4) *	-68.5 \pm 2.60 (n=4) NS	30 pps 13.08 \pm 1.28 (n=4) NS 1 pulse 8.7 \pm 1.70 (n=4) **	30 pps 6.24 \pm 0.27 (n=4) *** 1 pulse 5.88 \pm 0.28 (n=4) **	18.78 \pm 2.29 (n=4) NS	1.94 \pm 0.24 (n=4) NS	4.13 \pm 0.44 (n=4) NS

Values (means \pm SE) represent maximal effect of nickel at 30 min postinfusion; (n) = number of animals. NS = $P > 0.05$; *, $P < 0.05$; **, $P < 0.01$; ***, $P < 0.001$. Treatments were compared to relevant controls. § $P > 0.05$, DMP vs. MyP TSW amplitude controls. Single pulses were 100 msec, 10 to 20 V square waves.

Table 3. Electrophysiological effects of 0 Ca²⁺ (100 μM EGTA) on cells near the regions of the myenteric plexus (MyP) (A) and the deep muscular plexus (DMP) (B) of the full-thickness preparations and near the DMP region of isolated circular muscle (ICM) (C).

TREATMENT	SW Frequency (cycles/min)	SW Amplitude (mV)	SW Duration (sec)	Resting Membrane Potential (mV)	TSW Amplitude (mV)	TSW Duration (sec)	IJP Amplitude (mV)	IJP Duration (sec)	TSW _{30pps} Induction Delay (sec)
A. Control Near MyP	9.12 ± 0.38 (n=6)	22.02 ± 1.80 (n=6)	4.60 ± 0.33 (n=6)	-65.33 ± 1.89 (n=6)	<u>30 pps</u> 14.48 ± 1.97 (n=6) <u>1 pulse</u> 20.16 ± 2.00 (n=5)	<u>30 pps</u> 4.03 ± 0.12 (n=6) <u>1 pulse</u> 4.26 ± 0.88 (n=5)	15.75 ± 1.11 (n=6)	1.62 ± 0.18 (n=6)	2.45 ± 0.13 (n=6)
A. 0 Ca ²⁺ Near MyP 10-12 min.	5.46 ± 0.44 (n=6) **	10.25 ± 1.12 (n=6) ***	3.82 ± 0.65 (n=6) NS	-58.5 ± 3.45 (n=6) *	<u>30 pps</u> 9.48 ± 1.00 (n=6) ** <u>1 pulse</u> 8.88 ± 2.07 (n=5) ***	<u>30 pps</u> 3.73 ± 0.43 (n=6) NS <u>1 pulse</u> 3.16 ± 0.94 (n=5) NS	2.41 ± 0.92 (n=6) ***	0.73 ± 0.29 (n=6) **	6.40 ± 1.04 (n=6) **
B. Control Near DMP	8.41 ± 0.40 (n=7)	14.64 ± 1.57 (n=7)	4.53 ± 0.22 (n=6)	-54.67 ± 1.09 (n=6)	<u>30 pps</u> 7.08 ± 1.19 (n=5) † <u>1 pulse</u> 10.72 ± 2.33 (n=5) ‡	<u>30 pps</u> 4.12 ± 0.44 (n=5) <u>1 pulse</u> 4.09 ± 0.32 (n=5)	15.04 ± 2.37 (n=7)	2.12 ± 0.14 (n=7)	3.34 ± 0.15 (n=7)
B. 0 Ca ²⁺ Near DMP 10-12 min.	5.57 ± 0.20 (n=7) ***	6.13 ± 0.68 (n=7) ***	2.5 ± 0.21 (n=6) **	-52.07 ± 1.21 (n=6) NS	<u>30 pps</u> 4.60 ± 1.04 (n=5) * <u>1 pulse</u> 5.60 ± 1.03 (n=5) *	<u>30 pps</u> 3.77 ± 0.72 (n=5) NS <u>1 pulse</u> 3.08 ± 0.86 (n=5) NS	0.91 ± 0.69 (n=7) ***	0.31 ± 0.20 (n=7) ***	5.36 ± 0.68 (n=7) *

C. Control Near DMP in ICM	8.30 ± 0.58 (n=5)	10.3 ± 1.0 (n=5)	5.82 ± 0.28 (n=5)	-56.20 ± 2.40 (n=5)	Not triggered	N o t triggered	22.04 ± 1.17 (n=5)	6.0 ± 1.07 (n=5)	N o t triggered
C. 0 Ca ²⁺ Near DMP in ICM 10 min.	5.25 ± .25 (n=5) **	1.9 ± 0.3 (n=5) ***	N o t detectable	-49.60 ± 2.73 (n=5) NS	Not triggered	N o t triggered	1.24 ± 0.76 (n=5) ****	0.42 ± 0.26 (n=5) **	N o t triggered

Data are means ± SE; (n) = number of animals. NS = not significant, P>0.05; *, P<0.05; **P<0.01; ***, P<0.001. Treatments (after 10-12 min. in Ca²⁺-free solutions) were compared to respective controls. † P<0.05, DMP vs. MyP TSW (30 pps) control amplitudes. ‡ P<0.05, DMP vs. MyP TSW (1 pulse) control amplitudes. Single pulses were evoked by 100 msec depolarizing square waves (10-20 V).

CHAPTER 3.4

PAPER No. 4 (*preliminary report*)

CANINE ILEUM MYENTERIC AND DEEP MUSCULAR PLEXUS SLOW WAVES: ELECTRICAL COUPLING OF INTERSTITIAL CELLS OF CAJAL TO MYOCYTES

To be submitted to *American Journal of Physiology*

Francisco Cayabyab's contribution:

- (i) performance of all electrophysiological studies; morphological studies were executed by Dr. Wang
- (ii) data presentation and statistical analysis
- (iii) preparation of manuscript for submission to *American Journal of Physiology*

**CANINE ILEUM MYENTERIC AND DEEP MUSCULAR
PLEXUS SLOW WAVES: ELECTRICAL COUPLING OF
INTERSTITIAL CELLS OF CAJAL TO MYOCYTES.**

Francisco S. Cayabyab¹, Yu-Fang Wang², Hubert deBruin¹, and E.E. Daniel^{2*}

Running Title: Gap Junctions and Interstitial Cells of Cajal in Ileum.

McMaster University

¹Department of Electrical and Computer Engineering and

²Department of Biomedical Sciences

Division of Physiology and Pharmacology

Hamilton, Ontario, Canada

* Author for correspondence

ABSTRACT

Previously we showed that two distinct types of slow waves originated near the myenteric and deep muscular plexuses, where the clear presence of interstitial cells of Cajal or ICC (putative pacemakers) have been demonstrated by others. In the present study we tested the hypothesis that the heterogeneity in slow wave configurations generated near both plexuses reflect the different gap junction coupling properties of ICC to circular muscle cells. Intracellular microelectrode studies revealed that two types of slow waves (plateau-type near the myenteric plexus and triangular near the deep muscular plexus) oscillated with similar frequencies of 8-11 cycles/min in the intact muscularis externa. Spontaneous circular muscle contractions accompanied both types of slow waves. Octanol at 0.5-1 mM, a gap junction blocker, depolarized (by 8-17 mV) the membrane potential of circular muscle cells near the myenteric plexus. This effect was accompanied by a reversible inhibition of slow wave amplitude (by 56-88%) and frequency (by 20-52%), a decrease in the rate of rise of slow waves, and an abolition of circular muscle contractions after 20 min of exposure (n=3). In contrast, octanol at 1 mM modestly depolarized (by 2-10 mV) the membrane potentials of circular muscle cells near the deep muscular plexus, reduced slow wave amplitudes (by 28-44%) and frequencies (by 10-12%), but abolished circular muscle contractions (n=3). The fast inhibitory junction potentials (IJPs) recorded from the myenteric plexus region were abolished, but a slow IJP occurred after a delay. In contrast, the IJPs from the deep muscular plexus were inhibited by 50% in amplitude and occurred without a delay. The differential inhibitory

effects of octanol on slow wave parameters may reflect the different densities of gap junctions between ICC and circular muscle near the two plexuses. Greater susceptibility of myenteric plexus slow waves to octanol correlates with the paucity of gap junctions found in that region. In contrast, ICC are well coupled by gap junctions to one another and to circular muscle in the deep muscular plexus. The inhibitory effects of octanol on IJP may reflect the inability of nitric oxide action on muscle to be transmitted to other gap junctionally coupled smooth muscle. Disappearance of phasic contractions may involve blockade of Ca^{2+} influx by octanol.

***Key Words:* octanol, gap junctions, myenteric and deep muscular plexuses, inhibitory junction potentials, slow waves, excitation-contraction coupling.**

INTRODUCTION

A major pathway for intercellular communication in the gastrointestinal tract is believed to occur mainly through the normal functioning of gap junctions and other cell-to-cell contacts that are heterogeneously distributed along the muscularis externa of the small bowel and colon (10,13,14,15). Gap junctions which represent low resistance cell contacts allow for the electrical and metabolic coupling between different cellular populations and consequently for the synchronization of electrical activity and phasic contractions in the muscularis externa (10,13,15). The molecular structure of the gap junction protein (connexin 43) in the gut musculature of several species has been identified by molecular (16) and immunohistochemical (17) techniques. It has been widely accepted that gap junctions are absent or not detectable by electron microscopy or immunocytochemistry (17) in the longitudinal muscle layer and that gap junctions between interstitial cells of Cajal or ICC (putative pacemaker cells) (26) of the myenteric plexus and adjacent circular muscle are also absent or undetectable by electron microscopic techniques used (10). However, dense distribution of gap junctions occur between the deep muscular plexus ICC and circular muscle and also between ICC in this region (10,12,14,28). Moreover, the presence of gap junctions between ICC and circular muscle of myenteric plexus has not been shown by electron microscopy. A recent study of the colon by Huizinga and colleagues (13) utilizing neurobiotin injection and detection of its spread by confocal microscopy has demonstrated the coupling of cells by low density gap junctions between the longitudinal muscle cells and between myenteric plexus ICC and

circular muscle cells. Neurobiotin spread was inhibited by the gap junction blocker octanol (13). Functional studies of gap junction channels that have been performed on cardiac (25), vascular (7), and some visceral smooth muscle (13,15,27) usually involved the detection of a spread of low molecular weight tracer molecules or monovalent and divalent cations. However studies of gap junction function and their influence on electrical coupling of pacemaking cells to smooth muscle are rare in the small intestine.

Recently we have shown that in the canine ileum muscularis externa, two distinct types of slow waves paced from the myenteric and deep muscular plexuses occur independently and interactively (see Chapters 3.1, 3.2, 3.3). We have suggested that the difference in slow wave configurations (plateau-type slow waves near the myenteric plexus region in contrast to the triangular ones near the deep muscular plexus) might be explained by the different structural coupling by gap junctions of the ICC to the longitudinal and circular muscle cells. The aim of this study was to investigate the effects of octanol on the slow waves, inhibitory junction potentials (IJPs), and phasic contractions associated with the myenteric and deep muscular plexus. Morphological evidence to elucidate the ultrastructural relationship of myenteric and deep muscular plexus ICC to circular smooth muscle was obtained in an attempt to correlate morphological structure with the pacemaking function of the small intestine. The results suggest that a difference in susceptibility of the slow waves or IJPs to gap junction blockade may relate to differences in gap junction densities near the myenteric and deep muscular plexuses. We propose that this marked difference in gap junction density between the two pacemaking

networks may be physiologically relevant and may account for the heterogeneity in electrical activity in canine ileum.

METHODS

Electrophysiological studies.

Tissues from six dogs were used in this study. Tissue preparations were as previously described (see Chapters 3.1, 3.2, and 3.3). Electrophysiological recording technique and sites of recording electrodes were also described in previous chapters (3.1, 3.2, and 3.3). Stable electrical recordings were obtained using glass microelectrodes filled with 3 M KCl with resistances of 30-90 M Ω . The Krebs solution was aerated with 95% O₂ - 5% CO₂ to maintain pH of approximately 7.4 and consisted of (in mM): NaCl, 115.5; NaH₂PO₄, 1.6; NaHCO₃, 21.9; KCl, 4.2; CaCl₂, 2.5; MgSO₄, 1.2 and glucose, 11.1. Tissue strips were pinned to the Sylgard floor of the muscle chamber and allowed to equilibrate for at least 2 hours before starting experiments. Octanol, purchased from Sigma, was superfused for 20-30 min.

Electron microscopic studies.

Methods for fixation and staining of tissues for electron microscopy have been described in detail and published in several publications (1,2,3,4,6,9). In brief, a segment of the canine ileum from an anaesthetized animal was perfused with 2% glutaraldehyde through a cannulated mesenteric artery. A segment of the perfused ileum was later removed and immersed for 2 hours in 2% glutaraldehyde, which contained 4.5% sucrose

and 1 mM CaCl₂ in 75 mM sodium cacodylate buffer (pH of 7.4 at room temperature). Tissues were subsequently washed overnight in cacodylate buffer (6% sucrose and 1.25 mM CaCl₂, pH of 7.4 at 4 °C) and postfixed in OsO₄ in 0.05 M cacodylate buffer at room temperature for 90 min. Tissue blocks were stained with saturated uranyl acetate for 60 min, dehydrated in graded ethanol and propylene oxide, and then embedded in Spurr resin. Ultra-thin sections (96 nm) were obtained using a Sorvall MT-2B ultramicrotome, stained in lead citrate for 3 min, and viewed with a Philips 301 electron microscope at 60 kV.

Statistical analysis.

Data are presented as mean \pm S.E.M. Student *t*-tests were performed to check for statistical significance. Mean values were considered significantly different when $P < 0.05$.

RESULTS

Figure 1 shows the reversible inhibitory effects of octanol (1 mM) on slow waves and contractions near the myenteric plexus and deep muscular plexus recordings. The slow waves recorded from the myenteric plexus region were more effectively inhibited by octanol (amplitude: by 50-90%; and frequency: by 20-50%), but the slow waves recorded from the deep muscular plexus were less effectively inhibited in amplitude (by 30-50%) and frequency (about 10%) (see Table 1 for summary of actual values). Phasic contractions were abolished within 5 minutes of octanol superfusion and prior to changes

in membrane potential and significant inhibition of slow waves (Figures 1). Myenteric plexus slow waves were rapidly inhibited even by 0.5 mM octanol (amplitude: 19.4 mV (control) vs 12.4 mV (treated); and frequency: 8 cycles/min (control) vs 7 cycles/min (treated) n=1). Octanol at 0.5 mM had no detectable effect on slow wave parameters near the deep muscular plexus, but abolished circular muscle contractions. Near the myenteric plexus, octanol depolarized the membrane potential by 10-15 mV (Table 1), but this was accompanied by abolition of the "fast" component of IJPs (Figure 2A). A "slow" IJP occurring after a delay was unmasked; its nature and origin was not studied further in this study. In contrast, the IJPs recorded from the deep muscular plexus were inhibited by about 50% in amplitude and were not delayed (Figure 2B). The differential effects of octanol on the slow waves paced from the myenteric and deep muscular plexuses may be related to the different density and size of gap junctions that electrically couple the ICC to one another and to circular muscle myocytes. Gap junctions of greater density near the deep muscular plexus were found between ICC and between ICC and outer circular muscle (Figure 3). Gap junctions of smaller density near the myenteric plexus were difficult to show by electron microscopy, but were found to exist between ICC (Figure 4). Close appositional contacts were also found between ICC and circular muscle in this region (Figure 5). Nerve bundles were found to be in close proximity to ICC of the deep muscular plexus (Figure 3) while both nerve ganglia and nerve bundles were shown to be closely associated with the ICC of the myenteric plexus (Figures 4 and 5). Close appositional contacts and gap junctions were also found to exist between outer circular

muscle (E.E. Daniel, unpublished).

DISCUSSION

In the gastrointestinal tract, the molecular structure of gap junction protein (connexin 43) has been recently identified (16,17). Gap junctions represent intercellular communication pathways of least resistance allowing for the metabolic and ion-current carrying molecules to pass from cell to cell (7,10,13,25). Gap junctionally coupled circular smooth muscle cells act as a syncytium and ICC which are electrically well-coupled by visible gap junctions to circular muscle in the deep muscular plexus (20) may give rise to the triangular slow waves recorded from circular muscle. In contrast, the ICC in the myenteric plexus of the colon and small intestine are known to be less coupled by visible gap junctions (3,10,14,21). Either the gap junctions are too small to be detected by immunohistochemistry or electron microscopy or they are not present at all (10). However, other techniques have provided a further understanding of intercellular communication in the canine colon (13) and small intestine (16). Neurobiotin spread detection by confocal microscopy revealed that there are octanol-sensitive gap junctions able to metabolically and electrically couple longitudinal muscle to longitudinal muscle and ICC to adjacent circular muscle cells where gap junctions were previously believed to be absent (13). These studies on colonic tissues are consistent with recent studies done on small intestinal tissues which suggest the presence of connexin 43 in the longitudinal

muscle (16). The present study provided evidence of occasional gap junction coupling between ICC of myenteric plexus and between ICC and circular muscle but never between ICC and longitudinal muscle. Close appositional contact have been found to occur between ICC and longitudinal muscle, and evidence of visible gap junctions between ICC and longitudinal muscle was not obtained (E.E. Daniel, unpublished).

In this study, we showed that the myenteric plexus slow waves were more effectively diminished by octanol than those slow waves recorded near the deep muscular plexus. The greater susceptibility of the myenteric plexus pacemakers to gap junction blockade may be related to the paucity of gap junctions in this region (Berezin, Wang, and Daniel, unpublished observations). Close appositions and intermediate contacts but never visible gap junctions were observed between myenteric plexus ICC and longitudinal muscle cells and between adjacent circular muscle cells (Berezin, Wang, and Daniel, unpublished). Similar observations were recently reported in the colon (13,15,19). Previous studies have shown the presence of numerous gap junctions between outer circular smooth muscle cells and ICC of the deep muscular plexus and also between ICC of the deep muscular plexus (reviewed in 10,16,20). Arrays of connecting ICC were not found between the two pacemaking networks (21; Daniel E.E., unpublished), but visible gap junctions were found connecting the outer circular muscle cells in the canine ileum (12,14; Daniel, E.E., unpublished) and in other regions of the small intestine of other species (19,21). However, slow waves persisted during inhibition of gap junction function by octanol, suggesting that alternate coupling mechanisms (e.g., via electrical field

coupling (15) strengthened by appositional contacts and interdigitations of ICC and muscle cells) between myenteric plexus ICC and outer circular muscle may help coordinate the pacemaking function of the canine ileum. The different sensitivity of slow waves to octanol may relate to the marked heterogeneity in gap junction densities. Consequently, this graded gap junction density seen across the canine ileum musculature may explain the physiological observations of marked heterogeneity in slow waves, membrane potentials, and IJPs.

The inhibition of IJPs from both regions remains unclear. The full abolition of the fast IJP component and an apparent unmasking of a "slow" IJP component as observed near the myenteric plexus may reflect the electrotonic transmission of the IJP from the deep muscular plexus. This requires further investigation by studying the effects of octanol on the time delays of IJPs evoked by a single pulse electrical field stimulation. If the "slow" IJP originated in the deep muscular plexus region, then octanol is expected to increase the resistance and the time delay for the IJP to reach the myenteric plexus recording site. These IJPs are sensitive to the K^+ channel blocker, apamin (8). Octanol may inhibit IJPs which may result from inhibitions of Ca^{2+} and K^+ channels as it does in pancreatic acinar cells (18). Also octanol has been shown to block low threshold, voltage-activated T-type Ca^{2+} currents in neurons (22); this current was not inhibited by the N-type Ca^{2+} channel blocker ω -conotoxin GVIA, but was sensitive to Ni^{2+} . In our earlier study (see Chapter 3.3), we showed that the ω -conotoxin GVIA abolished IJPs. Whether octanol inhibits Ca^{2+} channels required for neurotransmitter release or it blocks K^+

channels responsible for the IJP needs further studies. Inhibition of K^+ channels would be consistent with the observed membrane depolarizations and reduction of IJPs in the canine ileum.

Previously we have shown (see preceding Chapter 3.3) that slow waves from both pacemaking regions were unaffected by antagonists of voltage-operated Ca^{2+} channels (L-type blocker, nifedipine, and N-type blocker, ω -conotoxin GVIA) and slowly affected by removal of extracellular Ca^{2+} . In the present study, octanol also abolished contractions even before slow waves were significantly affected. Either octanol inhibited a gap junction-mediated diffusion of Ca^{2+} from cell to cell as shown by others (7,24) or octanol was inhibiting the diffusion of second messenger molecules involved in the Ca^{2+} influx pathway (11) which may be involved in the excitation-contraction coupling. Because octanol is not very selective as a gap junction blocker, the nonspecific blockade of Ca^{2+} channels by octanol, like heptanol in the colon (23), may explain the inhibitory effect of octanol on abolishing contractile activity associated with excitations by slow waves and also on reducing slow wave amplitude and frequency.

ACKNOWLEDGEMENTS

This investigation was supported by the M.R.C. and N.S.E.R.C. of Canada.

REFERENCES

1. **Berezin, I., H.D. Allescher, and E.E. Daniel.** Ultra-structural localization of VIP-immunoreactivity in canine distal esophagus. *J. Neurocytology* 16:-749-757, 1987.
2. **Berezin, I., J.D. Huizinga, and E.E. Daniel.** Interstitial cells of Cajal in canine colon: A special communication network at the inner border of the circular muscle. *J. Comp. Neurocyt.* 273:42-51, 1988.
3. **Berezin, I., J.D. Huizinga, and E.E. Daniel.** Structural characterization of interstitial cells of Cajal in myenteric plexus and muscle layers of canine colon. *Can. J. Physiol. Pharmacol.* 68: 1419-1431, 1990.
4. **Berezin, I., J.D. Huizinga, L. Farraway, and E.E. Daniel.** Innervation of interstitial cells of Cajal by VIP-containing nerves in canine colon. *Can. J. Physiol. Pharmacol.* 68: 922-932, 1990.
5. **Berezin, I., S. Sheppard, E.E. Daniel, and N. Yanaiharu.** Ultrastructural immunocytochemical distribution of VIP-like immunoreactivity in dog ileum. *Regulatory Peptides* 11: 287-298, 1985.
6. **Berezin, I., S.H. Snyder, D.S. Bredt, and E.E. Daniel.** Ultrastructural localization of NOS in canine small intestine and colon. *Am. J. Physiol.* 266:C981-C989, 1994.
7. **Christ, G.J., A.P. Moreno, A. Melman, and D.C. Spray.** Gap junction-mediated intercellular diffusion of Ca^{2+} in cultured human corporal smooth muscle cells. *Am. J. Physiol.* 263:-C373-C383, 1992.
8. **Christinck, F., J. Jury, F. Cayabyab, and E.E. Daniel.** Nitric oxide may be the final mediator of nonadrenergic, noncholinergic inhibitory junction potentials in the gut. *Can. J. Physiol. Pharmacol.* 69: 1448-1458, 1991.
9. **Daniel, E.E., and V. Posey-Daniel.** Neuromuscular structures in opossum esophagus: role of interstitial cells of Cajal. *J. Physiol.* 246: G305-G315, 1984.
10. **Daniel, E.E., and I. Berezin.** Interstitial cells of Cajal: are they major players in control of gastrointestinal motility? *J. Gastrointestinal Motility.* 4: 1-24, 1992.
11. **DeLisle, S., G.W. Mayr, and M.J. Welsh.** Inositol phosphate structural requisites for Ca^{2+} influx. *Am J. Physiol.* 268: C1485-C1491, 1995.

12. **Duchon, G., R. Henderson, and E.E. Daniel.** Circular muscle layers in the small intestine. In: *Proceedings of the International Symposium of Gastrointestinal Motility*. edited by E.E. Daniel. Vancouver: Mitchell Press 1974, p. 635-646.
13. **Farraway, L., A.K. Ball, and J.D. Huizinga.** Intercellular metabolic coupling in canine colon musculature. *Am. J. Physiol.* 268: C1492-C1502, 1995.
14. **Henderson, R.M., G. Duchon, and E.E. Daniel.** Cell contacts in duodenal smooth muscle layers. *Am. J. Physiol.* 221: 793-799, 1971.
15. **Huizinga, J.D., L.W.C. Liu, M.G. Blennerhasset, L. Thuneberg, and A. Molleman.** Intercellular communication in smooth muscle. *Experientia Basel* 48: 932-941, 1992.
16. **Li, Z., Z. Zhou, and E.E. Daniel.** Expression of gap junction connexin 43 and connexin 43 mRNA in different regional tissues of intestine in dog. *Am. J. Physiol.* 265: G911-G916, 1993.
17. **Mikkelsen, H.B., J.D. Huizinga, L. Thuneberg, and J.J. Rumessen.** Immunohistochemical localization of a gap junction protein (connexin 43) in the muscularis externa of murine, canine, and human intestine. *Cell Tissue Res.* 274: 249-256, 1993.
18. **Perez-Armendariz, E.M., P.C. Spray, and M.V.L. Bennet.** L-octanol reduced calcium, potassium and gap junctional currents in mouse pancreatic β -cells. *Biophys. J.* 55:218a, 1989.
19. **Rumessen, J.J., H.B. Mikkelsen, K. Qvortrup, and L. Thuneberg.** Ultrastructure of interstitial cells of Cajal in circular muscle of human intestine. *Gastroenterology.* 104: 343-350, 1993.
20. **Rumessen, J.J., H.B. Mikkelsen, and L. Thuneberg.** Ultrastructure of interstitial cells of Cajal associated with deep muscular plexus of the human small intestine. *Gastroenterology.* 102: 56-58, 1992.
21. **Rumessen, J.J., and L. Thuneberg.** Interstitial cells of Cajal in human intestine. Ultrastructural identification and organization between the main smooth muscle layers. *Gastroenterology.* 100: 1417-1431, 1991.
22. **Scott, R.H., J.F. Wootton, and A.C. Dolphin.** Modulation of neuronal T-type calcium channel currents by photoactivation of intracellular guanosine 5'-O(3-

- thio)triphosphate. *Neuroscience* 38: 285-294, 1990.
23. **Serio, R., C. Barajas-Lopez, E.E. Daniel, I. Berezin, and J.D. Huizinga.** Slow-wave activity in colon: role of network of submucosal interstitial cells of Cajal. *Am. J. Physiol.* 260:G636-G645, 1991.
 24. **Sneyd, J., B.T.R. Wetton, and A.C. Charles.** Intercellular calcium waves mediated by diffusion of inositol triphosphate: a two-dimensional model. *Am. J. Physiol.* 268: C1537-C1545, 1995.
 25. **Spray, D.C., and J.M. Burt.** Structure-activity relations of the cardiac gap junction channel. *Am. J. Physiol.* 258: C195-C205, 1990.
 26. **Thuneberg, L.** Interstitial cells of Cajal: intestinal pacemakers? *Adv. Anatomy, Embryology and Cell Biol.* 71: 1-130, 1982.
 27. **Zamir, O., and M. Hanani.** Intercellular dye-coupling in intestinal smooth muscle. Are gap junctions required for intercellular coupling? *Experientia Basel* 46: 1002-1005, 1990.
 28. **Zhou, D.S., and T. Komuro.** Interstitial cells associated with the deep muscular plexus of the guinea-pig small intestine, with special reference to the interstitial cells of Cajal. *Cell Tissue Res.* 268: 205-216, 1992.

FIGURE LEGENDS

Figure 1. Octanol inhibition of slow waves and contractions. Effects of octanol (1 mM) on slow waves and contractions after 15 min of superfusion. *A.* Myenteric plexus (MyP) recording. *B.* Deep Muscular plexus (DMP) recording. Slow wave amplitude and frequency (see Table 1) were more effectively diminished by octanol in the MyP than in the DMP recordings. Contractions were abolished within 5 min (not shown). Inhibitory effects of octanol on electrical and mechanical activities were reversible after about 30 minutes of washout of octanol (not shown).

Figure 2. Octanol effects on IJPs near two pacemaking regions. Faster speed traces of experiments from Figure 1 showing the effects of octanol (1 mM) on slow waves, inhibitory junction potentials, and contractions after 25 min of superfusion. *A.* Myenteric plexus (MyP) recording. *B.* Deep Muscular plexus (DMP) recording. The "fast" (f) IJP component was abolished in *A*, but a "slow" (s) IJP component was uncovered by octanol. The "fast" IJP, slow wave parameters, and mechanical activity return to near control values after withdrawal of octanol (not shown). In *B*, the IJP was slightly reduced in amplitude but not delayed.

Figure 3. Electron micrograph of the deep muscular plexus region. At top is the inner circular muscle (ICM) layer, at bottom outer circular muscle (OCM), and at middle the deep muscular plexus (DMP) which contains interstitial cells of Cajal (IC) and nerve

endings. Note the profile of one IC shows its nucleus (n) and its numerous caveolae (c) which is characteristic of an IC. This IC is coupled to other IC (one with only a cross section of one of its processes showing) by gap junction (gj) and close appositional (ca) contacts (see a portion of an IC with its characteristic mitochondria (mit) showing). The IC are closely innervated by nerve bundles (nb). Calibration bar is shown at bottom.

Figure 4. Electron micrograph of the myenteric plexus region: gap junctions. Note three interstitial cells of Cajal (IC) that are coupled by a gap junctions (GJ) and close appositions (ca). Characteristic caveolae (c) found on IC and outer circular muscle (OCM) are shown. Gap junction contact between IC and circular muscle are rare, but close appositional contacts exist between IC and circular muscle. IC are densely innervated by nerve ganglia (G) and nerve fibers. Calibration bar shown at bottom.

Figure 5. Electron micrograph of the myenteric plexus region: close appositions. Note two apparent types of interstitial cells of Cajal (ICC) differentiated by the density of staining. Note the numerous caveolae (c) and mitochondria (mit) and the large nucleus (N), which are characteristic features of ICC. The light staining ICC forms close contact (see large hollow arrows) with two outer circular muscle (OCM). ICC are close to nerve bundles (NB). An endothelial cell (E) with its many characteristic caveolae, encloses a red blood cell (large dark stain). Calibration at bottom.

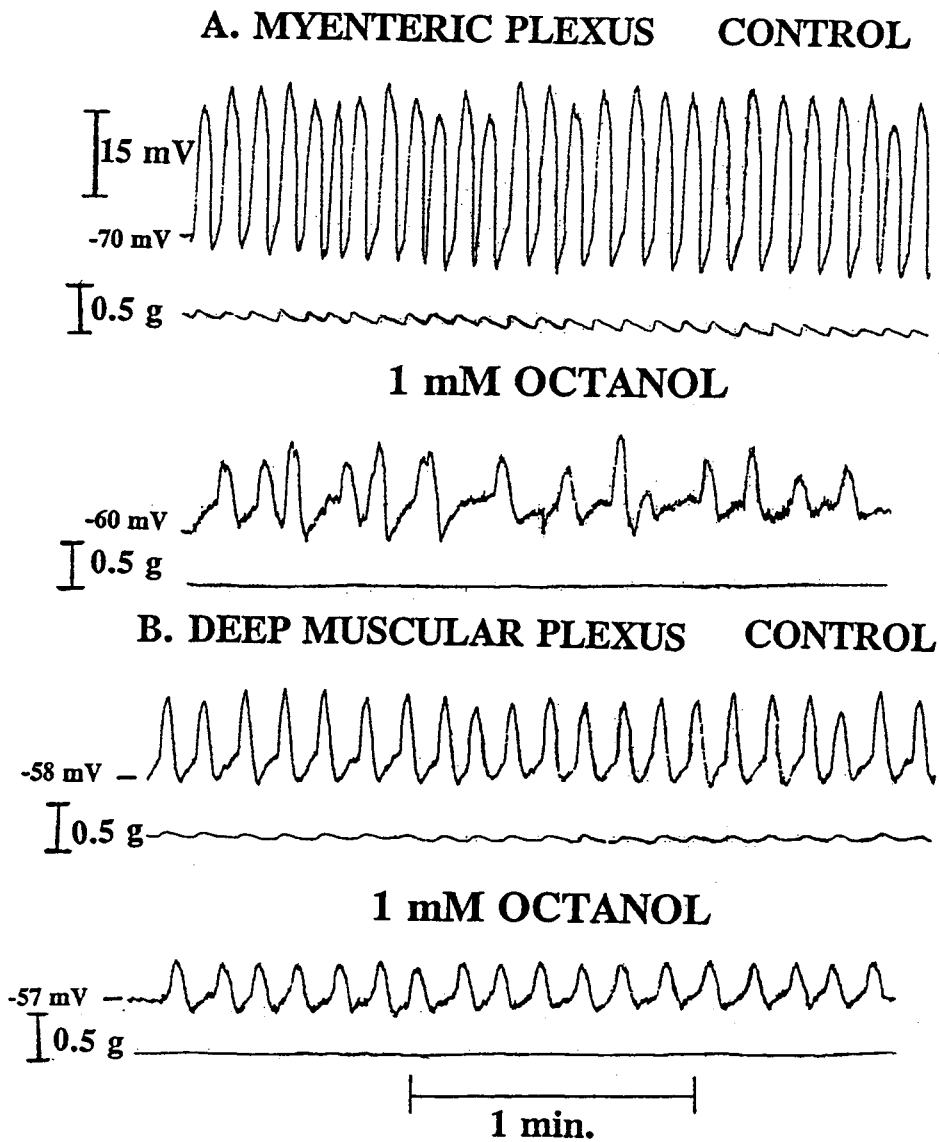


Fig. 1. Octanol inhibition of slow waves and contractions

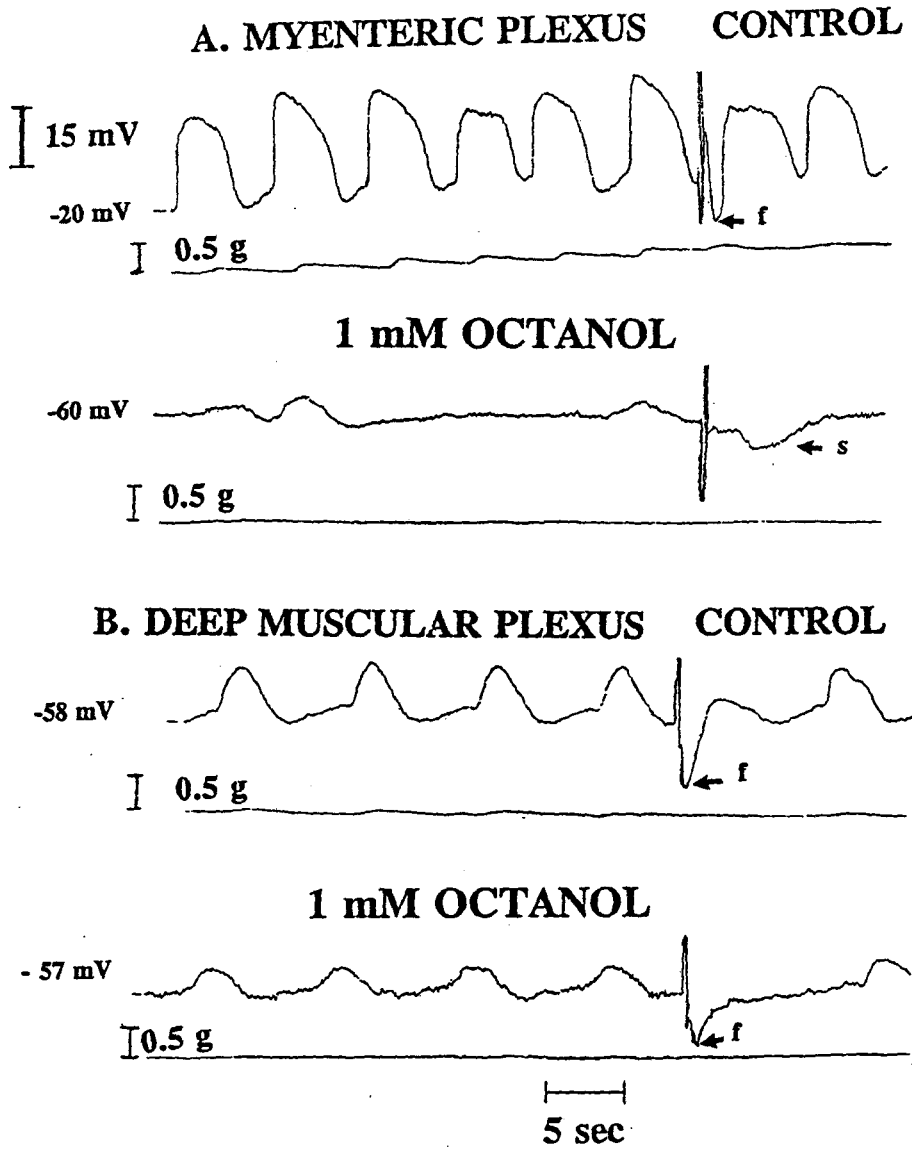
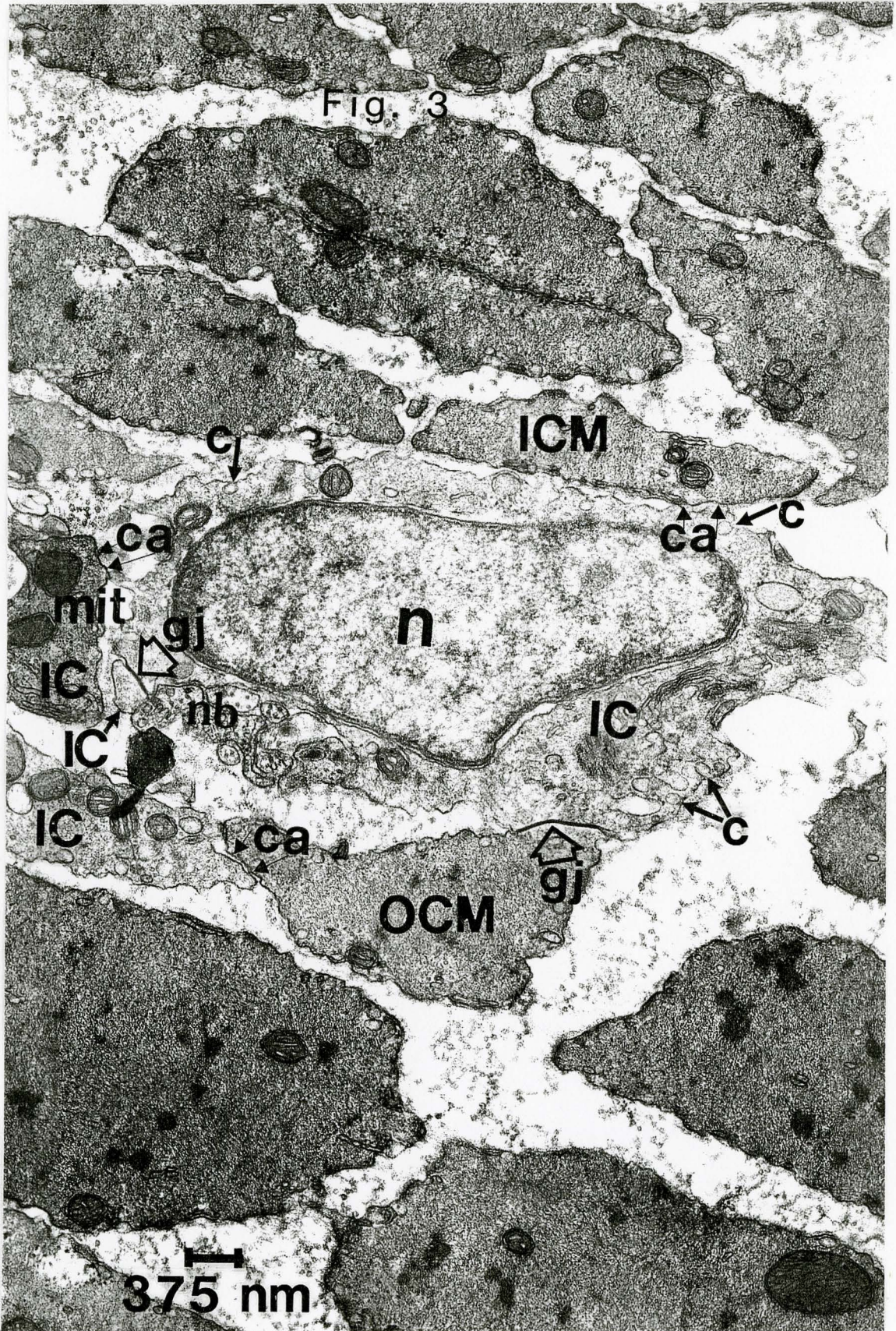
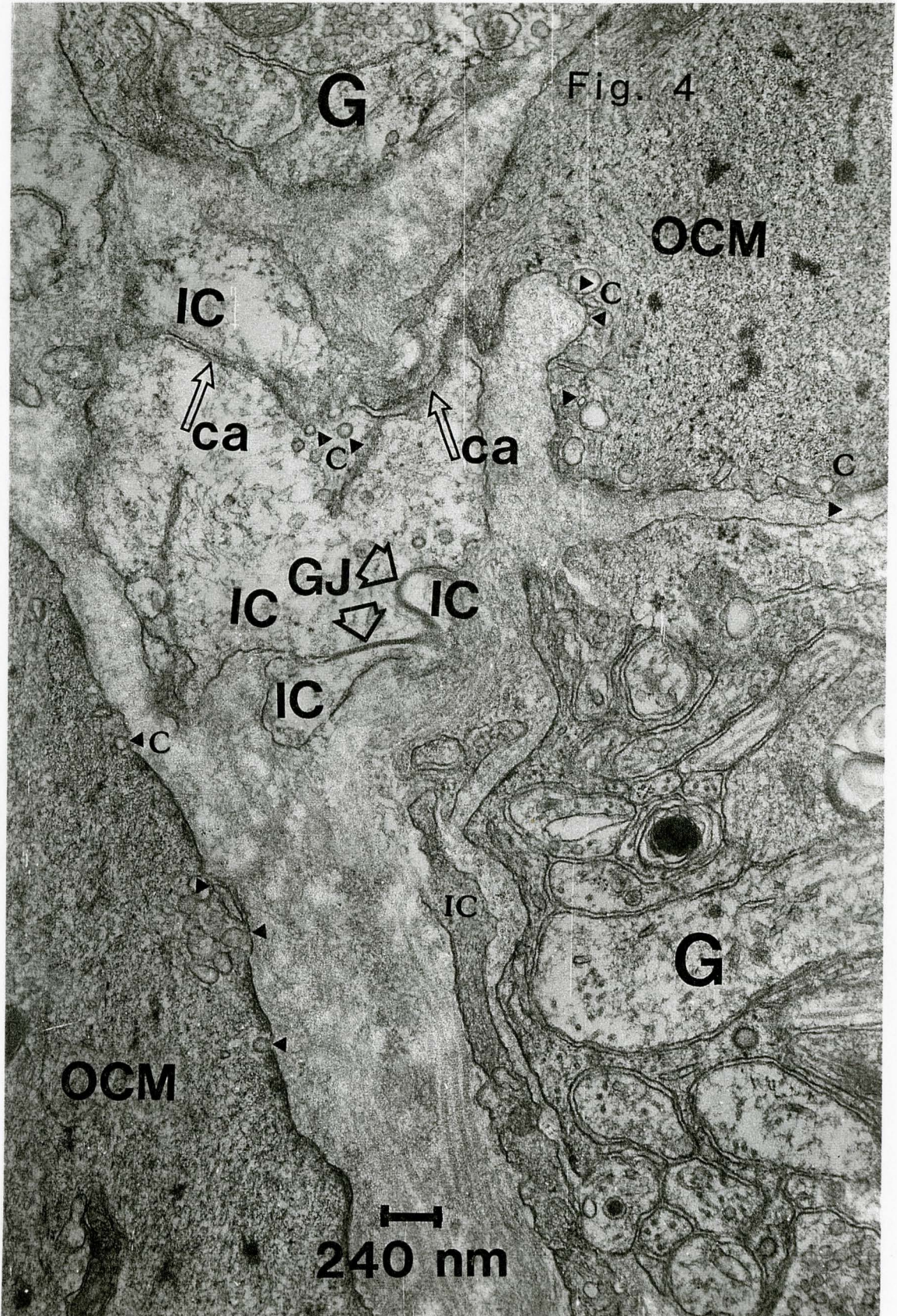


Fig. 2. Octanol effects on IJPs near two pacemaking regions





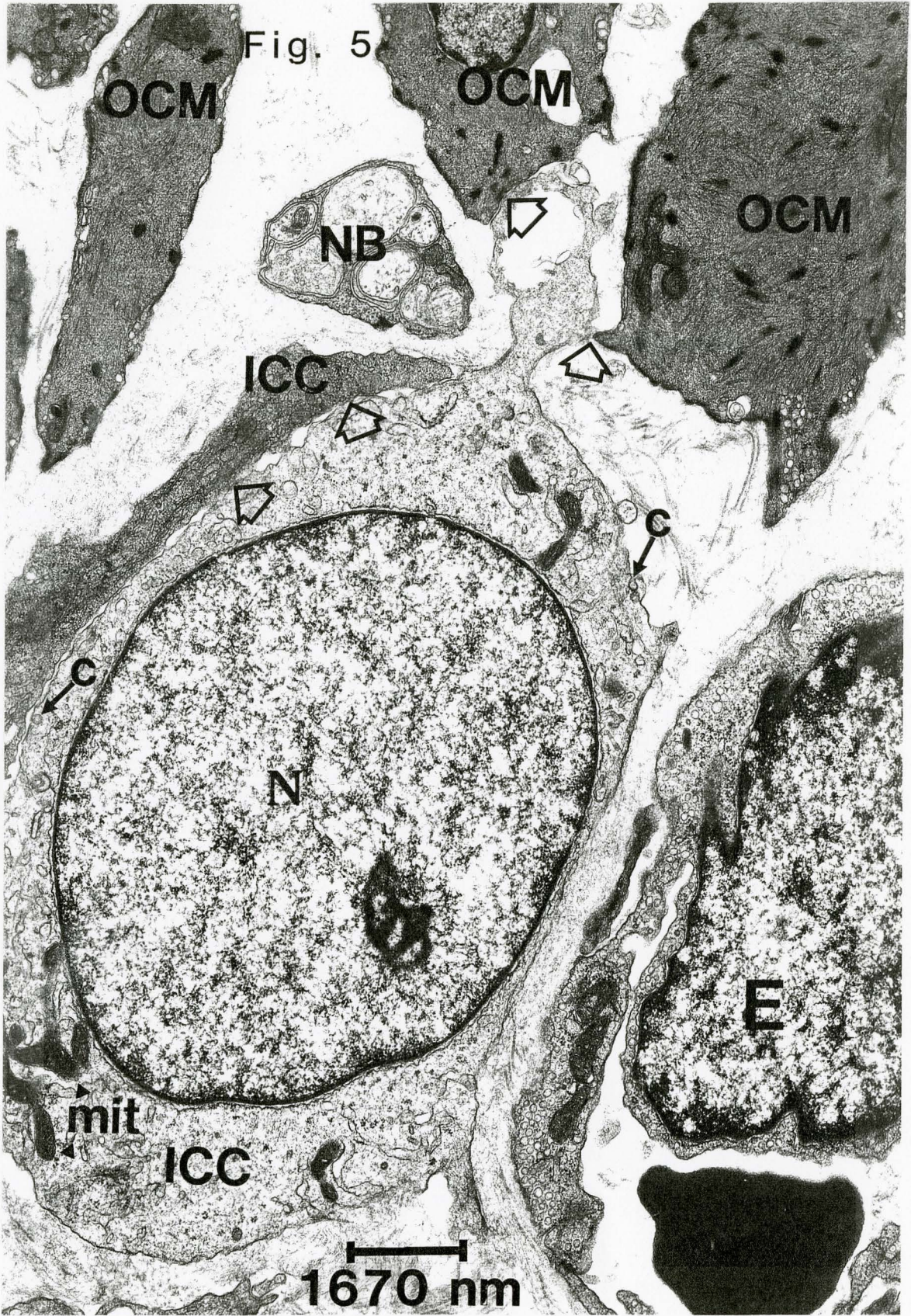


Table 1. Effects of octanol (1 mM) in the myenteric plexus (MyP, A) and deep muscular plexus (DMP, B) regions of the canine ileum.

Region and Treatment	Resting Membrane Potential (mV)	Slow Wave Amplitude (mV)	Slow Wave Frequency (mV)	Inhibitory Junction Potential Amplitude (mV)
A. MyP Control	-71.00 ± 0.58 (n=3)	22.33 ± 2.93 (n=3)	8.67 ± 0.93 (n=3)	10.8 (fast IJP) (n=1)
Treated	-60.67 ± 3.33 (n = 3) P=0.04	5.73 ± 1.51 (n = 3) P=0.007	5.50 ± 0.29 (n = 3) P=0.03	5.33 (slow IJP; fast IJP abolished) (n=1)
B. DMP Control	-54.00 ± 2.00 (n=3)	12.10 ± 1.80 (n=3)	7.83 ± 0.17 (n=3)	18.2 (fast IJP) (n=1)
Treated	-49.00 ± 8.0 (n = 3) P=0.61	7.56 ± 0.16 (n = 3) P=0.13	6.95 ± 0.05 (n = 3) P=0.04	8.8 (fast IJP) (n=1)

Values (mean ± SEM) represent measurements 5 min before and 20-25 min after addition of 1

mM octanol. *n* = number of strips from different animals; *P* = unpaired Student's *t* test *P*-value.

Fast IJP is the amplitude of a monophasic IJP characterized by a fast repolarization; slow IJP represents the amplitude of the delayed IJP characterized by a slower repolarization (longer duration, see Figure 2A).

CHAPTER 4

DISCUSSION

4.1 Dual Pacemaking Mechanism in Canine Ileum: Role of Interstitial Cells of Cajal.

4.1.1 Electrical Coupling Mechanisms in Gastrointestinal Musculature.

In the canine small intestine and stomach, the electrical oscillations called slow waves were driven by electrically-coupled relaxation oscillators (see reviews in [27,87,98]). In the rabbit intestine [112], slow waves were affected in frequency and amplitude by current clamp with polarizing and depolarizing current. However, in guinea-pig stomach [112], the slow waves were unaltered in frequency by current clamping the membrane potential, suggesting poor electrotonic coupling of pacemakers to smooth muscle. Alternatively, there was rectification in the coupling mechanism such that currents applied to smooth muscle were poorly transmitted to the pacemakers. Later studies of the rabbit intestine provided evidence of unusually large amplitude (about 40 mV vs. average 10-20 mV) slow waves recorded near the myenteric plexus region [112]; the investigators attributed this observation to the unusual penetration of a cell (possibly ICC) located between the circular and longitudinal muscle layers. In the present study (see Chapter 3.2), we also recorded very large slow waves near the myenteric and deep muscular plexus. Coupling mechanisms between the two muscle layers in the rabbit intestine were poor since inhibitory junction potentials and electrotonic potentials were not propagated from the circular into the longitudinal muscle layer (see review in [27]). Cheung and Daniel (1980) later obtained evidence to suggest that in the rabbit intestine, the pacemaking cells driving slow waves to occur simultaneously in the two muscle layers were located between them. Later work by Thuneberg and others (see review by Daniel and Berezin

[28]) has led to the hypothesis that these pacemaking cells have to be the interstitial cells of Cajal (ICC) found in that region. In the present study (see Chapter 3.4) and in reports by others (see [28]), these ICC located in the myenteric plexus are not well coupled to the two muscle layers by numerous gap junctions but do have gap junctions between one another and do make close contacts to the two muscle layers. They make occasional gap junction contacts to circular muscle.

4.1.2 Electrical Coupling of ICC as Pacemakers in Canine Ileum.

In the present study, the slow waves had characteristically different shapes when recorded in circular muscle near the myenteric plexus compared to those recorded near the deep muscular plexus (see Chapters 3.1, 3.2, 3.3, and 3.4). The former had a typical plateau and arose from a steady baseline while the latter had a more triangular shape and arose from a slowly depolarizing baseline. Intermediate regions often had slow waves with characteristics of both types. If the myenteric plexus and longitudinal muscle were removed, the remaining muscle still showed regular triangular slow waves but these were present everywhere (Chapter 3.1). We concluded that there are two potential pacemakers each of which might be associated with a set of ICC, one near the myenteric plexus and the other near the deep muscular plexus. As in the rabbit intestine, we have also provided evidence in the canine ileum of unusually large slow waves which we attribute to the occasional penetration of circular muscle cells closely coupled to ICC. These and other data (discussed below) lead us to suggest that there are two sets of pacemakers associated with two sets of ICC, and that these might be electrically coupled by gap junctions.

Many morphological and physiological characteristics of the interstitial cells of Cajal or ICC (the putative pacemaking cells) in the ileum (this study) and in other regions of the gastrointestinal tract support the widely held hypothesis that the ICC are the pacemaking cells of the gut [28, 113]. Morphologically, the circular smooth muscle and ICC are closely apposed with structures such as gap junctions and close appositions, which provide coupling mechanisms between cells [32, 53, 54, 59, 115, 121, 122, reviewed in 28]. Electrical oscillations of smooth muscle cells are thought to be generated from pacemaking regions and attributed to ICC [113]. These oscillations have been variously referred to as electrical control activity, slow wave type action potentials, pacesetter potentials, or electrical slow waves. In this thesis, these intracellular electrical events were called slow waves.

In whole thickness preparations, the pacemaker cells and the electrically well-coupled circular smooth muscle cells near both the myenteric plexus and deep muscular plexus can be considered as a system of coupled oscillators with different intrinsic electrical properties, which may provide gradients in intrinsic frequency and resting membrane potentials across the circular muscle layer (Chapter 3.1). In isolated circular muscle preparations where only the deep muscular plexus pacemakers are intact, no gradient in frequency and membrane potential was observed (Chapter 3.1). This suggests that functional coupling is present in the outer circular muscle such that communication between the two pacemaker networks occurs through electrotonic coupling of outer circular muscle cells. We observed that the myenteric plexus pacemakers oscillated with higher frequencies and arose from more hyperpolarized membrane potentials, whereas the

deep muscular plexus pacemakers, when isolated from the myenteric plexus pacemakers, oscillated with lower frequencies and arose from more depolarized membrane potential and exhibited a sigmoidal onset. The mechanical activity was often dissociated from the slow waves generated from the deep muscular plexus pacemakers when the two oscillators were coupled (Chapter 3.3). This frequency and resting membrane potential gradient along a series of coupled oscillators in the circular muscle layer may provide the basis for the direction and velocity of propagation of electrical and temporally associated mechanical activity. It is also possible that the gradient in frequency, resting membrane potential, and inhibitory junction potential can be modulated by putative neurotransmitters which would either depolarize or hyperpolarize the membrane. Note that the postulated electrotonic coupling of pacemaking potentials within smooth muscle cells does not establish electrotonic coupling of pacemakers to smooth muscle.

We also observed heterogeneity in inhibitory junction potentials recorded near both pacemaking networks. A triggered slow wave (TSW) which occurred with increasing delay and decreasing amplitude from the myenteric to deep muscular plexus region can be induced by the ending of an inhibitory junction potential. It can also be evoked by a 50-100 msec single pulse which did not produce a delay, but its amplitude decayed away from the myenteric plexus (Chapter 3.1). We suggested that triggered slow wave activity originated from pacemaker cells found in the myenteric plexus. Also this triggered activity appeared to be propagated passively via gap junctionally coupled outer circular muscle, to the deep muscular plexus region to affect the pacemaking function of pacemakers in that region. This electrical interaction of two sets of pacemakers which

results in phase-locking and entraining slow waves, reflects the dominance of the myenteric plexus pacemakers over the deep muscular plexus ones.

4.2 Role of NO and Other Neuromediators in Pacemaking Activity

4.2.1 NO as NANC Mediator

In the two plexuses, the presence of NADPH-diaphorase (marker for the NO-synthase which synthesizes NO) have been observed not only in nerve cell bodies and their varicosities but also from cells (possibly ICC) which are close to nerves (Wang, Mao, and Daniel, unpublished). Ultrastructural electron microscopic studies involving immunohistochemistry and immunogold staining techniques [14] suggested that NO and vasoactive intestinal polypeptide (VIP) are colocalized in the same nerve but may be stored in different cell organelles. Occasionally ICC in the ileum have also been found to have immunoreactivity to NO-synthase [14]. It is possible that the oscillatory properties such as frequency, resting membrane potential, and refractoriness of the two coupled oscillators, are susceptible to regional differences in inhibitory and excitatory innervation of the two pacemakers.

The roles of NO and NO-synthase and their modulation in control of gastrointestinal nerves, smooth muscle and ICC have been elucidated in part in Chapter 3.2. Previously we and others have claimed that NO is the major inhibitory mediator of non-adrenergic, non-cholinergic (NANC) nerves in canine and opossum gastrointestinal tract (reviewed in [107]). We have shown that NO or a NO-related compound mediated inhibitory junction potentials in the opossum esophagus [17, 22], the canine intestine [22;

see also Chapter 3.2] and the lower esophageal sphincter [61]. In each case, VIP did not mimic the action of the inhibitory mediator and VIP, if active, remained so after inhibition of NO-synthase which blocked inhibitory junction potentials and relaxation. However, a substantial body of evidence has been published to the effect that VIP is a major inhibitory mediator which relaxes in part by activating a constitutive NO-synthase in smooth muscle cells (reviewed in [76]). We attempted to provide a resolution to this issue by studying the effects of NO-donors (Chapter 3.2) and VIP and pituitary adenylate cyclase activating peptide (PACAP) on our intestinal muscle preparations (see below).

4.2.2 Possible Non-Neural Source of NO

We have developed a slab preparation of canine intestine ileal muscularis externa and shown that there are two networks of pacemakers which can work independently if isolated by dissection but in synchrony if coupled [62]. One near the myenteric plexus and the other near the deep muscular plexus probably consist of ICC connected to one another and to smooth muscle by gap junctions (see review in [28]). An inhibitory junction potential in this preparation, can trigger a slow wave after the inhibitory junction potential and delay and reset the pacemaker located near the myenteric plexus region. A single 50 msec pulse triggered a slow wave without inhibitory junction potential or delay. Tetrodotoxin (which blocks axonal conduction in nerves by blocking Na⁺ channels) or NO-synthase inhibitors abolished the inhibitory junction potential and the delay in triggering of slow waves, but ω -conotoxin GVIA (which blocks N-type Ca²⁺ channels involved in Ca²⁺ entry into nerve endings) inhibited the Inhibitory junction potential

without affecting the delay in triggering slow waves. Subsequent inhibition of NO-synthase abolished the delay and enhanced slow wave amplitude and regularity. These findings may result from basal NO release from a non-neural source (possibly ICC), not blocked by ω -CTX GVIA and affecting ICC pacemaking activity. Earlier, it was shown that VIP and also NO-synthase containing nerves innervate ICC closely [9, 10, 12, 14, 57(Berezin, I., J.D. Huizinga, L. Farraway, and E.E. Daniel, 1990; and Huizinga, J.D., I. Berezin, E.E. Daniel, and E. Chow, 1990). These studies point to future directions in research about the possibility of finding a non-neural source of NO (smooth muscle and/or ICC).

4.2.3 NO, VIP and PACAP and Their Modulation of Pacemaking Activity.

We showed that NO inhibited slow wave amplitude, slightly increased its frequency, hyperpolarized circular muscle membrane potential, and abolished contractions (Chapter 3.2). These effects were shown to be independent of tetrodotoxin-sensitive nerve mediator release. We concluded that both a neural and non-neural source of NO (possibly ICC, the pacemaker cells) contributed to the pacemaking function of the ICC in the myenteric and deep muscular plexuses. Other studies suggest that other neuromediators like VIP [64, 73] stimulate NO release from gastric smooth muscle cells. We have performed preliminary studies to determine if VIP or PACAP exhibit electromechanical effects in canine ileum. VIP did not have significant effect on slow wave amplitude and frequency but inhibited circular muscle contractions during prolonged exposure (see Table 4.1).

Table 4.1. Effects of vasoactive intestinal polypeptide (VIP) and pituitary adenylate cyclase activating peptide (PACAP) on pacemaking activity in the canine ileum.

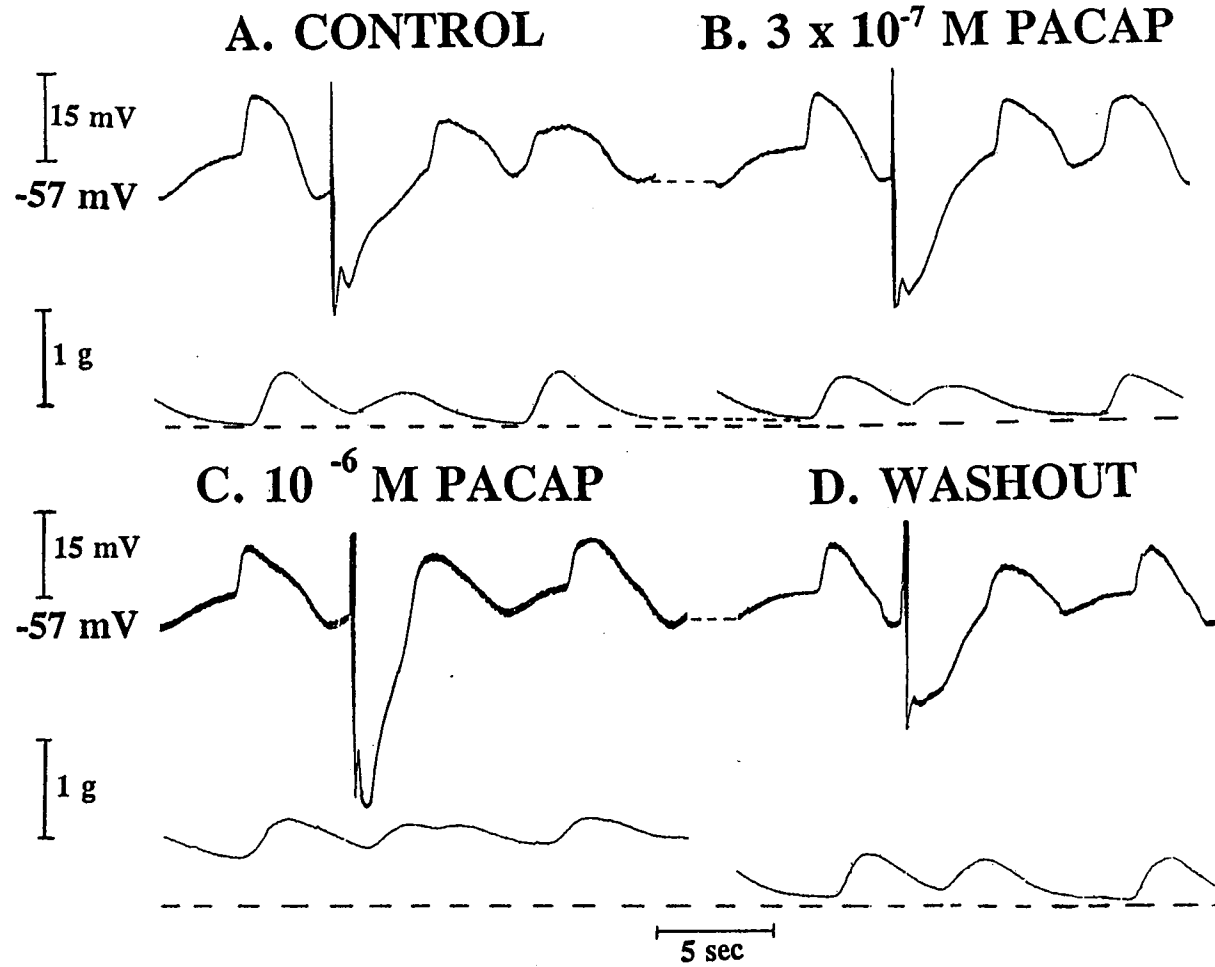
Region of Impalement and Treatment	Slow Wave Amplitude (mV)	Slow Wave Frequency (cycles/min)
A. Myenteric Plexus Control	16.83 ± 4.27 (n=4)	8.71 ± 0.60 (n=4)
VIP (10 ⁻⁶ M) 10-15 min	16.48 ± 7.05 (n=3) P>0.05	8.75 ± 0.75 (n=3) P>0.05
B. Deep Muscular Plexus Control	19.31 ± 2.15 (n=6)	9.05 ± 0.30 (n=6)
VIP (10 ⁻⁶ M) 10-15 min	17.87 ± 2.17 (n=5) P>0.05	8.70 ± 0.18 (n=5) P>0.05
C. Myenteric (n=1) and Deep Muscular Plexus (n=2) Combined Region and Treatment Control	23.59 ± 0.91 (n=3)	9.30 ± 0.50 (n=3)
PACAP (3x10 ⁻⁷ M) (10-15 min)	18.4 ± 1.70 (n=3) P=0.02	8.30 ± 0.80 (n=3) P=0.09

Data are means ± SEM and the means are significant if the two-tailed Student's *t*-test *P*-value is *P*<0.05. VIP and PACAP did not significantly affect membrane potentials during the superfusion.

VIP did not produce significant effects on the inhibitory junction potential amplitude or duration (data not shown). In some experiments, VIP caused a small tonic contraction during the first 5 min of exposure and then it caused inhibition of contraction. PACAP, on the other hand, produced increased tone of circular muscle and inhibited slow wave parameters (amplitude and frequency) more significantly than VIP, especially in recordings near the deep muscular plexus. PACAP increased the inhibitory junction

Legend to Figure 4. 1

Effect of PACAP on inhibitory junction potential and contractions. PACAP, unlike VIP, increased the circular muscle tone and amplitude of IJP.

Fig. 1. Effects of PACAP on slow waves, IJPs and contractions in canine ileum

potential amplitude but decreased its duration (Figure 4.1). This suggested that PACAP may have enhanced the apamin-sensitive K^+ -channel opening mediating the NO-mediated fast inhibitory junction potential and associated relaxation. However, this needs further investigation. Recently, PACAP has been shown to induce apamin-sensitive relaxation in taenia-coli [reviewed in 76], to stimulate contraction in guinea-pig ileum mediated via neural release of acetylcholine and substance P [65], and also to activate NOS and NO production in dispersed rabbit gastric muscle cells [64]. Preliminary biochemical results from our lab (Daniel and Mao, unpublished) indicate that PACAP binds to both muscle and nerves in the small intestine, while VIP has been shown earlier in biochemical studies [77] to have no significant specific binding to receptors on muscle. Preliminary results from studies of isolated preparations and measurement of acetylcholine release from nerves located in the deep muscular plexus revealed that VIP (to a lesser extent) and PACAP (to a greater extent) increased the release of acetylcholine and increased circular muscle contractions (Woskowska, Fox-Threlkeld, and Daniel, unpublished observations). These studies with NO, VIP and PACAP, so far incomplete, suggest that NO and not VIP is the main NANC inhibitory mediator in canine ileum circular muscle. PACAP may have both neural and myogenic actions which need mechanistic evaluations, but it is not the main inhibitory mediator in canine intestine.

4.2.4 Future studies to understand functions of and interplay among NO, VIP, and PACAP.

We will study how NO alone or together with VIP or other neural inhibitors, independently or interactively, mediates inhibition of intestinal motility. Many diseases

result from pathology of intestinal inhibitory nerves resulting in intestinal spasm and obstruction of transit. Some conditions result from overproduction of NO [69, 107], usually at non-neural sites (eg. macrophages, vascular smooth muscle, endothelial cells [81, 88] induced by inflammation.

The objective will be to determine the contributions of NO and other NANC mediators (VIP and PACAP, for example) in inhibitory control of gastrointestinal motor function in our intestinal slab preparations using intracellular microelectrodes. We will examine the sites of interactions of the neural mediators/modulators on NO function using intestinal slab preparations which enable study of the myenteric plexus and nerve endings in the deep muscular plexus, together or separately.

We need to study whether there are differences in the locus of actions of VIP and PACAP. It is possible that only when the myenteric plexus is removed that significant inhibitory effects of VIP and PACAP on slow wave parameters and inhibitory junction potentials can be observed. It will be important to look at blockade of nerve function with tetrodotoxin or ω -conotoxin GVIA before and after superfusion with either VIP or PACAP, in order to determine if the effects of VIP or PACAP can be abolished. Also it will be interesting to see if blockade of NOS function with known NOS blockers can abolish the inhibitory effects of VIP (at 3×10^{-7} M) and PACAP (at 10^{-9} - 3×10^{-7} M) on circular muscle contractions. Another objective is to test whether substance P or other tachykinin agonists can affect pacemaking; if so, it is possible that the excitatory actions of VIP or PACAP may involve tachykinin release from nerves as suggested elsewhere [65, 76].

Extension of this work may include examining VIP or PACAP receptor expression by immunocytochemistry. If ICC or the pacemakers are affected by these neuromediators it would be important to find if ICC or the smooth muscle closely coupled to them have receptors to either or both transmitters. Electrophysiological studies involving electrical field stimulation using single and repetitive pulses, in the presence and absence of VIP, PACAP, or other putative inhibitory and excitatory neuromediators, will provide information about how neural activity would modulate activity of circular muscle cells that are electrically well-coupled to the pacemaker networks. These studies will also provide fundamental information about the oscillators (ICC) themselves, since they are often found in close proximity to nerves containing these neuromediators.

Cellular mechanisms of actions of NO and VIP or PACAP can be studied also by using primarily patch clamp technique to record ion channel currents on single small intestinal smooth muscle cells. The effects of second messenger molecules involved in transducing the signals from NO or VIP can also be examined. Elevation of cGMP, cAMP, and cyclic adenosine diphosphate ribose by NO or VIP have been implicated in either direct or indirect actions on ion channels and intracellular Ca^{2+} [64, 72]. These studies will clarify the functioning of NO which is an important normal mediator of gastrointestinal muscle function and its interplay with other mediators.

4.3 Role of Gap Junctions and Other Cell Contacts in Electrical and Mechanical Coupling of Pacemaking Activity.

Gap junction coupling may be essential to transmission of pacemaking function

including propagation of Ca^{2+} waves. We studied the importance of gap junctional mechanisms using electrophysiological techniques. Octanol which blocks gap junction was used as a pharmacological tool. Gap junction coupling allows metabolic and electrical communications between pacemaking cells and circular smooth muscle. In the present study, functional coupling when the two oscillators were coupled and phase-locked in the whole thickness preparations (Chapter 3.1) was assessed using octanol (Chapter 3.4). Other ways of manipulating gap junction conductances including acidification and using other blockers of gap junction (for example, halothane and heptanol) to decrease gap junction conductance or alkalinization to increase conductance, were not used in this study. We obtained experimental evidence supporting electrotonic interactions of two pacemaking networks in the generation of slow waves (Chapter 3.4). The morphological basis for communication and interaction between the two pacemaking networks in the ileum was studied. Gap junction contacts and other cell-to-cell contacts were found to provide coupling between the ICC and between ICC and outer circular muscle near the regions of the deep muscular and myenteric plexuses. The paucity of visible gap junctions between ICC and between ICC and outer circular muscle, in contrast to the many gap junctions in ICC and coupling to outer circular muscle in the deep muscular plexus, may explain the differential sensitivity to octanol (Chapter 3.4) and Ca^{2+} removal (Chapter 3.3) of slow waves paced from the two sets of pacemakers. Production of inhibitory junction potentials in the myenteric plexus region was absent in the presence of octanol, and that generated from the deep muscular plexus appeared to spread electrotonically to the myenteric region. We concluded that electrotonic coupling between

outer circular muscle and between ICC in the pacemaker regions, may contribute substantially to the synchronization of pacemaker activity.

Further electron microscopic analysis coupled with light microscopy and staining of the structural relationships of cell-to-cell contacts between outer circular muscle and ICC and between ICC, will identify intercellular organization and distribution of ICC in relation to muscle cells and nerve bundles. This will provide insight into the relationships between the ICC and gradients in slow wave frequency, resting membrane potential, and inhibitory junction potential. The significance of these studies lies in advancing our understanding of how the pacemaking system and its innervation work in concert to provide orderly motor patterns for transit in the small intestine.

4.4 White Noise Current Input to Obtain Junctional Resistances and Capacitances.

Application of gaussian white noise current input through the recording microelectrode and simultaneous recordings of this input and the voltage output of the muscle, will allow the determination of the transfer function (Output/Input) and hence impedance of the system (see derivation in [25] to determine input impedance using z -transforms). The aim is to gain the relative impedance of circular muscle cells that are highly coupled by gap junctions and appositional contacts to the ICC of the myenteric and deep muscular plexuses. Hence, with the recent identification of a group of proteins (connexin 43) in gap junctions of the colon and small bowel [40, 74, 80], we postulate that the electrotonic coupling between the ICC and muscle and between ICC may be not be purely resistive. Membrane capacitance [5] may also be important and may account

for the shape of membrane potentials; a pure resistive contact cannot explain the shape of junctional potentials obtained from intracellular recordings near the pacemaker networks. Electrical field coupling introduced by the close appositional contacts of membranes of adjacent cells may contribute to the net input impedance. The prediction is that lower input impedance can be estimated near the deep muscular plexus where numerous gap junction contacts representing low resistive pathways can be found. Gap junctions in this region can act as current sinks, such that electrotonic potentials propagate at shorter distances from the point of current injection since they will encounter greater number of cell-to-cell contacts. In contrary, a higher input impedance or a low gap junction conductance in the myenteric plexus can be seen as an advantage for the pacemakers, since less current shunting occurs and less current is required to generate slow waves [59]. Relative differences in impedances will, therefore, provide a measure of the difference in gap junction densities between the two pacemaking networks. Once the junctional resistances and capacitances are determined, these initial parameters can be used to model the oscillatory behaviour generated from the two pacemaker networks.

A system model approach identification (see presentation of theoretical concepts in [42]) of the electrical properties of the gap junctionally coupled pacemakers should yield insight into the passive electrical properties of ICC and smooth muscle cells. Two intracellular microelectrodes can be used along with a system model approach for obtaining the passive electrical properties of the membrane along with the length and time constants. This method of analysis identifies the system parameters (membrane, myoplasmic and junctional impedances) using a frequency domain analysis of impedance

or voltage transfer function [42]. This will provide a complete description of the entire oscillator system [42, 44].

4.5 Biological Oscillators and Modelling

The electrical slow waves recorded from smooth muscle layer of the gut have been likened to and has been modelled by populations of coupled relaxation oscillators (see reviews in [6, 35, 27, 87, 98]. The significance of the coupled oscillator concept and its application to the stomach, small bowel, and colon has been documented in several review articles [27, 28, 87]. The interaction among coupled relaxation oscillators produces the final electrical and motor patterns of different regions in the gut. Three important parameters variable in space and time, namely 1) individual oscillator properties such as frequency, resting potential, refractory period, and amplitude and slow wave shape of the intrinsic oscillations; 2) electrical coupling; and 3) extrinsic stimuli applied to one or more oscillators. Differences in frequency, resting membrane potential, refractory period, and coupling can influence the interaction and behaviour of coupled oscillators. For example, differences in refractory period may determine the frequency to which an oscillator can be driven. When oscillators of different frequencies are entrained at the same frequency, there is a phase lag or delay between the oscillators with the oscillator having the highest frequency leading. When oscillators are separated in space, as along the circular muscle layer of the ileum, an apparent propagation occurs. The greater the difference in frequency or resting membrane potential, the greater the delay (i.e. apparent propagation velocity decreases). The stronger the coupling between the oscillators, the stronger the

interaction between them. Furthermore, coupling can occur not only through direct current passage from one oscillator to another, but also through "field" effects [5]. Further simplification and modification of the composite relaxation oscillator [6] allowed for more general applications.

Two recent conceptual advances have been made: 1) an oscillator can be seen as being composed of interactive units, its clock which determines its intrinsic periodicity and the absolute time varying phenomena, and 2) an oscillator can be influenced at different entry points or portals to produce different effects (eg. chaotic behaviour), known as "a multi input portal system" [4]. The first hypothesis states that an oscillator as a functional unit does not have to have its clock and the observed output in the same cell membrane, or in the same cell, or in a group of similar cells. For example, the ICC as a pacemaker source may serve as a clock for the electrical slow wave activity observed across the smooth muscle cell membrane [28]. The second concept holds that multi input portals allow any oscillator to be influenced by different receptors and different intercellular communication pathways, each potentially producing a different response. Both of these concepts have potential relevance to understanding the dual mechanisms of pacemaking in canine ileum. Our data showed that the pacemaking activity can be modulated by activity of NO-synthase and by actions of VIP or PACAP on receptors (probably located on muscle, nerves and ICC). Our data also showed that when the oscillators are coupled, application of octanol reduces the coupling factor for interaction of pacemakers and slow waves are markedly reduced or abolished (Chapter 3.4). This is explained by the inhibition of gap junction conductance and reduction of cell-to-cell

coupling of electrical signals and metabolites.

4.6 CONCLUSION

The results of this study bear on the nature of pacemaking in canine ileum muscle, on the relationship of neural activity to pacemaking and provide information about the basis for slow waves and their relationship to contraction. This study adds support to the hypothesis that there are two sources of pacemaking activity in the canine ileum, each source producing slow waves of different configuration but of similar frequency and each source capable of independently coupling the slow wave excitation to contraction. The two distinct types of slow waves have been described in relation to the presence of two pacemaker networks found near the myenteric and deep muscular plexuses. A triggered slow wave activity originated in the absence of neural function from the myenteric plexus region. The absence of the triggered slow wave in isolated circular muscle implies that the pacemaking activity of this region is difficult or impossible to trigger electrically. Since earlier studies (reviewed in [27, 28] showed that slow waves of the intact canine intestine *in vivo* could be driven by electrical stimuli, this implies that the pacing likely occurred at the myenteric plexus pacemaker. The ICC (pacemaker cells) found in the myenteric plexus were electrically coupled to circular muscle by few gap junctions but numerous close appositions, while the ICC in the deep muscular plexus were electrically well coupled by numerous gap junctions and close appositions. These results suggested that slow wave propagation may occur via either the low resistive pathway (gap junctions) or close apposition membranes which introduce an electrical field between membranes of

adjacent cells (termed "electrical field coupling") [5, 103]. The nature of coupling between the two pacemakers remains to be elucidated. Moreover, a difference in sensitivity to 0 Ca^{2+} between the two ICC networks suggest that the myenteric plexus ICC network, having lesser sensitivity, may dominate pacemaking activity under certain physiological or pathological conditions where intracellular or extracellular supply of Ca^{2+} is lowered. Slow waves and triggered slow waves occurred without spikes but were associated with contractions. Contractions but not slow waves were inhibited by block of L- Ca^{2+} channels. We presented evidence that there are two independent inhibitory neural inputs which can release NO, a NANC neurotransmitter responsible for the inhibitory junction potential. Finally, the ionic mechanisms that determine a triangular or sigmoidal mechanism for slow waves near the deep muscular plexus in contrast to the more common plateau type slow waves near the myenteric plexus were not clearly established in this study. However, our results showed that the slow waves were unaffected by inhibitors of N- or L-type Ca^{2+} channels. This raises the possibility that other non-L or non-N type Ca^{2+} channels are involved in generation of ileal slow waves, while L-channels provide Ca^{2+} to initiate contraction.

The cellular organizations of the pacemaker network and the cellular mechanisms of dual pacemaking activity that are elucidated in these studies provide insight into the coordination of electrical and motor patterns of the small intestine. Future studies will need to evaluate the structural and functional integrity of ICC in health and disruption in disease. It is of interest that in the gut, there may be an interplay among NO, VIP and PACAP (as well as other neuropeptides) with the regulation of relaxation and intestinal

pacemaking. Mechanistic evaluations of these neuromediators will provide insight into the sites and mechanisms of their action(s) in the gut, and will be essential if their physiological and pathophysiological functions are to be understood and used for therapeutic interventions. The experimentally derived pacemaking characteristics of the two sets of pacemakers in the canine ileum can lay the foundation for computer modelling of oscillators in the small intestine.

BIBLIOGRAPHY

1. **Ahmad, S., J. Rausa, E. Jang, and E.E. Daniel.** Calcium channel binding in nerves and muscle of canine small intestine. *Biochem. Biophys. Res. Comm.* 159(1):119-125, 1989.
2. **Alagarsamy, S., G. Lonart, and K.M. Johnson.** The role of P-type calcium channels in the depolarization-induced activation of NOS in frontal cortex. *J. Neurochem.* 62: 400-403, 1994.
3. **Allescher, H.D., G. Tougas, P. Vergara, S. Lu, and E.E. Daniel.** Nitric oxide as a putative nonadrenergic, noncholinergic inhibitory transmitter in the canine pylorus. *Am. J. Physiol.* 262:G695-G702, 1992.
4. **Bardakjian, B.L., and N.E. Diamant.** A mapped clock oscillator model for transmembrane electrical rhythmic activity in excitable cells. *J. Theor. Biol.* 166: 225-235, 1994.
5. **Bardakjian, B.L., and N.E. Diamant.** Electronic models of oscillator to oscillator communication. In: *Cell Interaction and Gap Junctions*, N. Sperelakis and W.C. Cole, Eds. Florida: CRC Press, Boca Raton, 1989. pp. 211-224.
6. **Bardakjian, B.L., S.K. Sarna, and N.E. Diamant.** Composite synthesized relaxation oscillators. Application to modelling of colonic electrical control and response activity. *J. Gastrointest. Motil.* 2: 109-116, 1990
7. **Bauer, A.J., J.B. Reed, and K.M. Sanders.** Slow wave heterogeneity within the circular muscle of the canine gastric antrum. *J. Physiol. (London)* 366:221-232, 1985.
8. **Bayguinov, O., F. Vogalis, B. Morris, and K.M. Sanders.** Patterns of electrical activity and neural responses in canine proximal duodenum. *Am. J. Physiol.* 263:G887-G894, 1992.
9. **Berezin, I., H.D. Allescher, and E.E. Daniel.** Ultra-structural localization of VIP-immunoreactivity in canine distal esophagus. *J. Neurocytology* 16: 749-757, 1987.
10. **Berezin, I., J.D. Huizinga, and E.E. Daniel.** Interstitial cells of Cajal in canine colon: A special communication network at the inner border of the circular

- muscle. *J. Comp. Neurocyt.* 273:42-51, 1988.
11. **Berezin, I., J.D. Huizinga, and E.E. Daniel.** Structural characterization of interstitial cells of Cajal in myenteric plexus and muscle layers of canine colon. *Can. J. Physiol. Pharmacol.* 68: 1419-1431, 1990.
 12. **Berezin, I., J.D. Huizinga, L. Farraway, and E.E. Daniel.** Innervation of interstitial cells of Cajal by VIP-containing nerves in canine colon. *Can. J. Physiol. Pharmacol.* 68: 922-932, 1990.
 13. **Berezin, I., S. Sheppard, E.E. Daniel, and N. Yanaihara.** Ultrastructural immunocytochemical distribution of VIP-like immunoreactivity in dog ileum. *Regulatory Peptides* 11: 287-298, 1985.
 14. **Berezin, I., S.H. Snyder, D.S. Brecht, and E.E. Daniel.** Ultrastructural localization of NOS in canine small intestine and colon. *Am. J. Physiol.* 266:C981-C989, 1994.
 15. **Brecht, D.S., P.M. Hwang, and S.H. Snyder.** Localization of nitric oxide synthetase indicating a neural role for nitric oxide. *Nature* 347: 768-770, 1990.
 16. **Carl, A., B.W. Frey, S.M. Ward, K.M. Sanders, and J.L. Kenyon.** Inhibition of slow-wave repolarization and Ca^{2+} -activated K^+ channels by quaternary ammonium ions. *Am. J. Physiol.* 264:C625-C631, 1993.
 17. **Cayabyab, F.S., and E.E. Daniel.** K^+ channel opening mediates hyperpolarizations by nitric oxide donors and IJPs in opossum esophagus. *Am. J. Physiol.* 268: G831-G842, 1995.
 18. **Cayabyab, F.S., H. deBruin, and E. E. Daniel.** NO and NANC inhibitory mediation in the canine ileum (Abstract). *Can. J. Physiol. Pharmacol.* 72: 234, 1994.
 19. **Cayabyab, F.S., M. Jiménez, P. Vergara, and E.E. Daniel.** Two independent pacemakers drive the electrical and mechanical activities of the canine ileum (Abstract). *Neurogastroenterology and Motility.* 6: 152, 1994.
 20. **Cheung, D.W., and E.E. Daniel.** Comparative study of the smooth muscle layers of the rabbit duodenum. *J. Physiol.* 309: 13-27, 1980.
 21. **Christ, G.J., A.P. Moreno, A. Melman, and D.C. Spray.** Gap junction-

- mediated intercellular diffusion of Ca^{2+} in cultured human corporal smooth muscle cells. *Am. J. Physiol.* 263:C373-C383, 1992.
22. **Christinck, F., J. Jury, F. Cayabyab, and E.E. Daniel.** Nitric oxide may be the final mediator of nonadrenergic, noncholinergic inhibitory junction potentials in the gut. *Can. J. Physiol. Pharmacol.* 69: 1448-1458, 1991.
 23. **Christinck, F. E.** Effect of nerve stimulation and neurotensin on intestinal smooth muscle: Mechanism of action of inhibitory junction potentials and neurotensin in canine ileum circular muscle. (Thesis). McMaster University, 1990.
 24. **Christinck, F., E.E. Daniel, and J.E.T. Fox-Threlkeld.** Inhibitory and excitatory mechanisms of neurotensin action in canine intestinal circular muscle *in vitro*. *Can. J. Physiol. Pharmacol.* 70:1423-1431, 1992.
 25. **D'Aguanno, A., B.L. Bardakjian, and P.L. Carlen.** A system model for investigating passive electrical properties of neurons. *Biophys. J.* 55: 1169-1182, 1989.
 26. **Dalziel, H.H., K.D. Thornbury, S.M. Ward, and K.M. Sanders.** Involvement of nitric oxide synthetic pathway in inhibitory junction potentials in canine proximal colon. *Am. J. Physiol.* 260: G789-G792, 1991.
 27. **Daniel, E.E., B.L. Bardakjian, J.D. Huizinga, and N.E. Diamant.** Relaxation oscillator and core conductor models are needed for understanding of GI electrical activities. *Am. J. Physiol.* 266: G339-G349, 1994.
 28. **Daniel, E.E., and I. Berezin.** Interstitial cells of Cajal: are they major players in control of gastrointestinal motility? *J. Gastrointestinal Motility* 4: 1-24, 1992.
 29. **Daniel, E.E., J.E.T. Fox-Threlkeld, Y.K. Mao, Y.F. Wang, F. Cayabyab, M. Jiminez, P. Vergara, and C. Memeh.** Interactions of VIP (vasoactive intestinal polypeptide) and nitric oxide (NO) in mediating intestinal inhibition. *Biomed. Res.* 15: 69-77, 1994.
 30. **Daniel, E.E., J.B. Furness, M. Costa, and L. Belbeck.** The projections of chemically identified nerve fibers in canine ileum. *Cell Tissue Res.* 247: 377-384, 1987.
 31. **Daniel, E.E., C. Haugh, Z. Woskowska, S. Cipris, J. Jury, and J.E.T. Fox-Threlkeld.** Role of nitric oxide-related inhibition in intestinal function: relation

- to vasoactive intestinal polypeptide. *Am. J. Physiol.* 266: G31-G39, 1994.
32. **Daniel, E.E., and V. Posey-Daniel.** Neuromuscular structures in opossum esophagus: role of interstitial cells of Cajal. *J. Physiol.* 246: G305-G315, 1984.
 33. **Darby, P.J., C.Y. Kwan, and E.E. Daniel.** Use of calcium pump inhibitors in the study of calcium regulation in smooth muscle. *Biol. Signals* 2:293-304, 1993.
 34. **DeLisle, S., G.W. Mayr, and M.J. Welsh.** Inositol phosphate structural requisites for Ca^{2+} influx. *Am J. Physiol.* 268: C1485-C1491, 1995.
 35. **Diamant, N.E., P.K. Rose, and E.J. Davison.** Computer simulation of intestinal slow-wave frequency gradient. *Am. J. Physiol.* 219:1684-1690, 1970.
 36. **Duchon, G., R. Henderson, and E.E. Daniel.** Circular muscle layers in the small intestine. In: *Proceedings of the International Symposium of Gastrointestinal Motility*, edited by Daniel E.E., Vancouver: Mitchell Press, pp 635- 646, 1974.
 37. **Elbert, T., W.J. Ray, Z.J. Kowalik, J.E. Skinner, K.E. Graf, and N. Birbaumer.** Chaos and Physiology: Deterministic chaos in excitable cell assemblies. *Physiol. Rev.* 74:1-47, 1994.
 38. **El-Sharkawy, T.Y. and E.E. Daniel.** Electrical activity of small intestine smooth muscle and its temperature dependence. *Am. J. Physiol.* 229:1268-1276, 1975.
 39. **El-Sharkawy, T.Y. and E.E. Daniel.** Ionic mechanisms of intestinal electrical control activity. *Am. J. Physiol.* 229:1287-1298, 1975.
 40. **Farraway, L., A.K. Ball, and J.D. Huizinga.** Intercellular metabolic coupling in canine colon musculature. *Am. J. Physiol.* 268: C1492-C1502, 1995.
 41. **Fox, J.E.T., E.E. Daniel, J. Jury, and H. Robotham.** Muscarinic inhibition of canine small intestinal motility *in vivo*. *Am. J. Physiol.* 248:G526-G531, 1985.
 42. **Fu, P., and B.L. Bardakjian.** System identification of electrically coupled smooth muscle cells: the passive electrical properties. *I.E.E.E. Trans. Biomed. Eng.* 38: 1130-1140, 1991.
 43. **Fu, P., B.L. Bardakjian, and P.L. Carlen.** Ethanol uncouples dentate granule neurons by increasing junctional resistance: a multineuronal system model approach. *Neuroscience* 51: 47-54, 1992.

44. **Fu, P., B.L. Bardakjian, A. D'Aguanno, and P.L. Carlen.** Computation of the passive electrical parameters of neurons using a system model. *IEEE Trans. Biomed. Eng.* 36: 55-64, 1989.
45. **Furness, J.B., and M. Costa.** Types of nerves in the enteric nervous system. *Neurosci.* 5:1-20, 1980.
46. **Furness, J.B., and M. Costa.** The Enteric Nervous System. London, Churchill-Livingstone, 1987.
47. **Furness, J.B., S. Pompolo, C.W.D. Shuttleworth, and D.E. Burleigh.** Light and electron microscopic immunohistochemical analysis of nerve fiber types innervating the taenia of the guinea pig caecum. *Cell Tissue Res.* 270: 125-137, 1992.
48. **Gelband, C.H. and J.R. Hume.** Ionic currents in single smooth muscle cells of the canine renal artery. *Circ. Res.* 71:745-758, 1992.
49. **Grider, J.R., K.S. Murthy, J.G. Jin, and G.M. Makhlouf.** Stimulation of nitric oxide from muscle cells by VIP: prejunctional enhancement of VIP release. *Am. J. Physiol.* 262: G774-G777, 1992.
50. **Goyal, R.K., S. Rattan, and S. Said.** VIP as a possible neurotransmitter of non-adrenergic, non-cholinergic inhibitory neurons. *Nature* 288: 378-380, 1980,
51. **Hara, Y., M. Kubota, and J.H. Szurszewski.** Electrophysiology of smooth muscle of the small intestine of some mammals. *J. Physiol.* 372: 501-520, 1986.
52. **Hara, Y., and J.H. Szurszewski.** Effect of potassium and acetylcholine on canine intestinal smooth muscle. *J. Physiol. (London)* 372:521-537, 1986.
53. **Henderson, R.M.** Cell-to-Cell Contacts. In: *Methods in Pharmacology*. E.E. Daniel and D.M. Paton, Eds. New Yew York: Plenum, 1975. Ch. 2, pp.44-77.
54. **Henderson, R.M., G. Duchon, and E.E. Daniel.** Cell contacts in duodenal smooth muscle layers. *Am. J. Physiol.* 221: 793-799, 1971.
55. **Hirning, L.D., A.P. Fox, E.W. McCleskey, B.M. Olivera, S.A. Thayer, R.J. Miller, and R.W. Tsien.** Dominant role of N-type Ca^{2+} channels in evoked release of norepinephrine from sympathetic neurons. *Science* 239:57- 60, 1988.

56. **Hryhorenko, L.M., Z. Woskowska, and J.E.T. Fox-Threlkeld.** Nitric oxide (NO) inhibits release of acetylcholine from nerves of isolated circular muscle of the canine ileum: Relationship to motility and release of nitric oxide. *J. Pharmacol. Exp. Ther.* 271(2):918-926, 1994.
57. **Huizinga, J.D., I. Berezin, E.E. Daniel, and E. Chow.** Inhibitory innervation of colonic smooth muscle cells and interstitial cells of Cajal. *Can. J. Physiol. Pharmacol.* 68: 447-454, 1990.
58. **Huizinga, J.D., L. Farraway, and A. Den Hertog.** Generation of slow-wave-type action potentials in canine colon smooth muscle involves a non-L-type Ca^{2+} conductance. *J. Physiol. (London)* 442:15-29, 1991.
59. **Huizinga, J.D., L.W.C. Liu, M.G. Blennerhasset, L. Thuneberg, and A. Molleman.** Intercellular communication in smooth muscle. *Experiential Base* 48: 932-941, 1992.
60. **Jiménez, M., P. Vergara, and E.E. Daniel.** Origin of the "off"-response after field stimulation in the canine ileum (Abstract). *J. Gastrointestinal Motility.* 5: 197, 1993.
61. **Jury, J., N. Ahmedzadeh, and E.E. Daniel.** A mediator derived from arginine is released from sphincteric intrinsic nerves to mediate inhibitory junction potentials and relaxations. *Can. J. Physiol. Pharmacol.* 70: 1182-1189, 1993.
62. **Jiménez, M. P. Vergara, F. Christinck, and E.E. Daniel.** Mechanism of action of somatostatin on the canine ileal circular muscle. *Am. J. Physiol.* 268: ___ - ___, 1995.
63. **Linkens, D.A., I. Taylor, and H.L. Duthie.** Mathematical modeling of the colorectal myoelectrical activity in humans. *IEEE Trans. Biomed. Eng.* 23: 101-110, 1976.
64. **Murthy, K.S., and G.M. Makhlof.** Vasoactive intestinal peptide/pituitary adenylate cyclase-activating peptide-dependent activation of membrane-bound NO synthase in smooth muscle mediated by pertussis toxin-sensitive G_{i1-2} . *J. Biol. Chem.* 269(23):15977-15980, 1994.
65. **Katsoulis, S., A. Clemens, H. Schworer, W. Creutzfeldt, and W.E. Schmidt.** PACAP is a stimulator of neurogenic contraction in guinea pig ileum. *Am. J. Physiol. Gastrointest. Liver Physiol.* 265(28): G295-G302, 1993.

66. **Keef, K.D., C.W.R. Shuttleworth, C. Xue, O. Bayguinov, N.G. Publicover, and K.M. Sanders.** Relationship between nitric oxide and vasoactive intestinal polypeptide in enteric inhibitory neurotransmission. *Neuropharm.* 33(11):1303-1314, 1994.
67. **Keef, K.D., C. Du, S.M. Ward, B. McGregor, and K.M. Sanders.** Enteric inhibitory neural regulation of human colonic circular muscle: role of nitric oxide. *Gastroenterology* 105: 1009-1016, 1993.
68. **King, B.F.** Excitatory and inhibitory junction potentials in canine antral circular muscle. *Neurogastroenterology and Motility* 6: 59-65, 1994.
69. **Konturek, S.K., and P.C. Konturek.** Role of nitric oxide in the digestive system. *Digestion* 56:1-13, 1995.
70. **Kostka, P., E. Jang, E.G. Watson, J.L. Stewart, and E.E. Daniel.** NOS in the autonomic nervous system of the canine ileum. *J. Pharmacol. Exp. Therap.* 264(1): 234-239., 1993
71. **Langton, P.D., E.P. Burke, and K.M. Sanders.** Participation of Ca currents in colonic electrical activity. *Am. J. Physiol.* 257:C451-C460, 1989.
72. **Lee, H.C..** A signalling pathway involving cyclic ADP-ribose, cGMP, and nitric oxide. *News Physiol. Sci.*-9:134-137, 1994.
73. **Lee, H.K., O. Bayguinov, and K.M. Sanders.** Role of nonselective cation current in muscarinic responses of canine colonic muscle. *Am. J. Physiol.* 265:C1463-C1471, 1993.
74. **Li, Z., Z. Zhou, and E.E. Daniel.** Expression of gap junction connexin 43 and connexin 43 mRNA in different regional tissues of intestine in dog. *Am. J. Physiol.* 265: G911-G916, 1993.
75. **Maklouf, G.M.** Smooth Muscle of the Gut. In: *Textbook of Gastroenterology.* Yamada, T., D.H. Alpers, C. Owyang, D.W. Powell, and R. Silverstein eds. New York, Lippincott. pp. 61-84. 1991.
76. **Makhlouf, G.M., and J.R. Grider.** Nonadrenergic noncholinergic inhibitory transmitters of the gut. *News Physiol. Sci.* 8: 195-199, 1993.
77. **Mao, Y.K., W. Barnett, D.H. Coy, G. Tougas, and E.E. Daniel.** Distribution

- and characterization of vasoactive intestinal polypeptide (VIP)-binding in circular muscle and characterization of VIP-binding in canine small intestinal mucosa. *J. Pharmacol. Exp. Therap.* 258: 986-991, 1991.
78. **Mason, M.J., C. Garcia-Rodriguez, and S. Grinstein.** Coupling between intracellular Ca^{2+} stores and the Ca^{2+} permeability of the plasma membrane: comparison of the effects of thapsigargin, 2,5-di-(tert-butyl)-1,4-hydroquinone, and cyclopiazonic acid in rat thymic lymphocytes. *J. Biol. Chem.* 266:20856-20862, 1991.
 79. **McCarron, J.G., J.G. McGeown, S. Reardon, M. Ikebe, F.S. Fay, and J.V. Walsh Jr.** Calcium-dependent enhancement of calcium current in smooth muscle by calmodulin-dependent protein kinase II. *Nature* 357:74-77, 1992.
 80. **Mikkelsen, H.B., J.D. Huizinga, L. Thuneberg, and J.J. Rumessen.** Immunohistochemical localization of a gap junction protein (connexin 43) in the muscularis externa of murine, canine, and human intestine. *Cell Tissue Res.* 274: 249-256, 1993.
 81. **Moncada, S., and R.M.J. Palmer.** Inhibition of the induction of nitric oxide synthase by glucocorticoids: yet another explanation for their anti-inflammatory effects? *Trends Pharmacol. Sci.* 12: 130-131, 1991.
 82. **Nichols, K., A. Krantis, and W. Staines.** Histochemical localization of nitric oxide-synthesizing neurons and vascular sites in the guinea-pig intestine. *Neurosci.* 51(4): 791-799, 1992.
 83. **Nishizuka, Y.** Intracellular signalling by hydrolysis of phospholipids and activation of protein kinase C. *Science* 258:607-614, 1992.
 84. **Ozaki, H., L. Zhang, I.L.O. Buxton, K.M. Sanders, and N.G. Publicover.** Negative-feedback regulation of excitation-contraction coupling in gastric smooth muscle. *Am. J. Physiol.* 263:C1160-C1171, 1992.
 85. **Perez-Armendariz, E.M., P.C. Spray, and M.V.L. Bennet.** L-octanol reduced calcium, potassium and gap junctional currents in mouse pancreatic β -cells. *Biophys. J.* 55:218a, 1989.
 86. **Publicover, N.G., E.M. Hammond, and K.M. Sanders.** Amplification of nitric oxide signaling by interstitial cells isolated from canine colon. *Proc. Nat. Acad. Sci. (U.S.A.)* 90: 2087-2091, 1993.

87. **Publicover, N.G., and K.M. Sanders.** Are relaxation oscillators an appropriate model of gastrointestinal electrical activity? *Am. J. Physiol.* 256: G265-G274, 1989.
88. **Randomski, M.W., R.M. J. Palmer, and S. Moncada.** Glucocorticoids inhibit the expression of an inducible but not constitutive nitric oxide synthase in vascular endothelial cells. *Proc. Natl. Acad. Sci. USA.* 87:10043-10047. 1990.
89. **Rembold, C.M.** Regulation of contraction and relaxation in arterial smooth muscle. *Hypertension* 20:129-137, 1992.
90. **Renzetti, L.M., M.B. Wang, and J.P. Ryan.** Modulation of cat antral slow waves by ion substitution, Ca^{2+} and K^{+} channel blockade, and acetylcholine stimulation. *Am. J. Physiol.* 263:G880-G886, 1992.
91. **Rumessen, J.J., H.B. Mikkelsen, K. Qvortrup, and L. Thuneberg.** Ultrastructure of interstitial cells of Cajal in circular muscle of human intestine. *Gastroenterology.* 104: 343-350, 1993.
92. **Rumessen, J.J., H.B. Mikkelsen, and L. Thuneberg.** Ultrastructure of interstitial cells of Cajal associated with deep muscular plexus of the human small intestine. *Gastroenterology.* 102: 56-58, 1992.
93. **Rumessen, J.J., and L. Thuneberg.** Plexus muscularis profundus and associated interstitial cells. I. Light microscopical studies of mouse small intestine. *Anat. Rec.* 203:115-127, 1982.
94. **Rumessen, J.J., L. Thuneberg, and H.B. Mikkelsen.** Plexus muscularis profundus and associated interstitial cells. II. Ultrastructural studies of mouse small intestine. *Anat. Rec.* 203: 129-146, 1982.
95. **Rumessen, J.J., and L. Thuneberg.** Interstitial cells of Cajal in human small intestine. Ultrastructural identification and organization between the main smooth muscle layers. *Gastroenterology.* 100: 1417-1431, 1991.
96. **Sanders, K.M.** Excitation-contraction coupling without Ca^{2+} action potentials in small intestine. *Am. J. Physiol.* 224: C356-C361, 1983.
97. **Sanders, K.M.** Ionic mechanisms of electrical rhythmicity in gastrointestinal smooth muscles. *Annu. Rev. Physiol.* 54: 439-453, 1992.

98. **Sarna, S.K., E.E. Daniel, and Y.U. Kingma.** Simulation of the electric-conotorl activity of the stomach by an array of relaxation oscillators. *Am. J. Dig. Dis.* 17: 299-310, 1972.
99. **Scott, R.H., J.F. Wootton, and A.C. Dolphin.** Modulation of neuronal T-type calcium channel currents by photoactivation of intracellular guanosine 5'-O(3-thio)triphosphate. *Neuroscience* 38: 285-294, 1990
100. **Serio, R., C. Barajas-Lopez, E.E. Daniel, I. Berezin, and J.D. Huizinga.** Slow-wave activity in colon: role of network of submucosal interstitial cells of Cajal. *Am. J. Physiol.* 260:G636-G645, 1991.
101. **Smith, T.K., J.B. Reed, and K.M. Sanders.** Interaction of two electrical pacemakers in muscularis of canine colon. *Am. J. Physiol.* 252: C290-C299, 1987.
102. **Sneyd, J., B.T.R. Wetton, and A.C. Charles.** Intercellular calcium waves mediated by diffusion of inositol triphosphate: a two-dimensional model. *Am. J. Physiol.* 268: C1537-C1545, 1995.
103. **Sperelakis, N.** Electric field model: An alternate mechanism for cell-to-cell propagation in cardiac muscle and smooth muscle. *J. Gastrointest. Motil.* 3: 1-19, 1991.
104. **Spray, D.C., and J.M. Burt.** Structure-activity relations of the cardiac gap junction channel. *Am. J. Physiol.* 258: C195-C205, 1990.
105. **Stark, M.E., A.J. Bauer, and J.H. Szurszewski.** Effect of nitric oxide on circular muscle of the canine small intestine. *J. Physiol.* 444: 743-761, 1991.
106. **Stark, M.E., A.J. Bauer, M.G. Sarr, and J.H. Szurszewski.** Nitric oxide mediates inhibitory nerve input in human and canine jejunum. *Gastroenterology* 104:398-409, 1993.
107. **Stark, M.E., and J.H. Szurszewski.** Role of nitric oxide in gastrointestinal and hepatic function and disease. *Gastroenterology* 103:1928-1949, 1992.
108. **Stockland, J., A. Sultan, D. Molony, T. DuBose Jr., and S. Sansom.** Interactions of cadmium and nickel with K channels of vascular smooth muscle. *Toxicol. Appl. Pharmacol.* 121:30-35, 1993.
109. **Stull, J.T., L.-C. Hsu, M.G. Tansey, and K.E. Kamm.** Myosin light chain

- kinase phosphorylation in tracheal smooth muscle. *J. Biol. Chem.* 265:16683-16690, 1990.
110. **Suzuki, N., C.L. Prosser, and V. Dahms.** Boundary cells between longitudinal and circular layers: essential for electrical slow waves in cat intestine. *Am. J. Physiol.* 250: G287-G294, 1986.
 111. **Szurszewski, J.H.** Electrical basis for gastrointestinal motility. In: *Physiology of the Gastrointestinal Tract* (2nd ed.) edited by L.R. Johnson. New York: Raven Press. 1987. p. 383-423.
 112. **Taylor, G.S., E.E. Daniel, and T. Tomita.** Origin and mechanism of intestinal slow waves. In: *Proceedings of the Fifth International Symposium on Gastrointestinal Motility*, edited by Van-Trappen, G., Belgium: Typoff Press, pp. 102-106, 1975.
 113. **Thuneberg, L.** Interstitial cells of Cajal: intestinal pacemakers? *Advances in Anatomy, Embryology and Cell Biology* 71: 1- 130, 1982.
 114. **Thuneberg, L., V. Johansen, J.J. Rumessen, and B.G. Anderson.** Interstitial cells of Cajal: selective uptake of methylene blue inhibits slow wave activity. In: *Gastrointestinal Motility*, edited by Roman, C. pp. 495-502. Lancaster, England: MTP Press, pp. 495-502, 1984.
 115. **Torihashi, S., S. Kobayashi, W.T. Gerthoffer, and K.M. Sanders.** Interstitial cells in deep muscular plexus of canine small intestine may be specialized smooth muscle cells. *Am. J. Physiol.* 265: G638-G645, 1993.
 116. **Töttrup, A., D. Svane, and A. Forman.** Nitric oxide mediating NANC inhibition on opossum lower esophageal sphincter. *Am. J. Physiol.* 260: G385-G389, 1991.
 117. **Ward, S.M., H.H. Dalziel, K.D. Thornbury, D.P. Westfall, and K.M. Sanders.** Nonadrenergic, noncholinergic inhibition and rebound excitation in canine colon depend on nitric oxide. *Am. J. Physiol.* 262: G237-G243, 1992.
 118. **Ward, S.M., C. Xue, W. Shuttleworth, D.S. Bredt, S.H. Snyder, and K.M. Sanders.** NADPH diaphorase and NOS colocalization in enteric nerves of canine colon *Am. J. Physiol.* 263: G277-G248, 1992.
 119. **Wheeler, D.B., A. Randall, and R.W. Tsien.** Roles of N-type and Q-type Ca²⁺

channels in supporting hippocampal synaptic transmission. *Science* 264: 107-111, 1994.

120. **Yoshino, M., T. Someya, A. Nishio, K. Yazawa, T. Usuki, and H. Yabu.** Multiple types of voltage-dependent Ca channels in mammalian intestinal smooth muscle cells. *Pflügers Arch.* 414:401-409, 1989.
121. **Zamir, O., and M. Hanani.** Intercellular dye-coupling in intestinal smooth muscle. Are gap junctions required for intercellular coupling? *Experientia Basel* 46: 1002-1005, 1990.
122. **Zhou, D.S., and T. Komuro.** Interstitial cells associated with the deep muscular plexus of the guinea-pig small intestine, with special reference to the interstitial cells of Cajal. *Cell Tissue Res.* 268: 205-216, 1992.

LIST OF PUBLICATIONS

PAPERS (Published)

1. **Cayabyab, F.S.** and Daniel, E.E. K^+ channel opening mediates hyperpolarizations by NO-donors and inhibitory junction potentials in opossum esophagus. *American Journal of Physiology (Gastrointestinal and Liver Physiology)* **268**:G831-G842, 1995.
2. Daniel, E.E., Fox-Threlkeld, J.E.T., Mao, Y.K., Wang, Y.F., **Cayabyab, F.S.**, Jimenez, M., Vergara, P., Memeh, C. Interactions of VIP (vasoactive intestinal polypeptide) and nitric oxide (NO) in mediating intestinal inhibition. *Biomedical Research* **15**:69-77, 1994.
3. Daniel, E.E., Jury, J., Christinck, F., and **Cayabyab, F.** Chloride-mediated inhibitory junction potentials in opossum esophageal circular smooth muscle. Letter to the Editor. *American Journal of Physiology (Gastrointestinal and Liver Physiology)* **263**: G135-G138, 1992.
4. Christinck, F., Jury, J., **Cayabyab, F.**, and Daniel, E.E. Nitric oxide may be the final mediator of nonadrenergic, noncholinergic inhibitory junction potentials in the gut. *Canadian Journal of Physiology and Pharmacology* **69**: 1448-1458, 1991.

PAPERS (submitted, *pertaining to this thesis)

- *1. **Cayabyab, F.S.**, Wang, Y.F., deBruin, H., and Daniel, E.E. Myenteric and deep muscular plexus slow waves: different gap junction coupling properties of interstitial cells of Cajal. *American Journal of Physiology (Gastrointestinal and Liver Physiology)*, Submitted August, 1995.
- *2. **Cayabyab, F.S.**, Jiménez, M., deBruin, H., and Daniel, E.E. Ca^{2+} role in canine ileum slow wave formation, nerve activation, and excitation-contraction coupling. *American Journal of Physiology (Cell Physiology)*, submitted June, 1995.
- *3. Jiménez, M., **Cayabyab, F.S.**, Vergara, P., and Daniel, E.E. Heterogeneity in electrical activity of the canine ileal circular muscle: interaction of two pacemakers. *American Journal of Physiology (Gastrointestinal and Liver Physiology)*, submitted June, 1995.

Physiology), in revision. Submitted March, 1995.

- *4. **Cayabyab, F.S., Jiménez, M., Vergara, P., deBruin, H., and Daniel, E.E.** Influence of nitric oxide on the spontaneous and triggered electrical and mechanical activities of the canine ileum. *American Journal of Physiology (Gastrointestinal and Liver Physiology)* in revision. Submitted March, 1995.
5. **Cayabyab, F.S., and Daniel, E.E.** Internal Ca^{2+} store and Ca^{2+} influx modulate esophageal inhibitory junction potentials in opossum esophagus. *Journal of Pharmacology and Experimental Therapeutics*, in revision. Submitted March, 1995.
6. **Cayabyab, F.S. and Daniel, E.E.** Modulation of non-specific cation channels and inhibitory junction potentials by neurotensin in opossum esophagus. *Regulatory Peptides*, Submitted February, 1995.

ABSTRACTS (* pertaining to this thesis)

- *1. **Cayabyab, F.S., deBruin, H., Jimenez, M., and Daniel, E.E.** Ca^{2+} and canine ileal slow waves, contractions and IJPs. The XV International Symposium on Gastrointestinal Motility, November 5-9, 1995, Rome, Italy. Abstract in *Neurogastroenterology and Motility* 1995.
- *2. **Cayabyab, F.S., Berezin, I., deBruin, H., and Daniel, E.E.** Electrical coupling of interstitial cells of Cajal (ICC) to smooth muscle of canine ileum. The XV International Symposium on Gastrointestinal Motility, November 5-9, 1995, Rome, Italy. Abstract in *Neurogastroenterology and Motility* 1995.
- *3. **Cayabyab, F.S., deBruin, H., Jimenez, M., and Daniel, E.E.** Differential Ca^{2+} sensitivity of two pacemaking networks in the canine ileum. American Gastroenterological Association Annual Meeting, Digestive Diseases Week, San Diego, California, May 14-17, 1995. Abstract in *Gastroenterology* 108:A579, 1995.
- *4. **Cayabyab, F.S., Jimenez, M., Vergara, P., and Daniel, E.E.** Two independent pacemakers drive the electrical and mechanical activities of the canine ileum. The 7th European Symposium on Gastrointestinal Motility. Toulouse, France, July 7-9, 1994. Abstract in *Neurogastroenterology and Motility*, 6:152, 1994.
- *5. **Cayabyab, F.S., deBruin, H., and Daniel, E.E.** NO and NANC inhibitory mediation in the canine ileum. The XIIth International Congress of Pharmacology.

- International Union of Pharmacology (IUPHAR) Meeting. Montreal, Quebec, Canada, July 24-29, 1994. Abstract in *Canadian Journal of Physiology and Pharmacology*, 72:234, 1994.
6. **Cayabyab, F.S.** and Daniel, E.E. The superficial buffer barrier role in K⁺ channel opening in opossum esophagus. The XIIth International Congress of Pharmacology. International Union of Pharmacology (IUPHAR) Meeting. Montreal, Quebec, Canada, July 24-29, 1994. Abstract in *Canadian Journal of Physiology and Pharmacology*, 72:513, 1994.
 7. Daniel, E.E., Fox-Threlkeld, J.E.T., Mao, Y.K., Wang, Y.F., **Cayabyab, F.**, Jimenez, M., Vergara, P., and Memeh, C. Interactions of VIP and nitric oxide (NO) in mediating intestinal inhibition. The International Conference on Gut Hormone (GUT HORMONE '93). Shizuoka, Japan, October 19-22, 1993. Abstract in *Biomedical Research*, 1993.
 8. **Cayabyab, F.S.**, Daniel, E.E, and C.Y. Kwan. T-type, not L-type, Ca²⁺ channels and sarcoplasmic reticulum modulate Ca²⁺-activated K⁺ channels in opossum esophagus. 14th International Symposium on Gastrointestinal Motility, Minnet, Muskoka, Canada, August 29-September 3, 1993. *Journal of Gastrointestinal Motility*, 5:184, 1993.
 9. **Cayabyab, F.S.** and Daniel, E.E. Mechanisms of neurotensin excitatory actions on the opossum esophagus: *role of intracellular Ca²⁺ stores*. American Gastroenterological Association, American Association for the Study of Liver Diseases, Boston, Massachusetts, May 16-19, 1993. *Gastroenterology* 104:A1033, 1993.
 10. **Cayabyab, F.S.** and Daniel, E.E. Dual Mechanisms for NO or SIN-1 hyperpolarization of opossum esophagus: *role of cGMP and Ca²⁺*. American Gastroenterological Association, American Association for the Study of Liver Diseases, Boston, Massachusetts, May 16-19, 1993. *Gastroenterology* 104:A1033, 1993.
 11. **Cayabyab, F.S.** and Daniel, E.E. Increased K⁺ conductance mediates inhibitory junction potential (IJP) and nitrovasodilator hyperpolarization of the opossum esophagus. American Gastroenterological Association, American Association for the Study of Liver Diseases, Boston, Massachusetts, May 16-19, 1993. *Gastroenterology* 104:A1033, 1993.
 12. **Cayabyab, F.S.** and Daniel, E.E. Ionic mechanisms of inhibitory junction

potentials (IJP) in opossum esophageal body circular muscle. Presented in the Seventh Biennial Symposium of the American Motility Society, Lake Tahoe, California, September 13-17, 1992. *Gastroenterology* 103(4):1405, 1992.

13. Daniel, E.E., Jury, J., **Cayabyab, F.**, Christinck, F., Kostka, P., Berezin, I. Role of neurally-derived NO-related compounds in gastrointestinal motor function *in vitro* studies. Seventh Biennial Symposium of the American Motility Society, Lake Tahoe, California, September 13-17, 1992. *Gastroenterology* 103(4):1405, 1992.
14. **Cayabyab, F.** and Daniel, E.E. Nitric oxide may mediate inhibitory responses in opossum esophagus. Presented at the Digestive Disease Week, American Gastroenterological Association (AGA) meeting. New Orleans, Louisiana, May 19-22, 1991. Abstract in *Gastroenterology* 100(5):A821, 1991
15. Daniel, E.E., Christinck, F., **Cayabyab, F.**, and Jury, J. NO, not VIP mediator of non-adrenergic, non-cholinergic inhibition (NANC) in enteric nerves. Third IBRO World Congress of Neuroscience, Montreal, Quebec, August, 1991.
16. Daniel, E.E., Jury, J., Christinck, F., and **Cayabyab, F.** What are the roles of VIP and NO-related compounds in NANC neurotransmission? The Fifth International Symposium on VIP and related peptides, Shizuoka, Japan, November, 1991.
17. Daniel, E.E., Jury, J., Christinck, F., and **Cayabyab, F.** What are the roles of VIP and NO-related compounds in NANC neurotransmission? Thirteenth International Symposium on Gastrointestinal Motility, Kobe, Japan, November, 1991. *Journal of Gastrointestinal Motility* 3:__, 1991.